



McElroy, Daniel (2018) Elucidating the functions of fibroblast growth factor 9 in multiple sclerosis. PhD thesis.

<https://theses.gla.ac.uk/30798/>

Copyright and moral rights for this work are retained by the author

A copy can be downloaded for personal non-commercial research or study, without prior permission or charge

This work cannot be reproduced or quoted extensively from without first obtaining permission in writing from the author

The content must not be changed in any way or sold commercially in any format or medium without the formal permission of the author

When referring to this work, full bibliographic details including the author, title, awarding institution and date of the thesis must be given

Enlighten: Theses

<https://theses.gla.ac.uk/>
research-enlighten@glasgow.ac.uk

ELUCIDATING THE FUNCTIONS OF FIBROBLAST GROWTH FACTOR 9 IN MULTIPLE SCLEROSIS

DANIEL MCELROY BSc (Hons)

Thesis submitted in fulfilment of the requirements for the degree of

Doctor of Philosophy



College of Medical, Veterinary, and Life Sciences

Institute of Infection, Immunity, and Inflammation

University of Glasgow

January 2018

ABSTRACT

Multiple sclerosis (MS) is a chronic demyelinating disease of the central nervous system. In around 85% of cases, the disease progresses through two distinct stages: relapsing-remitting MS (RRMS) is driven by repeated bouts of demyelination caused by autoimmune inflammation; and progressive MS, in which inflammation gives way to neurodegenerative processes that lead to axonal loss and the steady accumulation of disability. There is no cure for MS and the majority of disease-slowing treatments target the immune response in RRMS. These interventions are ineffective in progressive MS and other treatment options are extremely limited. Understanding the mechanisms underlying neurodegeneration in MS is critically important to developing therapeutics for progressive disease.

Fibroblast growth factor 9 (FGF9) has recently been implicated in the pathogenesis of MS. FGF9 inhibits myelination and promotes the production of inflammatory chemokines. This led to the hypothesis that FGF9 is involved in remyelination failure and may promote neurodegeneration via tissue remodelling and inflammatory pathways. FGF signaling is complex and the findings in MS raised many questions: what cells respond to FGF9 in MS? Why is FGF9 expression induced in the first place? Can FGF9 cause demyelination as well as inhibit myelination? This thesis has focused on the roles of FGF9 in MS and tried to answer these questions.

Through *in vitro* models, astrocytes, oligodendrocytes, and macrophages were shown to express feedback inhibitors of FGF signaling when treated with FGF9. Astrocytes produced FGF9 in response to hypoxic stress, macrophages expressed FGF9 when polarized towards an anti-inflammatory phenotype, suggesting hypoxia, and repair processes may drive FGF9 expression in the CNS. FGF9 did not cause demyelination *in vitro* but over-expression *in vivo* induced severe demyelination over the course of several months. Oligodendrocytes exposed to FGF9 failed to differentiate properly when the factor was removed which led to aberrant myelination. Long-term treatment with FGF9 induced axonal pathology, potentially via deficits in axon-transport. Over-expression of FGF9 in rat cortex also produced an axonal pathology, which suggests chronic exposure is detrimental to neurons. Together, these findings indicate that increased levels of FGF9 are detrimental to myelination and neurons in the CNS. Demyelination, and

axonal pathology are hallmarks of MS and these studies provide evidence that FGF9 can mediate these processes in *in vitro* and *in vivo* models.

AUTHOR'S DECLARATION

I declare that, except where referenced to others, this thesis is the product of my own work and has not been submitted for any other degree at the University of Glasgow or any other institution.

Signature: _____

Printed name: DANIEL MCELROY

ACKNOWLEDGEMENTS

First I would like to thank my supervisor, Professor Chris Linington. I started in Chris' lab as an undergraduate on an Honours project and I have not left since. Chris has been a font of knowledge and enthusiasm (and pints), which were invaluable in completing this PhD. I would like to thank our Post Doc Katja, who is a great teacher and master of organisation, and great to talk to when squeezed into a tissue culture hood together. Next, I would like to thank Tiia, my lab wife. If we were as good at science as we were at driving each other mad we would have cured MS by now. Thanks to Diana, the hardest working scientist I know, for all your help and baking all those amazing cakes. Thanks to Dr Julia Edgar for all the knowledge and expertise you brought to the lab, as well as teaching me your skills in EAE. I am also grateful to Prof Hans Lassmann and Dr Corneila Schuh for teaching me the ways of neuropathology, and giving me the opportunity to visit Vienna. For setting up the FGF9 rat model and allowing me to visit Göttingen, thank you Prof Christine Stadelmann and Dr Claudia Wrzos. Thanks to my second supervisor, Prof Sue Barnett and my assessors, Prof Hugh Willison and Prof Rob Nibbs for your ideas and guidance. To the whole Barnett lab/office buddies, Susan, Mike 1, Mike 2, Sara, and George you are a truly marvellous group of people and the finest drinking companions a man can have. Bilbao and Edinburgh were particular highlights of our adventures. To the newbies in the lab, Lorna and Colin, good luck and enjoy yourselves. To Craig, Dennis, Stewart, Joanna, Dougie, and Colin, and all the CRF staff, thanks for your help over the years. Moreover, to everyone in the GBRC, thank you. In four years, I never came across a person who wouldn't go out of their way to help me, or spend their time teaching me what they know and I am very grateful. I would like to thank my parents and siblings who supported me throughout the PhD, even though they still do not really know what I do. Lastly, I would like to thank my amazing girlfriend Liz, for all your support and the endless proofreading you have endured. Thank you all, I have had an amazing time.

Table of Contents

Abstract	II
Authors Declaration	IV
Acknowledgements	V
List of Figures	XII
List of Tables	XVI
Abbreviations	XV
Conference Poster Presentations	XX
1. General Introduction	1
1.1 General introduction to multiple sclerosis	2
1.1.1 Historical perspective of multiple sclerosis	2
1.1.2 Pathogenesis of multiple sclerosis	4
1.1.2.1 Relapsing remitting multiple sclerosis	6
1.1.2.2 Progressive multiple sclerosis	7
1.2 The fibroblast growth factor signalling family	10
1.2.1 Fibroblast growth factor ligands	11
1.2.2 Fibroblast growth factor receptors	14
1.2.3 Fibroblast growth factor signalling pathways	15
1.2.3.1 MAPK signaling	18
1.2.3.2 PI3K-AKT pathway	18
1.2.3.3 PLC γ signalling	19
1.2.3.4 Stat signalling	19
1.2.3.5 FGFs in the nucleus	20
1.2.4 Regulation of FGF signalling	21
1.2.4.1 Heparan sulphates	21

1.2.4.2 Sproutys	22
1.2.4.3 DUSPs	23
1.2.4.4 Extracellular FGF signalling regulators	23
1.3 Fibroblast growth factors in the central nervous system	24
1.3.1 FGF1, 2, and 9 in CNS development	24
1.3.2 Roles of FGFs in the adult CNS.....	27
1.3.2.1 FGF and FGFR expression in the adult CNS.....	27
1.3.2.2 FGFs in adult CNS homeostasis.....	28
1.4 Fibroblast growth factors in multiple sclerosis.....	30
1.4.1 Localisation of FGFs in MS lesions.....	30
1.4.2 Roles of FGFs in MS pathogenesis.....	31
1.4.2.1 FGF1	31
1.4.2.2 FGF2	32
1.4.2.3 FGF9	35
1.5 Thesis aims	39
2. Materials and Methods.....	40
2.1 Animals.....	41
2.2 Cell Culture.....	41
2.2.1 Generation of myelinating spinal cord cultures.....	41
2.2.1.1 Generation of neurospheres.....	41
2.2.1.2 Generation of astrocyte monolayers from neurospheres.....	42
2.2.1.3 Seeding of embryonic spinal cord cells on astrocyte monolayers.....	43
2.2.2 Generation of low-density astrocyte cultures.....	44
2.2.3 Generation of purified oligodendrocyte cultures.....	47
2.2.4 Generation of bone marrow-derived macrophage cultures.....	48
2.2.5 Generation of enriched neuronal cultures.....	50
2.2.6 <i>In vitro</i> culture experiments.....	50
2.2.6.1 Myelination experiments.....	50

2.2.6.2 Astrocyte experiments.....	50
2.2.6.3 FGF9 experiments.....	51
2.2.6.4 Cytokine experiments.....	51
2.2.6.5 Hypoxia experiments.....	51
2.2.6.6 Macrophage experiments.....	51
2.2.6.7 Purified oligodendrocyte experiments.....	51
2.2.6.8 Enriched neuron experiments.....	52
2.2.7 Immunofluorescence staining of <i>in vitro</i> cultures.....	52
2.2.8 Imaging and quantitative analysis.....	52
2.3 Immunohistochemical analysis of human tissues.....	55
2.4 Molecular biology.....	57
2.4.1 RNA extraction.....	57
2.4.1.1 RNA extraction from <i>in vitro</i> cultures.....	57
2.4.1.2 RNA extraction from tissues.....	57
2.4.2 cDNA synthesis.....	58
2.4.3 Primer design.....	58
2.4.4 Quantitative real-time PCR.....	60
2.5 Recombinant rat MOG ₁₋₁₂₅ production and purification.....	60
2.5.1 Culture of rMOG-expressing <i>E. coli</i>	60
2.5.2 Lysis of <i>E. Coli</i>	61
2.5.3 Dissolving inclusion bodies.....	62
2.5.4 Nickel-chelate affinity chromatography.....	62
2.5.5 Dialysis of protein.....	62
2.5.6 BCA protein concentration assay.....	63
2.5.7 X-ray sterilization of purified rMOG.....	63
2.6 <i>In Vivo</i> experiments.....	63
2.6.1 MOG-induced EAE in DA rats.....	63
2.6.1.1 Clinical scoring of EAE	63
2.6.1.2 Perfusion and harvesting of rat spinal cord.....	64
2.6.1.3 Preparing rat spinal cord for immunohistochemistry.....	64

2.6.2 Cortical injection of AAV 6 viral vectors in Lewis rats.....	65
2.6.2.1 Stereotactic injections.....	65
2.6.2.2 Harvesting and preparing rat brain for immunohistochemistry.....	65
2.6.3 Staining and imaging of rat brain and spinal cords.....	67
2.7 Statistical Analysis.....	67
3. Feedback inhibitors of FGF9 in MS and myelinating cultures.....	68
3.1 Introduction.....	69
3.2 Results.....	71
3.2.1 FGF-feedback inhibitor expression was increased in acute and chronic MS	71
3.2.1.1 There was constitutive expression of FGF feedback-inhibitors in healthy human brain.....	71
3.2.1.2 FGF-feedback inhibitor expression was highest in acute MS lesions.....	74
3.2.1.3 FGF-feedback inhibitor expression is a feature of chronic MS but is less pronounced compared to acute disease	80
3.2.2 Assessing feedback-inhibitor expression in myelinating cultures	84
3.2.2.1 FGF9 induced feedback-inhibitor expression in myelinating cultures while FGF1 and FGF2 did not.....	84
3.2.2.2 Mature OLs, OPCs, and neurons responded to FGF2 and FGF9.....	86
3.2.2.3 Feedback inhibitor expression in astrocytes was induced only by FGF9.....	90
3.3 Discussion.....	94
4. Induction of FGF9 In Cells Involved In Pathogenesis of MS	99
4.1 Introduction.....	100
4.2 Results.....	103
4.2.1 Inflammatory mediators had little effect on myelination or axon density....	103
4.2.2 Treatment with inducers of FGF9 in cancer or inflammatory mediators did not induce expression of FGFs.....	105
4.2.3 Inflammatory mediators did not induce FGF9 expression at the protein level.....	109
4.2.4 Hypoxia upregulated FGF9 in myelinating cultures.....	112

4.2.5 Macrophages polarised towards an anti-inflammatory phenotype upregulate FGF9 gene expression	118
4.2.6 FGF-treatment does not induce feedback inhibitor expression or alter cytokine production in polarised macrophages	121
4.3 Discussion.....	124
5. FGF9 disrupted myelination and induced axonal pathology.....	130
5.1 Introduction.....	131
5.2 Results.....	133
5.2.1 FGF9 had different effects depending on the duration of treatment and age of cultures when treatment was initiated.....	133
5.2.1.1 FGF9 did not cause demyelination after day 10 treatment.....	133
5.2.1.2 Removing FGF9 from cultured treated from DIV 18-28 led to increased but aberrant myelination.....	136
5.2.1.3 Long term treatment with FGF9 was detrimental to axons in myelinating cultures	141
5.2.1.4 Oligodendrocyte numbers increased by FGF9 treatment return to control levels after the factor is withdrawn.....	143
5.2.2 FGF9 treatment reduced neuronal numbers, axonal density, and axonal transport-gene expression in enriched neuronal cultures.....	147
5.2.2.1 Expression of genes involved in axonal transport were reduced in myelinating cultures treated with FGF9.....	147
5.2.2.2 Neuronal cell numbers and axon density were reduced by FGF9 treatment.....	150
5.3 Discussion.....	153
6. Chronic over-expression of FGF9 induced demyelination and axonal pathology.....	160
6.1 Introduction.....	161
6.2 Results.....	163
6.2.1 FGF9 expression appeared in neurons following AAV6 infection.....	163
6.2.2 FGF9 overexpression caused extensive demyelination.....	165
6.2.3 Demyelinated lesions accumulated β -APP+ axonal swellings over time .	168
6.2.4 Astrocytes in FGF9-overexpressing lesions upregulated Sprouty2 but not FGF9	171

6.3 Discussion 174

7. General Discussion 178

8. Appendices 185

8.1 Positive control stainings for Sprouty, DUSP, and FGF9 antibodies ... 186

8.2 Cell culture purity analysis 188

8.3 FGF9 induced proliferation in astrocytes 191

8.4 Expression of FGFs and feedback inhibitors in EAE 192

8.5 FGF9 and Sprouty2 were associated with macrophages in EAE 195

LIST OF FIGURES

Figure 1.1 Ligand-receptor interactions of the canonical FGFs	13
Figure 1.2 Simplified FGF signaling schematic	17
Figure 1.3 Schematic diagram of FGF signaling events throughout oligodendrocyte differentiation.....	26
Figure 1.4 FGF9 inhibits myelination in a dose dependant manner	37
Figure 1.5 Representative images of myelinating cultures after FGF9 treatment	38
Figure 2.1 Representative images of cells which constitute myelinating cultures at DIV 28.....	46
Figure 2.2 Adeno-associated viral vectors used in in vivo experiments.....	66
Figure 3.1 FGF9 and Sproutys were associated with neurons in healthy adult brains	73
Figure 3.2 FGF9 and Sproutys label astrocytes in acute lesions	77
Figure 3.3 FGF9 and Sproutys label astrocytes and macrophages in Balo's concentric sclerosis	78
Figure 3.4 Swollen neurons in a grey matter lesion from case 70-93-6 displayed intense granular staining for FGF9 and the Sproutys	79
Figure 3.5 Representative images from chronic MS case 146-01-8	82
Figure 3.6 FGF9 and Sprouty2 colocalized in astrocytes in white matter lesions	83
Figure 3.7 Feedback inhibitor expression was increased and FGFR expression decreased in myelinating cultures treated with FGF9.....	85
Figure 3.8 Mature OLs upregulated feedback inhibitors and downregulated Fgfr2 when treated with FGF2, and FGF9.....	87
Figure 3.9 OPCs were less responsive to FGFs than mature OLs.....	88
Figure 3.10 Neurons similarly upregulated feedback inhibitors when treated with FGF2 and FGF9	89
Figure 3.11 Only FGF9 upregulated feedback inhibitor expression in astrocytes	91
Figure 3.12 FGF feedback inhibitor expression was increased by FGF9, but not other FGFs in astrocytes	92

Figure 3.13 Representative images of FGF feedback inhibitors in cultures astrocytes following treatment with FGF9	93
Figure 4.1 A selection of inflammatory mediators had little effect on myelination or axon density	104
Figure 4.2 Inflammatory mediators did not upregulate <i>Fgf1</i> expression in myelinating cultures	106
Figure 4.3 Inflammatory mediators did not upregulate <i>Fgf2</i> expression in myelinating cultures	107
Figure 4.4 Inflammatory mediators did not upregulate <i>Fgf9</i> expression in myelinating cultures	108
Figure 4.5 Representative images FGF9 and GFAP staining in control myelinating cultures	110
Figure 4.6 FGF9 was not induced at the protein level by inflammatory mediators	111
Figure 4.7 Myelinating cultures lost axons and myelin following hypoxia and reperfusion	113
Figure 4.8 Representative images of myelin and axons in hypoxia experiment	114
Figure 4.9 Astrocytes increased FGF9 expression in response to hypoxia	115
Figure 4.10 Representative images of astrocytes and FGF9 in hypoxia experiment	116
Figure 4.11 FGF9 expression was reduced at the mRNA level following hypoxia while FGF2 expression was elevated	117
Figure 4.12 Polarisation of bone marrow-derived macrophages with IFN γ and IL-13	119
Figure 4.13: FGF2 and FGF9 were induced by IL-13 in BMDMs	120
Figure 4.14: FGF treatment did not induce feedback-inhibitor expression in macrophages	122
Figure 4.15 FGF9 did not influence macrophage polarization or cytokine expression.....	123
Figure 5.1 FGF9 was not a demyelinating factor and pre-treatment increased myelination production	134
Figure 5.2 Representative images of myelinating cultures after alternating FGF9 treatment.....	135

Figure 5.3 Pre-treatment with FGF9 disrupted myelination and causes an axonal pathology	138
Figure 5.4 Confocal imaging of MOG ⁺ PLP ⁺ cells reveals stark morphological differences from normal OLs	139
Figure 5.5 Microglia did not phagocytose irregular myelin produced as a result of FGF9-treatment	140
Figure 5.6 Axonal pathology preceded reduction in density in FGF9-treated myelinating cultures	142
Figure 5.7 OPC and OL lineage cell numbers increased after FGF9 treatment and returned to baseline levels after it is withdrawn.....	144
Figure 5.8 Representative images of NG2 staining after alternating FGF9 treatment.....	145
Figure 5.9 Representative images of Olig2 staining after alternating FGF9 treatment.....	146
Figure 5.10 Axonal transport gene expression was reduced by FGF9 treatment	149
Figure 5.11 Axon density and neuronal cell counts were reduced in neuronal cultures following 10-day FGF9 treatment.....	151
Figure 5.12 Representative images of neurons and axons in FGF9-treated neuronal cultures.....	152
Figure 6.1 FGF9 was expressed by neurons following injection with AAV6-Fgf9 vectors	164
Figure 6.2 Representative images of progressive demyelination in AAV6- <i>Fgf9</i> lesions	166
Figure 6.3 Demyelination took place between 1 and 3 months following injection with AAV- <i>Fgf9</i>	167
Figure 6.4 Representative images of β -APP staining in rat cortex following AAV6 infection	169
Figure 6.5 β -APP ⁺ swellings appeared 30 days PI in pAAV-Fgf9 lesions and accumulate as lesions persist	170
Figure 6.6 Astrocytes did not express FGF9 in AAV6- <i>Fgf9</i> lesions	172
Figure 6.7 Sprouty2 staining appeared in astrocytes in AAV- <i>Fgf9</i> lesions	173
Figure 8.1 Positive control stainings for FGF9 antibodies used in immunohistochemistry and immunofluorescence	186

Figure 8.2 Positive control stainings for antibodies used in immunohistochemistry and immunofluorescence	187
Figure 8.3 Quantification of different cell types in astrocyte monolayers	189
Figure 8.4. Quantification of different cell types in enriched neuronal cultures .	190
Figure 8.5 FGF9 induced proliferation in astrocytes <i>in vitro</i>	186
Figure 8.6 MOG1-125 induced EAE caused biphasic disease in Lewis rats	193
Figure 8.7 FGF and feedback inhibitor expression was variable in EAE	194
Figure 8.8 FGF9 and Sprouty2 expression was visualised in macrophages/ microglia in EAE	196

LIST OF TABLES

Table 1.1. Currently approved treatment for multiple Sclerosis	3
Table 2.1 Primary antibody list	54
Table 2.2 Fluorescent secondary antibody list	54
Table 2.3 List of patient samples used in human lesion studies.....	56
Table 2.4 List of primers used in qPCR experiments.....	59
Table 3.1 Differentially expressed genes in rat myelinating cultures treated with FGF1, 2 or 9 for 24 hours and 10 days	70
Table 3.2 Characterisation of FGF9, Sprouty2, and Sprouty4 staining in human control brain sections.....	72
Table 3.3 Characterisation of FGF9, Sprouty2 and Sprouty4 staining in acute MS lesions.....	76
Table 3.4 Characterisation of FGF9, Sprouty2 and Sprouty4 staining in chronic MS lesions.....	81
Table 5.1 Differentially expressed neuronal genes in myelinating cultures treated with FGF1, 2 or 9 for 24 hours and 10 days.....	148

ABBREVIATIONS

AAV	adeno-associated virus
AhR	aryl hydrocarbon receptor
ATP	adenosine tri-phosphate
BaP	benzo[a]pyrene
BBB	blood-brain barrier
BCA	bicinchoninic acid
BMDM	bone marrow-derived macrophages
BSA	bovine serum albumin
cDNA	complementary deoxyribonucleic acid
CFA	complete Freund's adjuvant
CIS	clinically isolated syndrome
CNPase	(2',3'-cyclic-nucleotide 3'-phosphodiesterase)
CNS	central nervous system
cRPMI	complete Roswell Park Memorial Institute-1640 media
CSF	cerebrospinal fluid
CT	cycle threshold
DA	Dark Agouti
DAB	3,3'diaminobenzidine
DAG	diacylglycerol
DAPI	4'-6'diamidino-2-phenylindole
DIV	day <i>in vitro</i>
DM-	differentiation media (without insulin)
DM+	differentiation media (with insulin)
DMEM	Dulbecco's Modified Eagle Medium
DMSO	dimethyl sulfoxide
DNA	deoxyribonucleic acid
DUSP	dual-specificity phosphatase
E	embryonic day
E. Coli	<i>Escherichia coli</i>
EAE	experimental autoimmune encephalitis
EBV	Epstein-Barr virus
ECM	extracellular matrix
EDTA	ethylenediaminetetraacetic acid
EGF	epidermal growth factor
eGFP	enhanced-green fluorescent protein
ELISA	enzyme-linked immunosorbent assay
ETS	E26 transformation-specific
FBS	foetal bovine serum
FdU	5-fluoro-2 deoxyuridine
FGF	fibroblast growth factor
FGFBP	fibroblast growth factor binding protein
FGFR	fibroblast growth factor receptor

FGFRL1	fibroblast growth factor receptor-like 1
FRS2 α	fibroblast growth factor receptor substrate 2- α
g	relative centrifugal force
GAB1	growth factor receptor-bound 2-associated binding protein 1
GFAP	glial fibrillary acidic protein
GM	grey matter
GM-CSF	granulocyte-macrophage colony-stimulating factor
GRB2	growth factor receptor-bound 2
H ₂ O ₂	hydrogen peroxide
HBSS	Hank's balanced salt solution
HIF1 α	hypoxia-inducible factor 1- α
HK2	hexokinase 2
HLA	human leukocyte antigen
HRP	horseradish peroxidase
HSPGs	heparin sulphate proteoglycans
iFGFs	intracrine fibroblast growth factors
IFN γ	interferon- γ
IFN γ	interferon- γ
Ig	immunoglobulin
IL-	interleukin
IP3	inositol 1,4,5-triphosphate
IPTG	isopropyl β -D-1-thiogalactopyranoside
KO	knock out
L. broth	L lysogeny broth
LDAO	N,N-dimethyldodecylamine N-oxide
LIF	leukocyte inhibitory factor
MAG	myelin-associated glycoprotein
MAPK	mitogen-activated protein kinase
MBP	myelin basic protein
M-CSF	macrophage colony-stimulating factor
MFI	mean fluorescent intensity
MHC	major histocompatibility complex
MOG	myelin oligodendrocyte glycoprotein
MRI	magnetic resonance imaging
mRNA	messenger ribonucleic acid
MS	multiple sclerosis
mTORC1	mammalian target of rapamycin complex 1
MW	molecular weight
NaCl	sodium chloride
NAGM	normal appearing grey matter
NaHCO ₃	sodium bicarbonate
NAWM	normal appearing white matter
NFAT	nuclear factor of activated T cells
NiCl	nickel chloride
NO	nitric oxide
NSM	neurosphere media

OD	optical density
OL	oligodendrocyte
OPC	oligodendrocyte precursor cell
OPC	oligodendrocyte precursor cell
P	post-natal day
PBS	phosphate buffered saline
PCR	polymerase chain reaction
PDGF	platelet-derived growth factor
PDGFR	platelet-derived growth factor receptor
PDGF α	platelet-derived growth factor α
PFA	paraformaldehyde
PGE2	prostaglandin E2
PI	post-injection
PI3K	phosphoinositide 3-kinase
PI3K-AKT	phosphoinositide 3-kinase/protein kinase B
PLC γ 1	phospholipase C γ 1
PLL	poly-L-lysine
PLP	phospholipid protein
PM	plating media
PPMS	primary progressive
qPCR	quantitative real-time polymerase chain reaction
rMOG	recombinant myelin oligodendrocyte glycoprotein ₁₋₁₂₅
RNA	ribonucleic acid
rpm	revolutions per minute
RRMS	relapsing-remitting multiple sclerosis
RSK	ribosomal S6 kinase
RTKs	receptor tyrosine kinases
SCI	spinal cord injury
SD	Sprague Dawley
SDS-PAGE	sodium dodecyl sulphate polyacrylamide gel electrophoresis
SOS	son of sevenless
SPMS	secondary progressive multiple sclerosis
STAT	signal transducer and activator of transcription
SVZ	subventricular zone
TF	transcription factor
TGF β 1	transforming growth factor- β 1
TNF α	tumour necrosis factor- α
TSC2	tuberous sclerosis complex 2
VEGF	vascular endothelial growth factor
WM	white matter
WPRE	Woodchuck Hepatitis virus posttranscriptional regulatory element
β -APP	beta-amyloid precursor protein

CONFERENCE POSTER PRESENTATIONS

July 2017, Edinburgh, Scotland. Glia: Glial Cells in Health and Disease

- Lesion Development in a Rat Model of Fibroblast Growth Factor 9 Overexpression: Implications for Multiple Sclerosis

May 2016, Lucca, Italy. Gordon Research Conference: Myelin – Rethinking Functions, Revealing Mechanisms, Developing Medicines

- Inhibition of Myelination by FGF2 is Dependent on Wnt/ beta-catenin Signaling

July 2015, Bilbao, Spain. Glia: Glial Cells in Health and Disease

- FGF9 is Upregulated in Astrocytes after Exposure to Hypoxia

March 2014, California USA | Gordon Research Conference: Fibroblast Growth Factors in Development & Disease

- Elucidating the Roles of FGF Signaling in Multiple Sclerosis

CHAPTER ONE

GENERAL INTRODUCTION

1 GENERAL INTRODUCTION

1.1 General introduction to multiple sclerosis

1.1.1 Historical perspective of multiple sclerosis

The earliest known description of symptoms thought to be caused by multiple sclerosis (MS) comes from 12th century Iceland; from the account of a woman that suffered transient paresis and vision loss (Holmøy, 2006). The first descriptions and illustrations of MS lesions come from Sir Robert Carswell, a Professor of pathology in the early 19th Century (Compston, 1988). Carswell described the hallmarks of lesions of the brain and spinal cord but did not identify MS as a disease in its own right (Murray, 2009). This had to wait a further 40 years until the French neurologist, Professor Jean-Martin Charcot collated clinical and pathological descriptions of the disease he named “sclerose en plaque” (Compston, 1988). Charcot described three clinical symptoms that were used in the early diagnosis of MS: nystagmus, intention tremor, and telegraphic speech, known as Charcot’s neurological triad. Charcot also described cognitive symptoms of MS such as memory loss, difficulty grasping new concepts, and emotional disturbances (Özakbaş, 2015). This marked the beginning of defining diagnostic guidelines for MS which now draw extensively on magnetic resonance imaging (MRI) based criteria and cerebrospinal fluid (CSF) findings, as well as symptomology (Polman et al., 2011).

The development of effective treatments for MS followed these improvements in disease diagnosis. High dose, intravenous steroid therapy replaced adrenocorticotrophic hormone based treatments (Eisen and Norris, 1969) in the 1970’s and is still used in the treatment of clinically severe acute relapses (Milligan et al., 1987, Caster and Edwards, 2015). However, the first treatments to show real efficacy in reducing relapse frequency were β -interferons which became available in the 1990’s (Ebers, 1998). There are currently a dozen approved immunomodulatory treatments for relapsing-remitting MS (RRMS) (Table 1.1), but their efficacy remains limited by large numbers of non-responders and their failure to halt accumulation of disability in patients with progressive forms of the disease.

Table 1.1. Currently approved treatments for multiple sclerosis

Treatment	Year Approved	In use for	Efficacy	Mechanism of Action
Corticosteroids (Myhr, 2009)	1950's	RRMS	Shorten the duration of relapses.	General anti-inflammatory and immunosuppressive.
Plasma exchange (Tumani, 2008)	1980	RRMS	Improves recovery from relapses.	Reduces levels of circulating lymphocytes and immunoglobulins.
β-interferons (Kieseier, 2011)	1993	RRMS	Reduces relapse rate by 30%. Only effective in 70% of patients.	Increase expression of anti-inflammatory cytokines and nerve growth factor. Reduces expression of pro-inflammatory cytokines and ingress of immune cells to the CNS.
Glatiramer acetate (Neuhauser et al., 2001)	1997	RRMS	Reduces relapse rate but not progression disability.	Mimics MBP and perhaps acts as a decoy antigen. Promotes regulatory T cell induction.
Mitoxantrone (Fox, 2006)	2000	RRMS, SPMS	Reduces relapse rate, formation of new lesions and disability progression in both conditions.	Disrupts DNA synthesis which reduces immune cell proliferation.
Natalizumab (Hutchinson, 2007)	2004	RRMS	Reduces relapse rate by 68% and disability progression by 42%.	Blocks α 4 β 1-integrin receptor which prevents immune cells crossing the blood-brain barrier.
Fingolimod (Khatri, 2016)	2010	RRMS	Reduces relapse rate by up to 50%.	Sphingosine-1-phosphate receptor inhibitor. Sequesters lymphocytes in lymph nodes
Teriflunomide (Gandoglia et al., 2017)	2012	RRMS	Reduces relapse rate and disability progression by 30%.	Thought to limit T and B cell proliferation via inhibition of dihydroorotate-dehydrogenase.
Alemtuzumab (Havrdova et al., 2015)	2013	RRMS	Reduces relapse rate by 78% and disability progression by 71%.	Targets lymphocytes for destruction by binding to lymphocyte-specific antigen, CD52.
Dimethyl fumarate (Linker, 2016)	2013	RRMS	Reduces relapse rate by 50% and progression of disability.	Mechanisms still unclear but immunomodulatory and neuroprotective effects.
Dacizumab (Lycke, 2015)	2016	RRMS	Reduces relapse rate by 41%.	Blocks IL-2 receptor α chain which leads to T cell depletion.
Ocrelizumab (Hauser et al., 2017)	2017	RRMS, PPMS	Reduces relapse rate by 46% and disability progression by 40% in RRMS. Reduces disability progression from 36% to 30% over 6 months in PPMS.	Targets B cells for destruction by binding to CD20.

The introduction of these immunomodulatory treatments can be traced back studies in the 1930's that lead to the development of experimental autoimmune encephalitis (EAE) as an animal model for MS (Chaudhuri and Behan, 2005). EAE is a CD4⁺ T-cell mediated autoimmune disease that reproduces many of the clinical and pathological features of RRMS in which disease activity is driven by inflammatory activity in the central nervous system (CNS). Unfortunately, other pathological mechanisms appear to be responsible for disease activity in progressive forms of MS for which there are currently no effective treatments available.

1.1.2 Pathogenesis of multiple sclerosis

Several demyelinating diseases of the CNS share common features with, and can be difficult to differentiate from, classical MS. Neuromyelitis optica, for example, produces inflammatory demyelinating lesions and has a relapsing disease course, but mostly affects the optic nerves and spinal cord while sparing the brain (Wingerchuk et al., 1999). Acute disseminated encephalomyelitis causes widespread CNS inflammation and demyelination but occurs as a single bout of inflammation and is triggered by infections or immunization although the mechanism responsible is still unknown (Sanderson et al., 2017). Classification and diagnosis of the different demyelinating diseases is still difficult due to the overlapping mechanisms of damage and the unknown triggers in most cases.

Several hypotheses for the cause of MS have been proposed such as vitamin deficiency, hygiene, infections, vaccination, gut microbiota, etc. yet the trigger or triggers remain a mystery. It has however, become clear that a combination of genetic susceptibility and environmental factors determine ones likelihood of developing the disease. If one twin has MS, a monozygotic twin has a 30% chance of developing MS while a dizygotic twin has only a 7.5% chance (Willer et al., 2003). Having two affected parents carries a higher risk of developing MS than having just one, 25% vs 15% respectively (Robertson et al., 1997). These observations point towards a clear genetic component and genome-wide association studies have identified over 50 susceptibility genes for MS (Lin et al., 2015). The majority of these genes are involved in the immune system with the strongest association in human leukocyte antigen (HLA) genes (Olerup and Hillert, 1991). HLA genes are highly variable amongst the population as they transcribe

components of the major histocompatibility complex (MHC) class I and II, which mediate antigen presentation between antigen presenting cells, and B and T cells. Polymorphisms in interleukin receptor genes and in the myelin oligodendrocyte glycoprotein (MOG) have also been associated with a greater susceptibility to MS (Hafler et al., 2007, Lin et al., 2015).

Prevalence of MS generally increases further north and south from the equator and in the last few decades, rates of MS have increased drastically in some areas pointing to the involvement of strong environmental factors. In Canada for example, the female to male ratio has increased over the last half century to exceed 3.2 : 1 (Orton et al., 2006). Several studies focusing on different populations have shown migration from a high-risk area to a low-risk area correlates with a decrease in risk for MS and vice versa (Elián et al., 1990, Hammond et al., 2000). These studies indicate that sun exposure may be a factor in the latitudinal gradient of MS prevalence. This is supported by extensive studies, which demonstrate a strong correlation between high levels of vitamin D and a reduced risk of MS (Riccio and Rossano, 2017, Munger et al., 2006, Alharbi, 2015). The most substantial environmental risk factor so far identified is Epstein-Barr virus (EBV) infection in childhood or early adulthood associated with a 15 - and 30 - fold increased risk of MS respectively (Levin et al., 2003). The mechanisms linking MS with EBV infection are still not fully understood but B and T cells in MS lesions have been independently implicated. In one study the vast majority of MS brains contained infiltrating B cells infected with EBV while brains with other inflammatory diseases did not (Serafini et al., 2007). T cells from MS patients with MS-linked MHCII alleles recognise EBV and myelin basic protein (MBP) peptides suggesting molecular mimicry may lead to an autoimmune response against myelin (Lang et al., 2002). None of these factors can account for all cases of MS or the underlying mechanisms that facilitate disease. Especially lacking is evidence for the causes of progressive forms of MS, which mainly lack inflammatory components that most of the genetic and environmental risk factors are associated with.

1.1.2.1 Relapsing remitting multiple sclerosis

RRMS accounts for about 85% of MS cases diagnosed and mostly strikes people in their 20s with around 5% of cases occurring in children (Özakbaş, 2015). RRMS normally presents as clinically isolated syndrome (CIS) in which patients present with one or more neurological symptoms such as optic neuritis and numbness in the extremities. If patients with CIS also have lesions or white matter (WM) abnormalities detectable by MRI, they have a 60 - 80% chance of developing MS within 5 years vs 20% for CIS patients without detectable lesions (Fisniku et al., 2008). Patients that develop MS will typically experience relapses every 1.5 years but the frequency is highly variable and can be reduced with current treatments. 95% of MS patients have white matter lesions detectable by MRI and 90% have evidence of intrathecal antibody synthesis, detected as oligoclonal bands on gel electrophoresis of CSF (Polman et al., 2011).

Patients with RRMS develop spontaneous and erratic neurological symptoms accompanied by the appearance of inflammatory lesions in the corresponding brain or spinal cord region. Patients will then go through periods of remission where symptoms may partially or totally disappear, this is more common in early stages of disease and over the course of 20 - 30 years patients will accumulate a variety of disabilities and cognitive impairments.

Although the trigger of MS is unknown, pathogenesis is thought to begin with the entry of self-reactive T cells into the CNS. CD4⁺ T helper-17 (Th17) cells secrete IL-17 and -22, which activate endothelial cells of the blood-brain barrier (BBB) to upregulate integrin expression (Kebir et al., 2007, Tzartos et al., 2008). Circulating monocytes as well as CD8⁺ T cells, B cells, and plasma cells are recruited into the CNS via the activated BBB and inflammatory lesions begin to develop. Infiltrating immune cells become activated and in turn secrete a variety of inflammatory cytokines, which activate and recruit resident microglia into the lesion. B cells and plasma cells secrete antibodies that opsonise myelin and axons, and are detected as oligoclonal bands in CSF. Antibody deposition further opsonises myelin and facilitates damage via complement activation as serum proteins cross the damaged BBB (Lucchinetti et al., 2000). Monocytes and microglia secrete tumour necrosis factor α (TNF α) and nitric oxide (NO), which kills oligodendrocytes (OLs) and impairs mitochondrial function respectively (Nakazawa et al., 2006, Zajicek et

al., 1992, Lan et al., 2017). NO can kill neurons directly, as well as via mitochondrial impairment (Smith et al., 2001, Dutta et al., 2006). CD8⁺ T cells are the predominant T cell population in MS lesions but their role in disease is still controversial as different groups find they have pathological and beneficial functions depending on the experimental model used (Sinha et al., 2015). This combination of inflammatory pathological mechanisms results in extensive loss of mature OLs, degradation of myelin sheathes and damage to underlying axons (Bitsch et al., 2000).

Myelin debris is phagocytosed by infiltrating macrophages, which become laden with lipids and take on an anti-inflammatory phenotype; they are termed foamy macrophages due to their appearance in histology (Boven et al., 2006, Brück et al., 1995). At this stage remyelination may occur, as the brain's resident oligodendrocyte precursor cell (OPC) population migrate into lesions and mature (Chandran et al., 2008). The new OLs ensheath denuded axons and account for the appearance of so-called shadow plaques, partially remyelinated lesions observed in histology of MS brains. Remyelination is highly variable in the population with only 20% of RRMS patients exhibiting extensive remyelination, which was correlated with longer disease duration and life expectancy, suggesting that remyelination is protective in MS (Patrikios et al., 2006). Although remyelination has long been considered a therapeutic target, there are currently no approved treatments for RRMS that enhance or promote remyelination.

1.1.2.2 Progressive multiple sclerosis

Within 20 years of disease onset, most RRMS patients will transition into secondary progressive MS (SPMS) (Tutuncu et al., 2013). In around 10% of patients, disease is progressive from the onset, known as primary progressive MS (PPMS) (Tutuncu et al., 2013). Primary progressive MS (PPMS) shares many similarities with SPMS and some key distinctions, however from here they will be referred to together as progressive MS unless otherwise stated. Progressive MS is characterised by a steady worsening of symptoms without periods of recovery and the majority of disability associated with MS is acquired during progressive stages of disease (Nandoskar et al., 2017).

In SPMS, the change in clinical symptoms reflects the shift from inflammatory to neurodegenerative mechanisms that drive pathogenesis. This also renders the majority of RRMS treatments, which target the immune system, ineffective against progressive forms of MS. The trigger for progressive MS is unknown, however the strongest risk factor is age; onset of progressive MS occurs at 40 – 50 years old, regardless of whether the patient had RRMS or the age of the patient when disease first presented (Tutuncu et al., 2013).

New lesions can develop in progressive MS and relapses can occur but the main drivers of disease are lesion expansion and diffuse white matter pathology. Around 5% of patients present with progressive MS but also suffer relapses that may or may not recover (Trapp and Nave, 2008). Post-mortem progressive MS brains display two major types of lesion, chronic-active and chronic-inactive lesions (Prineas et al., 2001). Chronic active lesions consist of an inactive lesion core surrounded by a slowly expanding, active rim. The active rim resembles acute lesions in composition; activated macrophages and microglia are numerous and actively phagocytose myelin breakdown products (Lucchinetti et al., 2000). OL numbers are reduced and lymphocytes are present in the active rim, and penetrate beyond the rim into normal appearing white matter (NAWM). Grey matter (GM) lesions are uncommon in RRMS but become more frequent in progressive MS and are more strongly associated with disability progression than white matter pathology (Calabrese et al., 2012). The core of chronic-active lesions is hypocellular, containing mainly reactive astrocytes, a few scattered lymphocytes and myeloid cells and few if any OLs. Axonal pathology is more apparent in chronic-active lesions than acute lesions in which axons are mostly spared (Frischer et al., 2009). Some remyelination can occur in the chronic-active lesion rim and is sometimes observed throughout the lesion, however it is rarer in progressive MS than RRMS (Lassmann et al., 1997).

Chronic-inactive lesions, also known as burnt-out lesions have a sharply demarcated border between demyelinated areas and NAWM. These lesions are quiescent and lymphocytes and myeloid cells are sparsely distributed throughout the rim and core (Frischer et al., 2009). Chronic-inactive lesions are mainly composed of reactive astrocytes that form a fibrotic scar. OLs are very rare in chronic-inactive lesions and axon numbers are reduced by up to 80% (Wilson et

al., 2006, Frischer et al., 2009). These lesions do not undergo remyelination and inflammatory damage has for the most part ceased, hence the term 'burnt-out'.

Another hallmark of progressive MS is diffuse white matter injury. Activated microglia, reactive astrocytes, and scattered lymphocytes are found throughout the white matter and cortex in progressive MS patients (Allen et al., 2001). Quantitative real-time polymerase chain reaction (qPCR) studies found that a mixture of pro- and anti-inflammatory genes, such as *Il-10*, *Il-1 β* , *Stat4*, *Stat6*, and *Csf1* are upregulated in white matter in progressive MS (Zeis et al., 2008). These changes are believed to contribute to diffuse myelin injury, axonal death, and general atrophy associated with progressive MS (Ceccarelli et al., 2007, Kutzelnigg et al., 2005). Around 50% of SPMS and 30% PPMS patients have a variable degree of meningeal inflammation (Choi et al., 2012). This is characterised by infiltration of T cells, B cells and macrophages in the meninges. Meningeal inflammation correlates with greater cortical demyelination, subpial lesion load, loss of neurites, and microglia activation in the cortex. Patients with more severe meningeal inflammation have a shorter disease course with more rapid accumulation of disability and earlier death. Interestingly, B-cell follicular structures, containing T- and B-cells, are found in the meninges of over 40% of SMPS patients, but they are not seen in PPMS (Magliozzi et al., 2007). Meningeal B-cell follicles were associated with earlier onset of MS and more severe disease; they were also always adjacent to cortical lesions, suggesting they may contribute to lesion development through production of inflammatory cytokines and antibodies.

Besides low-grade inflammation, several neurodegenerative mechanisms have been implicated in the pathogenesis of progressive MS. The most obvious cause of neurodegeneration in SPMS is from repeated bouts of inflammatory demyelination and axonal injury that occurs in RRMS leaving irreparable damage in an aged CNS. Loss of OLs and myelin sheathes leaves axons without the trophic support they need to survive and so axonal loss occurs (Nave, 2010). Loss of myelin also leaves axons more vulnerable to direct damage and more susceptible to metabolic stressors. Demyelinated axons have a greater requirement for adenosine triphosphate (ATP) as Na⁺ ion channels, normally concentrated at the nodes or Ranvier, become spread out along the axon, making it harder to maintain the correct ion gradients for neurotransmission (Nave and

Trapp, 2008). This, combined with chronic mitochondrial dysfunction as a result of NO production by activated microglia and reactive astrocytes, contribute to axonal loss (Trapp and Stys, 2009). A further consequence of Na⁺ imbalance is increased Ca⁺⁺ levels, which can cause axon degeneration and contributes to deficits in ATP production (Trapp and Stys, 2009). In the aged brain, release of reactive iron species from dying OLs and microglia causes oxidative damage of surrounding cells and contributes to neurodegeneration (Lassmann et al., 2012). Most of the neurodegenerative mechanisms associated with progressive MS feed into each other and therefore perpetuate and amplify damage. By promoting remyelination, it is thought that axons will be protected from downstream degeneration.

1.2 The fibroblast growth factor signaling family

Research into the fibroblast growth factor (FGF) signaling has its roots in 1939 when it was discovered that brain extracts were particularly good inducers of proliferation in periosteal fibroblasts (Trowell and Willmer, 1939). Nearly half a century later a protein in bovine pituitary extracts was shown to be mitogenic for 3T3 mouse fibroblasts *in vitro* (Armelin, 1973), but, it was not until 1983 this factor was purified and named basic-FGF, now known as FGF2 (Lemmon and Bradshaw, 1983). Subsequently, several other FGFs were identified as oncogenes, endothelial cell growth factors, and tumour-promoting factors (Itoh, 2007). Genetic studies eventually led to the consolidation of these factors into one family based on their high sequence homology (Beenken and Mohammadi, 2009). The first fibroblast growth factor receptor (FGFR) was purified from chicken embryos using a tagged, truncated FGF2 protein (Lee et al., 1989). The peptide sequence of the purified chicken FGFR was used to generate a complementary deoxyribonucleic acid (DNA) clone that was found to have high sequence homology with human and mouse versions of the same gene, now known to encode for FGFR1 (Lee et al., 1989). Stimulation of these receptors with purified FGFs resulted in phosphorylation and subsequent tyrosine-kinase activity (Huang and Huang, 1986, Coughlin et al., 1988). Screening of a chicken embryo complementary DNA (cDNA) library led to the identification of additional FGFRs, which were then also identified in human, and mouse by homology-based cloning (Pasquale, 1990a, Keegan et al., 1991, Partanen et al., 1991).

Since their discovery, the secreted FGFs have been found in all organs and tissues in the developing embryo with more limited expression in the adult (Sekine et al., 1999, Xu et al., 1998, Fon Tacer et al., 2010). FGF signaling is now known to be involved in the induction and patterning of germ layers, organogenesis and morphogenesis, cell migration, differentiation, survival, and wound healing (Ornitz and Itoh, 2015). FGF signaling occurs in simple invertebrates such as *Caenorhabditis elegans*, *Drosophila*, as well as all vertebrate species, but is absent in unicellular organisms such as *Escherichia coli* (*E.coli*) (Itoh, 2007, Itoh and Ornitz, 2011). These findings support the hypothesis that FGF signaling developed through metazoan evolution to mediate body patterning of multicellular organisms (Itoh, 2007, Itoh and Ornitz, 2011).

Due to their prominent roles in development, mutations in genes involved in FGF signaling have been shown to cause a wide variety of developmental disorders that can impact every organ in the body (Itoh and Ornitz, 2011). Dysregulated FGF signaling is also a well-known facet of cancer development and is normally associated with a worse prognosis (Turner and Grose, 2010). During wound healing and tissue repair in the adult, FGFs are upregulated and mediate cell proliferation, differentiation and angiogenesis. Although roles for FGF signaling in developmental disorders and cancer are now well established, its involvement in the pathogenesis of inflammatory, autoimmune and acquired neurological diseases remains controversial. Its effects are likely to be context-dependent, as it is influenced by cross-talk with other signaling pathways associated with inflammation and tissue repair. Nonetheless, recent research identifies FGFs as promising therapeutic targets in cardiovascular disease, osteoarthritis, neurodegenerative disorders and neuropsychiatric conditions (Beenken and Mohammadi, 2009, Kiyota et al., 2011, Aurbach et al., 2015).

1.2.1 Fibroblast growth factor ligands

There are 22 FGFs expressed in humans, which are classified into two families, secreted and intracrine FGFs (iFGFs). The iFGFs do not signal through FGFRs and function mainly as co-factors for voltage gated sodium channels (Zhang et al., 2012). The secreted FGFs are grouped into five paracrine-acting subfamilies and one endocrine-acting subfamily based on their structural similarities and evolutionary history. The paracrine FGF subfamilies and their interactions with

FGFRs are summarized in Figure 1.1. The endocrine-FGF subfamily evolved only in vertebrates and is involved in the regulation of bile acid, energy, phosphate, and vitamin D metabolism, their dysfunction being associated with a variety of metabolic diseases (Itoh et al., 2015). Knock out (KO) studies of endocrine FGFs in mice demonstrate they are also required for the normal morphogenesis of some organs such as the heart and inner ear (Vincentz et al., 2005, Lysaght et al., 2014). As well as circulating throughout the body to affect distant cell populations, endocrine FGFs require a distinct protein co-factor known as the Klotho receptors in order to initiate signaling (Itoh et al., 2015).

The paracrine FGFs share a regular globular β -trefoil core composed of 12 β -strands whereas endocrine FGFs lack the β -11 strand and so have an atypical β -trefoil (Goetz and Mohammadi, 2013). Paracrine FGFs are first expressed in the inner cell mass during the earliest stage of embryonic development, before implantation into the endometrium (Yamanaka et al., 2010). Paracrine, also known as canonical, FGF signaling then facilitates organogenesis and morphogenesis throughout the embryo via the formation of tightly controlled ligand gradients (Pera et al., 2014, Xu et al., 2000) established by their interactions with heparan sulphate proteoglycans (HSPGs). HSPGs are co-factors for paracrine FGF-signaling found on the surface of all cells and in the extracellular matrix (Mohammadi et al., 2005).

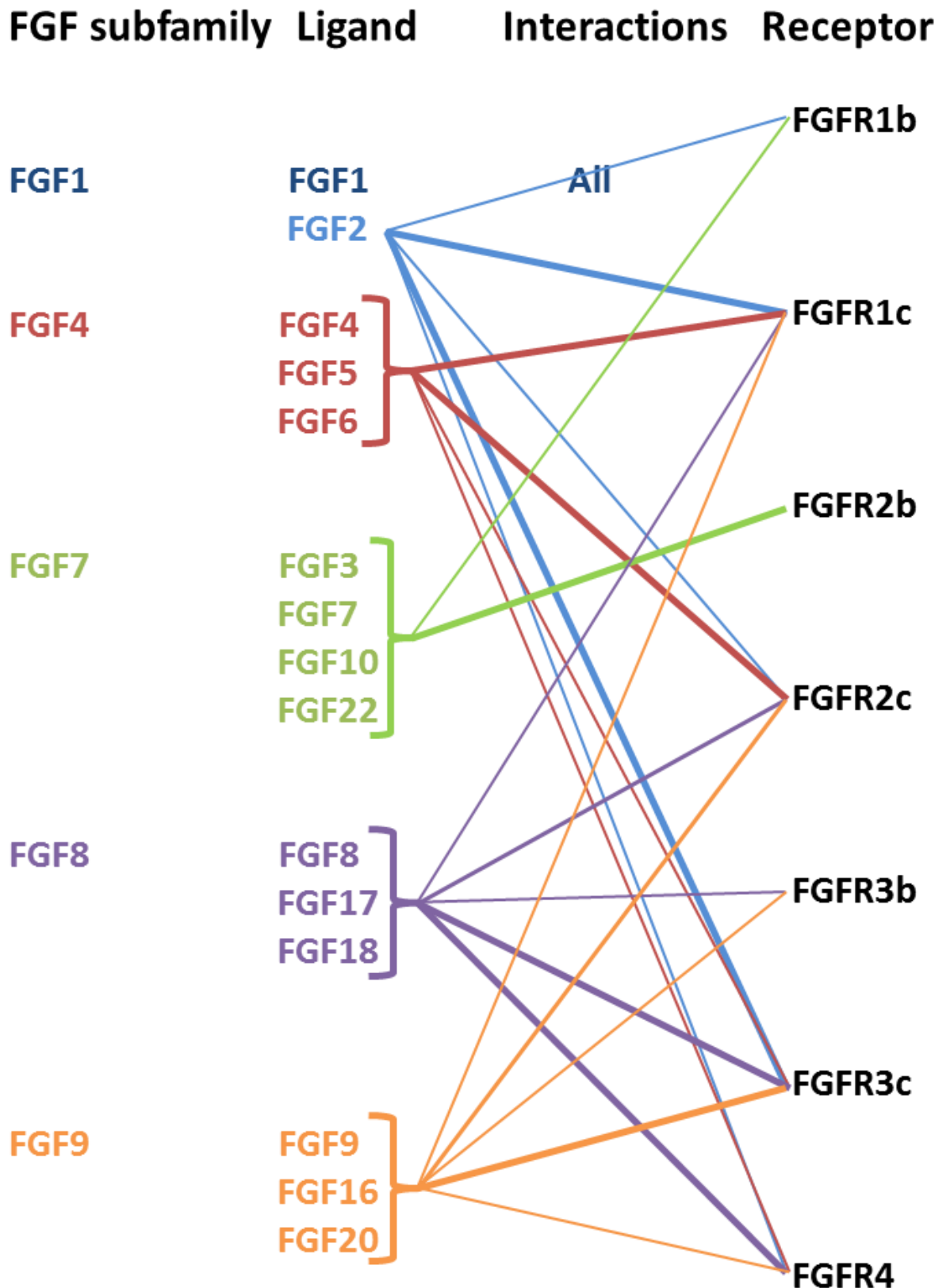


Figure 1.1 Ligand-receptor interactions of the canonical FGFs. Canonical FGFs are paracrine/autocrine signaling molecules and require heparan sulphates to activate FGFRs. Receptor preference is indicated by the weight of the lines linking ligands and receptors. Data is derived from experiments using Baf3 cells transfected with FGFR splice variants, and treated with FGFs, using mitogenic activity as a readout to determine binding specificity (Zhang et al., 2006).

1.2.2 Fibroblast growth factor receptors

FGFs function as ligands for cell surface receptor tyrosine kinases (RTKs) known as FGFRs. Humans express four distinct FGFR genes which are all highly related with over 50% identical amino acid sequence (Johnson and Williams, 1993, Pasquale, 1990b). FGFRs are single pass transmembrane receptors with three extracellular immunoglobulin-like domains termed D1 - D3 with functional linker domains between each, and an intracellular tyrosine kinase domain (Groth and Lardelli, 2002). FGFRs 1 - 3 can undergo two different alternative splicing events; the first occurs when the exons encoding the D1 and D1 - D2 linker domains are not transcribed so these domains are absent from the final, truncated receptor (Mohammadi et al., 2005, Yeh et al., 2003). Real-time binding studies demonstrate truncated FGFRs have the same or higher binding affinity for FGFs and HSPGs compared to their full-length isoforms and retain biological activity (Olsen et al., 2004, Mohammadi et al., 2005). Structural studies revealed the D1 and D1-D2 linker domains interact with the D2-D3 region to occlude the portion of the receptor involved in FGF and HSPG-binding (Olsen et al., 2004). In this way, the D1 and the D1-D2 linker serves as an auto-inhibitory mechanism that regulates ligand-binding specificity and promiscuity.

A second possible splicing event in FGFR expression involves the D3 domain; the exon encoding the N-terminal portion of D3 is termed IIIa and two alternative exons, termed IIIb and IIIc, encode the C-terminal portion (Schlessinger, 1991, Yeh et al., 2003). Expression of each alternative exon is tissue specific: epithelial tissues tend to express the IIIb isoforms of FGFRs (FGFR1b – FGFR3b) and mesenchymal tissues express the IIIc isoforms (FGFR1c – FGFR3c) (Orrurtreger et al., 1993). This alternative splicing event was shown to affect ligand binding affinity when Miki *et al* observed that FGF7 will exclusively bind to FGFR2b and not FGFR2c (Miki et al., 1991). Subsequently, Yeh *et al* showed FGF10, which is also highly specific for FGFR2b, induces a conformational change in D2 of the spliced receptor which contributes to ligand binding, suggesting alternative splicing in the D3 domain may enhance or diminish the interaction of ligand with other domains of the receptor, further increasing ligand-receptor specificity (Yeh et al., 2003). The crystal structures of FGF/ FGFR complexes reveal that interactions between the N-terminal region of FGF ligand and the alternatively spliced regions

of D3 (IIIb or IIIc) confer ligand specificity and mutations in these regions that results in aberrant ligand binding are responsible for some human skeletal disorders (Plotnikov et al., 2000). These discoveries effectively increased the number of FGFRs with distinct ligand binding capabilities from four to seven. Further examples of alternatively spliced receptors with different ligand-binding affinities led to the realization that mesenchymal FGFRs were specific for FGF ligands secreted by epithelial tissues and vice versa. This provided the basis for paracrine FGF signaling loops that regulate complex developmental processes; for example, branching and budding of lung epithelia is coupled to proliferation of lung mesenchymal cells via bi-directional FGF9 and FGF10 signaling (Colvin et al., 2001, Sekine et al., 1999). Normal organogenesis and tissue morphogenesis depend on the establishment of these paracrine-signaling loops; i.e. mesenchymal and epithelial tissues produce a variety of FGF ligands that could be promiscuous and bind to FGFRs on the cells that secreted them, which is prevented by the expression of alternatively spliced FGFRs on each type of tissue.

1.2.3 Fibroblast growth factor signaling pathways

FGFR activation involves two FGF ligands interacting with two receptor monomers at the cell surface, with each FGF interacting with both receptors at the same time (Mohammadi et al., 2005). Binding occurs at the D2-D3 domains of the FGFR and the formation of the ligand-receptor complex causes two FGFRs to dimerize (Ueno et al., 1992); this brings the intracellular tyrosine kinase domains into close contact and allows them to transphosphorylate each other (Mohammadi et al., 2005). FGFRs have six tyrosine residues that are sequentially phosphorylated in order to fully activate the tyrosine kinase domain. In this state, FGFRs can recruit CRKL, an adapter protein with several Src homology (SH2) and SH3 domains, required for the recruitment of signaling proteins to the plasma membrane (Pawson et al., 1993, Seo et al., 2009). Activated FGFR and CRKL phosphorylate and activate FGFR substrate 2 α (FRS2 α), an adapter protein that is constitutively bound to FGFR monomers at the plasma membrane (Wang et al., 1996, Ong et al., 2000). Despite its name, FRS2 α has been shown to play a role as an adaptor molecule for other growth factors such as epidermal growth factor (EGF), platelet-derived growth factor (PDGF), vascular endothelial growth factor (VEGF), nerve growth factor, and neurotrophic factors (Lax et al., 2002, Kouhara et al., 1997, Xu and

Goldfarb, 2001, Chen et al., 2014). Phosphorylated FRS2 α contains multiple binding sites for SH2 domains of other signaling proteins, and so acts as a docking protein on which multiprotein signaling complexes can be formed (Ong et al., 2000). Activated FRS2 α recruits and activates proteins required for initiation of the mitogen-activated protein kinase (MAPK) and phosphoinositide 3-kinase/protein kinase B (PI3K-AKT) signaling cascades (Kouhara et al., 1997). FGFRs possess two additional tyrosine residues which, when phosphorylated, activate two other signaling pathways. Signal transducer and activator of transcription (STAT) signaling is initiated when tyrosine 677 is phosphorylated and phospholipase C γ 1 (PLC γ 1) is bound to the receptor by phosphorylated tyrosine 766 (Dudka et al., 2010, Mohammadi et al., 1992). Which pathways will be activated by FGF signaling is dependent on a number of variables: the specific FGF ligand and receptor involved, the availability of ligand and receptor at the cell membrane, and the influence of downstream regulators and cross-regulation between each signaling pathway (Ornitz and Itoh, 2015). A schematic diagram of the three FGF-signaling pathways and the signaling cascades involved is shown in Figure 1.2.

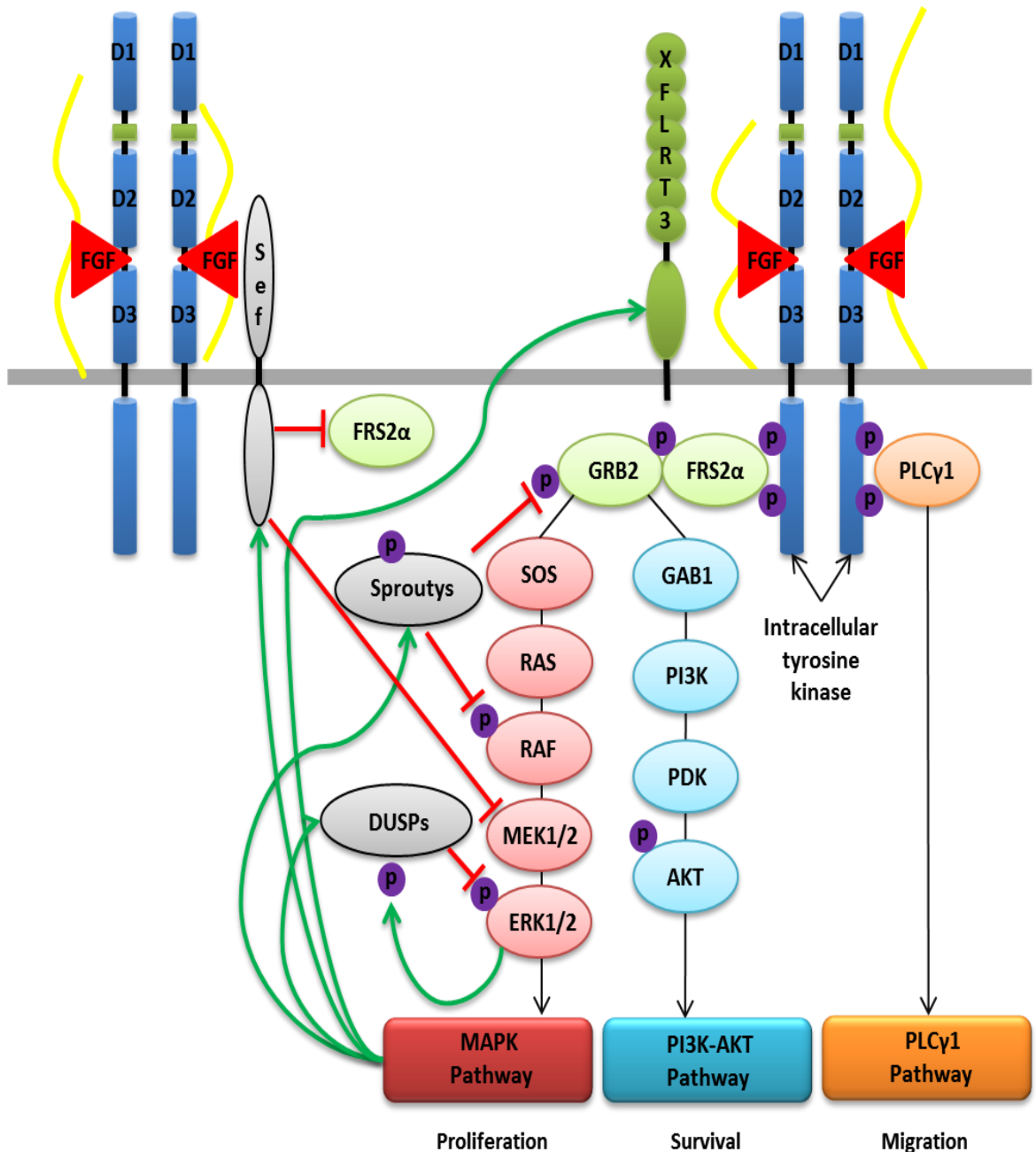


Figure 1.2 Simplified FGF Signaling Schematic. Red arrows denote inhibition, green arrows denote promotion of expression. Heparan sulphates are represented in yellow, phosphate groups are purple. Heparan sulphate and bound FGF interact with D2 and D3 domains of two FGFRs, which leads to transphosphorylation of intracellular tyrosine kinase domains. Activated RTKs phosphorylate FRS2 α , GRB2, and PLC γ 1. Activation of each signaling cascade leads to transcription of distinct sets of genes. Several inhibitory mechanisms (shown in grey) regulate FGF signaling; Sef interacts with FGFRs directly to prevent FRS2 α phosphorylation. Sproutys are activated by MAPK signaling which they regulate by interacting with GRB2 at the membrane or with RAF. DUSPs form part of the negative feedback loop of MAPK signaling as they are phosphorylated and activated by MAPK proteins. Sproutys, DUSPs, Sef, XFLRT3, and various other FGF signaling regulators are induced at the transcriptional level by MAPK signaling.

1.2.3.1 MAPK signaling

When activated, FRS2 α recruits and activates the adapter protein growth factor receptor-bound 2 (GRB2), which in turn recruits either GRB2-associated binding protein 1 (GAB1) or the guanine nucleotide exchange factor son of sevenless (SOS) (Kouhara et al., 1997, Ong et al., 2000). Activated SOS in turn activates membrane-bound Ras, which initiates the mitogen-activated protein kinase (MAPK) signaling cascade (Kato and Kato, 2006). FGF signaling can lead to activation of ERK1/2, JNK and p38 MAP kinases (Tsang and Dawid, 2004, House et al., 2005). MAPK signaling leads to the phosphorylation and activation of the ETS (E26 transformation-specific) family of transcription factors (TFs). ETS TFs can then enter the nucleus and induce the expression of genes involved in cell proliferation, growth, and survival (McCubrey et al., 2000). MAPK is the pathway most commonly activated by FGF signaling.

1.2.3.2 PI3K-AKT pathway

If GRB2 binds to GAB1 instead of SOS, PI3K is recruited and activated, which leads to downstream phosphorylation of AKT (Lamothe et al., 2004). AKT inhibits a number of apoptotic signaling pathways; for example, AKT phosphorylates caspase 9, which inhibits activation of caspase 3 (Fujita et al., 1999). AKT also phosphorylates the forkhead box class O transcription factors, which prevents them from transcribing death-receptor ligands and Bcl2 family members by forcing them to exit the nucleus (Fu and Tindall, 2008, Zhang et al., 2011). Another protein phosphorylated and inactivated by AKT is tuberous sclerosis complex 2 (TSC2), a tumour suppressor gene that regulates cell growth and size (Manning and Cantley, 2007). Phosphorylation of TSC2 by AKT causes it to lose its GTPase activating protein activity which constitutively inhibits mammalian target of rapamycin complex 1 (mTORC1) (Durán and Hall, 2012). mTORC1 is a protein complex that determines whether the intracellular environment (amino acid, oxygen, and growth factor concentrations, etc.) is favourable towards growth, and if so, activates protein synthesis which leads to cell growth and proliferation (Manning and Cantley, 2007, Rafalski and Brunet, 2011). Carballada et al. showed PI3K-AKT signaling is required for mesoderm induction in xenopus embryos, and acts in parallel with MAPK signaling to do so (Carballada et al., 2001). FGF signaling is often observed to activate the MAPK and PI3K-AKT signaling

pathways in parallel to enhance cell growth and proliferation while preventing apoptosis.

1.2.3.3 PLC γ signaling

The phospholipase C- γ (PLC γ) signaling pathway is initiated when PLC γ is recruited directly to phosphorylated FGFR (Mohammadi et al., 1992). Active PLC γ hydrolyzes phosphatidylinositol-4,5-diphosphate to inositol 1,4,5-triphosphate (IP3) and diacylglycerol (DAG). DAG activates protein kinase C which then phosphorylates and activates regulators of cell motility, such as the actin filament reorganisation protein, myristoylated alanine-rich C kinase substrate (Hartwig et al., 1992). IP3 functions by inducing the release of calcium ions from intracellular stores which activates calcineurin, that in turn, dephosphorylates and activates the transcription factor nuclear factor of activated T cells (NFAT) (Hogan et al., 2003). NFAT is then able to enter the nucleus and initiate the transcription of genes involved in cell motility and migration (Li et al., 2011). The PLC γ pathway was shown to regulate motility and migration downstream of FGF signaling when PLC γ binding site on FGFRs were blocked in neurons and neurite outgrowth was inhibited (Hall et al., 1996).

1.2.3.4 STAT signaling

SH2 domain-containing STAT1, 3, and 5 are recruited to the plasma membrane and phosphorylated by the FGFR tyrosine kinase (Ornitz and Itoh, 2015, Hart et al., 2000). Phosphorylated STATs combine to form hetero- or homodimers which translocate to the nucleus and induce gene transcription (Hebenstreit et al., 2005). STATs are typically regarded as downstream mediators of interferon and immune mediated signaling, however they are also known to induce genes associated with cell proliferation, differentiation, migration, and apoptosis (Kuzet and Gaggioli, 2016, Au-Yeung et al., 2013). The roles of STATs in FGF signaling are still controversial as it has been difficult to delineate the effects of STAT activation from other pathways induced by FGFRs as several pathways are usually activated in concert.

1.2.3.5 FGFs in the nucleus

FGFs and FGFRs have been visualised in the nuclei of some cell types where they regulate gene expression (Planque, 2006). Endocytosis and degradation of ligands and receptors is a common regulatory mechanism in cell signaling, however some FGFs have been shown to persist inside the cell for over 24 hours (Wiedłocha and Sørensen, 2004). FGFR1 and FGFs 1, 2, and 3 have been visualised in the nuclei of a variety of cell types but no other FGF ligands or receptors, suggesting these abilities are not shared between all FGF family members (Planque, 2006). Several high and low molecular weight (MW) isoforms of FGF1 and FGF2 can be expressed depending on where translation is initiated on the genes (Iberg et al., 1989). High MW isoforms are not secreted and can enter the nucleus directly from the cytoplasm of the cell in which they have been translated. Low MW isoforms bind to FGFR1 at the cell surface and translocate to the nucleus via importin β , under the control of PI3K signaling and the chaperone protein, heat shock protein-90 (Reilly and Maher, 2001, Małeckci et al., 2004, Wesche et al., 2006). The nuclear isoform of FGF3 contains three polycationic sequences, lacked by the secreted isoform, that mediate entry into the nucleus (Antoine et al., 1997). In the nucleus, FGFR1 binds to CREB-binding protein and ribosomal S6 kinase 1 (RSK1) which recruit RNA (ribonucleic acid) polymerases, modify histones and induce gene transcription (Stachowiak et al., 2003, Fang et al., 2005, Hu et al., 2004). Cyclin D1, c-jun, neuron specific enolase, and microtubule associated protein-2 genes are all upregulated by nuclear FGFR1 and are essential for neuronal differentiation (Stachowiak et al., 2003, Reilly and Maher, 2001). The mechanisms by which nuclear FGF1, 2, and 3 regulate gene expression are less well understood although there is some evidence they interact with TFs and RSK2 (Soulet et al., 2005, Sheng et al., 2005). High levels of nuclear FGFs are features of some cancers, and are associated with a poor prognosis (Joy et al., 1997, Fukui et al., 2003). Overexpression of high MW FGF2 is sufficient to transform cultured primary cells and stimulate their proliferation (Couderc et al., 1991). Interestingly, nuclear and secreted FGF3 have been found to have opposing effects on cell proliferation (Antoine et al., 1997). Results from cancer studies show that nuclear FGFs enhance the expression of genes associated with cell survival and proliferation which contributes to tumour progression (Planque, 2006).

1.2.4 Regulation of FGF signaling

1.2.4.1 Heparan sulphates

(Moscatelli, 1987) discovered that cells express high and low affinity receptors for FGFs. The high affinity receptors are FGFRs and low affinity receptors are heparan sulphates. Heparan sulphates are linear glycan polymers that are expressed in all tissues, in the extracellular matrix (ECM) and on the surface of cells where they modulate cell surface receptor-ligand interactions (Bernfield et al., 1999). Heparan sulphates are bound to cell membranes via core proteins such as transmembrane proteins as in the syndecans or through glycosylphosphatidylinositol-anchored core proteins as in the glypicans (Fransson et al., 2004, Tkachenko et al., 2005); these proteins and the bound heparan sulphates comprise the heparan sulphate proteoglycan.

Heparan sulphate had previously been reported to enhance FGF signaling in epithelial cells (Thornton et al., 1983) and (Yayon et al., 1991) showed heparan sulphate was absolutely required for FGF signaling through the use of mutant heparan sulphate-deficient cells. Heparan sulphate is required for the formation of a stable 2:2 symmetric dimer between FGFs and FGFRs. Stable dimer formation allows each FGF to interact with both receptors and the receptors to interact with each other via the D3 domains (Schlessinger et al., 2000).

Heparan sulphates are composed of repeating disaccharides of N-substituted glucosamine and glucuronic acid (Bernfield et al., 1999, Sasisekharan and Venkataraman, 2000). The glucosamine in heparan sulphate can be either N-acetylated or N-sulphated. N-acetylated glucosamine does not undergo modification whereas N-sulphated glucosamine can undergo a variety of modifications, such as 2-O-, 3-O-, and 6-O- sulphation, and C5-epimerization (Perrimon and Bernfield, 2000). These modified sites interact with FGFs and the D2 domains of FGFRs via hydrogen bonds (Schlessinger et al., 2000, Gallagher, 2001). The golgi enzymes, N-deacetylase, uronosyl C5-epimerase, and the N-sulphotransferases, modify heparan sulphate in a tissue specific manner to generate heparan sulphates with unique fine structures (Habuchi et al., 1998, Rosenberg et al., 1997).

Heparan sulphates have a distinct pattern of expression during embryogenesis and development, which affect FGF-FGFR interactions (Allen and Rapraeger, 2003). The fine structure determines heparan sulphates affinity for FGFs, which regulates how far FGFs can diffuse from their site of secretion. In this way, heparan sulphates mediate and maintain complex FGF signaling-gradients, which are vital for normal morphogenesis during development. The requirement for these three components: heparan sulphate, FGF ligand, and FGFR, to be compatible, allows for multiple ligands and receptors to be expressed in the same vicinity without the danger of promiscuous signaling. This tertiary layer of regulation by heparan sulphates also allows for more intricate and complex signaling without the need for additional ligands or receptors.

1.2.4.2 Sproutys

A number of positive and negative regulators of FGF signaling have been discovered in xenopus, zebrafish, and drosophila (Tsang and Dawid, 2004). The first to be identified were the Sproutys (Hacohen et al., 1998), antagonists of RTK signaling (Frank et al., 2009). There are four Sprouty isoforms, all of which are highly conserved in vertebrates and all of which inhibit MAPK signaling downstream of FGFR but upstream of ERK, the major protein phosphorylating component of the MAPK pathway. PLC γ signaling can also induce Sprouty expression, and is in turn regulated by Sproutys (Akbulut et al., 2010, Abe and Naski, 2004). Gain- and loss-of-function experiments in mice and chicks show FGF signaling induces Sprouty gene expression through MAPK (Minowada et al., 1999, Chambers and Mason, 2000). Sproutys have a conserved tyrosine phosphorylation site and cysteine-rich domain which allows them to translocate to the plasma membrane when activated by MAPK signaling (Lim et al., 2002). Sproutys function by inhibiting MAPK signaling at two points in the pathway: Sprouty can bind to Grb2 at the membrane to prevent it from binding SOS which prevents Ras activation, and Sprouty can also interact downstream with Raf to attenuate signaling (Hanafusa et al., 2002, Sasaki et al., 2003).

1.2.4.3 DUSPs

The mammalian genome encodes over 60 members of the dual-specificity phosphatase (DUSP) family, all of which have an intrinsic ability to dephosphorylate tyrosine or serine/threonine kinases (Alonso et al., 2004, Owens and Keyse, 2007). Eleven members of the DUSP family comprise the MAPK phosphatase subfamily, which regulate components of the MAPK pathway in different cellular compartments. Throughout this thesis, only the MAPK phosphatase DUSPs are discussed and they are simply referred to as DUSPs. DUSP1 dephosphorylates p38 in the nucleus, while DUSP6 dephosphorylates ERK in the cytosol (Patterson et al., 2009). DUSPs are phosphorylated and activated by MAPK signaling and are therefore feedback inhibitors of MAPK (Brondello et al., 1999). DUSPs 1, 5, and 6, are early response genes to FGF signaling (Branney et al., 2009). DUSP6 expression is only induced in response to FGFR1 or FGFR2 signalling and strongly correlates with the pattern of active FGF signaling during embryonic development (Urness et al., 2008, Li et al., 2007).

1.2.4.4 Extracellular FGF signaling regulators

Several proteins act in the ECM or at the plasma membrane to positively or negatively regulate FGF signaling. FGF-binding protein 1 (FGFBP1) is a secreted protein that can bind to heparan sulphate and FGF1, 2, 7, 10, and 22 (Wu et al., 1991). FGFBP1 was originally identified as an inhibitor of FGF signaling, but has since been shown to enhance ligand-receptor interactions and promote angiogenesis and wound healing (Rosenberg et al., 1997, Tassi et al., 2011). XFLRT3 is a member of a leucine-rich-repeat transmembrane protein family that interacts with FGFRs to propagate MAPK signaling (Böttcher et al., 2004). XFLRT3 expression is induced by FGF signaling and inhibited by MAPK signaling regulators. Sef (similar expression to FGF) is another transmembrane protein that interacts with the FGFR, but Sef inhibits signaling by blocking phosphorylation of FRS2 α (Tsang et al., 2002). Sef-b is a splice-isoform of Sef which lacks the transmembrane portion of the protein and inhibits MAPK signaling in the cytosol. It accomplishes this by binding to and preventing ERK1/2 from dissociating from the MEK complex and entering the nucleus (Preger et al., 2004). FGFR1 (fibroblast growth factor receptor like 1) is a transmembrane protein structurally similar to other FGFRs but lacking intracellular tyrosine kinase activity (Trueb et al., 2003).

FGFRL1 acts as a decoy receptor and can be shed from the membrane to bind FGFs in the ECM (Steinberg et al., 2010). Interestingly, the intracellular domain of FGFRL1 contains an SH2 binding motif that can bind SHP-1 and induce MAPK signaling without ligation. This suggests that FGFRL1 can also function as a non-tyrosine kinase signaling receptor (Silva et al., 2013).

1.3 Fibroblast growth factors in the central nervous system

1.3.1 FGF1, 2, and 9 in CNS development

FGF1 expression begins late in mouse CNS development on embryonic day 11 (E11) and does not peak until adulthood (Elde et al., 1991, Alam et al., 1996, Ford-Perriss et al., 2001). *In vitro* experiments have shown that downregulating FGF1 expression in cultured retinal cells was detrimental to neuronal differentiation and survival (Désiré et al., 1998). Treating PC12 cells with FGF1 activated MAPK and STAT3 signaling which led to enhanced neurite outgrowth, suggesting FGF1 may be involved in neuronal differentiation and maintenance *in vivo* (Lin et al., 2009).

FGF2 stimulates proliferation of neural crest cells, which go on to make up most of the peripheral nervous system in the embryo (Murphy et al., 1994). FGF2 is the most abundantly expressed FGF in the CNS during development and in the adult (Woodbury and Ikezu, 2014). Like FGF1, FGF2 is produced by neurons but the majority is derived from astrocytes during development and adulthood (Woodbury and Ikezu, 2014). In early stages of CNS development FGF2 is a proliferative and survival factor for neuroepithelial cells (Arakawa et al., 1990, Murphy et al., 1990). Several studies have also shown that FGF2 stimulates differentiation of neuroepithelial cells into neurons and astrocytes (Murphy et al., 1990, Baron et al., 2012, Dono et al., 1998, Qian et al., 1997). FGF2 also induces expansion of dopaminergic and GABAergic neuronal precursor cells while delaying their differentiation (Bouvier and Mytilineou, 1995, Deloulme et al., 1991). FGF2 further affects neuronal development by enhancing axonal branching and neurite outgrowth (Kalil et al., 2000, Morrison et al., 1986). FGF2 promotes the proliferation of oligodendrocyte precursor cells (OPCs) and increases their expression of platelet-derived growth factor receptor (PDGFR), which binds PDGF α , the most important mitogen and survival factor for early OPCs (Mckinnon

et al., 1990). FGF2 is a chemoattractant for OPCs, and transgenic OPCs expressing a truncated FGFR1 failed to migrate after transplantation into neonatal rat brain (Osterhout et al., 1997, Mckinnon et al., 1993). A schematic diagram of OL lineage development and interactions with FGFs at each stage can be seen in Figure 1.3.

FGF9 is expressed at high levels early in murine CNS development (E10 - 14) and is mainly localized to developing motor neurons in the spinal cord, for which it is an important survival factor (Nakamura et al., 1999, Nakamura et al., 1997, Kanda et al., 1999, Garcès et al., 2000). *In vitro* studies have also shed some light on the roles of FGF9 in glial cell development; FGF9 promoted the proliferation and survival of neural progenitor cells while inhibiting their differentiation into neurons and glia (Lum et al., 2009). Differentiation to all cell types was reduced following FGF9 treatment but astrocyte differentiation was markedly reduced; these results suggest FGF9 may be involved in maintenance of the progenitor cell populations. The effect on astrocyte differentiation is particularly interesting as FGF9 promotes proliferation in already differentiated astrocytes (Naruo et al., 1993) demonstrating how FGF signaling can have different effects at different stages of lineage progression.

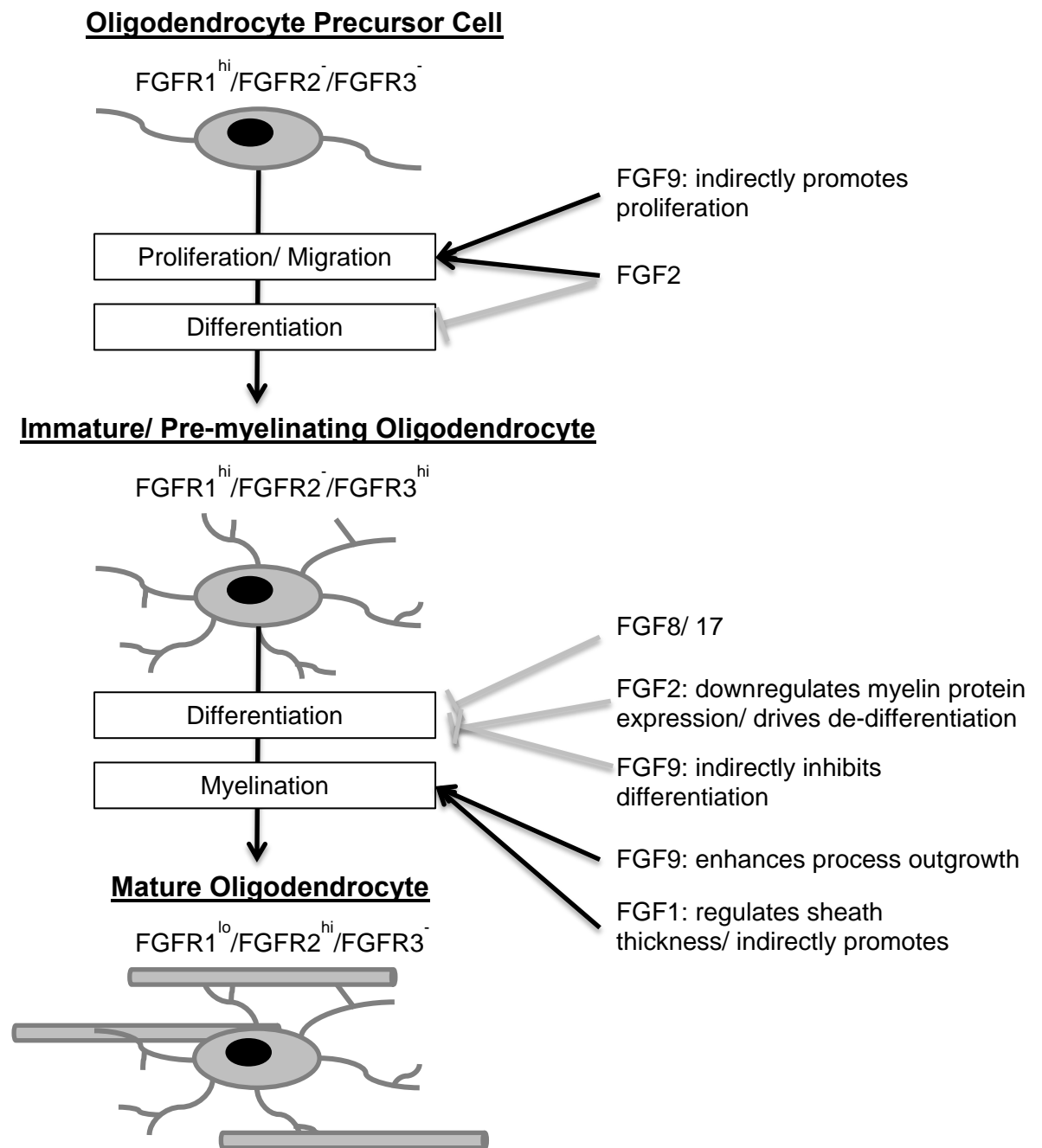


Figure 1.3 Schematic diagram of FGF signaling events throughout oligodendrocyte differentiation. Grey arrows denote inhibition; black arrows denote promotion. OLs proceed through three major developmental stages from migratory and proliferative precursor cells to mature, myelinating oligodendrocytes. These stages are accompanied by changes in FGFR expression and interactions with members of the FGF signaling pathway.

1.3.2 Roles of FGFs in the adult CNS

1.3.2.1 FGF and FGFR expression in the adult CNS

After development, the FGFs involved in regionalisation and patterning of the CNS are down regulated. In the healthy adult CNS only FGF1, 2, and 9 are known to be constitutively expressed and their functions in homeostasis are still not fully elucidated. FGF1 is produced by neurons in the adult, and unlike other FGFs, FGF1 expression increases throughout development and peaks in adulthood (Elde et al., 1991, Alam et al., 1996). FGF2 is also produced by neurons in the adult CNS but the majority is astrocyte-derived and it is expressed mainly in sites of neurogenesis (Woodward et al., 1992). FGF2 is a known mitogen for neuroprogenitor cells (which express FGFR1) in the subventricular zone (SVZ) and subgranular zone (Ohkubo et al., 2004, Woodward et al., 1992, Werner et al., 2011). Like in development, FGF9 is mainly produced by neurons, particularly motor neurons and is expressed at higher levels in the spinal cord and brain stem (Kanda et al., 1999). FGF9 is also produced by white matter astrocytes in the spinal cord and by CNPase-positive OLs in the white matter of the cerebellum and corpus callosum (Nakamura et al., 1999).

The major CNS cell types, neurons, astroglia, OLs and microglia have different FGFR expression profiles. Neurons, the first cell type to differentiate in the developing CNS, express FGFR1 while exclusively retinal neurons also express FGFR4 (Fuhrmann et al., 1999). Astrocytes are the most abundant cell type in the CNS and constitutively express FGFRs 1, 2, and 3 (Miyake et al., 1996, Choubey et al., 2017). Oligodendrocyte lineage cells are responsible for ensheathing axons in insulating myelin and express variable levels of FGFRs depending on their stage of maturation (Fortin et al., 2005). OPCs only express FGFR1 but as OPCs differentiate, they transiently express FGFR3, which is lost by the time the cells have fully matured, and begun producing myelin. Mature OLs express FGFR2 specifically on the myelin sheath; FGFR1 is still expressed but at a reduced level compared to OPCs. OLs and astrocytes express the IIIc isoform of each FGFR (Miyake et al., 1996). While different CNS cell types express different combinations of FGFRs, RNA sequencing data has shown that by far, astrocytes have the highest level of expression of FGFRs compared to neurons, OLs, and

microglia, suggesting that they will be the main target of FGF signaling in the CNS (Zhang et al., 2014).

Since concomitant expression of several FGFs occurs during development and in the adult CNS, altering FGFR expression as OLs mature allows them to temporally regulate FGF signaling. Fortin *et al* demonstrated that signaling through FGFR3 by FGFs 8 and 17 inhibits OPC maturation, while FGF2 stimulated OPC proliferation via FGFR1 (Fortin et al., 2005). FGF9 appeared to have no effect on OPCs but enhanced process elongation in mature OLs via FGFR2 (Furusho et al., 2012). Several studies have shown that FGF2 stimulates OPC proliferation while inhibiting their maturation and subsequent myelination. FGF2 has also been shown to have detrimental effects on mature OLs in which it induces downregulation of expression of myelin-associated genes and re-entry into the cell cycle (Bansal and Pfeiffer, 1997, Zhou et al., 2006). Most of the studies that have shown FGF2 to be an inhibitor of myelination have done so using pure OL cultures. A study by Mayer *et al* found that the inhibition of OL differentiation by FGF2 was overcome in the presence of astrocytes (Mayer et al., 1993). These findings demonstrate that the outcome of FGF signaling is often context dependant and cells will react to FGFs differently depending on their stage of maturation.

1.3.2.2. FGFs in adult CNS homeostasis

FGF1-null mice appear phenotypically normal; They have no deficiencies in embryonic development, adulthood, old age, or reproduction (Miller et al., 2000). This suggests absence of FGF1 can be functionally compensated for by other FGFs or growth factors. However, FGF1 has been shown to regulate some neuron and OL functions. Treating rat hippocampal slices with FGF1 reduced the basal amplitude of spikes and facilitated generation of long-term potentiation (Sasaki et al., 1994). Subcutaneous injections of FGF1 improved learning and long-term memory in senescence-accelerated mice and preserved medial septum cholinergic neurons (Sasaki et al., 1999). These findings suggest FGF1 contributes to learning and memory formation. FGF1 signaling through FGFR1 and FGFR2 has also been shown to regulate the thickness of myelin sheathes produced by OLs. OLs lacking FGFR1 and FGFR2 genes had had reduced

expression of myelin genes and thinner myelin sheathes, which was associated with reduced MAPK signaling (Furusho et al., 2012).

FGF2 serves some of the same functions in the adult CNS as it does in the embryonic CNS and is a proliferative and survival factor at sites of neurogenesis. FGF2 is produced by neurons and astrocytes throughout the CNS but it is expressed at highest levels in the hippocampus, striatum, SVZ, and subgranular zone, all areas with populations of neuroprogenitor cells (Ohkubo et al., 2004, Woodbury and Ikezu, 2014). Subcutaneous injection of FGF2 in mice stimulated proliferation in these sites (Wagner et al., 1999). Cultured hippocampal cells treated with FGF2 proliferate and express genes associated with neuronal and glial cell differentiation (Gage et al., 1995). Neurons derived from these precursors go on to exclusively populate the granule cell layer. Neuroprogenitor cells from the striatum can also differentiate into neurons, astrocytes, and OLs when treated with FGF2. The concentration of available FGF2 determined this cell fate decision with lower concentrations favouring neuronal differentiation and higher levels favouring glial cell development (Dono et al., 1998, Qian et al., 1997, Gritti et al., 1996).

FGF2 regulates neuronal morphology and is the most potent enhancer of axon branching currently known. *In vitro* cortical neurons treated with FGF2 have larger growth cones and three times more axon branching than untreated neurons (Patel and Mcnamara, 1995, Kalil et al., 2000). This is thought to increase the complexity of axonal trees in development and regulate axonal remodelling in the adult CNS (Ramirez et al., 1999). FGF2 is also involved in neuronal signaling and, like FGF1, lowers the threshold required to induce long-term potentiation (Ishiyama et al., 1991). *In vitro* experiments and injury models have shown that FGF2 has a variety of effects on glial cells but its roles in homeostasis are still unclear.

The functions of FGF9 in the healthy adult CNS are unclear. Its expression is mostly detected in the brainstem and spinal cord where it is thought to provide tonic signaling to spinal cord motor neurons (Kanda et al., 1999). Like FGF2, FGF9 is a mitogen and survival factor for neuroprogenitor cells, but is less potent and inhibits their differentiation into neurons and glia (Lum et al., 2009).

1.4 Fibroblast growth factors in multiple sclerosis

1.4.1 Localisation of FGFs in MS lesions

In situ hybridisation and immunohistological studies of tissue biopsies and post-mortem MS brains have identified three FGFs that are upregulated in and around lesions: FGF1, 2, and 9. In healthy control brains FGF1 staining was observed in subsets of cortical neurons and OL lineage cells throughout the white matter (Eckenstein, 1994, Mohan et al., 2014). In MS lesions of the grey matter, neuronal FGF1 expression was comparable to controls. FGF1 staining was also observed in OLs in the NAWM surrounding MS lesions, particularly lesions that have undergone remyelination. Hypertrophic astrocytes in remyelinated lesions tended to be FGF1-positive whereas astrocytes in demyelinated areas and NAWM were mostly FGF1-negative. In active and chronic active lesions a subset of IBA1⁺ microglia/macrophages expressed FGF1. Double staining for lymphocyte markers in lesions with high numbers of perivascular infiltrates showed that both T and B cells express FGF1 (Mohan et al., 2014). In all cases where FGF1 staining was observed, only subsets of each cell type displayed FGF1 expression, suggesting it is a feature of different subsets of cells.

FGF2 concentrations in CSF from MS patients peaks during a relapse suggesting it is involved in the pathogenesis of the disease (Sarchielli et al., 2008). FGF2 is detected at higher levels in the serum and CSF of MS patients than healthy controls. FGF2 levels were highest during relapses in RRMS and correlated with higher lesion loads in SPMS (Sarchielli et al., 2008, Harirchian et al., 2012). In MS lesions, FGF2 expression has been observed in damaged neurons, astrocytes, macrophages, and microglia, with the highest levels in active lesions and the penumbra of chronic lesions (Mizuno, 2014, Albrecht et al., 2002, Albrecht et al., 2003, Clemente et al., 2011). Perivascular astrocytes located near lesions were FGF2-positive suggesting that it is involved in breakdown of the BBB. Astrocytes are the main source of FGF2 in the healthy CNS and the same appears to be true in MS, however it is only upregulated in actively demyelinating lesions and does not appear to be present in chronic inactive lesions with little inflammation (Clemente et al., 2011).

In healthy control brains, FGF9 staining is observed in neurons and infrequently in astrocytes and OLs in white matter (Todo et al., 1998). FGF9 staining appears as diffuse background immunoreactivity thought to be due to FGF9 in axons and dendrites of neurons, and bound to cells and components of the ECM. In MS brains, there is generally higher intensity of diffuse FGF9 immunoreactivity in the NAWM. Higher levels of FGF9 expression were seen in active lesions and chronic active lesion rims compared to inactive lesions and inactive cores of chronic lesions (Lindner et al., 2015). However, unlike FGF2, FGF9 staining was present in chronic lesions, albeit to a lesser extent than observed in actively demyelinating lesions. FGF9 staining colocalized with markers for OLs, OPCs, and astrocytes in active lesions and NAWM. Like FGF1, only subsets of each cell type were found to be FGF9-positive: around 50% of astrocytes in active lesions and the surrounding periplaque stained for FGF9 and occasional NogoA⁺ OL lineage cells at the rim of actively demyelinating lesions were FGF9-positive (Lindner et al., 2015).

1.4.2 Roles of FGFs in MS pathogenesis

1.4.2.1 FGF1

qPCR analysis found that FGF1 was the most highly expressed myelination-regulatory factor in remyelinated MS lesions (Han et al., 2008, Mohan et al., 2014). Levels of FGF1 expression in demyelinated areas were lower than in control brain white matter. Treating dissociated spinal cord cultures and cerebellar slice cultures with FGF1 accelerated myelination and remyelination respectively, however treating isolated OLs inhibited their differentiation. This suggests promotion of myelination by FGF1 was an indirect effect and transcriptional profiling revealed that FGF1-treated astrocytes increased expression of CXCL8 and LIF (Leukaemia inhibitory factor). Both of these factors are known to enhance OPC recruitment and myelination respectively. Lesions in a cuprizone-demyelination model displayed reduced levels of FGF1 expression (Berghoff et al., 2017). When these mice were treated with dietary cholesterol, levels of FGF1 increased in astrocytes, and *in vitro*, FGF1 was shown to enhance OPC differentiation.

In a rat spinal cord injury (SCI) model, injection of FGF1 into the injury site resulted in significantly greater functional recovery 28 days after injury (Tsai et al., 2008). Proteomic analysis showed proteins associated with axonal survival and

regeneration were upregulated in FGF1-treated rats while proteins involved in astrocyte activation, scar formation and inflammation were reduced. Together, these data suggest that FGF1 is beneficial in demyelinating disease and is likely involved in the remyelination observed early in MS. Several studies have shown that FGF1 is a neuronal survival factor and transgenic overexpression of FGF1 protects neurons from apoptosis in ischemia and stroke models (Russell et al., 2006, Ghazavi et al., 2017). FGF1 is detected at higher levels in the serum and CSF of Alzheimer's patients and reactive astrocytes surrounding senile plaques express high levels. (Mashayekhi et al., 2010, Kimura et al., 1994). In diseases associated with neurocognitive impairment, lower levels of FGF1 in CSF correlated with poorer performance in five of seven cognitive tests (Bharti et al., 2016). Taken together these studies suggest that the presence of FGF1 in MS is likely to perform several beneficial functions. FGF1 reduces inflammation and glial scar formation, promotes neuronal survival, and promotes OL differentiation and myelination.

1.4.2.2 FGF2

Studies of FGF2 highlight the complexity and wide ranging effects of FGF signaling as research in the areas of inflammation and neurodegeneration has produced varied and often contradictory findings. FGF2 can bind to all FGFRs except IIIb isoforms of FGFR2 and FGFR3 (Zhang et al., 2006). FGF2 performs a variety of functions in the CNS and likely mediates a host of effects in the course of many CNS pathologies. Some groups have shown that FGF2 activates astrocytes and induces Glial fibrillary acidic protein (GFAP) production (Goddard et al., 2002, Ballabriga et al., 1997); while other groups have found that FGF2 suppresses astrocyte activation and inhibits GFAP messenger RNA (mRNA) expression (Kang et al., 2014, Reilly et al., 1998). A similar disparity was observed in the investigation of FGF2 on microglial activation: *in vivo*, injections of FGF2 into the lateral ventricle increased microglial ED1 expression (a marker of phagocytosis) and number of cytoplasmic granules (Goddard et al., 2002). However, in another study FGF2 inhibited microglia activation indirectly by enhancing CD200 expression on neurons and astrocytes (Cox et al., 2013); CD200 is an anti-inflammatory ligand and ligation maintains microglia in a quiescent state (Lyons et al., 2007).

FGF2 is upregulated in numerous CNS pathologies including brain/spinal cord injury, Parkinson's, Alzheimer's, stroke, and MS (Woodbury and Ikezu, 2014). In most of these conditions, research has shown FGF2 to be a potent neuroprotective agent, and several groups have investigated FGF2 as a therapeutic target for degenerative brain diseases and CNS injuries. In cortical lesions induced by aspiration or stereotactically localized knife wounds, FGF2 mRNA levels were increased from four hours post-injury and remained elevated two weeks later (Frautschy et al., 1991, Logan et al., 1992). Microglia and reactive astrocytes were the main sources of FGF2, with some produced in vascular endothelial cells. FGF2 is expressed by neurons and reactive astrocytes in SCI in and around the lesioned area and is still upregulated three weeks post-injury (Madiati et al., 2003).

Many studies have shown FGF2 is a potent survival factor for different neuronal populations: in the presence of FGF2, hippocampal and dopaminergic neurons are more resistant to glutamate-induced cell death and cholinergic/non-cholinergic neurons are more likely to survive axon transection (Mattson et al., 1993, Casper and Blum, 1995, Otto et al., 1989, Cummings et al., 1992). FGF2 promoted survival of grafted dopaminergic neurons in a rat Parkinson's model which led to greater behavioural improvements over grafts without FGF2 (Takayama et al., 1995). Degenerating neurons secrete FGF2 which attracts microglia and enhances phagocytosis of neuronal debris which helps to protect neurons from glutamate toxicity (Noda et al., 2014). In another study, FGF2 gene delivery to retinal ganglion cells promoted axon regrowth following acute optic nerve injury (Sapieha et al., 2003). FGF2 also indirectly promotes neuronal survival by inducing proliferation of glial cells that produce a range of trophic factors (Perkins and Cain, 1995). Ischemia as the result of stroke or CNS injury results in rapid neuronal loss, which several studies have shown, is prevented by FGF2 treatment (Martone et al., 2000, Nakata et al., 1993, Bethel et al., 1997, Wei et al., 2000). FGF2 is doubly beneficial for ischemic injuries as it is a potent angiogenic factor that stimulates VEGF expression in endothelial cells (Issa et al., 2005, Thau-Zuchman et al., 2012, Seghezzi et al., 1998). In a Huntington's disease transgenic mouse model, injection of FGF2 in neurogenic niches increased neural stem cell proliferation and differentiation into neurons. Newly formed neurons from the SVZ migrated to the basal ganglia and projected axons. FGF2 injection also increased

neuronal survival and improved the life span and motor functions of Huntington's disease-transgenic mice (Jin et al., 2005, La Spada, 2005, Tao et al., 1996).

FGF2 gene delivery in an Alzheimer's disease model improved spatial learning, enhanced neurogenesis and amyloid- β clearance by microglia, and reduced amyloid- β production by neurons (Kiyota et al., 2011, Takami et al., 1998). Intrathecal injection of FGF2 and EGF in the injured rat spinal cord reduced size of the injury site and more white matter was preserved compared to untreated injuries (Jimenez Hamann et al., 2005). In a mouse SCI model, subcutaneous injection of FGF2 reduced TNF α expression, monocyte/macrophage infiltration, and reactive gliosis, while enhancing neurogenesis and axon regeneration in the lesion, which led to improved recovery of hind limb function (Goldshmit et al., 2014). Blocking endogenous FGF2 with neutralising antibodies reduced functional recovery from motor cortex injury in rats which was associated with decreased neuronal survival (Rowntree and Kolb, 1997). A similar reduction in neuronal survival was observed in FGF2-null mice in neurotoxin-induced lesions (Timmer et al., 2007). Together these studies show that FGF2 is neuroprotective in the face of a variety of insults and an important component of the brains endogenous recovery processes.

(Butt and Dinsdale, 2005) showed that doses of FGF2 at or above 350 ng/mL injected into the CSF of healthy rats is sufficient to disrupt myelin and OL physiology. Mature OLs in these animals lost the ability to support myelin sheathes and began to express OPC markers, which led to pronounced demyelination. Armstrong *et al* have published a series of papers delineating the effects of FGF2 signaling in demyelinating mouse models: they first showed that FGF2 was upregulated by astrocytes in focally demyelinated spinal cord lesions and FGFR expression was highest at the onset of remyelination (Messersmith et al., 2000). They then induced cuprizone-demyelination in FGF2 null mice and found remyelinating lesions in the null animal contained more OLs than the wildtype (Armstrong et al., 2002). Using these KO mice the group then induced chronic cuprizone-demyelination from which wildtype mice do not spontaneously recover, and found that lesions in the KOs underwent spontaneous remyelination (Armstrong et al., 2006). By downregulating FGFR expression in *in vitro* OPCs treated with FGF2 they showed FGFR1 signaling was responsible for the inhibition of OPC maturation (Zhou et al., 2006). More recently, they showed that deleting

FGFR1 in OL lineage cells in the cuprizone-demyelination model resulted in increased remyelination and OL maturation compared to wildtypes (Zhou et al., 2012). Improved remyelination in FGF2 and FGFR1 null mice leads to functional recovery following acute or chronic demyelination (Mierzwa et al., 2013) suggesting that this signaling pathway contributes to the inhibition of remyelination observed in MS.

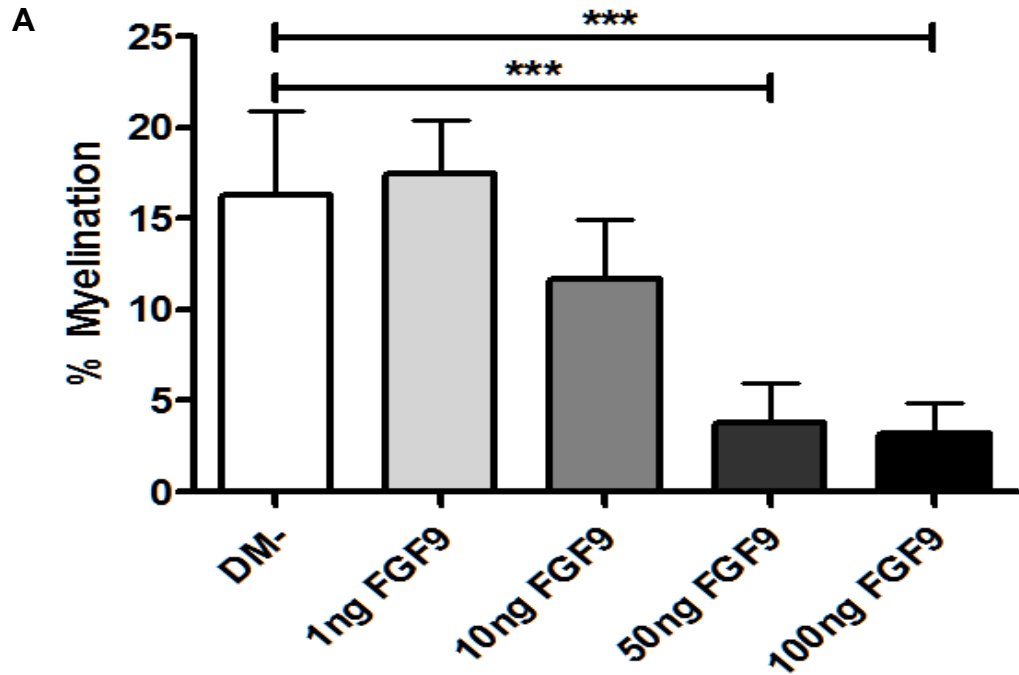
In contradiction to findings from Armstrong *et al*, studies by groups using the inflammatory EAE model have shown that FGF2 improves lesion recovery and reduces inflammation (Rottlaender et al., 2011). Increasing FGF2 expression via viral gene transfer led to robust recovery in a chronic EAE mouse model. Inducing active EAE in FGF2 null mice resulted in more severe disease marked by enhanced microglia/macrophage and CD8⁺ T cell infiltration, and reduced remyelination. In a model of toxin-induced demyelination, animals treated with FGF2 had increased OPC and mature OL numbers in lesions and improved remyelination (Azin et al., 2015). Injections of FGF2 restored MBP expression and axonal function following lyssolecithin-induced demyelination in the optic chiasm and hippocampus (Dehghan et al., 2012, Azin et al., 2015). Furusho et al. employed the toxin-induced acute and chronic cuprizone-demyelination models to investigate remyelination in mice that had FGFR1 and FGFR2 deleted in OL lineage cells (Furusho et al., 2015). They reported no difference in recovery following acute disease, but compromised remyelination after chronic disease. This was due to reduced expression of myelin proteins and myelin sheath thickness. OL numbers and maturation were unaffected in the KOs. Together, the studies of FGF2 in demyelinating animal models seem to suggest it has beneficial and detrimental properties. FGF2 appears to be anti-inflammatory and promote progenitor proliferation and migration, while at the same time inhibiting OPC maturation and myelination which prevents remyelination and functional recovery.

1.4.2.3 FGF9

FGF9 was identified as a target of interest when an *in vitro* screen of FGFs on a rat myelinating culture system revealed that FGF9 is a more potent inhibitor of myelination than FGF2. FGF9-treated myelinating cultures show a marked decrease in myelination at day *in vitro* 28 (DIV 28) without an obvious effect on underlying axons as shown in Figures 1.4 and 1.5.

FGF9 acts via a different mechanism than FGF2 but similarly promotes OPC proliferation and inhibits their differentiation to mature myelinating OLs. FGF2 inhibits myelination directly by binding to FGFRs on OL lineage cells and so can inhibit differentiation of purified OPCs *in vitro*. Myelinating cultures treated with FGF9-conditioned astrocyte media displayed similar inhibition of myelination as FGF9-treated cultures (Lindner et al., 2015). This suggests that the mechanism of action of FGF9 is indirect and inhibits myelination by inducing the secretion of myelin inhibitory factors by astrocytes. FGF9 may be involved in promoting the recruitment of inflammatory cells via chemokine expression. Microarray and qPCR studies also showed that FGF9 induced the expression of proteases involved in tissue remodelling and pro-inflammatory cytokines, which could contribute to the impaired repair and inflammatory responses seen in MS (Lindner et al., 2015). A study in OL differentiation found that FGF9 had no significant effect in purified rat OPCs and induced little signaling, but activated MAPK in differentiated OLs (Cohen and Chandross, 2000). This led to a decrease in FGFR2 (OL maturation marker) expression and increase in FGFR1, with inhibition of myelin genes, *Cnp*, *Mbp*, and *Plp*. Similar changes were observed in differentiated OLs treated with FGF2. These findings suggest that FGF9 plays a pathogenic role in MS, by inhibiting myelination indirectly via astrocytes, and potentially by directly inhibiting OPC maturation. OPC proliferation was stimulated by FGF9 indicating that it may have some beneficial properties in MS where OLs have been depleted. Mice with cuprizone-induced EAE given dietary cholesterol display enhanced remyelination and axon-sparing which was associated with increased expression of FGF9 and FGF1 and a decrease in FGF2 (Berghoff et al., 2017). FGF9 is upregulated in Alzheimer's plaques and amyotrophic lateral sclerosis (ALS) spinal cord, suggesting it is involved in the pathogenesis of neurodegenerative diseases (Nakamura et al., 1998). FGF9 is a potent neuronal survival factor and protects neurons from metabolic damage in Parkinson's models (Kanda et al., 1999, Huang et al., 2009, Huang and Chuang, 2010). These findings suggest FGF9 may protect neurons and prevent axonal loss in MS, which is the main driver of disability.

DIV 18-28 Myelinating Culture Treatment



DIV 18-28 Myelinating Culture Treatment

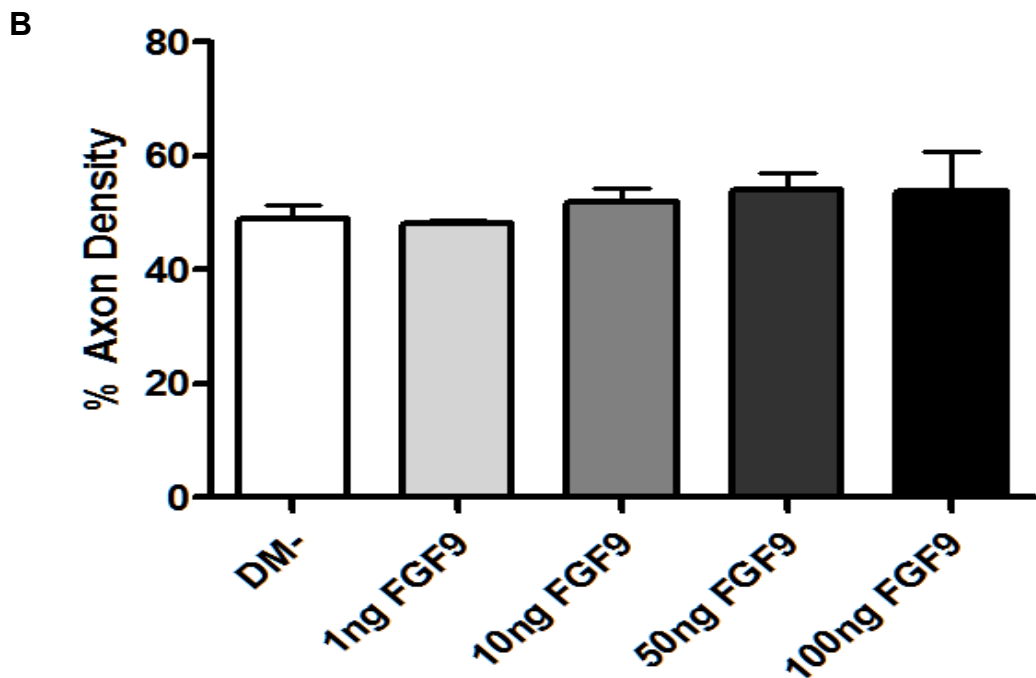


Figure 1.4. FGF9 inhibits myelination in a dose dependant manner. Myelinating cultures were treated with different concentrations of recombinant human FGF9 from DIV 18 - 28. DM- alone was used as a control to compare the effect on myelination. Cultures were fixed and stained with antibodies against MOG and SMI31 which label myelin and axons respectively. Myelination was quantified using CellProfiler as described in Section 2.2.7. 50 ng/ mL and 100ng/ mL FGF9 significantly inhibited myelination (A) and treatment had no effect on axon density (B). Data presented are the means \pm SD relative to controls. This experiment was performed three times. *, $p < 0.001$ (one-way ANOVA with Dunnett's Multiple Comparison Test).

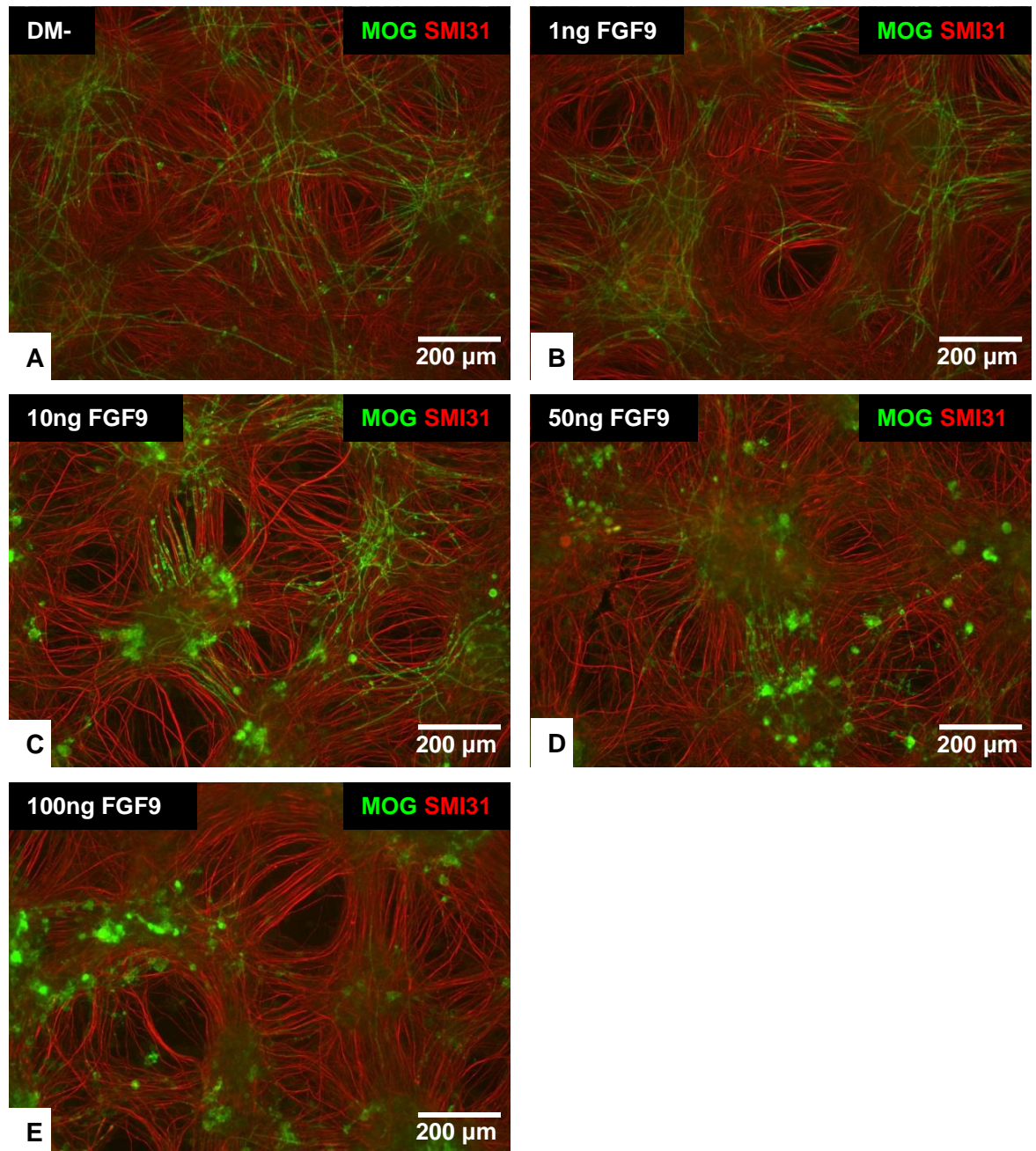


Figure 1.5. Representative images of myelinating cultures following FGF9 treatment. Myelinating cultures were treated with different concentrations of recombinant human FGF9 from DIV 18 - 28. Cultures were fixed and stained with antibodies against MOG (green) and SMI31 (red). Myelin appears normal in DM- control cultures (A) and following treatment with 1ng FGF9 (B). A decrease in myelination is observed in cultures treated with 10ng FGF9, concomitant with the appearance of irregular, brightly staining MOG⁺ cells (C). Myelination is almost totally inhibited in cultures treated with 50ng (D) and 100ng FGF9 (E).

1.5 Thesis aims

Following the recent discoveries made with regard to FGF9 in the pathogenesis of MS, the goals of this thesis were to further elucidate the mechanisms involved in FGF9 expression and signaling in MS. It was hypothesized that astrocytes and OL lineage cells would be the main target of FGF9-signaling in MS. To test this, studies of downstream FGF9 regulators were performed using post-mortem MS tissue, EAE samples, and *in vitro* cultures. Downstream regulators are expressed quickly in response to FGF-signaling making their presence a good indicator of where signaling is occurring. The trigger for FGF9 upregulation in MS is unknown and it was hypothesized that an aspect of the inflammatory process may be involved as higher FGF9 expression was seen in acute MS than in chronic stages. To test this hypothesis, several inflammatory mediators of MS and inducers of FGF9 in cancer were screened for their ability to induce FGF9 expression. As MS is a chronic disease characterised by bouts of inflammatory demyelination followed by remyelination it was hypothesized that downregulation of FGF9 following high levels would promote remyelination. The long-term effects of increased levels of FGF9 were investigated using *in vitro* and *in vivo* models. The impact of FGF9 on mature myelin and FGF9 withdrawal were also investigated using the *in vitro* myelinating culture system. In addition, FGF9-gene containing vectors were administered to rat brains which were examined over a nine month period to examine the effects of chronic exposure of FGF9 in the CNS. These experiments were performed with the goal of increasing understanding of the mechanisms that drive pathogenesis in MS.

CHAPTER TWO

MATERIALS AND METHODS

2 MATERIALS AND METHODS

2.1 Animals

Sprague Dawley (SD) and Dark Agouti (DA) rats were used in these studies. All animals were purchased from Harlan Laboratories (Blackthorn, UK) and were maintained at the University of Glasgow Central Research Facility. All animal care and procedures were in accordance with the Animals Scientific Procedures Act, 1986, under project license no. 60/4314 and personal license no. 60/10857 issued by the UK Home Office and with approval from the University of Glasgow Ethical Review Process Applications Panel.

2.2 Cell Culture

All culture preparation and maintenance was performed in an aseptic fashion. Instruments and dissection tools were sterilized prior to use by autoclave or 70% ethanol. Tissue dissections were mostly performed at the bench, all *in vitro* work was done using laminar flow hoods. All tissue culture media used in these experiments contained the antibiotics penicillin and streptomycin and were filter sterilized before use.

2.2.1 Generation of myelinating spinal cord cultures

2.2.1.1 Generation of neurospheres

The corpus striatum of P1 (post-natal day one) Sprague Dawley (SD) rats were dissected to generate neurospheres via the methods developed by (Reynolds and Weiss, 1996) with the modifications described by (Sorensen et al., 2008). P1 pups of both sexes were sacrificed by intraperitoneal injection of Euthanal. Once dead, the pups were decapitated and their brains excised and transferred to a petri dish containing cold Leibovitz's L-15 media (Invitrogen). Using a scalpel, the cerebral hemispheres of the brain were separated and the portion of the cortex containing the striatum was isolated by making coronal slices through the cortex at the corpus callosum and just prior to the olfactory bulb. The striatum was then carefully dissected out of the cortex and placed into a bijoux containing 1 mL of Leibovitz's L-15 media, on ice. 5 – 6 striata generated one flask of neurospheres. The striata were mechanically dissociated by trituration using a glass Pasteur pipette and

transferred into a 15 mL centrifuge tube. The suspension was centrifuged at room temperature for 5 minutes at 800rpm (~136g). The supernatant was discarded and the cell pellet resuspended in 2 mL neurosphere media (NSM) consisting of DMEM/F12 (Dulbecco's Modified Eagle Medium: Nutrient Mixture F-12) (1:1, DMEM containing 4500 mg/L glucose), supplemented with 7.5% NaHCO₃, 2 mM glutamine, 5000 U/mL penicillin, 5 µg/mL streptomycin, 5.0 mM HEPES, 0.0001% bovine serum albumin (BSA) (all from Invitrogen), 25 g/mL insulin, 100 g/mL apotransferrin, 60 M putrescine, 20 nM progesterone, and 30 nM sodium selenite (all from Sigma). To this mixture, 4 µL of EGF (20 ng/mL mouse submaxillary gland epidermal growth factor from R&D Systems) was added and the whole suspension was plated into a 75 cm³ uncoated tissue culture flask (Greiner), containing 18 mL of 37° C NSM. The cultures were incubated at 37° C in a humidified atmosphere of 7% CO₂/93% air. The cultures were fed twice a week by the addition of 5 mL NSM + 4 µL EGF. After 7-10 days, the neurospheres were visibly large enough to be plated down to form astrocytes.

2.2.1.2 Generation of astrocyte monolayers from neurospheres

Differentiation of astrocytes was performed as described by (Thomson et al., 2006). Firstly, glass coverslips (13 mm diameter; VWR International) were coated with poly-L-lysine (PLL) (13 g/mL, Sigma Aldrich) by incubating them at 37° C for at least 1 hour. Twenty-four well plates (Corning Life Sciences) were prepared by placing PLL-coverslips individually into each well and letting them dry overnight in a laminar flow hood. Prepared 24 well plates were sealed in an autoclave bag and kept at 4° C until use. After 7 - 10 days in culture, flasks of neurospheres were scraped using a cell scraper (Grenier) and the suspension was transferred into a 50 mL centrifuge tube

. One flask of neurospheres would typically generate 5 – 6 plates of astrocyte monolayers. The neurospheres were centrifuged at 800rpm (~136g) for 5 minutes at room temperature and the pellet was triturated using a glass Pasteur pipette to produce a single cell suspension. The suspension was diluted to in 12 mL/ 24 well plate with low-glucose DMEM supplemented with 10% foetal bovine serum and 2 mM L-glutamine (DMEM-FBS) (Sigma Aldrich). 0.5 mL of suspension was pipetted into each well followed by 0.5 ml of DMEM-FBS. The monolayers were incubated at 37° C in a humidified atmosphere of 7% CO₂ /93% air and were maintained by

replacing half the media in each well with fresh DMEM-FBS twice a week until the cells formed a confluent monolayer, 7 - 10 days later. Astrocyte monolayers are produced without any cell-specific selection and as such are subject to contamination by other CNS cell types. Data of astrocyte monolayer purity is shown in Figure 8.3. OL lineage cells are the major contaminating cell type in astrocyte monolayers at DIV 7 however as this culture is mainly used as a base for myelinating cultures this is not considered to be a negative issue.

2.2.1.3 Seeding of embryonic spinal cord cells on astrocyte monolayers

The methods of generating myelinating cultures were developed by (Thomson et al., 2008) for mouse cultures and adapted by (Sorensen et al., 2008) for use in rat cultures with some modifications. Time-mated SD female rats were sacrificed by asphyxiation in a CO₂ chamber on embryonic-day 15.5 (E15.5). The rats' abdomen and dissection tools were sterilized with 70% ethanol. Using scissors the skin and abdominal wall were cut in a V shape to expose the embryos. The gravid uterus was removed and placed in a petri dish containing Hank's balanced salt solution (HBSS) on ice. The embryos were removed from their embryonic sacs and transferred to 35 mm petri dish containing ice cold HBSS. Using forceps and pointed-tweezers the embryos were dissected under a microscope. First, the embryos were decapitated rostral to the cervical flexure to preserve the structure. The skin over the spinal cord was then carefully removed along its length and the cord was gently lifted out of the embryo. The meninges were peeled from the cord along with any attached dorsal root ganglia, and the cords placed in a bijoux containing 1 mL HBSS without calcium or magnesium on ice. Up to five cords were collected in each bijoux.

The cords were dissociated by trituration with a glass Pasteur pipette and enzymatically digested with trypsin (2.5%, 100 μ L, Sigma Aldrich) and collagenase I (1.33%, 100 μ L, Invitrogen) in HBSS for 15 minutes at 37° C. To stop the enzymatic activity 2 mL of trypsin inhibitor containing 0.52 mg/mL soybean trypsin inhibitor, 3.0 mg/mL bovine serum albumin, and 0.04 mg/mL DNase (Sigma Aldrich) to prevent cell clumping, was added to the suspension. The spinal cord suspensions were shaken and incubated at room temperature for a few minutes to allow the DNase to work and the dissociated tissue to settle on the bottom of the bijoux. 2 mL of media was carefully pipetted off and discarded from each bijoux. The

dissociated cords were then triturated with a glass Pasteur pipette and pooled in a 15 mL centrifuge tube and centrifuged at 1200rpm (200g) for 5 minutes. The supernatant was removed and the pellet was resuspended in 10 mL plating media (PM) consisting of 50% low-glucose DMEM (Gibco Life Sciences), 25% horse serum (Sigma Aldrich), 25% HBSS with calcium and magnesium, and 2 mM L-Glutamine (Invitrogen). Cell numbers and viability were measured by diluting a sample of the suspension 1:1 with Trypan Blue and counting the living cells under a microscope using a Haemocytometer. The suspension was then diluted to 3×10^6 cells/mL with PM.

Coverslips with neurosphere-derived astrocyte monolayers, described in section 2.2.1.2 were removed from the 24 well plate using ethanol sterilized tweezers and placed into 35 mm petri dishes (3 per dish). 50 μ L (150,000 cells) of the dissociated spinal cord suspension was pipetted onto each cover slip and the petri dishes were incubated at 37° C for 2 hours to allow the cord cells to adhere to the monolayer. After incubation 450 μ L PM + 600 μ L differentiation media + insulin (DM+) was added to each dish. DM+ consists of DMEM (4500 mg/mL glucose) (Gibco Life Sciences), 10 ng/ml biotin (Sigma Aldrich), 50 nM hydrocortisone (Sigma Aldrich), 0.5X N1 supplement (Sigma Aldrich), and 0.5 mg/mL insulin from bovine pancreas (Sigma Aldrich). These cultures were maintained in a humidified atmosphere of 7% CO₂ /93% air and fed with DM+ 3 times per week by swapping half the culture media with fresh DM+ until day-*in vitro* 12 (DIV 12). From DIV 12, the cultures were fed with DM- (DM+ without insulin) to allow OL lineage cells to differentiate and produce myelin.

2.2.2 Generation of low-density astrocyte cultures

Neurospheres were harvested and pelleted as described in Section 2.2.1.1. The supernatant was discarded and using a glass Pasteur pipette the pellet was triturated with 1 mL DMEM-FBS. This 1 mL cell suspension was divided between 2 75 cm³ uncoated tissue culture flasks (Greiner) containing 11.5 mL DMEM-FBS. The cultures were maintained in a humidified atmosphere of 7% CO₂ /93% air at 37° C and were fed by removing 6 mL of media and adding 6 mL fresh DMEM-FBS twice a week. After 1 week in culture the media was removed from the flask, the cells were gently aspirated with 10 mL cold sterile phosphate buffered saline (PBS) then trypsinised with 1 mL trypsin Ethylenediaminetetraacetic acid (EDTA)

0.05% (Invitrogen) and incubated at 37° C for 1 - 2 minutes. After incubation, 10 mL DMEM-FBS was added to each flask to inhibit the trypsin. The adherent cells were separated from the flasks using cell scrapers (Greiner) and then pipetted into a 50 mL centrifuge tube before centrifugation at 1200rpm (200g) for 5 minutes. The supernatant was discarded and the cells were resuspended in 10 mL DMEM-FBS and counted using Trypan Blue and a haemocytometer. The suspension was diluted to 25,000 cells/mL with DMEM-FBS. 1 mL of suspension was pipetted into each well of a 24 well plate containing PLL-coated glass coverslips as described in section 2.2.1.2. Cells were maintained in a humidified atmosphere of 7% CO₂ /93% air. After 24 hours, the astrocytes had adhered to the coverslips and were transferred to 35 mm petri dishes, flooded with 1 mL DM-, and then fed twice weekly by removing and replacing half of the media in each dish.

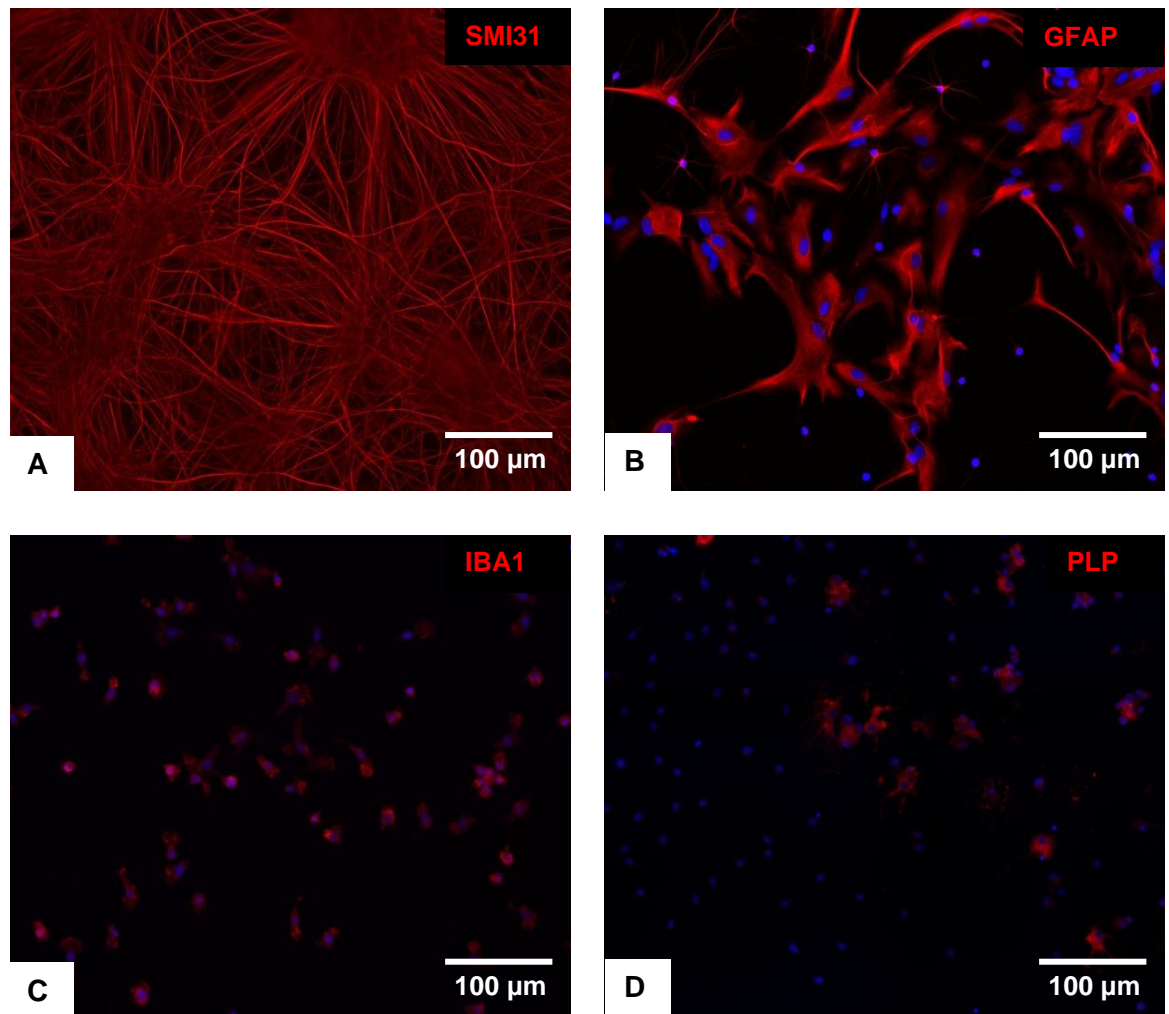


Figure 2.1. Representative images of cells that constitute myelinating cultures at DIV 28. The projected axons of neurons are visualised by staining with SMI31 (A). Astrocytes that make up the supporting monolayer are stained with GFAP (B). Microglia are stained with IBA1 (C) and myelinating oligodendrocytes with PLP (D).

2.2.3 Generation of purified oligodendrocyte cultures.

Purified oligodendrocyte cultures were generated from the cortices of P1 SD rat pups that were used to generate neurospheres. After the striatum was dissected out of the coronal section of the cortex, tweezers were used to peel away the meninges surrounding the cortex and within the ventricles. Four cortices were collected in a bijoux containing 2ml HBSS without calcium or magnesium (ThermoFisher Scientific) on ice. Dissociation of the cortices was performed using a neural-tissue dissociation kit (Miltenyi Biotec) followed by A2B5 MACS microbead purification of oligodendrocyte lineage cells (Miltenyi Biotec). Cortices were minced in a 9 cm petri dish using a sterilized razor blade and collected in a 15 mL centrifuge tube. The tissue was centrifuged at 300g for 2 minutes at room temperature and the supernatant discarded. 100 µL buffer X + 100 µL enzyme P were added to the centrifuge tube and the cortices were triturated slightly. The tube was incubated at 37° C for 10 minutes then 50 µL buffer Y and 25 µL enzyme A was added to the tube and the cortices were triturated again before another 10 minute incubation at 37° C. Following one more trituration and 10 minute incubation at 37° C the cortices were spun down at 300g for 2 minutes, some of the enzyme solution was removed and the cells resuspended in the remaining solution and centrifuged again at 300g for 5 minutes. The remaining solution was removed and the cells were resuspended in 10ml HBSS with calcium and magnesium and counted using a haemocytometer. The cells were centrifuged at 300g for 5 minutes at room temperature and resuspended in 1 mL MACS buffer (PBS + 0.5% BSA) then centrifuged again at 300g for 5 minutes at room temperature. The buffer was removed and the cells resuspended in 70 µL MACS buffer/ 10 million cells. 20 µL anti-A2B5 coated microbeads/ 10million cells was added and the cells were incubated on ice for 15 minutes. Anti-A2B5 monoclonal antibodies recognise a cell surface ganglioside epitope expressed by oligodendrocyte progenitor cells. During this incubation, an LS column (Miltenyi Biotec) was set up in a MACS separator magnet and washed with 500 µL MACS buffer. 2 mL MACS buffer was added to the cell suspension for washing and the tube was centrifuged at 300g for 5 minutes. The supernatant was removed and the magnetically labelled cells were resuspended in 500 µL MACS buffer and put onto the column through a 30 µm pre-separation filter (Miltenyi Biotec). The column was then washed with 3 x 3 mL MACS buffer and the negative cells collected in a 15

mL centrifuge tube. After washing the column was removed from the magnet and magnetically labelled cells were eluted by pressing 5 mL MACS buffer through the column into a 15 mL centrifuge tube. The eluted cells were centrifuged at 300g for 5 minutes, the buffer was removed and the cells were resuspended in 0.5 mL oligodendrocyte differentiation media (BDM media) and counted with a haemocytometer. From this stage the cells were cultured under different conditions depending on the experiment as described below:

For fluorescence microscopy studies the cells were resuspended in BDM media at 20,000 cells/mL and 40,000 cells/mL for RNA extraction.

In experiments involving mature oligodendrocytes PDGF α and FGF2 (both from Peprotech) were added to the cell suspensions at 50 ng/mL prior to plating. 1 mL of suspension was plated onto a PLL coated coverslip in a 24 well plate as described in Section 2.2.1.2. The cells were maintained in a humidified atmosphere of 7% CO₂ /93% air. After two days the coverslips were transferred into 35 mm tissue culture dishes and 1mL Sato's media was added to each dish without PDGF α and FGF2 to allow the cells to differentiate. OLs were checked daily by bright field microscopy to assess viability and differentiation state. Cells were fed by exchanging half of the media with fresh Sato's 3 times per week. Treatments for these experiments began at DIV 6.

In studies of immature OLs, cells were suspended and diluted in Sato's media instead of BDM. These cells were cultured for 2 days before treatments were initiated. Experiments performed by previous members of the lab showed that OLs purified by these methods are over 90% pure throughout the first seven DIV. The only contaminating cell type is astrocytes which begin to proliferate and take over the cultures after DIV 7.

2.2.4 Generation of bone marrow-derived macrophage cultures.

SD female rats were sacrificed by asphyxiation as in Section 2.2.1.3. The animals' hind legs and dissection instruments were sterilized with 70% ethanol. Using pointed scissors and forceps the skin was cut from the abdomen along the inside of the hind leg to the ankle. The skin around the ankle was cut and peeled back towards the abdomen to expose the musculature of the leg up to the hip. Most of the muscle surrounding the upper and lower legs was removed with scissors and

the leg was twisted to dislocate the hip joint. Any tissue still connecting the hind leg to the body was cut away and the leg transferred to a 50 mL centrifuge tube containing ice-cold PBS. Both legs from one animal were typically collected. In a laminar flow hood the legs were removed from the centrifuge tube and sterilized with 70% ethanol. Sterilized medium duty bone shears were used to remove the foot, fibula, and separate the knee joint of each leg. Using fine banded scissors the remaining muscle was removed from the femurs and tibias. The trabeculae of the bones were removed by one clean cut with the bone shears, being careful not split the bone along its length and expose the bone marrow. A 10 mL syringe was filled with ice cold complete Roswell Park Memorial Institute -1640 media (cRPMI), containing RPMI-1640 with 10% FBS, and connected to a 25G needle. Marrow was flushed from the bones into a 9 cm petri dish and then dissociated by drawing the suspension through the needle several times. The bone marrow was passed through a 70 μ m cell strainer (Corning) into a 50 mL centrifuge tube and pelleted by centrifugation at 2000 rpm (~480g) for 5 minutes at room temperature. The supernatant was discarded and the pellet was agitated and incubated with 2 mL ACK lysis buffer (ThermoFisher Scientific) for 90 seconds to lyse erythrocytes. An excess of PBS was then added to the centrifuge tube to inhibit lysis followed by another centrifugation at 2000rpm. The pellet was resuspended in 10 mL cRPMI and the cells were counted using Trypan Blue and a Haemocytometer. The cells were diluted with cRPMI to a density of 1 million cells/mL and 50 ng/mL rat macrophage colony-stimulating factor (M-CSF, peprotech) was added to the suspension. M-CSF promotes differentiation of macrophages from bone marrow progenitor cells. 1 mL of cell suspension was plated into 35 mm petri dishes. The cultures were incubated at 37^o C in a humidified atmosphere of 5%CO₂/95% air. Every 2-3 days all media were removed from each dish and the cells were carefully washed with PBS before adding fresh cRPMI + 50 ng/mL M-CSF. Macrophage progenitors adhere to the dishes while other bone marrow cells remain in suspension and were removed by washing with PBS. Bone marrow-derived macrophages (BMDMs) were fully differentiated after 7 days in culture. Purity of BMDM cultures was not analysed as part of these experiments however this is a well-established protocol for BMDM generation which is described to produce cultures that are 95 – 99% pure (Ying et al., 2013).

2.2.5 Generation of enriched neuronal cultures.

E15.5 embryos from SD rats were harvested and dissected as described in section 2.2.1.3. Brains from the decapitated heads of the embryos were carefully dissected from the skulls using forceps. The meninges were removed and the brains transferred into a bijoux containing 1 mL HBSS without calcium and magnesium, striata from two brains were placed in each bijoux which were kept on ice. The brains were digested and pelleted identically to E15.5 spinal cords. The final pellet was resuspended in 10 mL neuron media: Neurobasal media (Gibco) containing 1 X B27 supplement (Gibco), 2 mM L-Glutamine (Invitrogen), and 5000 U/mL penicillin, 5 µg/mL streptomycin. Cell numbers and viability were measured with Trypan Blue using a Haemocytometer and cells were diluted to a density of 80,000/ mL. 0.5 mL cell suspension was pipetted onto PLL-coated coverslips in a 24 well plate. Neurons were incubated in a humidified atmosphere of 7% CO₂ /93% air for 4 days. Coverslips were then transferred into 35 mm petri dishes and flooded with 300 µL conditioned neuron media and 800 µL fresh neuron media. After 6 DIV neurons were fully differentiated. Neurobasal media suppresses differentiation of cell types other than neurons however some contamination does occur as shown in Figure 8.4. In particular, astrocytes and OL lineage cells appear at DIV3 and continue to increase the longer the cultures are maintained.

2.2.6 *In vitro* culture treatments

2.2.6.1 Myelination experiments

The myelinating cultures (one petri dish per condition) were treated with human FGF9 (R&D systems) at a concentration of 100 ng/mL from DIV 18 for 1 to 10 days. The factor was added at the specified concentration to the DM- media for feeding (double the concentration was used on the first day of treatment).

2.2.6.2 Astrocyte experiments

For these experiments the low density astrocyte coverslips were placed in petri dishes and treated in the same way as the myelinating cultures with 100 ng/mL of each FGF. Low density astrocytes were used in imaging studies while astrocyte monolayers were used in qPCR experiments.

2.2.6.3 FGF9 experiments

The myelinating cultures (one petri dish per condition) were treated with human FGF9 (R&D systems) at a concentration of 100 ng/ml from DIV 18 for 10 or 20 days and from day 28 for 10 days. The factor was added at the specified concentration to the DM- media for feeding (double the concentration was used on the first day of treatment).

2.2.6.4 Cytokine experiments

Myelinating cultures were treated with a range of cytokines: tumour necrosis factor α (TNF α), interferon- γ (IFN γ), interleukin-6 (IL-6), IL-1 β , granulocyte-macrophage colony-stimulating factor (GM-CSF), IL-10, transforming growth factor- β 1 (TGF β 1), (all from Peprotech), prostaglandin E2 (Santa Cruz), or benzo[a]pyrene (Sigma) at concentrations of 5, 50, or 100 ng/ml from day 18 for 24 hours or 10 days.

2.2.6.5 Hypoxia experiments

Myelinating cultures and astrocyte monolayers were incubated in a hypoxic chamber (Modular Incubator Chamber (MIC-101) and flooded with 1% O₂ at a rate of 20 L/min for four minutes before being sealed and placed in a 37° C incubator for 6, 24, or 48 hours. Control cultures were maintained in a normal incubator at 7% CO₂. Some of the hypoxic cultures were then incubated at normal O₂ levels for a further 24 or 48 hours.

2.2.6.6 Macrophage experiments

After 7 days in culture BMDMs were treated with 100 ng/mL recombinant rat IFN γ (Peprotech) or 100 ng/mL recombinant rat IL-13 (Peprotech) to drive macrophage polarization towards the M1 (inflammatory) or M2 (repair) phenotype respectively. Polarized macrophages were then treated for a further 24 hours with 100 ng/mL FGF1, 2, or 9 before they were lysed to collect mRNA for qPCR.

2.2.6.7 Purified oligodendrocyte experiments

Mature and immature oligodendrocytes were treated with 100 ng/mL FGF1, 2, or 9 for 24 hours. The cultures were then fixed for immunofluorescence staining or lysed for RNA extraction.

2.2.6.8 Enriched neuron experiments

Neurons were treated from DIV6 with 100 ng/mL FGF9 for 10 days then processed for immunofluorescence. Where 5-Fluoro-2'-deoxyuridine (FDU) was used in conjunction with FGF9, FDU treatment was started at DIV 4.

2.2.7 Immunofluorescence staining of *in vitro* cultures

After treatment, the cultures were fixed and stained with antibodies for immunofluorescence microscopy. All staining steps were performed at the bench with incubations taking place at room temperature. Media was removed from culture dishes and cells were fixed with 4% paraformaldehyde (PFA) for 20 minutes followed by permeabilization with Triton X-100 0.5% (Sigma Aldrich) for 10 minutes. Coverslips were then blocked for 30 minutes in blocking buffer (1% BSA (bovine serum albumin), 10% horse serum, in PBS). Primary and secondary antibodies used in imaging experiments are detailed in Table 2.2 below. Primary antibodies were diluted in blocking buffer and 40 µl was applied to each coverslip and incubated for 45 minutes. Coverslips were then washed in PBS and incubated with fluorescently-tagged secondary antibodies, prepared in blocking buffer, for 15 minutes in the dark to avoid photo-bleaching. After incubation coverslips were washed 3 x in PBS followed by a final wash in distilled water and mounted on glass slides (ThermoFisher Scientific) with 10 µl Mowiol 4-88 + DAPI (4',6-Diamidino-2-Phenylindole, Dihydrochloride) (Sigma Aldrich).

2.2.8 Imaging and quantitative analysis

For all culture experiments imaging was performed using an Olympus BX51 fluorescent microscope and images were captured using Image-Pro software. For quantitative analysis of each culture system, 10 images from each coverslip were taken randomly at 20X magnification. Each condition was performed in triplicate (1 petri dish = 1 condition = 3 coverslips); therefore, 30 images were taken per condition per experiment and used for quantification and analysis in *in vitro* culture experiments.

Fluorescence intensity of staining of each antibody was quantified using CellProfiler software (<http://www.cellprofiler.org/>) with a pipeline developed to measure the pixel intensity from individual colour channels. Pipelines used in

these experiments can be downloaded from <https://github.com/muecs/cp>. Myelination percentage and axon densities were calculated using the myelin.cp pipeline. Total cell counts were measured using the dapi.cp pipeline to count cell nuclei. Total OL lineage cell numbers were counted using the olig2-aa3.cp pipeline to count green-labelled nuclei. Mean fluorescent intensities of FGF9 staining in hypoxia experiments was calculated using the pixel-int-g.cp pipeline. NG2⁺ OPCs were counted manually using the cell counter function of ImageJ. MAP2⁺ Neurons were also counted manually.

Table 2.1. Primary antibody list

Antigen	Host	Target	Isotype	Dilution	Source	Clone
PLP	Rat	M, R, H	IgG	1-100	Hybridoma	AA3
DUSP 5	Rb	H	IgG	1-200	Abcam	Poly
DUSP 6	Rb	M, R, H	IgG	1-2000	Abcam	EPR129Y
CD68	Ms	M, R, H	IgG1	1-1000	Abcam	ED1
FGF9	Rb	M, H	IgG	1-400	Abcam	Poly
FGF9	Rb	M, R, H	IgG	1-200	Abnova	Poly
GFAP	Rb	M, R, H	IgG	1-1000	DAKO	Poly
GFAP	Ms	M, R, H	IgG1	1-1000	Abcam	GF5
IBA1	Rb	M, R, H	IgG	1-1000	Alpha	Poly
MAP2	Rb	M, R, H	IgG	1-100	Abcam	Poly
MOG	Ms	M, R, H	IgG2a	1-500	Hybridoma	Z2
NeuN	Ms	M, R, H	IgG1	1-100	Millipore	A60
NG2	Rb	R, H	IgG	1-200	Abcam	Poly
Olig-2	Rb	M, R, H	IgG	1-500	Chemicon	Poly
NF-H	Ms	M, R, H	IgG1	1-1500	Affinity	SMI31
Sprouty 2	Ms	H	IgG1	1-200	Abcam	ab60719
Sprouty 4	Rb	H	IgG	1-200	Abcam	ab103114

Table 2.2. Fluorescent secondary antibody list.

Antibody	AlexaFluor 488	AlexaFluor 568	AlexaFluor 350
goat-anti-mouse IgG	+	+	
goat-anti-mouse IgG1	+	+	
goat-anti-mouse IgG2a	+	+	
goat-anti-mouse IgG2b	+	+	
goat-anti-rat IgG	+	+	
goat-anti-rabbit IgG	+	+	+

All secondary antibodies were purchased from Invitrogen and used at a working dilution of 1:400.

2.3 Immunohistochemical analysis of human tissues

Immunohistochemical studies were performed on archived, formalin-fixed, paraffin-embedded brain material from 14 patients with MS and six controls without neurological disease or evidence of brain lesions. Samples were provided by the archive of the Centre for Brain Research at the Medical University of Vienna for immunopathological studies of human MS and control brain tissue under license from Ethik Kommission of the Medical University of Vienna (EK No. 535/2004).

Immunohistochemical studies were performed on consecutive deparaffinized 5 μ m sections after endogenous peroxidase was blocked with H₂O₂/methanol. Antigen retrieval was performed using citrate buffer (pH 6.0) or EDTA buffer (pH 8.5) and non-specific antibody binding was blocked by incubating sections in 10% foetal calf serum. Primary antibodies to Sprouty2 (1:500) and Sprouty4 (phospho-Y75, 1:250) (both rabbit polyclonal IgG (immunoglobulin G) from Abcam) were applied overnight at 4°C. After incubation and washing, antibody binding was routinely visualized using the horse radish peroxidase conjugated secondary antibody, biotin-donkey-anti-rabbit IgG, (1:2000), and 3,3'-diaminobenzidine (DAB). Cell nuclei were counterstained with haematoxylin prior to mounting. Photomicrographs were taken under a light microscope at 10X or 25X magnification.

Confocal fluorescence immunohistochemistry was performed as described for light microscopy with some modifications. For fluorescent double labelling Sprouty2 rabbit polyclonal IgG, 1:250, or Sprouty2 mouse monoclonal IgG, 1:150 (Abcam), were applied with glial fibrillary acidic protein (GFAP), goat polyclonal IgG, 1:100, or GFAP rabbit polyclonal IgG, 1:1500. Primary antibodies from different species were applied simultaneously at 4 °C overnight. After washing, appropriate secondary antibodies: Cy5-conjugated donkey-anti-goat (1:100), Cy3-conjugated donkey-anti-mouse (1:500), biotinylated donkey-anti-mouse (1:500), and biotinylated donkey-anti-rabbit (1:2000) (all from Jackson ImmunoResearch, West Grove, PA, USA) were applied simultaneously for 1 hour followed by application of Streptavidin-Cy2 (Jackson ImmunoResearch) for 1 hour at room temperature. Images were acquired using a confocal laser scanning microscope (Leica SP5, Leica Mannheim, Germany) equipped with lasers for 488, 543 and 633 nm excitation.

Table 2.3. List of patient samples used in human lesion studies

Case Number	LesionType	Age	Sex
132-92-1	control	65	male
421-92-5	control	80	female
36989	control	36	female
579-91-3	control	46	female
37343	control	42	female
68-93-4	control	83	male
581-96-7A	acute MS	35	male
90-09-6	acute MS	69	female
A01-144	acute MS	34	female
S403-97	acute MS	45	male
270-99-2	acute MS	45	male
Spanien C2	RRMS	40	male
70-93-6	acute MS	78	male
146-01-8	active/ chronic active	41	male
67-05-9	chronic active	34	male
39-03-15	chronic active	67	male
144-90-3	chronic active/ inactive	77	female
244-94-7	chronic inactive	81	female
285-81-1	chronic inactive	78	female
72-83-6	chronic inactive	64	female

2.4 Molecular Biology

2.4.1 RNA extraction

2.4.1.1 RNA extraction from *in vitro* cultures

RNA was extracted from myelinating cultures, astrocyte monolayers, purified oligodendrocytes, neuronal cultures, and BMDM cultures using the Qiagen RNeasy Micro kit (Qiagen, #74034). At the bench, media were completely removed from the tissue culture dishes. 350 μ L RNeasy lysis buffer was then pipetted directly onto the coverslips. The coverslips were scraped with a cell scraper (Grenier) and the lysates were collected and homogenized by centrifugation through QIAshredder spin columns (Qiagen, #79654). Lysates were used immediately or stored at -80° C to aid homogenization. From this point, RNA extraction proceeded according to manufacturer's instructions; the lysates were centrifuged through a genomic DNA eliminator spin column, then mixed with an equal volume of 70% ethanol and transferred to RNeasy Mini Spin Columns. The columns were washed with provided buffers and RNA was eluted in 14 μ L RNase-free water and stored at -80° C. RNA quantity, quality, and integrity were measured using a Nanodrop ND-1000 Spectrophotometer (ThermoFisher Scientific).

2.4.1.2 RNA extraction from tissues

Tissue samples were added to RNase-free microcentrifuge tubes with 1 mL Trizol reagent (Ambion, #15596026) and a 5 mm stainless steel bead (Qiagen, #69989). Tubes were placed in a tissue homogeniser for 10 minutes at 50 oscillations/second. 400 μ L chloroform was added to the tubes which were shaken vigorously by hand for 15 seconds. The mixed homogenate was incubated on ice for 3 minutes and centrifuged at 12,000g for 15 minutes at 4° C. 700 μ L of the resulting clear interface was pipetted into a fresh RNase-free microcentrifuge tube containing 700 μ L 70% ethanol and mixed thoroughly. The mixture was pipetted onto a PureLink® RNA Mini Kit (Ambion, #12183030) and RNA was extracted according to manufacturer's instructions. RNA was eluted in 30 μ L RNase free water and stored at -80° C after measuring concentration and purity on a Nanodrop.

2.4.2 cDNA synthesis

The volume of each RNA sample containing 500 ng RNA was transferred to a PCR (polymerase chain reaction) tube and made up to 12 μ L with RNase free water. cDNA was synthesized using the Qiagen QuantiTect® Reverse Transcription Kit following the manufacturer's instructions. 2 μ l genomic DNA wipe-out buffer was added prior to the first cycling step followed by 4 μ L reaction buffer, 1 μ L reverse transcriptase and 1 μ L random primer mix. Cycling parameters were as follows: first cycle (DNA wipe-out step) 42°C for 2 minutes, after adding reverse transcriptase, reaction buffer and primer mix second cycle: 42°C for 20 minutes, then 3 min for 95°C.

2.4.3 Primer design

Primers for use in qPCR experiments were designed from FASTA sequences in the NCBI nucleotide database, using the NCBI Pick Primers tool. Primer sequences were tested with NCBI Primer BLAST (<http://blast.ncbi.nlm.nih.gov/Blast.cgi>) and were purchased from Integrated DNA Technologies. Before use, Primers were resuspended in RNase free water at a concentration of 100 μ M. A master mix of 1:1 forward and reverse primers were made in RNase free tubes and stored at -20° C. Primer sequences used in all experiments are detailed in Table 4 below.

Table 2.4. List of Primers used in qPCR experiments

Gene	Forward sequence	Reverse sequence
<i>Arg1</i>	CATATCTGCCAAGGACATCG	GGTCTCTTCCATCACTTTGC
<i>Ccl2</i>	TAGCATCCACGTGCTGTCTC	TGCTGCTGGTGATTCTCTTG
<i>Ccl7</i>	CCATCAGAAGTGGGTTGAGG	CAGAAAGGACAAGGGTGAGG
<i>Dnah3</i>	AACTGCCACCTGGCTACAAG	CTGAGTCCTTTTGGGGGCTC
<i>Dnah6</i>	TGCAGAACGAGTGCAGTCAA	AGAGCCGGAAAGTGCCTTG
<i>Dnah9</i>	CAAAGGGATGCTGGAGCAGA	TCACTTCGTTGTGGCTCTCC
<i>Dusp5</i>	TTGAGGGGGTAGCAGGAAC	CAGGGTAGGGAGGGAAACA
<i>Dusp6</i>	AGTTTCTCTTGGGCAGCATC	GCAAATCTCTCCCTCCGTAA
<i>Dync1i1</i>	CCGTTCCAGATGACTCCGAT	CAGCGGCTGCACTAGAGG
<i>Dynlrb2</i>	TCCAATCCGAACAACCCTGG	TCAGGTCATTCTGGGGGTCA
<i>Fgf1</i>	TGTAGCATCTGGAGGGGTCT	GGTAGGGGGAAGGGTAGTCA
<i>Fgf2</i>	CTGTCTCCCGCACCCCTATC	CTTTCTCCCTTCCTGCCTTT
<i>Fgf9</i>	GGAAAGACCACAGCCGATT	TCTCTGAACACGCACTCCTG
<i>Fgfr1</i>	AGAGACCAGCTGTGATGA	CGCGTGACCAAAGTGGCC
<i>Fgfr2</i>	GAGAGAAGGAGATCACAG	CGCCACGGTGACTGCCTC
<i>Fgfr3</i>	TGATGGAAACTGATGAGG	GGCCACGGTGACAGGCTT
<i>Gapdh</i>	ATGACTCTACCCACGGCAAG	TACTCAGCACCAGCATCACC
<i>Hk2</i>	GGTTTCAAAGCGGTGCGAACTG	GAAATTGGTCAACCTTCTGCACT
<i>Ifny</i>	GCCCTCTCTGGCTGTTACTG	CCAAGAGGAGGCTCTTTCT
<i>Il10</i>	CTCCCCTCGAGTGTCTTCAG	CCATCAGCTGGGAATTTGTC
<i>Kif5a</i>	GGCCAGAGCAGAGATCACATT	CTCCGACAGGTCAGCAAGAC
<i>Nefh</i>	AGGACACAGGGTTAGCAACG	TCACTAGCAGGGTGGCTTTG
<i>Nos2</i>	GAGACGCACAGGCAGAGG	AGGCACACGCAATGATGG
<i>Rbfox3</i>	TCTATGCAGTGACCAGTTTCCC	CCACGGGACTGGCATTTTAAC
<i>Spry2</i>	TGTCCCTCTTTCTGCCTTGT	AACGCTATGTGCGCTTTTCA
<i>Spry4</i>	TGAGGAAGAGGGAGGGTTTT	AAGGGCAGGTGAGGTGTATG
<i>Sv2b</i>	CTCTACCGCTGAATCGCTCG	TTTGACAAGGTCGGTCCGGAG
<i>Tnf</i>	CCCCTTTATCGTCTACTCCTCA	TTCAGCGTCTCGTGTGTTTC
<i>Tubb3</i>	CAATGAGGCCTCCTCTCACA	AATAGGTGTCCAAAGGCCCC

2.4.4 Quantitative real-time PCR

Real-time PCR was performed using 7.5 μL 1X SYBR Green master mix (Applied Biosystems), 10 ng cDNA template (2 μL), 50 pmol/ μL (0.3 μL) forward and reverse primers and 5.2 μL RNase free water per reaction. Amplifications for each sample were performed in triplicate on MicroAmp Fast 96-well Reaction Plates (Applied Biosystems). The reaction was amplified in an Applied Biosystems Fast Real-Time PCR System (ABI 7500) using the following cycle settings: 50°C for 5 minutes, 95°C for 10 minutes, followed by 40 cycles of 95°C for 15 seconds, 60°C for 1 minutes, and a final dissociation step at 95°C for 15 seconds. Melt curve analysis was then performed between 75 – 99°C in 1°C increments. The comparative CT method (or the 2- ΔCT (cycle threshold) method) (Livak and Schmittgen, 2001, Schmittgen and Livak, 2008) was used to determine differences in gene expression between conditions.

2.5 Recombinant rat MOG₁₋₁₂₅ production and purification

2.5.1 Culture of rMOG-expressing *E. coli*

E. coli expressing recombinant rat myelin oligodendrocyte glycoprotein₁₋₁₂₅ (rMOG) were cultured from frozen glycerol stocks generated previously. *E. coli* – strain DH5 α F'1q, were transformed using pQE12 vector (Qiagen) containing rMOG cDNA. This vector contained the inducible lac promoter which initiated gene expression when the bacteria were treated with Isopropyl β -D-1-thiogalactopyranoside (IPTG). Included at the C-terminal end of rMOG cDNA in the plasmid were six histidine residues to allow for HisTrap purification. The pQE12 vector confers ampicillin resistance on transformed *E. coli* allowing them to be positively selected in ampicillin-containing media.

10 L Lysogeny broth (L. broth) was prepared by combining 100g tryptone, 100g NaCl, and 50g Yeast in 10 L distilled H₂O. 2 L of L. broth was added to 4 x 4L flasks and 1 L in a 2 L bottle which were sealed with foil and autoclaved. 8 x 15 mL centrifuge tubes containing 5 mL L. broth, 5 μL kanamycin (25mg/mL), and 5 μL ampicillin (100mg/mL) were prepared and a glycerol stock of *E. coli* containing recombinant MOG expression vector was taken from a -80° C freezer. Once thawed slightly the pellet was scratched with a needle and *E. coli* was added to 7

of the prepared centrifuge tube, leaving the 8th as a control. The lids were loosely taped onto the tubes, which were secured in a shaking incubator at 37° C and 150 rpm for 5 hours. After incubation, the tubes containing *E. coli* turned cloudy, indicating bacterial growth, and the control tube remains clear; the contents of centrifuge tubes were pooled in a bottle containing 1 L L. broth plus 1 mL kanamycin and 1 mL ampicillin, and the bottle was put in the shaking incubator overnight with the lid loosely taped on. After overnight incubation, the contents were evenly distributed between the 4 prepared 4L flasks and put in the shaking incubator with loosely taped on lids. Samples of broth were taken from one flask before and after the addition of the *E. coli* and then subsequently every 30 minutes. The growth phase of *E. coli* was estimated by measuring the optical density (OD) of the samples at 600nm using the sample containing no *E. coli* as a blank. When exponential phase was reached (OD 600nm = 0.7-0.8, around 1 - 2 hours) the *E. coli* were induced to begin expressing rMOG by adding 20 mL 0.1 M IPTG to each flask. The flasks were put back in the incubator for 5 hours and then the bacteria were collected in one pellet by repeated centrifugation at 15,000rpm for 20 minutes, 4° C (Beckman Coulter, F10BCI). The pellet was weighed and frozen at -20° C.

2.5.2 Lysis of *E. coli*

The pellet was thawed at room temperature and then resuspended in 5 mL/g PBS. The bacterial suspension was transferred to a glass homogeniser in batches and homogenised on ice before being collected in a sterile glass bottle on ice. Lysis was achieved with the addition of lysozyme (1mg/mL) (Sigma Aldrich) and DNase (5ug/mL) (Sigma Aldrich) to the suspension which was shaken for 30 minutes on ice. N,N-Dimethyldodecylamine N-oxide (LDAO) was added to the bottle to make a 0.5% concentration and the whole suspension was transferred to a sterile 200 mL glass beaker. The suspension was sonicated on ice (Soniprep 150) for 10 minutes at 10 - 15 amplitude. The suspension was distributed between 4 x 35 mL centrifuge bottles which were topped up with PBS until full. The suspension was centrifuged at 15,000rpm for 20 minutes, then the supernatant was discarded and the pellets resuspended in 10 mL PBS and homogenized using a glass homogeniser. This step was repeated 3 times. After these washing steps the pellet was collected in one bottle, weighed, and frozen at -20° C.

2.5.3 Dissolving inclusion bodies

The frozen pellet was thawed and resuspended in 10 mL/g 8 M Urea buffer in a 50 mL centrifuge tube. To this, 8 μ L/mL β -mercaptoethanol was added to reduce disulphide bonds and the suspension put on a shaker for 30 minutes with the lid sealed with parafilm. The suspension was distributed between 4 x 35 mL centrifuge bottles and 20 mL urea buffer was added to each bottle. The suspension was centrifuged at 15,000 rpm for 20 minutes at 4^o C. The supernatant was collected and vacuum filtered (0.45 μ m, Nalgene) into a sterile glass bottle.

2.5.4 Nickel-chelate affinity chromatography

The supernatant containing rMOG was purified using an ÄKTAprime plus chromatography system (GE Healthcare). First, the ÄKTAprime loads a HisTrap column (GE Healthcare) with NiCl that binds to His-tagged rMOG. The bound protein is then eluted from the column by passing through excess imidazole (Sigma Aldrich) which displaces the His-tagged protein from the column. 10 μ L samples from each eluted fraction were analysed by sodium dodecyl sulphate polyacrylamide gel electrophoresis (15% SDS-PAGE). The gel was run at 200V for 30 minutes with 5 μ L SeeBlue Plus2 pre-stained protein standard (ThermoFisher Scientific) followed by a 2 hour stain with Coomassie Blue and 1 hour de-stain with 50% methanol/ 10% acetic acid solution.

2.5.5 Dialysis of protein

Eluted fractions which left rMOG-positive bands on the Coomassie-stained gel were selected for dialysis. The samples were dialysed in 1000:1 20mM sodium acetate buffer (pH3.5) at 4^o C. Strips of 12-14 kDA dialysis tubing (Spectra/ Por Biotech) were prepared by boiling in a 2% sodium bicarbonate + 1 mM EDTA solution for 10 minutes followed by 10 minute boil in 1 mM EDTA solution and then rinsed with distilled water. The tubing was sealed at one end using a clip and the protein-containing fractions were transferred into the tubing which was sealed with a buoyancy clip. The elution was dialysed 4 L at a time at 4^o C with the buffer being changed every 24 hours until the elution had been dialysed in 1000 x its volume.

2.5.6 BCA protein concentration assay

The concentration of rMOG in dialysed elution was determined using a Pierce bicinchoninic acid (BCA) assay (ThermoFisher Scientific) according to the microplate method in the manufacturer's instructions. BCA working reagent, protein standards, and dilutions of rMOG solution were added to a flat-bottomed 96 well plate (Corning Life Sciences) and incubated for 30 minutes at 37° C to allow the reaction to develop. The absorbance at 562 nm was measured using a Magellan Tecan Sunrise plate reader and a standard curve of known protein concentration vs light absorbance was used to determine the concentration of rMOG in the elution. rMOG was diluted to a concentration of 1 mg/mL using sterile water in a 50 mL centrifuge tube.

2.5.7 X-ray sterilization of purified rMOG

The rMOG sample was placed in an ARAD 225 X-ray generator and given a dose of 50,000 cGy. Following this, the sample was taken to a laminar flow hood and aliquoted in sterile cryotubes at 1 mL per tube. Aliquots were stored at -20° C.

2.6 *In vivo* experiments

2.6.1 MOG-induced EAE in DA rats

rMOG (1mg/mL) was thawed and mixed 1:1 with complete Freund's adjuvant (CFA) (Sigma Aldrich). An emulsion was formed by pumping the mixture through a 24 gauge connector using two glass syringes. The emulsion was kept at 4° C and mixed every 2 hours until very viscous. Twelve, 12-week-old, female DA rats were ear marked and weighed before 10 rats were given an injection of 100 µL emulsion (containing 50µg rMOG) subcutaneously at the base of the tail.

2.6.1.1 Clinical scoring of EAE

Following immunization with rMOG, rats were weighed and clinically assessed daily and twice daily after the first symptoms were detected. Rats were assigned a score from the following scale: 0 = no sign of disease; 0.5 = distal limp tail; 1 = limp tail; 2 = mild paraparesis, ataxia; 3 = moderate paraparesis, occasional tripping; 3.5 = one hind limb is paralysed; 4 = complete hind limb paralysis; 5 =

complete hind limb paralysis and incontinence; 6 = moribund, difficulty breathing, does not eat or drink, front limb paralysis; 7 = dead. A clinical score of 6 was considered the humane endpoint of the experiment and any animals that reached this score were immediately euthanized. Rats that did not develop a clinical score of 6 were euthanized at peak clinical severity during the first or second phase of EAE. Rats were scored consistently by the same person to minimize variation.

2.6.1.2 Perfusion and harvesting of rat spinal cord

Rats were sacrificed by asphyxiation in a CO₂ chamber. Once determined to be dead by assessing pain and blink reflexes were absent the rats were quickly perfused with PBS followed by 4% PFA. First the rat was decapitated then, using a scalpel to open the skin and cut away surrounding tissue, the vertebral column was exposed. Using fine pointed scissors, a laminectomy was performed and the spinal cord was carefully lifted out of the spinal column and submerged in a 15 mL centrifuge tube containing 4% PFA. The cords were kept at 4° C for 24 hours to ensure the tissue was well fixed. For qPCR experiments, the cords were removed after perfusion with PBS and the lumbar portion was placed in a sterile bijou and frozen at -80° C. RNA extraction was then performed as described in section 2.4.1.2.

2.6.1.3 Preparing rat spinal cord for immunohistochemistry

The lumbar portions of fixed spinal cords were cut into 2 mm coronal sections using a rat brain matrix and microtome blade. Sections were collected in cassettes and dehydrated using a Leica TP 1020 Tissue Processor. Paraffin embedding of the sections was then performed using a Leica EG1160 Embedding Center. Consecutive 6 µm coronal sections were made from paraffin embedded spinal cords and mounted on Superfrost™ Plus microscope slides (Thermo Fisher Scientific).

2.6.2 Cortical injection of AAV6 viral vectors in Lewis rats

2.6.2.1 Stereotactic injections

These procedures were performed by Dr Claudia Wrsoz in collaboration with Prof Christine Stadelmann from the Neuropathology department at the University of Göttingen. Adult female Lewis rats (n=60) were anaesthetised by intraperitoneal injection with Xylazine and Ketamine (100 mg/kg and 5 mg/kg respectively). The scalp was shaved and, using a scalpel, the skin was opened with a sagittal cut from the eyes to ears to reveal the bregma. Rats were fixed in a stereotactic frame, holes were drilled through the skull (Dremel 300-1/5 driller) 2 mm posterior, and 2 mm lateral of each side of the bregma. Using a fine glass capillary ($\varnothing = 0.05\text{--}0.1$ mm) 1 μL adeno-associated virus (AAV) vector solution (containing 10^8 vectors) (shown in Figure 2.2) was injected 2.5 mm into the cortex of each hemisphere. Monastral Blue (Sigma-Aldrich) was added as a marker dye to trace the injection site. 6 rats were injected with AAV6-*egfp* vectors and 6 with AAV6-*Fgf9* vector per time point. Time points were 10 days, 30 days, 3 months, and 9 months. After surgery the wound was closed with sutures and the animals were allowed to recover until they were euthanized at each given time point.

2.6.2.2 Harvesting and preparing rat brain for immunohistochemistry

Animals were euthanized by lethal intraperitoneal injection of 200 μL 14% chloral hydrate. When dead, animals were quickly perfused with PBS followed by 4% PFA. The rats were then decapitated and the heads were perfused for a further 48 hours in 4% PFA at 4^o C. After perfusion, the brains were dissected from the skull a coronal section was made using a razor blade to cut several mm anterior and posterior of the injection as identified by Monastral Blue. These sections were dehydrated and processed for paraffin embedding. Using a Microtome (Leica Biosystems) 6 μm sections were made and mounted on Superfrost™ Plus microscope slides (Thermo Fisher Scientific).

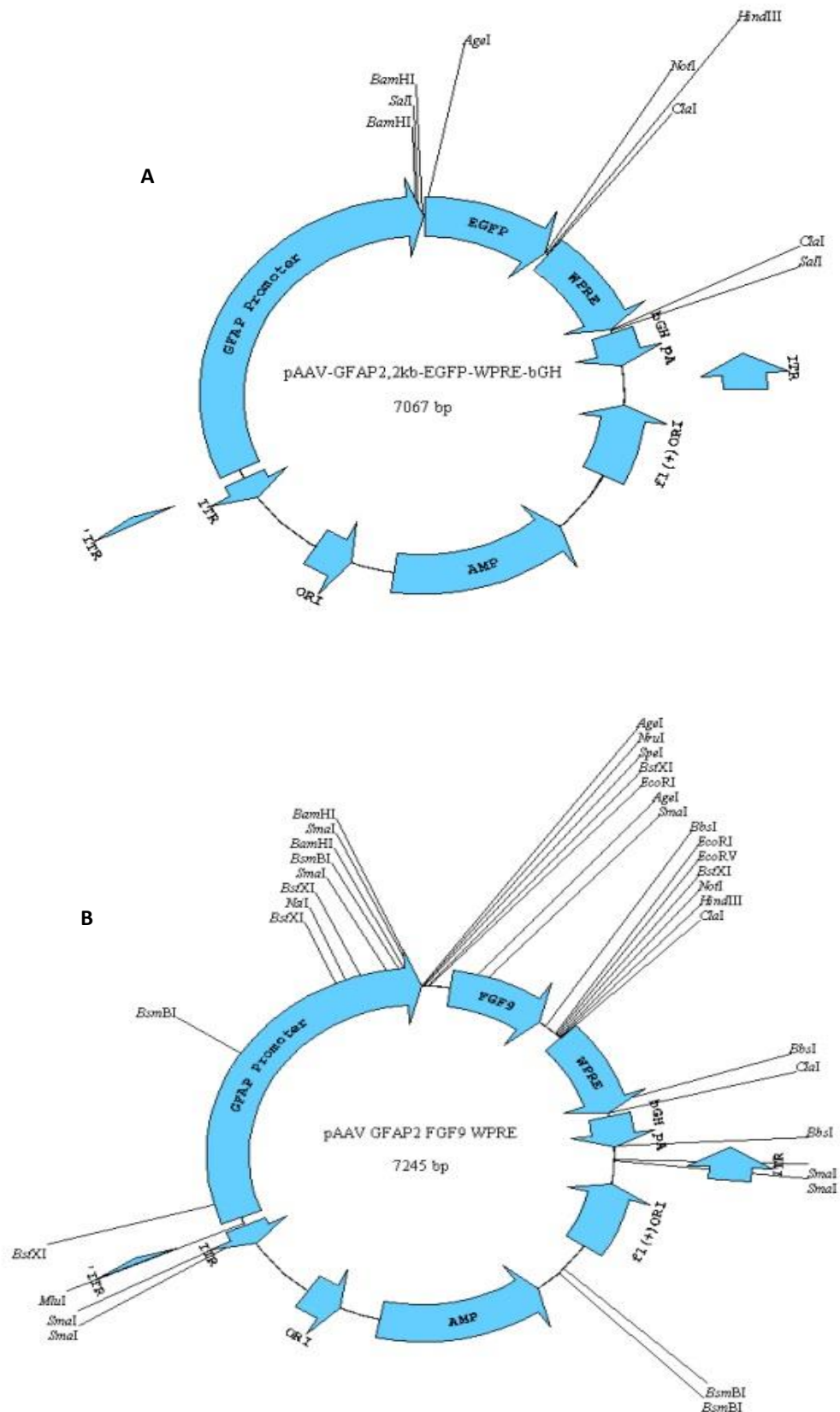


Figure 2.2. Adeno-associated viral vectors used in *in vivo* experiments. Infections were performed using (AAV-6)-based vectors containing the *Egfp* (pAAV-eGFP) (A) and *Fgf9* (pAAV-FGF9) (B) genes driven by the astrocyte GFAP promoter. These vectors also contain Woodchuck Hepatitis Virus Posttranscriptional Regulatory Element (WPRE) to enhance target gene expression.

2.6.3 Staining and imaging of rat brain and spinal cords

Immunohistochemical and immunofluorescence studies were performed on consecutive deparaffinized 5 μm sections after endogenous peroxidase was blocked with H_2O_2 /methanol. Antigen retrieval was performed using citrate buffer (pH 6.0) or EDTA buffer (pH 8.5) and non-specific antibody binding was blocked by incubating sections in 10% fetal calf serum. Primary antibodies against MOG, MBP, CNPase (2',3'-cyclic-nucleotide 3'-phosphodiesterase), MAG (myelin-associated glycoprotein), PLP (proteolipid protein), β -APP (beta-amyloid precursor protein), FGF9, and Sprouty2 were applied overnight at 4° C. After washing, appropriate horseradish peroxidase (HRP)-conjugated or fluorescently labelled secondary antibodies were applied simultaneously for 1 hour. Sections were incubated with DAB until staining was detected and cell nuclei were counterstained with haematoxylin. For myelin quantification, in AAV6-*Fgf9* lesions, FIJI image processing software was used to delineate lesions. Colour deconvolution software in FIJI was then used to select only the DAB staining and then the image was converted to binary to generate an image in which DAB staining appeared as black particles which could be measured with particle analysis. These data were then used to calculate the area of each lesion that was positive for myelin proteins. β -APP counts were obtained by counting β -APP⁺ axonal swellings in a grid from 6 different areas of each lesion at 40x magnification. Counts were performed twice.

2.7 Statistical analysis

Experimental data were analyzed using GraphPadPrism 5.0 (GraphPad Software, San Diego, CA, USA). Data were expressed as the means \pm standard deviation (SD). Two tailed T-tests and one-way analysis of variance (ANOVA) statistical analysis were performed with post hoc tests used where appropriate. Significance was set at $P < 0.05$.

CHAPTER THREE

**FEEDBACK INHIBITORS OF FGF9 IN MS AND
MYELINATING CULTURES**

3 FEEDBACK INHIBITORS OF FGF9 IN MS AND MYELINATING CULTURES

3.1 Introduction

FGFs play a role in every stage of embryonic development and accomplish their varied functions through the establishment of ligand gradients, activation of several signaling pathways, and an array of regulatory mechanisms (Ornitz and Itoh, 2015). The major positive and negative regulators of FGF signaling are discussed in section 1.2.4. Sproutys and DUSPs comprise two families of MAPK inhibitors that are induced by FGF signaling (Branney et al., 2009, Minowada et al., 1999). While DUSP1 and DUSP5 upregulation is a general response to ERK-MAPK signaling, Sprouty2 and Sprouty4 are only induced by ligation of IIIc isoforms of FGFRs, for which FGF9 is specific (Branney et al., 2009, Sylvestersen et al., 2011). DUSP6 expression requires FGF signaling through FGFR1 or FGFR2 (Li et al., 2007). Using the Sproutys and DUSPs as surrogate markers for FGF signaling could reveal which cell types are targets of FGF9 in MS and increase our understanding of its mechanisms of action.

Microarray analysis of FGF-treated myelinating cultures found Sprouty2, Sprouty4, DUSP5, and DUSP6, were significantly upregulated by FGF9 24 hours and 10 days after commencement of treatment (Table 3.1). FGF1 induced no significant changes in expression of these genes at 24 hours or 10 days. FGF2 induced upregulation at 24 hours but at 10 days, this effect had largely diminished. These findings suggest FGF9 signaling maintains higher levels of feedback inhibitor expression over a protracted period while signaling via other FGFs tails off. If the same is true in MS, this may mean that over time Sprouty/DUSP expression in lesions is a direct result of FGF9 signaling alone.

The aims of the experiments in this chapter were to analyse expression of FGF feedback inhibitors in MS lesions, and investigate the effects of FGF9 on feedback inhibitor expression *in vitro*. Human brain sections from patients with acute or chronic MS lesions, as well as healthy controls (Table 2.3), were stained with antibodies against Sprouty2 and Sprouty4 to assess in which condition feedback inhibitor expression was highest and how this related to FGF9 expression. Astrocytes, OLs, neurons, and macrophages were identified based on their

nuclear and cytoplasmic morphology. Some sections were double stained with cell-type specific antibodies to confirm which cells in the lesions were responding to FGF signaling. *In vitro* myelinating, OL, and astrocyte cultures were generated and treated with FGFs to assess negative-feedback inhibitor expression by qPCR and immunofluorescence.

Gene	FGF1		FGF2		FGF9	
	24 hours	10 Days	24 hours	10 Days	24 hours	10 Days
<i>Spry1</i>	1.66429	-1.13181	2.62865	1.15258	2.82015	3.20257
<i>Spry2</i>	1.39665	-1.34698	2.58598	1.16276	2.63593	3.76283
<i>Spry3</i>	-1.02506	-1.10525	1.01039	-1.13094	1.02613	1.03482
<i>Spry4</i>	1.59551	-1.10347	8.51173	1.28566	7.3989	5.58061

<i>Dusp1</i>	1.00992	1.0935	1.32224	1.19059	1.03682	1.63413
<i>Dusp2</i>	1.00202	-1.06506	1.18446	-1.01644	1.10998	-1.22667
<i>Dusp4</i>	2.27261	-1.1606	4.53533	-1.08873	4.8481	1.79124
<i>Dusp5</i>	1.38495	1.07075	8.21072	2.04495	6.81049	2.70486
<i>Dusp6</i>	1.57391	1.37269	5.51279	1.99727	5.01733	6.50911
<i>Dusp7</i>	1.07361	1.04134	1.54146	1.12073	1.52373	1.31843
<i>Dusp8</i>	-1.12153	-1.06968	-1.35298	-1.61927	-1.30864	-2.46719
<i>Dusp9</i>	1.01812	-1.03094	1.10596	1.00125	1.03068	1.02193
<i>Dusp10</i>	1.19886	-1.13546	1.69085	-1.27421	1.29386	1.03969
<i>Dusp16</i>	1.05861	-1.12203	1.27194	-1.03076	1.25538	1.02237

<i>Fgfr1</i>	-1.03445	-1.02274	-1.17369	1.10437	-1.12936	1.18193
<i>Fgfr2</i>	-1.34399	1.02231	-1.39775	-1.04508	-1.31047	-1.03827
<i>Fgfr3</i>	-1.08078	-1.00257	-1.35427	1.10586	-1.33396	2.39353
<i>Fgfr4</i>	-1.18494	1.0023	-1.25267	1.00702	-1.28403	-1.07927

Table 3.1. Differentially expressed genes in rat myelinating cultures treated with FGF1, 2, or 9, for 24 hours and 10 days. Microarray analysis of FGF-associated gene expression shows that negative feedback inhibitors, Sproutys and Dusps (fold changes marked in red), are similarly upregulated by FGF2 and FGF9 after 24 hours but only FGF9 maintains negative feedback regulator expression after 10 days. Data derived from Microarray performed by Lindner et al., 2015.

3.2 Results

3.2.1 FGF-feedback inhibitor expression was increased in acute and chronic MS

3.2.1.1 There was constitutive expression of FGF-feedback inhibitors in healthy human brain

FGF9 is present in the adult CNS of humans and rats (Lindner et al., 2015, Nakamura et al., 1999, Nakamura et al., 1997). To determine levels of constitutive feedback inhibitor expression in healthy brains, sections were stained with antibodies against Sprouty2 and Sprouty4. Expression was categorised by region and cell type and results are shown in Table 3.2 and representative images in Figure 3.1. FGF9 staining was mainly associated with neurons in grey matter and occasionally astrocytes of the grey and white matter. OL expression of FGF9 was rare in control brains. Sprouty2 and Sprouty4 staining deposition overlapped with areas of FGF9 expression and the same cell types expressing FGF9 were usually immunoreactive for Sprouty2 and Sprouty4. Sprouty2 staining was more pronounced and appeared in more cells than Sprouty4.

Control Cases	Region	FGF9	Sprouty2	Sprouty4
132-92-11	Grey Matter	Neurons	Neurons	Neurons
	White Matter	Astrocytes	Astrocytes	0
421-92-5	Grey Matter	Neurons	Neurons	Neurons
	White Matter	0	Astrocytes	0
8-04-1	Grey Matter	Neurons	Neurons	Neurons
	White Matter	0	Astrocytes	0
579-91-3	Grey Matter	Neurons	Neurons	Neurons
	White Matter	Astrocytes, OLs	Astrocytes, OLs	Astrocytes, OLs
28-03-2	Grey Matter	Neurons	Astrocytes, Neurons	0
	White Matter	OLs	Astrocytes	0
68-93-4	Grey Matter	Neurons	Astrocytes, Neurons	Neurons
	White Matter	Astrocytes	Astrocytes	0

Table 3.2. Characterisation of FGF9, Sprouty2, and Sprouty4 staining in human control brain sections. Sections from archived, formalin-fixed, paraffin embedded tissues processed for immunohistochemistry and stained with antibodies against FGF9, Sprouty2, and Sprouty4. Constitutive FGF9 expression is common to neurons in grey matter and less frequently, astrocytes and OLs in white matter. Sprouty2 and Sprouty4 expression profiles largely matched that of FGF9, but Sprouty4 staining was present in fewer cases than Sprouty2. 0 denotes areas where no staining was detected.

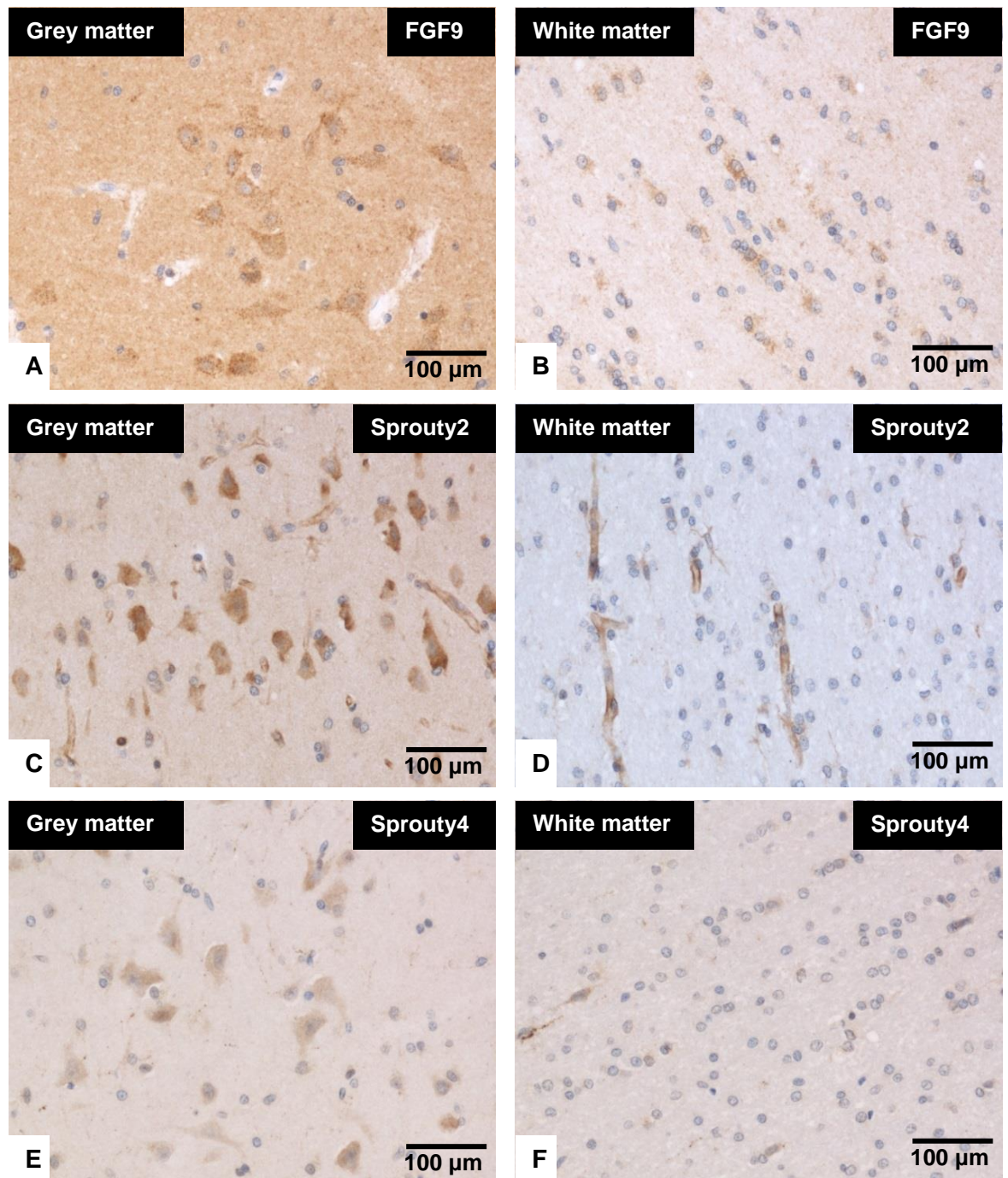


Figure 3.1 FGF9 and Sproutys were associated with neurons in healthy adult brains. Representative images of healthy brain stainings from case 132-92-11. Sections from archived, formalin-fixed, paraffin embedded tissues processed for immunohistochemistry. Antibodies against FGF9 (A, B), Sprouty2 (C, D), and Sprouty4 (E, F) stained serial sections from grey (A, C, E) and white (B, D, F) matter regions in healthy control brains. Cells that were positive for each protein were identified morphologically by DAB deposition under light microscopy. All three proteins are expressed by neurons in GM and in a small number of astrocytes and OLS in WM.

3.2.1.2 FGF-feedback inhibitor expression was highest in acute MS lesions

The previous study showed a correlation between the cell types expressing FGF9 and those expressing feedback inhibitors in healthy brains, suggesting autocrine FGF signaling. Lindner et al., 2015 showed astrocytes and OLs are the main source of FGF9 in acute MS lesions, and FGF9 signaling in astrocytes was responsible for inhibition of myelination seen in myelinating cultures. This indicated that astrocytes in MS lesions will upregulate feedback-inhibitor expression in response to FGF9.

The next step was to examine a variety of MS lesions and characterise feedback inhibitor expression in different regions of each. Astrocytes were the main cells associated with Sprouty2 and Sprouty4 staining (Table 3.3). Where macrophages were present they were strongly FGF9⁺, Sprouty2⁺, and Sprouty4⁺ to a lesser extent. Examination of NAWM in acute cases showed FGF9 and Sprouty expression profiles similar to those seen in healthy controls (Figure 3.2 A - D). FGF9 staining was diffuse and punctate throughout the NAWM, and weak Sprouty2 and Sprouty4 staining was observed mostly in OLs and infrequently in astrocytes. FGF9, Sprouty2, and Sprouty4 staining was common in hypertrophic astrocytes in acute lesion cores (Figure 3.2 F - H). Where they were present, OLs, stained for FGF9 and the Sproutys to a variable degree. Overall, acute lesion rims and cores displayed similar feedback inhibitor expression.

FGF9 staining appeared mostly in astrocytes in the core of a balo lesion, and astrocytes and macrophages around the active rim (Figure 3.3 F, J). Sprouty2 staining was strong in astrocytes and macrophages in both the lesion core and rim (Figure 3.3 G, K). Sprouty4 was also in astrocytes and macrophages but the staining was much weaker than Sprouty2 (Figure 3.3 H, L). In case 70-93-6, astrocytes and OLs were FGF9⁺ in the early active lesion whereas astrocytes and macrophages were FGF9⁺ in the late active lesion (Table 3.3). This was somewhat mirrored in Sprouty expression: astrocytes and OLs were Sprouty2⁺ in the early active lesion while weaker Sprouty4 staining was only observed in astrocytes (Figure 3.4). Astrocytes and macrophages were Sprouty2⁺ and Sprouty4⁺ in the late active lesion respectively. In normal-appearing grey matter (NAGM) neurons stained positive for FGF9, Sprouty2, and Sprouty4. Large distended neurons with irregular shapes were found in grey matter adjacent to the

lesion. These cells, thought to be a result of axonal transection with the lesion, stained intensely for FGF9, Sprouty2, and Sprouty4 (Figure 3.4).

Acute Cases	Region	FGF9	Sprouty2	Sprouty4
581-96-7A	NAWM	-	0	OLs
	Early active lesion core	-	0	0
	Early active lesion rim	-	0	0
	Late active lesion	-	Astrocytes, OLs	Astrocytes
90-09-6	NAWM	Astrocytes, OLs	Astrocytes, OLs	Astrocytes
	Inactive lesion core	Astrocytes	Astrocytes	Astrocytes
	Active lesion rim	Astrocytes	Astrocytes	Astrocytes
A01-144	NAWM	Diffuse extracellular	0	0
	Balo lesion core	Astrocytes, OLs	Astrocytes, Macrophages	Astrocytes, OLs
	Balo lesion rim	Macrophages	Astrocytes, Macrophages	Astrocytes, Macrophages
S403-97	NAWM	0	0	0
	Early active lesion	-	Astrocytes, Macrophages	0
	Late active lesion	-	Astrocytes, Macrophages	Astrocytes
270-99-2	NAWM	-	Astrocytes	Astrocytes
	Early active lesion	-	Astrocytes	Astrocytes
	Late active lesion	-	Astrocytes	Astrocytes
Spanien C2	NAWM	-	0	0
	Inactive lesion	Astrocytes	Astrocytes	Astrocytes
70-93-6	NAWM	Astrocytes	Astrocytes, OLs	Astrocytes
	Early active lesion core	Astrocytes, OLs	Astrocytes, OLs	Astrocytes
	Early active lesion rim	Astrocytes	Astrocytes	Astrocytes
	Late active lesion	Astrocytes, Macrophages	Astrocytes, Macrophages	Astrocytes
	NAGM	Neurons	Astrocytes, Neurons	Neurons
	GM at subcortical lesion	Neurons	Neurons	Neurons

Table 3.3. Characterisation of FGF9, Sprouty2 and Sprouty4 staining in acute MS lesions. Sections from archived, formalin-fixed, paraffin embedded tissues processed for immunohistochemistry. Sprouty2 stained intensely in astrocytes in active lesion cores and lesion rims while very little staining was seen in NAWM. In both cases where they were present, infiltrating macrophages stained for FGF9 and Sproutys. Sprouty4 had a similar staining pattern to Sprouty2 but was consistently weaker. 0 denotes areas where no staining was detected, - denotes cases not imaged.

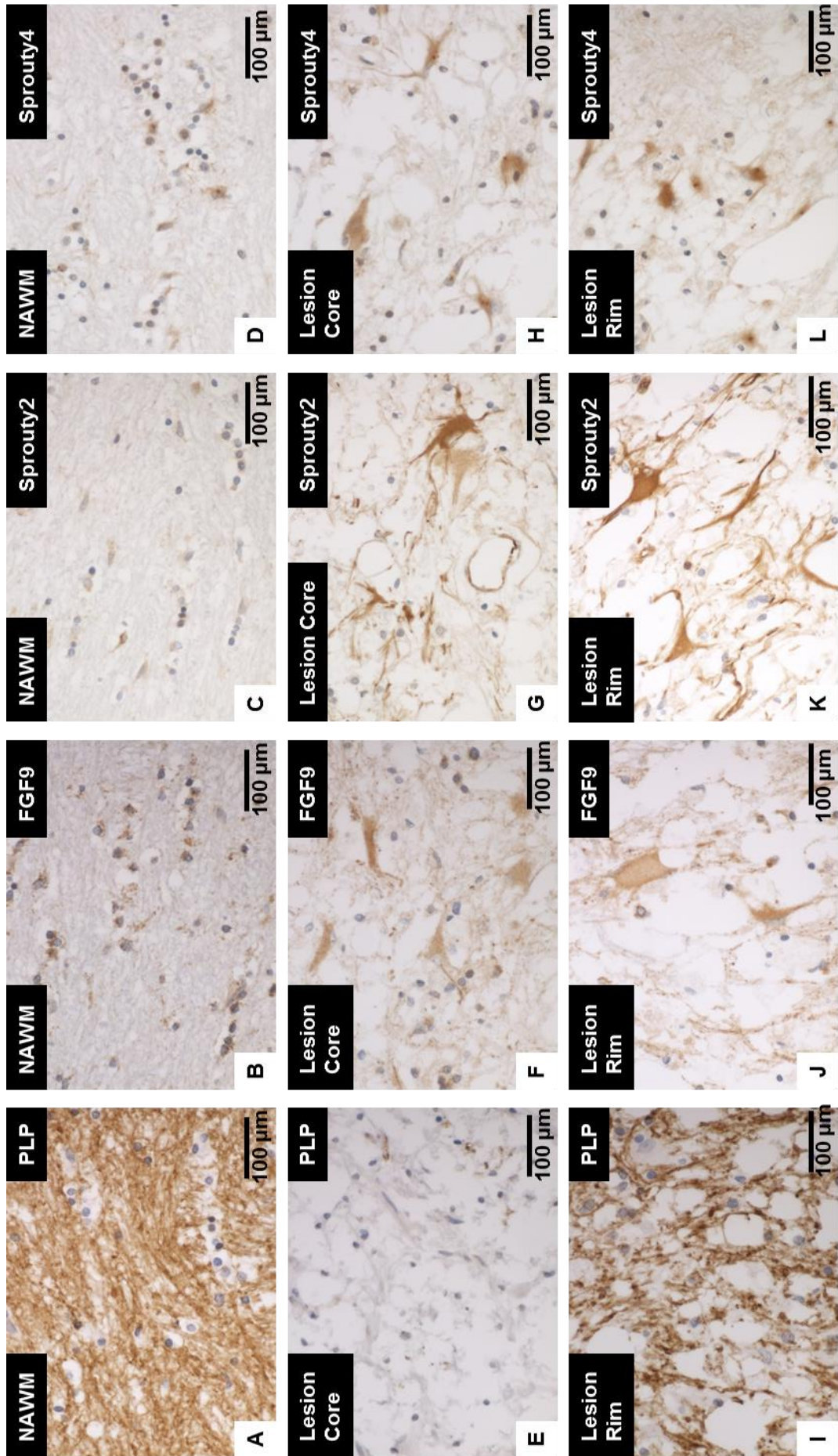


Figure 3.2 FGF9 and Sproutins label astrocytes in acute lesions. Representative images from acute MS case 90-09-06. Sections from archived, formalin-fixed, paraffin embedded tissues processed for immunohistochemistry. Antibodies against PLP (A, E, I), FGF9 (B, F, J), Sproutin2 (C, G, K), and Sproutin4 (D, H, L) stained areas of NAWM (A – D), lesion cores (E – H), and lesion rim (I – L). Demyelinated and demyelinating areas are associated with astrocytic expression of FGF9 and FGF-feedback inhibitors, Sproutin2 and Sproutin4.

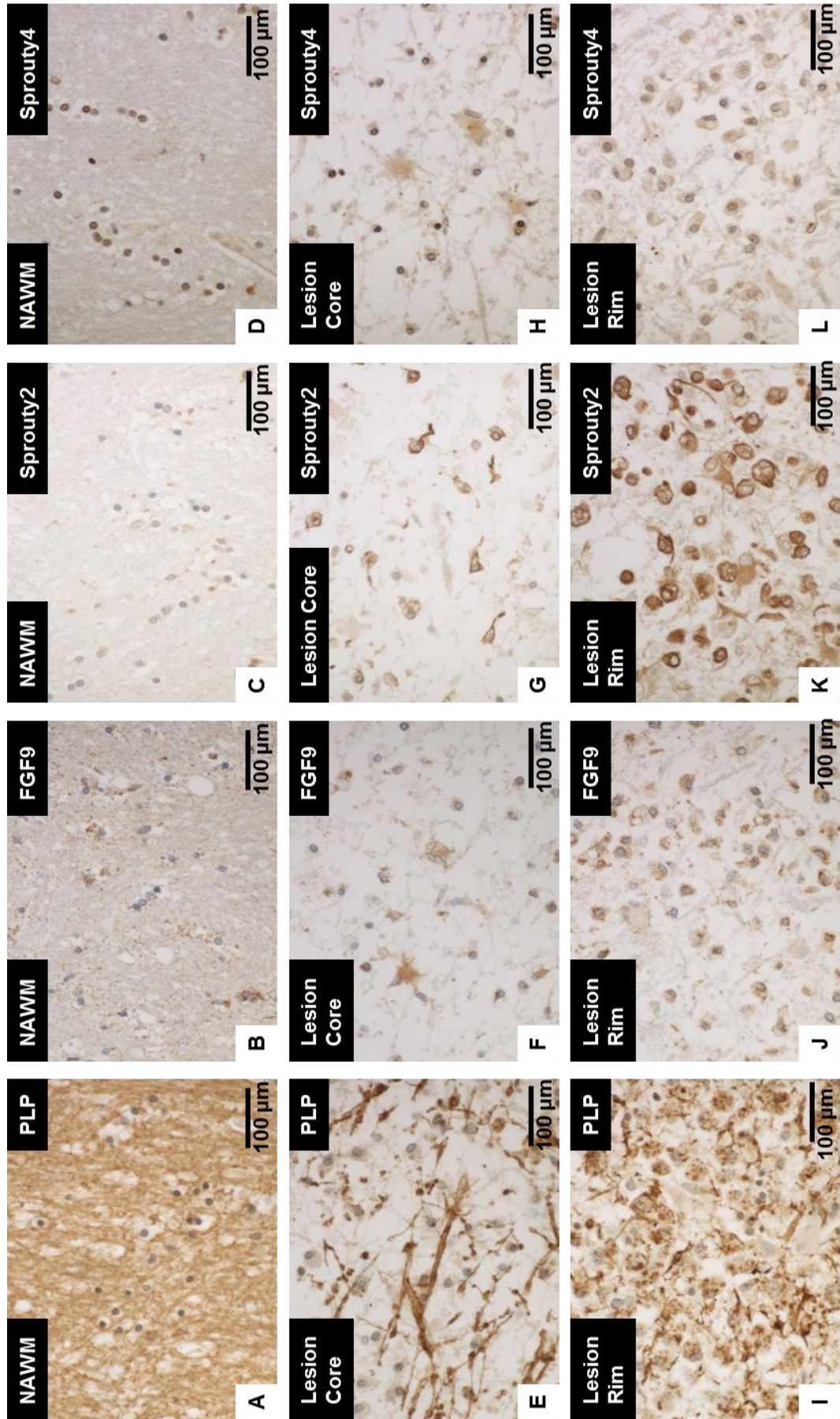


Figure 3.3 FGF9 and Sproutin label astrocytes and macrophages in Balb/c concentric sclerosis. Representative images from case A01-144. Sections from archived, formalin-fixed, paraffin embedded tissues processed for immunohistochemistry. Antibodies against PLP (A, E, I), FGF9 (B, F, J), Sproutin2 (C, G, K), and Sproutin4 (D, H, L) stained areas of NAWM (A – D), lesion cores (E – H), and lesion rim (I – L). FGF9 and feedback inhibitors are present in macrophages and astrocytes in lesion core but much more abundantly in the lesion rim.

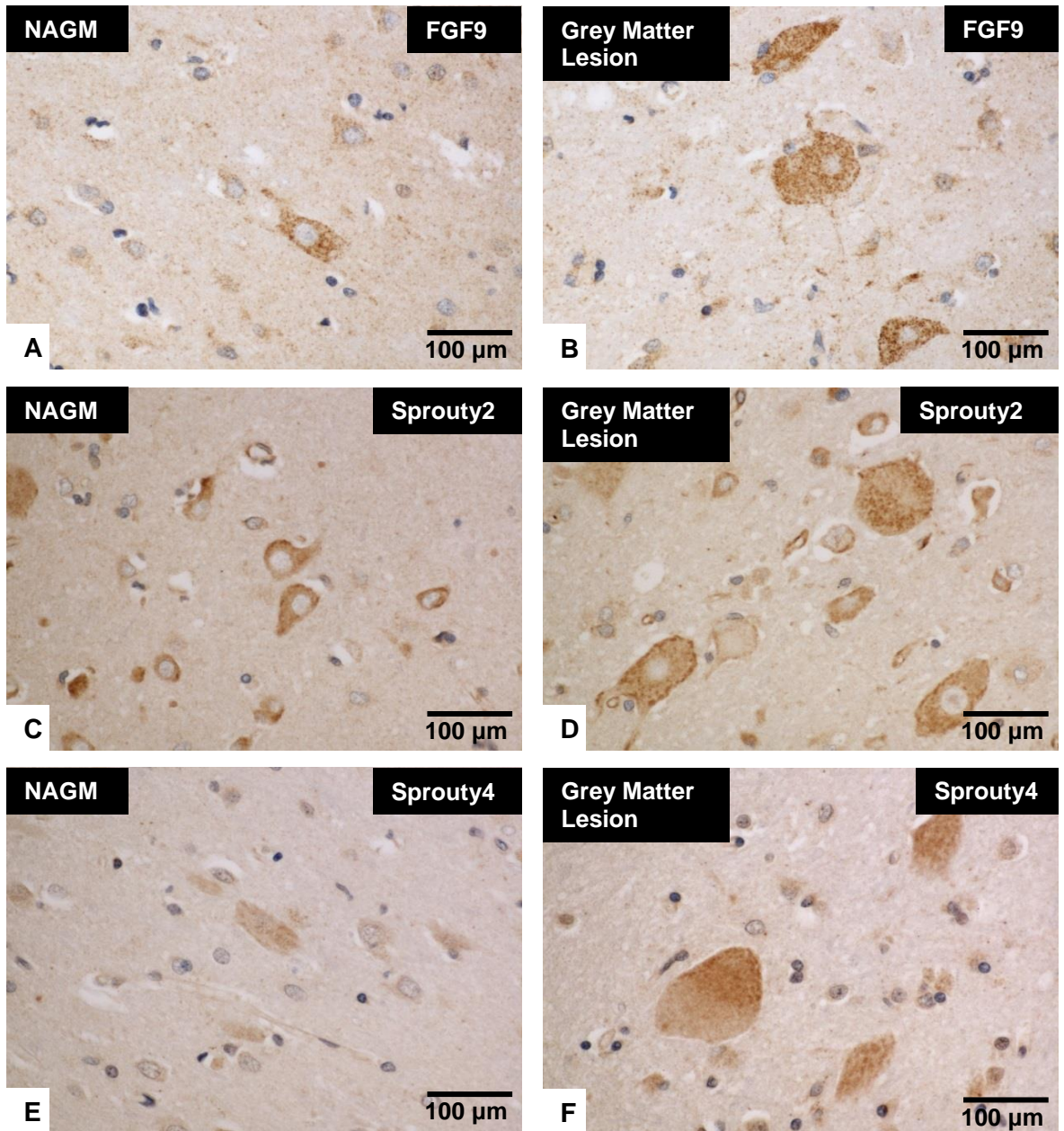


Figure 3.4 Swollen neurons in a grey matter lesion from case 70-93-6 displayed intense granular staining for FGF9 and the Sproutins. Sections from archived, formalin-fixed, paraffin embedded tissues processed for immunohistochemistry. Antibodies against FGF9, Sprouty2, and Sprouty4 were used to stain serial sections from different regions within and around lesion sites. Dense, granular FGF9, Sprouty2, and Sprouty4 staining was observed in swollen neurons in a grey matter lesion.

3.2.1.3 FGF-feedback inhibitor expression is a feature of chronic MS but is less pronounced compared to acute disease

FGF9 expression is more common in acute MS lesions than chronic lesions (Lindner et al., 2015). This suggests that feedback inhibitor expression would be less common in chronic lesions than acute. Imaging of chronic lesions showed this to be the case. FGF9 stained mainly astrocytes in white matter lesions and neurons in cortical lesions (Table 3.4). As in acute lesions, Sprouty2 expression closely mirrored that of FGF9 and staining was generally less intense for FGF9 and Sprouty2 versus acute lesions. Sprouty4 staining was detected in astrocytes in only a few of the chronic cases. FGF9 and Sprouty2 staining was more common in NAWM than in acute MS or healthy controls (Table 3.4). Representative images of staining in a chronic white matter lesion from case 146-01-8 are shown in Figure 3.5

The next step in these experiments was to perform double stainings and examine sections using confocal microscopy. Case 67-05-9 was stained with MAP2 (neuronal marker), GFAP (astrocytic marker), FGF9, and Sprouty2 antibodies. Imaging revealed prominent FGF9 staining in neurons of NAGM (Figure 3.6 A) and swollen neurons in a cortical lesion (Figure 3.6 B). NAWM astrocytes lacked FGF9 staining (Figure 3.6 C). Astrocytes in a white matter lesion contained variable amounts of granular FGF9 staining over a diffuse background of extracellular punctate FGF9 (Figure 3.6 D). Sprouty2 was also absent from NAWM (Figure 3.6 E) but stained intensely in astrocyte cell bodies as well as diffusely in the extracellular background of the white matter lesion (Figure 3.6 F).

Chronic Cases	Region	FGF9	Sprouty2	Sprouty4
146-01-8	NAWM	Astrocytes	Astrocytes	0
	Lesion core	0	Astrocytes	Astrocytes
	Lesion rim	Astrocytes	Astrocytes	Astrocytes
	NAGM	Neurons	Neurons	0
	Cortical lesion	Neurons	Neurons	0
67-05-9	NAWM	Astrocytes	0	0
	Lesion core	Astrocytes	Astrocytes	Astrocytes
	Lesion rim	Astrocytes	Astrocytes	0
	NAGM	Neurons	Neurons	Neurons
	Cortical lesion	Neurons	Neurons	Neurons
39-03-15	NAWM	Astrocytes	Astrocytes	0
	Lesion core	Astrocytes	Astrocytes	0
	Lesion rim	Astrocytes	Astrocytes	Astrocytes
144-90-3	NAWM	Astrocytes, OLs	0	0
	Lesion core	0	Astrocytes	0
	Lesion rim	Astrocytes	Astrocytes	0
244-94-7	NAWM	Astrocytes, OLs	Astrocytes	0
	Lesion core	0	Astrocytes	0
	Lesion rim	Astrocytes	Astrocytes	0
285-81-1	NAWM	0	0	Astrocytes
	Lesion core	0	0	Astrocytes
	Lesion rim	0	0	Astrocytes
72-83-6	NAWM	0	0	0
	Lesion core	0	Astrocytes	0
	Lesion rim	0	0	0

Table 3.4. Characterisation of FGF9, Sprouty2 and Sprouty4 staining in chronic MS lesions. Sections from archived, formalin-fixed, paraffin embedded tissues processed for immunohistochemistry. FGF9 and Sprouty2 stained astrocytes in lesion rims and was more common in NAWM of chronic cases than acute cases. Staining with all three antibodies was generally less intense than that seen in the acute lesions. Again, Sprouty4 had a similar staining pattern to Sprouty2 but was weaker in most cases. 0 denotes areas where no staining was detected.

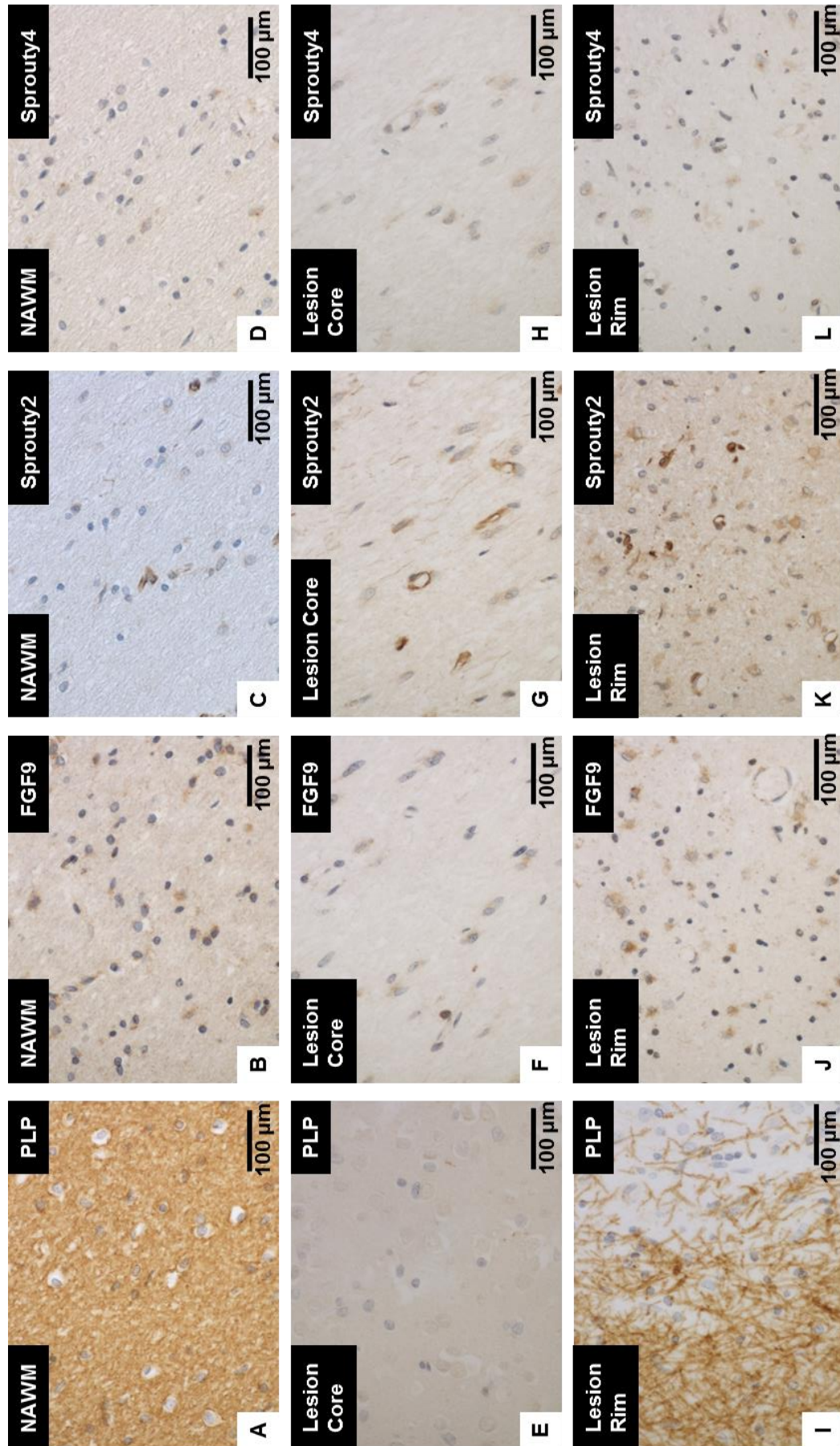


Figure 3.5 Representative images from chronic MS case 146-01-8. Archived formalin-fixed, paraffin embedded tissue sections were cut in 5 µm thick sections and processed for immunohistochemistry. Antibodies against PLP (A, E, I), FGF9 (B, F, J), Sprouty2 (C, G, K), and Sprouty4 (D, H, L) stained areas of NAWM (A – D), lesion cores (E – H), and lesion rim (I – L). FGF9 and feedback inhibitors staining is absent in NAWM but can be seen in some astrocytes of the lesion core and rim to an equal degree.

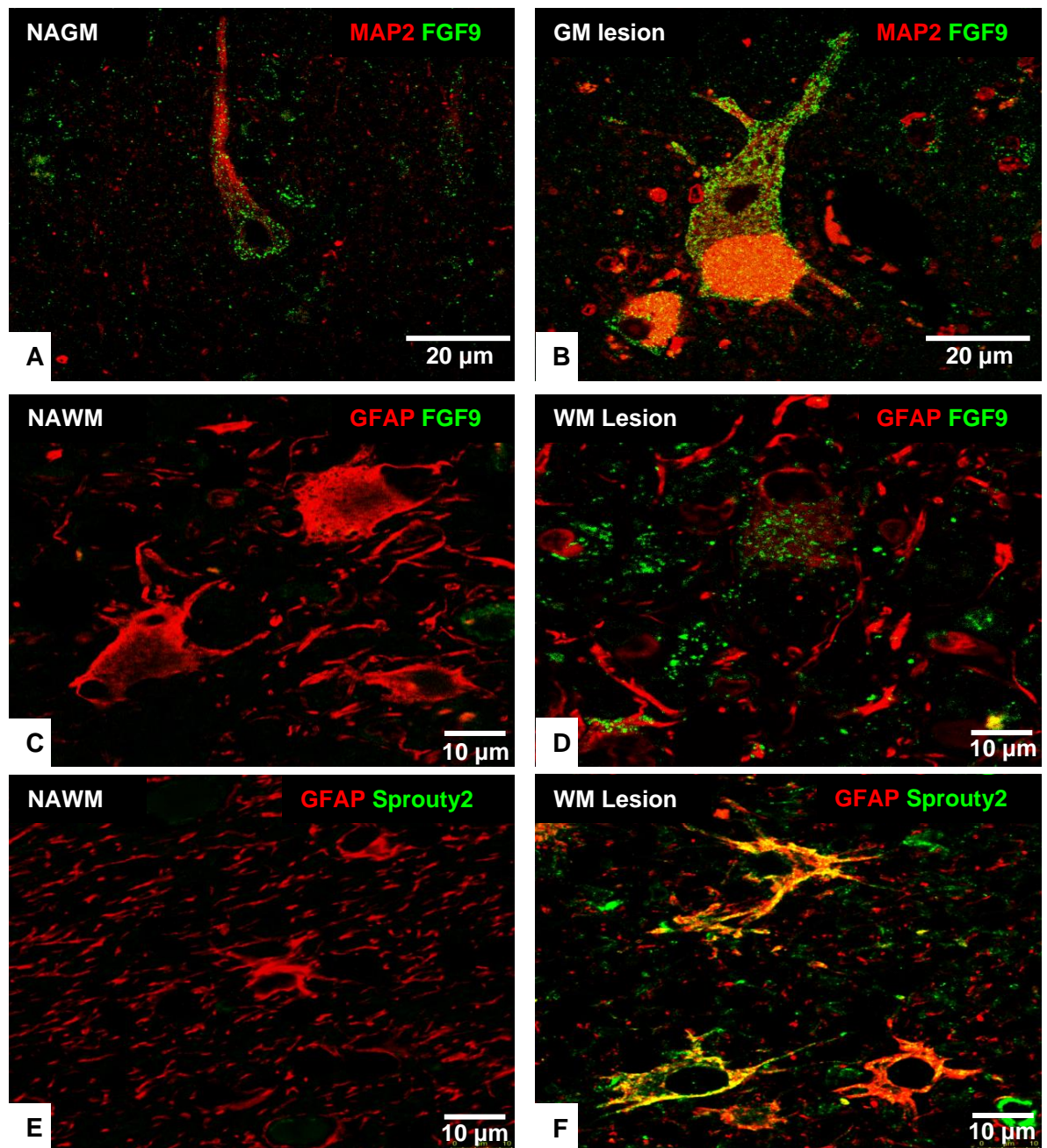


Figure 3.6 FGF9 and Sprouty2 colocalized in astrocytes in white matter lesions. Images from chronic case 67-05-9. Sections from archived, formalin-fixed, paraffin embedded tissues processed for immunofluorescence. Antibodies against FGF9, Sprouty2, MAP2, and GFAP were used to stain neurons and astrocytes. Neurons in NAGM and damaged-appearing neurons in GM lesion stain with FGF9 (A, B) Astrocytes in NAWM are negative for FGF9 (C) and Sprouty2 (E) but in WM lesions these cells stain strongly for FGF9 (D) and Sprouty 2 (F). Diffuse extracellular staining with FGF9 and Sprouty2 occurs within lesions.

3.2.2 Assessing feedback-inhibitor expression in myelinating cultures

3.2.2.1 FGF9 induced feedback-inhibitor expression in myelinating cultures while FGF1 and FGF2 did not

The previous sections showed that FGF-feedback inhibitor expression was increased in MS and correlated with cells and regions of FGF9 expression. To investigate the effects of FGF9 on cells of the CNS directly, feedback inhibitor and FGFR expression in myelinating cultures was assessed. Primers for rat *Spry2*, *Spry4*, *Dusp5*, *Dusp6*, *Fgfr1*, *Fgfr2*, and *Fgfr3* were designed. Myelinating cultures were generated as described in section 2.2, followed by treatment with 100 ng/ mL FGF1, 2, or 9 for 24 hours from DIV 18, then processed for qPCR as described in section 2.4. According to results from the microarray (Table 3.1), FGF1 and FGF2 should act as negative and positive controls for feedback inhibitor expression respectively.

Results from qPCR analysis showed that all four feedback inhibitors were upregulated after 24 hours by FGF9 but not FGF1 or FGF2 (Figure 3.7 A - D). *Spry2* expression was increased 5.1 ± 1.7 fold vs control, *Spry4* was increased 11.2 ± 5.9 fold, *Dusp5* was increased 10.5 ± 4.1 fold, and *Dusp6* was increased 6.2 ± 1 fold. Feedback inhibitor expression following treatment with FGF1 and FGF2 never varied far from baseline. Looking at *Fgfr* expression in these same samples revealed no changes in cultures treated with FGF1 or FGF2. However, there was downregulation of *Fgfr2* and *Fgfr3* following FGF9 treatment (Figure 3.7 E – F). These changes were significant but minor as *Fgfr2* expression only fell -2.1 ± 1 fold and *Fgfr3*, -2 ± 0.4 fold.

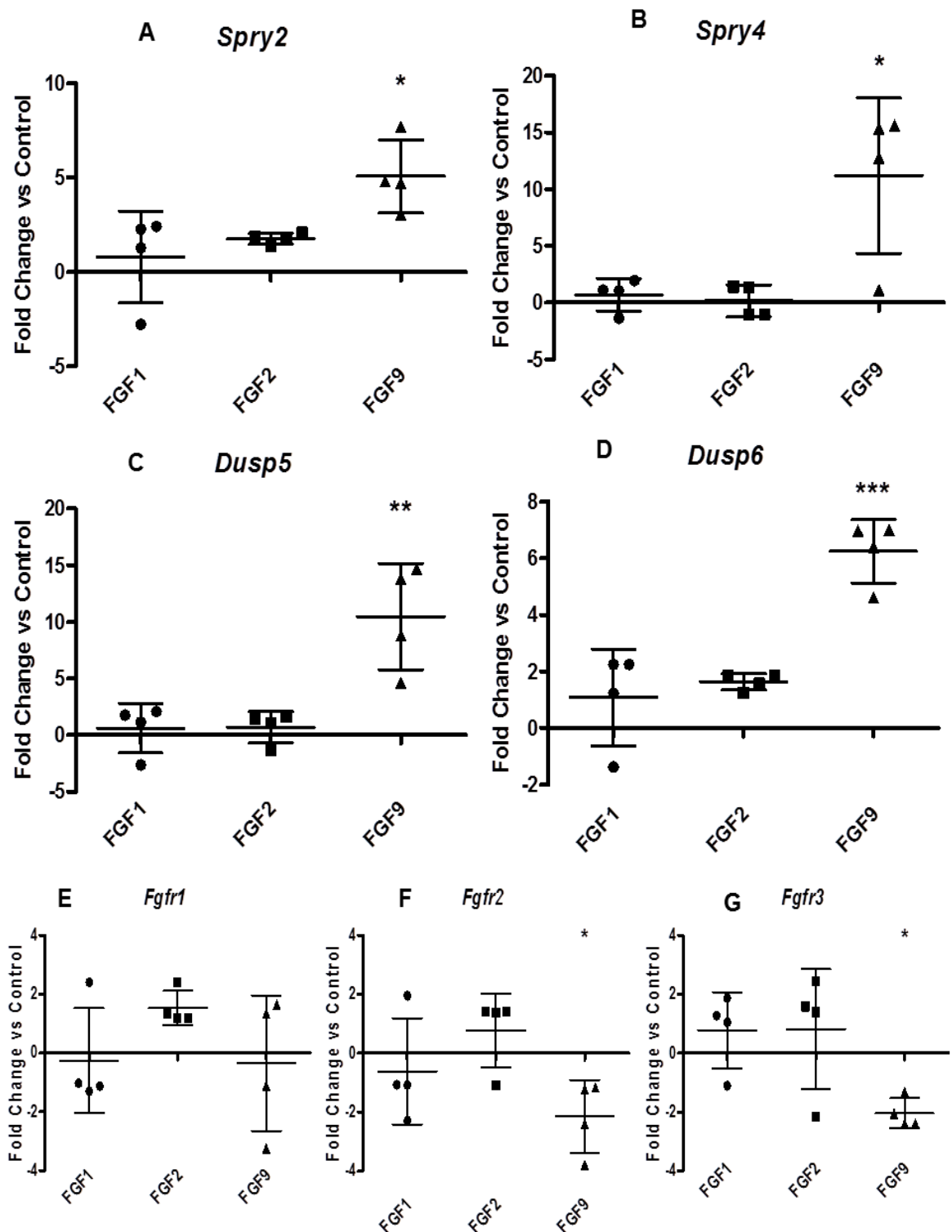


Figure 3.7. Feedback inhibitor expression was increased and FGFR expression decreased in myelinating cultures treated with FGF9. Myelinating cultures were treated with 100 ng/mL recombinant human FGF1, 2, or 9 for 24 hours on DIV 18. Cells were lysed and processed for RNA extraction and cDNA synthesis. qPCR was performed using primers for *Spry2*, *Spry4*, *Dusp5*, *Dusp6*, *Fgfr1*, *Fgfr2*, *Fgfr3* with *Gapdh* as the housekeeping standard. Treatment with FGF9 induced variable but significant upregulation of *Sprys* and *Dusps* (A – D) versus control cultures while FGF1 and FGF2 had no effect. *Fgfr2* and *three* were downregulated by FGF9 but not FGF1 or FGF2 and *Fgfr1* expression was unaffected by any of the FGFs tested (E – G). Fold changes in gene expression are shown relative to untreated control values, data presented are the means \pm SD. This experiment was performed four times. *, $p < 0.05$, **, $p < 0.01$ ***, $p < 0.001$ (one-way ANOVA with Dunnett's Multiple Comparison Test performed on delta CT values).

3.2.2.2 Mature OLs, OPCs, and neurons responded to FGF2 and FGF9

Purified cultures containing single cell types were produced to elucidate cell-type specific responses to FGF9. These cultures were treated with FGFs for 24 hours as in the previous section. Firstly, OLs were cultured from P1 rat cortices as described in section 2.2.3 then after 6 days in culture, OLs fully differentiated and were treated with FGF1, 2, and 9. Similar upregulation of feedback inhibitors was observed following treatment with FGF2 and FGF9, while FGF1 had no significant effect (Figure 3.8 A – D). *Spry2* expression increased 2.9 ± 0.5 fold after FGF2 and 2.4 ± 0.7 fold after FGF9. *Spry4* expression increased 16.1 ± 5.4 fold after FGF2 and 12.9 ± 3.7 fold after FGF9. *Dusp5* expression increased 13.6 ± 8.3 fold after FGF2 and 4.9 ± 2.5 fold after FGF9. *Dusp6* expression increased 11.7 ± 2.5 fold after FGF2 and 8.33 ± 0.8 fold after FGF9. *Fgfr2* and *Fgfr3* expression were downregulated following treatment with FGF2 and FGF9 but not FGF1 (Figure 3.8 E – G). *Fgfr2* was downregulated 6.6 ± 1.3 fold after FGF2 and 4.6 ± 0.7 fold after FGF9. *Fgfr3* was downregulated 7.3 ± 5.5 fold after FGF2 and 1.9 ± 1.3 fold after FGF9.

OPCs treated with FGFs from DIV 2, as described in section 2.2.5.7, displayed a similar but less pronounced effect on feedback inhibitor expression than fully differentiated OLs. (Figure 3.9 A – D). *Spry2* was upregulated 2.6 ± 0.1 fold by FGF2 and 4.6 ± 1.9 fold by FGF9. *Spry4* was upregulated 7.5 ± 3.5 fold by FGF2 and 8.7 ± 5.8 fold by FGF9. *Dusp5* was upregulated 38 ± 42.6 fold by FGF2, and *Dusp6* was upregulated 9.1 ± 2.3 fold by FGF2 and 5.7 ± 2.1 fold by FGF9. *Fgfr2* expression was downregulated -4 ± 3.5 fold by FGF2 and -3.9 ± 2.7 fold by FGF9, *Fgfr1* and 3 expression were unchanged following treatment (Figure 3.9 E – G).

Enriched neuronal cultures were generated as described in section 2.2.6 and treated with FGFs for 24 hours. Feedback inhibitor expression was similar following FGF2 and FGF9 treatment (Figure 3.10). *Spry2* was upregulated 1.9 ± 0.2 fold by FGF2 and 1.9 ± 0.3 fold by FGF9. *Spry4* was upregulated 10.3 ± 1.5 fold by FGF2 and 12.6 ± 5.9 fold by FGF9. *Dusp5* was upregulated 2.6 ± 1 fold by FGF2, and *Dusp6* was upregulated 4.2 ± 0.7 fold by FGF2 and 3.7 ± 1.7 fold by FGF9. *Dusp5* was not upregulated by FGF9 and *Spry4* was the only feedback-inhibitor upregulated by FGF1, 3.68 ± 1.7 fold.

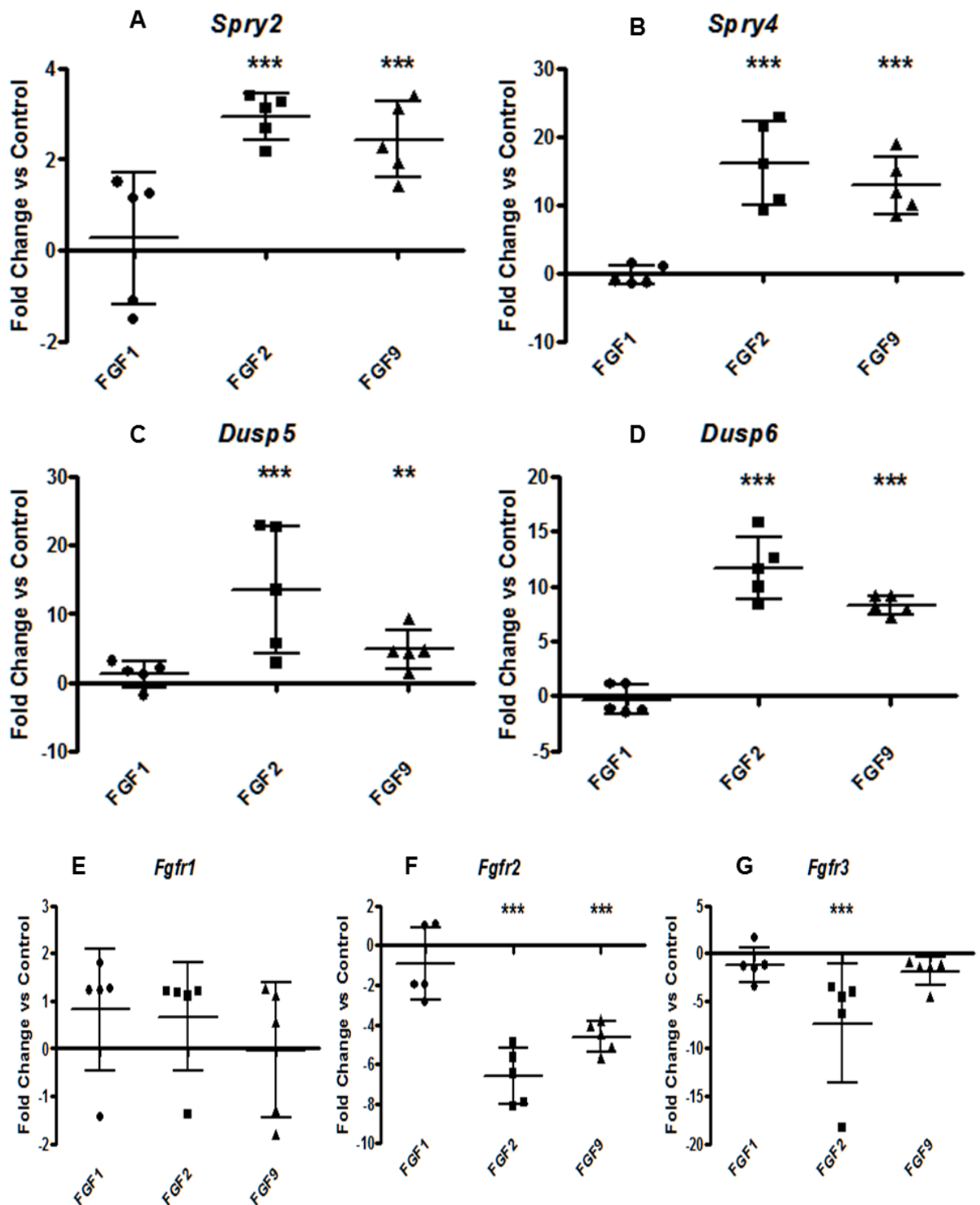


Figure 3.8. Mature OLs upregulated feedback inhibitors and downregulated *Fgfr2* when treated with FGF2, and 9. Oligodendrocytes were cultured as described in section 2.2.3 and maintained in Sato's media for four days without growth factors to allow them to differentiate. OLs were treated for 24 hours with 100 ng/mL FGF1, 2, or 9. Cells were lysed and processed for RNA extraction and cDNA synthesis. qPCR was performed using primers for *Spry2*, *Spry4*, *Dusp5*, *Dusp6*, *Fgfr1*, *Fgfr2*, *Fgfr3* with *Gapdh* as the housekeeping standard. All feedback inhibitors of FGF signaling were induced by FGF2 and FGF9 (A – D). *Fgfr1* expression was unaffected by FGF treatment (E). FGF2 and FGF9 downregulated *Fgfr2* while FGF1 had no effect (F) and only FGF2 downregulated *Fgfr3* (G). Fold changes in gene expression are shown relative to untreated control values, data presented are the means \pm SD. This experiment was performed five times. **, $p < 0.01$ ***, $p < 0.001$ (one way ANOVA with Dunnett's Multiple Comparison Test performed on delta CT values).

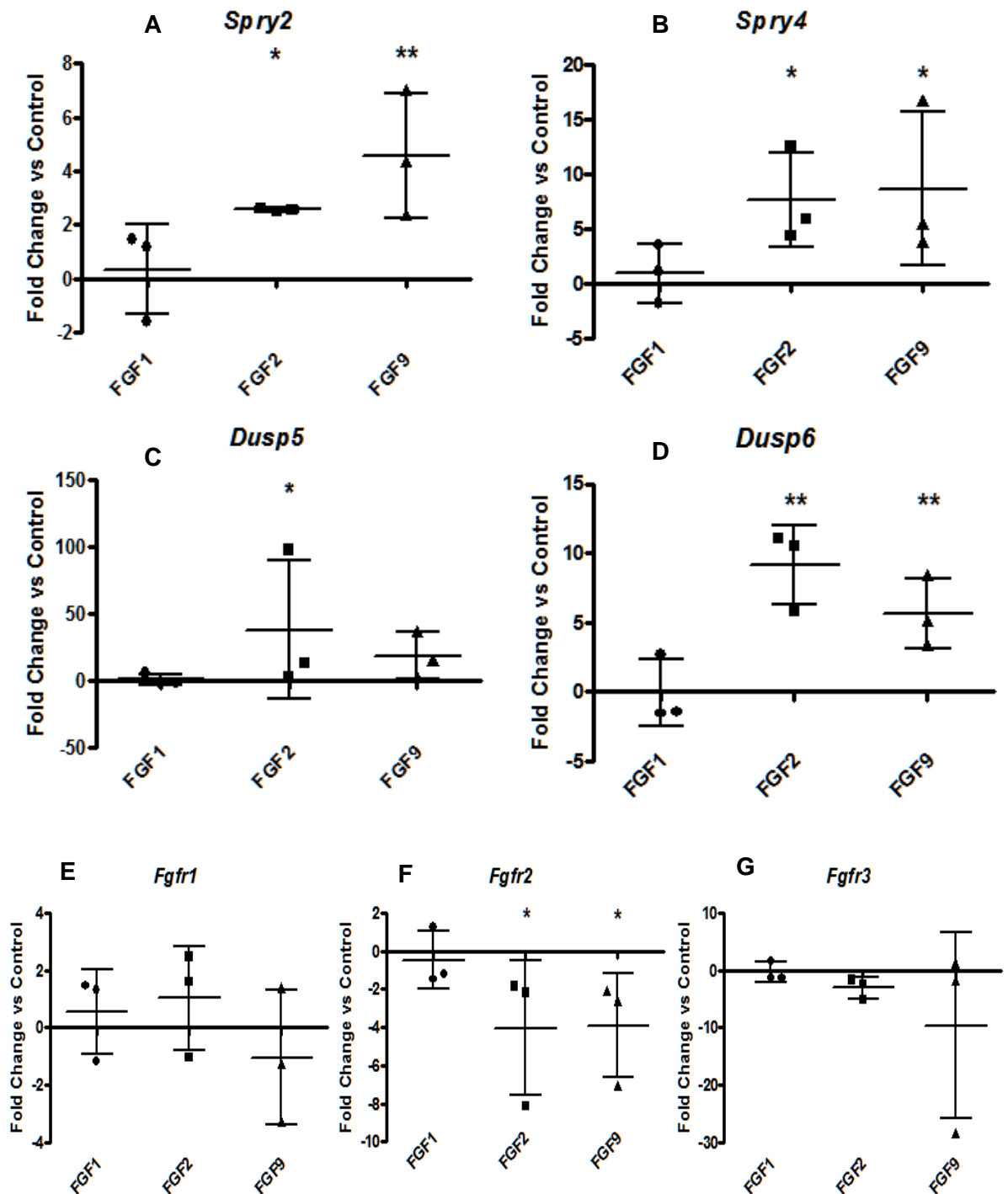


Figure 3.9. OPCs were less responsive to FGFs than mature OLs. Oligodendrocytes were cultured as described in section 2.2.3 and maintained in Sato's media for 2 days before treatment. OPC cultures were treated for 24 hours with 100 ng/mL FGF1, 2, or 9. Cells were lysed and processed for RNA extraction and cDNA synthesis. qPCR was performed using primers for *Spry2*, *Spry4*, *Dusp5*, *Dusp6*, *Fgfr1*, *Fgfr2*, *Fgfr3* with *Gapdh* as the housekeeping standard. OPCs similarly upregulated feedback inhibitors in response to FGF2 and FGF9 (A – D). FGF2 and FGF9 downregulated *Fgfr2* while FGF1 had no effect (F) *Fgfr1* and *Fgfr3* were unaffected by FGF treatment (E - G). Fold changes in gene expression are shown relative to untreated control values, data presented are the means ± SD. This experiment was performed three times. *, p < 0.05, **, p < 0.01 (one way-ANOVA with Dunnett's Multiple Comparison Test performed on delta CT values).

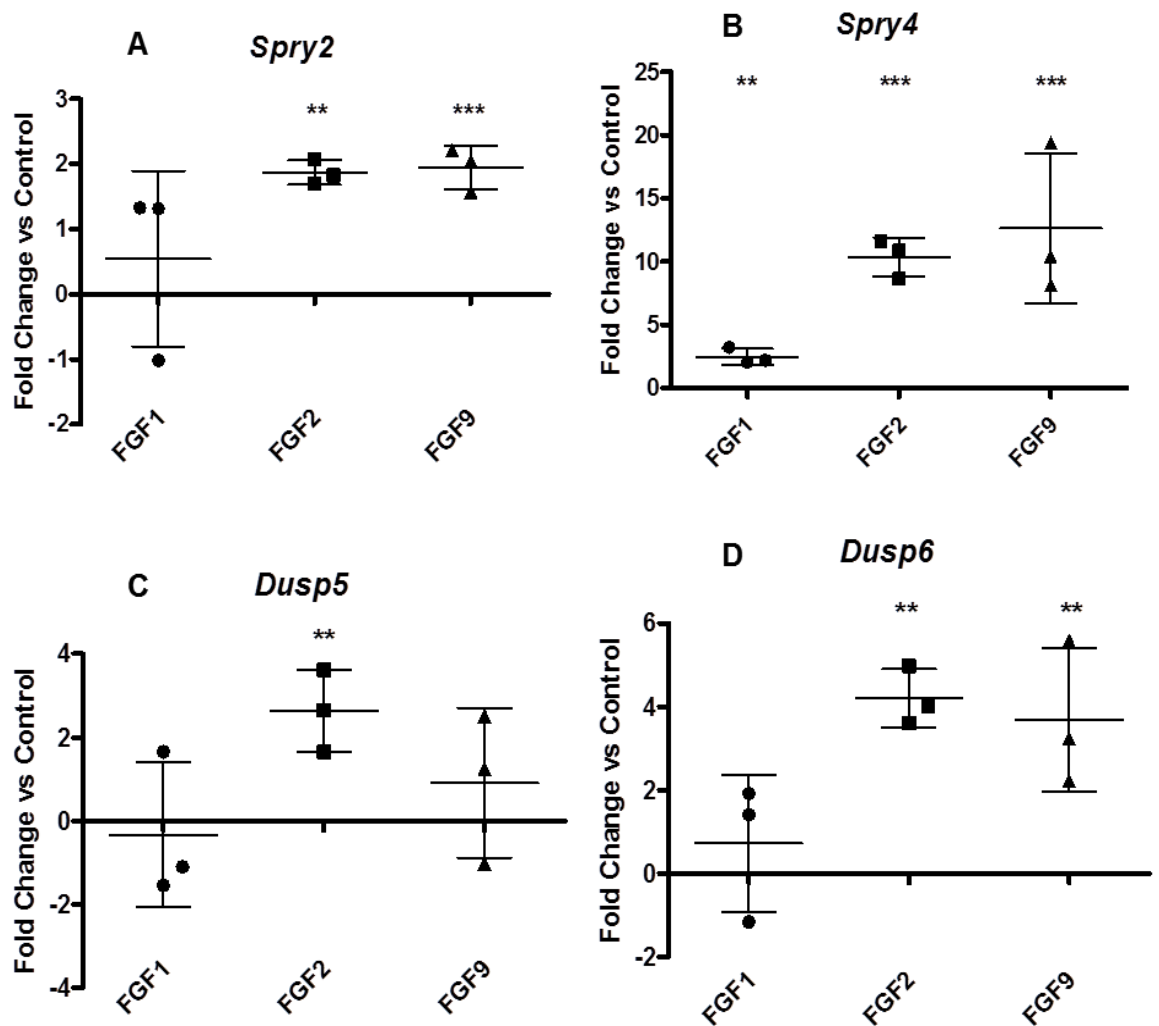


Figure 3.10. Neurons similarly upregulated feedback inhibitors when treated with FGF2 and FGF9. Neurons were purified as described in section 2.2.5 and cultured in neuro-basal medium for 6 days to allow them to differentiate. Neuronal cultures were treated for 24 hours with 100 ng/mL FGF1, 2, or 9. Cells were lysed and processed for RNA extraction and cDNA synthesis. qPCR was performed using primers for *Spry2*, *Spry4*, *Dusp5*, *Dusp6*, with *Gapdh* as the housekeeping standard. FGF2 and FGF9 induced negative feedback inhibitor expression to a similar degree in neurons. Fold changes in gene expression are shown relative to untreated control values, data presented are the means \pm SD. This experiment was performed three times. **, $p < 0.01$ ***, $p < 0.001$ (one-way ANOVA with Dunnett's Multiple Comparison Test performed on delta CT values).

3.2.2.3 Feedback inhibitor expression in astrocytes was induced only by FGF9.

The next cell type assessed for feedback-inhibitor and FGFR gene expression were astrocytes. Astrocyte monolayers were generated as described in section 2.2.1.2 and treated with FGFs from DIV 7. qPCR analysis revealed that *Spry4* and *Dusp6* were upregulated by FGF9 treatment but other feedback inhibitors and FGFR gene expression were unaffected (Figure 3.10). FGF1 and FGF2 induced no change in any of the genes examined in this study. FGF9 upregulated *Spry2* 17.5 ± 4 fold and *Dusp6* 8.3 ± 2.7 fold. *Fgfr* expression was highly variable following FGF treatment but no clear trends towards up or downregulation emerged (Figure 3.10 E – G).

To determine if similar effects were seen at the protein level, low-density astrocyte cultures were prepared as described in section 2.2.2 and treated for three days with FGF1, 2, and 9. After treatment, cultures were fixed and stained with antibodies against Sprouty2, Sprouty4, DUSP5, and DUSP6. The mean fluorescent intensity of staining for each feedback inhibitor was calculated using CellProfiler as detailed in section 2.2.7. Following treatment, Sprouty4, DUSP5, and DUSP6 were upregulated by FGF9 but not by FGF1 or FGF2 (Figure 3.11). Sprouty4, C = 8.2 ± 2.7 , FGF9 = 21.9 ± 1.2 . DUSP5, C = 11.3 ± 4.6 , FGF9 = 26.9 ± 3.4 . DUSP6, C = 6.1 ± 2.4 , FGF9 = 12.4 ± 2.9 . There was a slight trend for Sprouty2 to stain more strongly after treatment with all three FGFs but the changes were variable and not significant (Figure 3.11 A). Examining the cells using fluorescence microscopy revealed Sprouty2 stains in astrocyte nuclei and weakly in cell bodies (Figure 3.12 A, B). Sprouty4 is found in cell bodies in control astrocytes (Figure 3.12 C) and in cell bodies and nuclei after FGF9 treatment (Figure 3.12 D). DUSP5 stains in a few cell nuclei in controls (Figure 3.12 E) and is seen in cell bodies and nuclei following treatment (Figure 3.12 F). DUSP6 is present at low levels in nuclei and cell bodies in controls (Figure 3.12 G) and is upregulated mainly in cell bodies after FGF9 treatment (Figure 3.12 H).

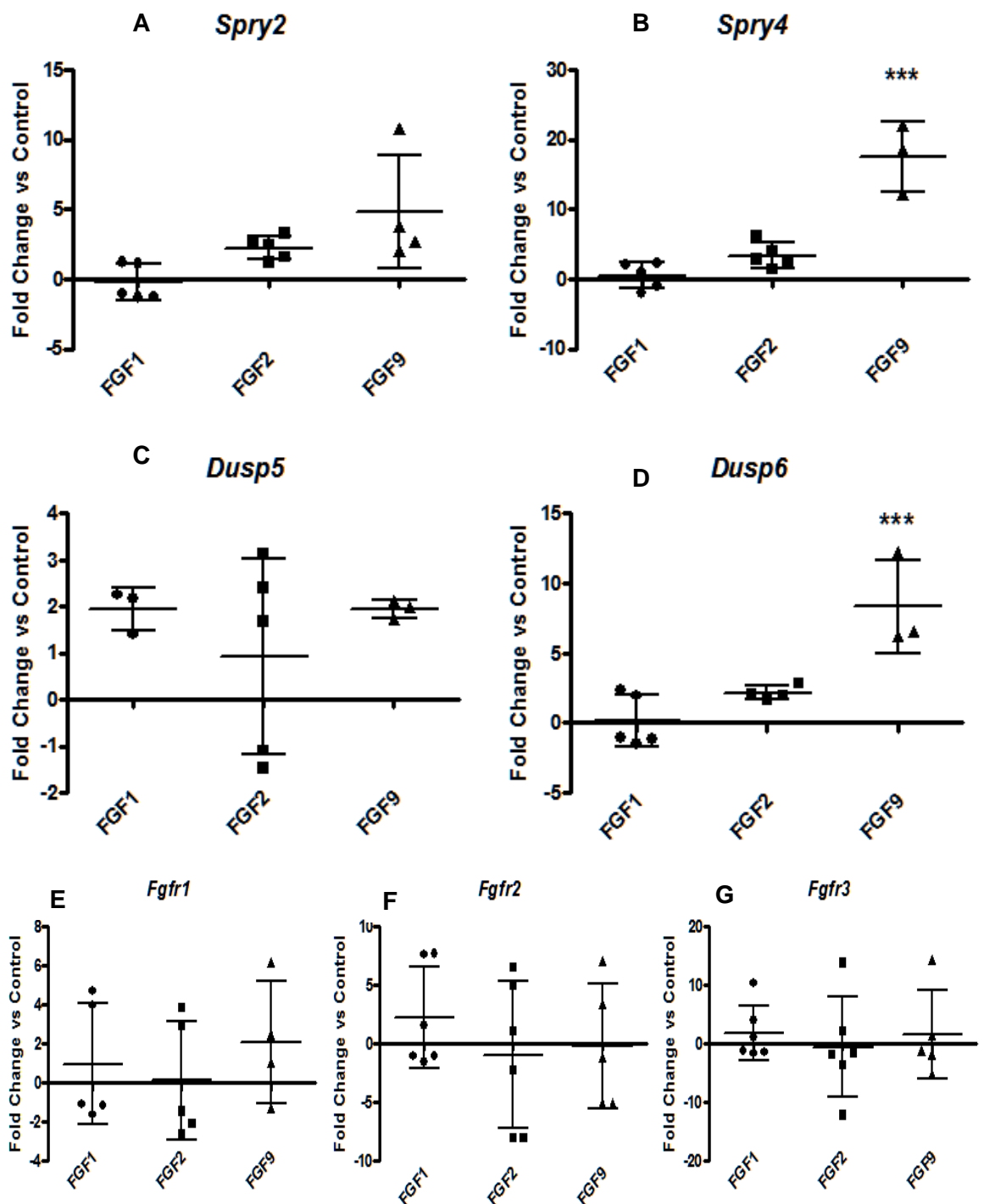


Figure 3.11. Only FGF9 upregulated feedback inhibitor expression in astrocytes. Astrocyte monolayers were generated as described in section 2.2.1.2 and cultured for 7 days before treatment. Cells were treated with 100 ng/mL recombinant human FGF1, 2, or 9 for 24 hours. Cells were lysed and processed for RNA extraction and cDNA synthesis. qPCR was performed using primers for *Spry2*, *Spry4*, *Dusp5*, *Dusp6*, *Fgfr1*, *Fgfr2*, *Fgfr3* with *Gapdh* as the housekeeping standard. FGF9 induced upregulation of *Spry4* and *Dusp6* (B, D) whereas FGF1 and FGF2 had no effect on any feedback inhibitors (A – D). *Fgfr* was highly variable following FGF treatment, but no trends emerged and mean expression was near control levels. Fold changes in gene expression are shown relative to untreated control values, data presented are the means ± SD. This experiment was performed five times. ***, $p < 0.001$ (one-way ANOVA with Dunnett's Multiple Comparison Test performed on delta CT values).

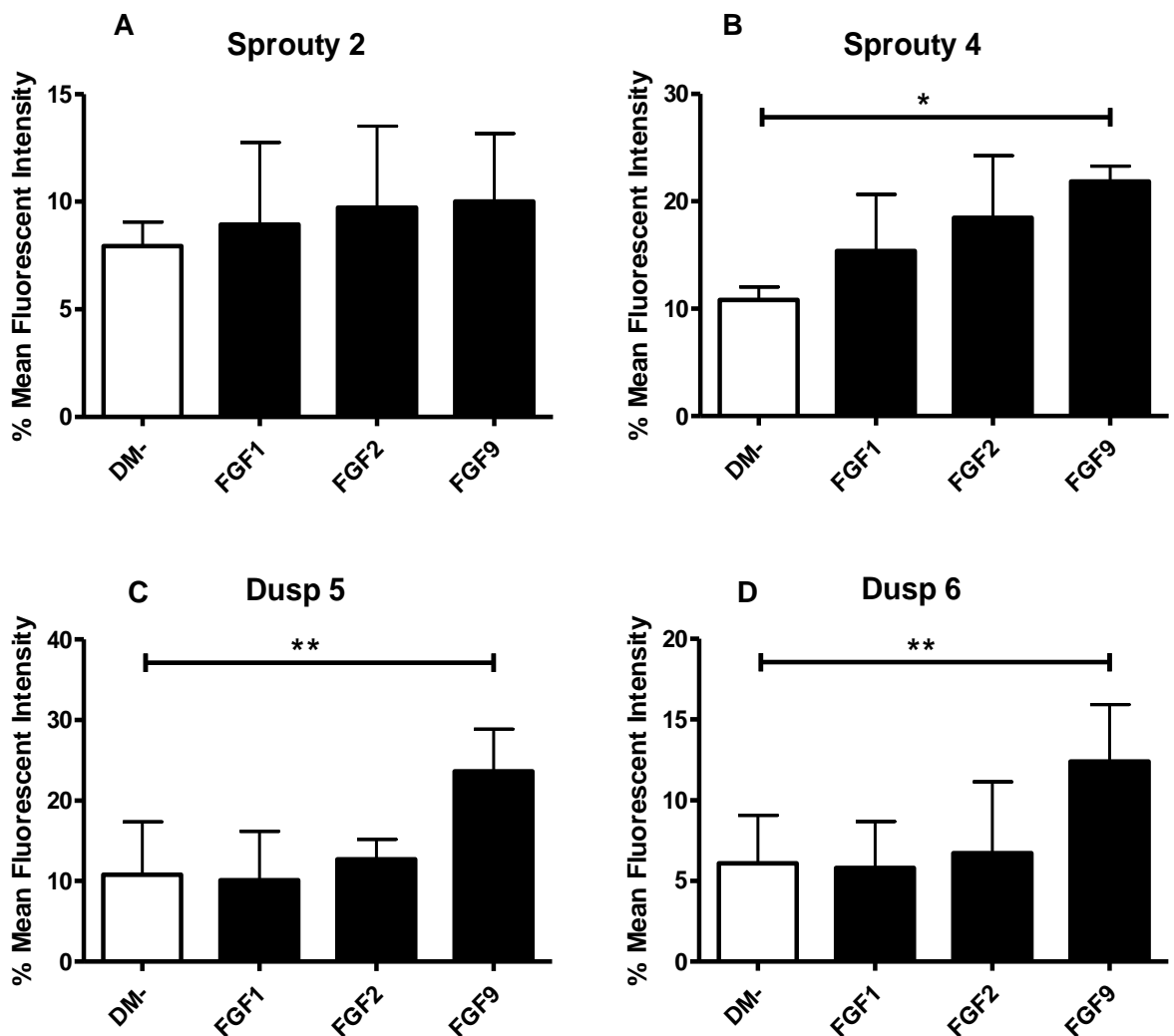


Figure 3.12. FGF feedback inhibitor expression was increased by FGF9, but not other FGFs in astrocytes. Low-density astrocyte cultures were generated as described in section 2.2.2 and treated for 72 hours with 100 ng/mL FGF1, 2, or 9. Cells were fixed and stained with antibodies against Sproutly2, Sproutly4, DUSP5, and DUSP6. Feedback-inhibitor expression was quantified as mean fluorescent intensities using CellProfiler as described in section 2.2.7. FGF9 significantly upregulated Sproutly4, DUSP5, and DUSP6 at the protein level. FGF1 and FGF2 did appear to have small effects on Sproutly2 and Sproutly4 but these were not significant. This experiment was performed three times. *, $p < 0.05$, **, $p < 0.001$ (one-way ANOVA with Dunnett's Multiple Comparison Test).

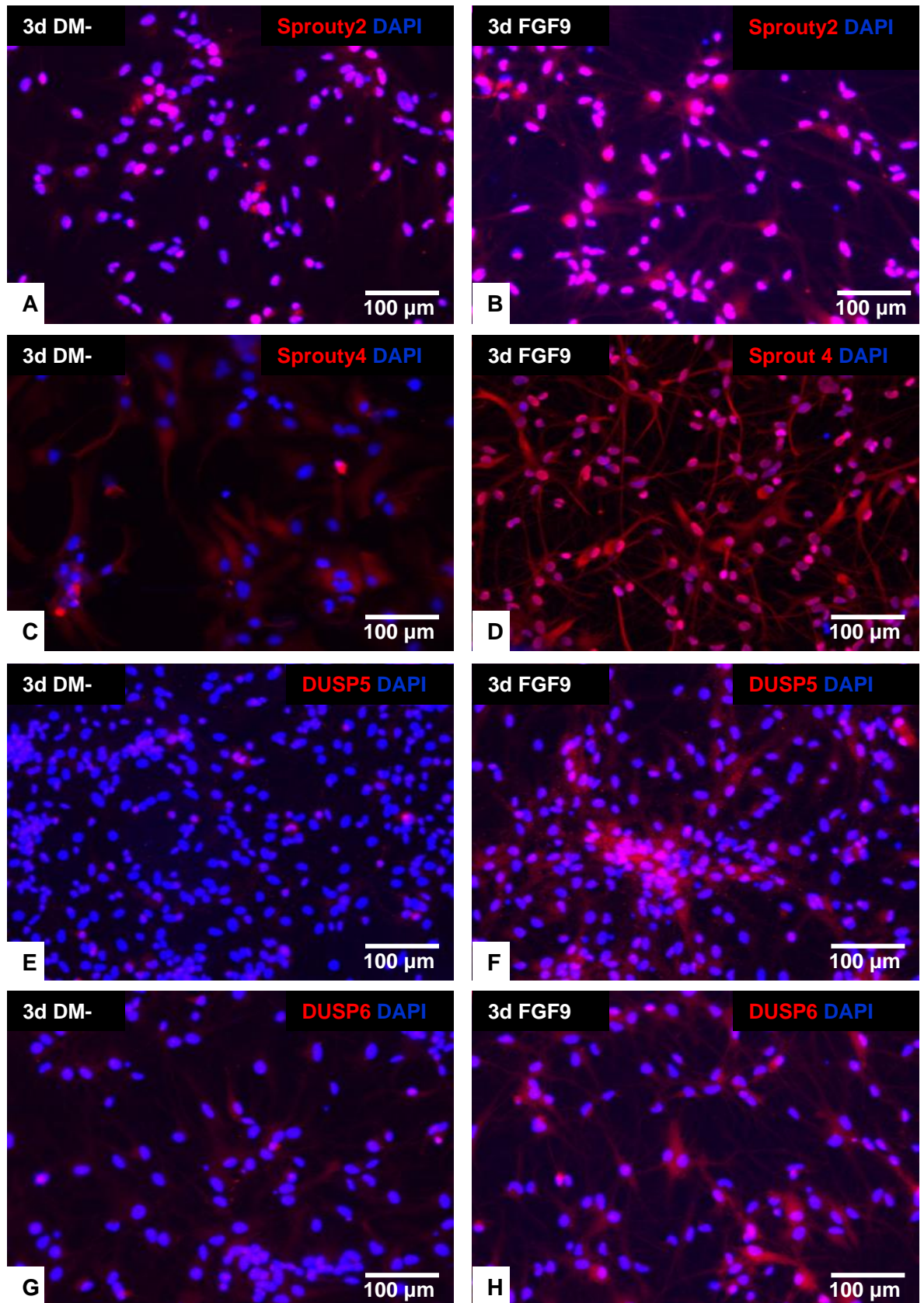


Figure 3.13. Representative images of FGF feedback inhibitors in cultured astrocytes following treatment with FGF9. Low-density astrocyte cultures were generated as described in section 2.2.2 and treated for 72 hours with 100 ng/mL FGF1, 2, or 9. Cells were fixed and stained with antibodies against Sprouty2, Sprouty4, DUSP5, and DUSP6. Treatment induced increases in Sprouty and DUSP staining increases in astrocyte cytoplasm. Sprouty4 is present in cell nuclei following treatment.

3.3 Discussion

FGF signaling is enormously complex and facilitates activation of several signaling pathways depending on ligand-receptor specificity and a host of regulatory mechanisms discussed in section 1.2.4. Expression of the appropriate FGFR does not ensure signaling by its cognate FGF ligand as heparan sulphates regulate FGF-FGFR interactions (Chang et al., 2000). This makes determining the target of FGF-signaling in tissues comprising multiple cell types difficult. Activation of downstream markers in cells can be used as an indicator that FGF signaling is occurring. Feedback inhibitors are rapidly induced in response to FGF signalling (Minowada et al., 1999, Branney et al., 2009). To determine if feedback inhibitors can be used as surrogate markers of FGF9 signaling in MS, feedback inhibitor expression was investigated in MS lesions and FGF-treated myelinating cultures.

Most of the sections used in this study were used to characterise FGF9 expression in MS lesions (Lindner et al., 2015), therefore direct comparisons between FGF9 and feedback inhibitor staining could be made. Sprouty2 and Sprouty4 staining was characterised on cell-type specific expression. Cell-type was determined by morphological examination of nuclei size and cell body shape which are unique in cells of the CNS. Sprouty2 and Sprouty4 staining was observed in grey matter neurons and occasional white matter astrocytes and OLs in healthy brains (Table 3.2, Figure 3.1). Sprouty2 staining closely mirrored FGF9 staining while Sprouty4 staining was generally much weaker. This suggested autocrine or paracrine FGF signaling is occurring in the healthy CNS.

FGF9 and Sprouty2 stained most intensely in acute MS lesions (Table 3.3, Figure 3.2, 3.3) and staining patterns in lesion rims and cores were very similar for both antibodies. Sprouty4 staining was also similar but consistently less intense and less common than Sprouty2. Astrocytes were immunoreactive for FGF9 and the Sproutys in most of the lesions examined. In three out of seven cases, OLs were immunoreactive for FGF9 and Sproutys. Infiltrating macrophages were also immunoreactive for FGF9 in the two acute cases in which they were present. This was surprising as macrophage FGF9 immunoreactivity was not detected in previous studies with these MS cases (Lindner et al., 2015). Macrophages are mostly associated with acute MS and populate the lesion rim where demyelination is taking place (Brück et al., 1995). FGF9 staining in macrophages was less

pronounced than in astrocytes, but Sprouty2 stained strongly. FGF2 has been shown to recruit and activate macrophages, and stimulate production of inflammatory cytokines and chemokines (Ribatti et al., 2006). Macrophages can also be a source of FGF2 under the right conditions (Vacca et al., 1999, Presta et al., 2009, Jetten et al., 2014). These findings suggest macrophages could be a source of FGF9 in acute MS and might be responding to FGF signaling. This prompted further investigation of FGF9 in the context of macrophages, which is discussed in the next chapter.

Of the cases examined, two displayed different lesions from those normally associated with acute MS. FGF9⁺ macrophages were associated with these lesions due to their high degree of lesion activity. Case A01-144 came from a patient with Balo's concentric sclerosis, in which demyelinated areas appear as concentric rings alternating with areas of undamaged myelin (Li et al., 2009). This disease is considered a rare variant of MS and, despite the bizarre lesion structure, possesses most of the same symptoms and pathological features as classical MS. At the rims of expanding MS lesions inflammation and demyelination are most active and phagocytosis of myelin breakdown products by macrophages can be observed (Figure 3.3 I). The second interesting lesion was in case 70-93-6, which contained examples of an early active lesion, and an acute subcortical lesion that appeared to be affecting neurons in the adjacent grey matter (Figure 3.4). Swollen neurons with intense FGF9, Sprouty2 and Sprouty4 staining were observed. Neuronal swelling is often associated with CNS injury and precedes neuronal death (Staub et al., 1993, Rungta et al., 2015). The presence of swollen neurons in this MS case was believed to be the result of axonal transection but the reason for accumulation of FGF9 and Sprouty⁺ cytoplasmic granules is unknown.

In chronic lesions astrocytes stained for FGF9 and Sprouty2 in lesion rims, and less frequently in inactive lesion cores (Table 3.4, Figure 3.5). Sprouty4 staining was of lower intensity and observed less frequently than in acute MS. Immunoreactivity for FGF9 and Sprouty2 was detected in all chronic-active cases but only in one of three chronic-inactive cases (case 244-94-7). Sections from chronic case 67-05-9 were double stained with the neuronal marker MAP2 and astrocytic marker GFAP (Figure 3.6). Confocal microscopy showed colocalization of FGF9 and MAP2 in NAGM and swollen neurons of a grey matter lesion (Figure 3.6 A, B). FGF9 and Sprouty2 were not detected in NAWM (Figure 3.6 C, E), but

colocalized with GFAP in the white matter lesion. There was also diffuse immunoreactivity of FGF9 and Sprouty2 throughout the lesion. FGF9 is normally localized on cell surfaces and the ECM as it is a secreted factor, but why Sprouty2 was detected outside of cells is unclear. In summary, FGF9 and Sprouty2 were detected in the same cell types in MS lesions, which suggests autocrine FGF9 signaling is occurring.

The next step in these experiments was to determine if the feedback inhibitor response in FGF9-treated myelinating cultures reflected the findings in MS lesions. qPCR experiments were performed to validate the microarray data, shown in Table 3.1. Unexpectedly, only FGF9 induced significant upregulation of *Spry2*, *Spry4*, *Dusp5*, and *Dusp6* after 24 hour treatment (Figure 3.7 A – D). *Fgfr2* and *Fgfr3* were downregulated (Figure 3.7 F, G), which suggests inhibition of OPC maturation or changes in astrocytic FGFR expression. As discussed in section 1.3.2.1, astrocytes express FGFR2 and FGFR3, and OLs express FGFR3 transiently during maturation, and FGFR2 on myelin membranes. These findings suggested that only FGF9 is capable of driving changes in feedback inhibitor and FGFR expression in myelinating cultures in contrast to the microarray data. FGF1 can interact with all seven FGFR variants and FGF2 interacts with all IIIc variants (Zhang et al., 2006) which suggests some signaling should occur in myelinating cultures. To try and understand these findings, the experiment was repeated on purified cultures of OPCs, mature OLs, and astrocytes.

Expression of all feedback inhibitors was increased by FGF2 and FGF9 in mature OLs (Figure 3.8 A – D) but no effect was seen with FGF1. *Fgfr2* expression was reduced by FGF2 and FGF9, which was expected as both of these factors are known to inhibit OL maturation and myelination (Figure 3.8 F). *Fgfr3* is expressed by OPCs transiently during maturation and while some downregulation was seen with FGF9, only FGF2 significantly reduced expression of this receptor (Figure 3.8 G). These results are in line with previous research showing FGF2 and FGF9 can signal in mature OLs (Fortin et al., 2005). OPCs were less responsive to FGF treatment but similarly upregulated feedback inhibitors in response to FGF2 and FGF9 (Figure 3.9 A – D). This was surprising, as OPCs are believed to be insensitive to FGF9 (Fortin et al., 2005, Lindner et al., 2015), but these results suggest FGF9 is initiating MAPK signaling. *Fgfr2* expression was reduced in OPCs after FGF2 and FGF9 treatment, which is in line with the finding that FGF9 inhibits

OPC maturation (Lindner et al., 2015). Neurons upregulated feedback inhibitor expression in a similar fashion after exposure to FGF2 and FGF9 (Figure 3.10). FGF9 was not predicted to stimulate signaling in neurons as their major FGF receptor, FGFR1 does not interact strongly with FGF9 (Choubey et al., 2017, Zhang et al., 2006). Neurons were the only cell type studied to respond to FGF1: *Spry4* expression was elevated but to a much lesser extent than in FGF2 or FGF9 treated neurons (Figure 3.10 B).

Astrocytes were only responsive to FGF9 treatment, despite expressing FGFR1, 2, and 3 (Miyake et al., 1996, Choubey et al., 2017). *Spry4* and *Dusp6* expression was elevated by FGF9, and FGFR expression was unaffected by any factor. There was a trend towards increased *Spry2* expression in FGF9-treated astrocytes but the change was not statistically significant. FGF1 has been shown to activate FGFR1 on astrocytes (Cassina et al., 2005) and FGF2 affects astrocytes in several ways: it regulates proliferation, differentiation, gap junction coupling, and reactivity (Gómez-Pinilla et al., 1995, Gómez-Pinilla et al., 1997, Reuss et al., 2000, Eclancher et al., 1996). This suggests feedback inhibitors would be upregulated in astrocytes exposed to FGF1 and FGF2 but this was not the case. There are two possibilities as to why astrocytes do not appear to respond to FGF1 and FGF2 in these experiments: either FGF1 and FGF2 are inducing signaling, but not feedback inhibitor expression, or astrocytic FGFRs are not being activated. Both of these reasons seem unlikely as FGF signaling is intrinsically linked to feedback inhibitor expression and FGF9 preferentially binds FGFR2 and FGFR3. FGF1 and FGF2 are promiscuous and should be able to bind FGFRs on astrocytes. Sulphation level of heparan sulphate has been shown to regulate FGFR activation by FGF1 and FGF9 in astrocytes (Higginson et al., 2012) so perhaps heparan sulphate expression in *in vitro* neurosphere-derived astrocytes is impermissible to signaling activation by FGF1 and FGF2. Either way, these results show expression of FGFRs does not guarantee signaling when cognate ligands are available and supports the idea that feedback inhibitor expression in MS lesions is a result of FGF9 signaling.

One important point to note is that while DUSP6 expression is a specific response to FGF signaling, this is not the case for other feedback inhibitors. Sprouty2, Sprouty4, DUSP5 antagonise ERK-MAPK, and have been shown to regulate FGF, EGF, VEGF, and PDGF signaling (Gross et al., 2001, Lee et al., 2001, Kramer et

al., 1999, Casci et al., 1999, Kucharska et al., 2009). VEGF is upregulated in RRMS and Progressive MS while EGF is mainly produced by immune cells in RRMS. VEGF is found at higher levels in progressive MS than RRMS (Tejera-Alhambra et al., 2015, Levy et al., 2013, Proescholdt et al., 2002). PDGF levels vary in RRMS but are decreased in progressive MS (Mori et al., 2013, Harirchian et al., 2012). In order to say for certain that the presence of feedback inhibitors in MS is a result of FGF9 signaling, these growth factors must be tested for their ability to induce Sproutys and DUSP5 in cells of the myelinating cultures.

Astrocytes were the only cell type studied to increase feedback inhibitor expression in response to FGF9 but not FGF2. This suggests the feedback inhibitor response to FGF9 in myelinating cultures is due to astrocytes as they are the most numerous cell-type present. OL and neuronal responses to FGF2 are potentially diluted beyond detection by qPCR. In conclusion, Sproutys and DUSPs can be upregulated in astrocytes *in vitro* by FGF9 treatment. Sprouty upregulation is also seen in astrocytes in human MS lesions and there was a strong correlation between cells expressing FGF9 and the Sproutys. This suggests autocrine/paracrine FGF9 signalling is occurring in MS lesions and astrocytes are the main target. These findings provide some further evidence to support the hypothesis that astrocytic responses to FGF9 are involved in the development of MS lesions.

CHAPTER FOUR

**INDUCTION OF FGF9 IN CELLS INVOLVED IN
PATHOGENESIS OF MS**

4 INDUCTION OF FGF9 IN CELLS INVOLVED IN PATHOGENESIS OF MS

4.1 Introduction

FGF9 availability is increased in the MS brain and the effects of this pleiotropic growth factor likely contribute to the failure of remyelination (Lindner et al., 2015). In order to manipulate FGF9 expression for therapeutic benefit in MS, it is important to understand the triggers for its upregulation. Despite its prominent roles in development and certain cancers, the mechanisms involved in regulation of FGF9 expression are mostly unknown. Aberrant inflammation is the main driver of lesion development in acute MS where FGF9 expression is greatest. Astrocytes, OLS, and macrophages appear to be the primary sources of FGF9 in acute MS. Inflammation is a critical component of the healing process, and not only precedes progenitor proliferation and tissue remodelling, but actively induces these processes (Eming et al., 2007, Donnelly and Popovich, 2008). Numerous studies have demonstrated the ability of astrocytes to respond local inflammation via the expression of multiple cytokine and chemokine receptors (Liberto et al., 2004, Barnett, 2012). Astrocytes respond to these stimuli by secreting cytokines, chemokines, and growth factors (Deng et al., 2010, Liberto et al., 2004), including FGF2 (Proia et al., 2008, Albrecht et al., 2002). These findings suggest inflammatory mediators might also induce astrocytic expression of FGF9 in MS lesions. If this hypothesis is correct it could explain why chronic MS lesions are associated with lower expression of FGF9 as there is less inflammation.

Cancer models have shed some light on mechanisms of FGF9 induction. Prostaglandin E₂ (PGE₂) was shown to induce FGF9 in an endometriosis model (Chuang et al., 2006). Briefly, PGE₂ activates PGE₂ receptor 3, which leads to protein kinase C and ERK1/2 signaling. This then leads to phosphorylation of the TF, Elk1, which binds to the promoter region of the FGF9 gene and induces expression. Elevated PGE₂ levels have been found in the CSF of MS patients (Mattsson et al., 2009), therefore this pathway may be involved in FGF9 expression.

FGF9 over-expression has been implicated in pathogenesis of lung adenocarcinomas where it has been linked to aryl hydrocarbon receptor (AhR)

activation (Wang et al., 2009). Ligation of AhR increased FGF9 mRNA levels via enhanced transcriptional activity at the FGF9 promoter. AhR activation leads to ligand-dependant promotion of Th17 or Treg cells (Quintana et al., 2008) and deletion of the AhR gene protected mice from EAE (Veldhoen et al., 2008). These findings suggest AhR might play a role in MS and could be involved in the regulation of FGF9 expression.

Another potential trigger for FGF9 induction in MS is hypoxia: breakdown of the vasculature around MS lesions, as a result of inflammatory damage of small blood vessels, limits oxygenation (Lassmann, 2003). An increase in overall metabolic processes and production of toxic metabolites by immune cells also reduces oxygen availability in lesions. A normal response to hypoxic injury is angiogenesis, which produces new blood vessels. FGFs have been shown to enhance angiogenesis in response to hypoxia and ischemia (Issa et al., 2005, Yang et al., 2015). Chen et al. described a mechanism whereby FGF9 upregulation is induced by hypoxia in colon cancer (Chen et al., 2014). They found an increase in FGF9 protein expression was due to increased translational efficiency. Translation of FGF9 is normally maintained at low levels by upstream open reading frame dependant repression. Hypoxia induces a conformational change in the internal ribosome entry site on FGF9 mRNA that overcomes this repression and promotes translation. Hypoxia-inducible factor 1-alpha (HIF1 α) and other stress response proteins are regulated in this way to facilitate rapid protein expression (Pagé et al., 2002, Lang et al., 2002). MS lesions display profound similarities to tissue alterations in acute white matter stroke and both involve induction of HIF1 α (Zeis et al., 2008, Aboul-Enein et al., 2003). This all suggests hypoxia may drive expression of FGF9 in MS.

Macrophages are highly plastic and can exhibit a range of phenotypes in response to their environment (Mosser and Edwards, 2008, Martinez and Gordon, 2014). The classification of macrophages into distinct subsets has become controversial but for simplicity, inflammatory and anti-inflammatory macrophages will be termed M1 and M2 respectively throughout this chapter. M1 macrophages are activated by IFN γ released by T cells in MS lesions and produce pro-inflammatory cytokines such as TNF α (Bsibsi et al., 2014). During remyelination, macrophages express anti-inflammatory cytokines including TGF β 1 and IL-10, and growth factors such as EGF, PDGF, and FGFs, which promote angiogenesis and proliferation (Lloyd

and Miron, 2016, Boven et al., 2006, Jetten et al., 2014). Macrophages display a spectrum of phenotypes in MS and up to 70% express markers of both M1 and M2 activation (Bogie et al., 2014, Vogel et al., 2013). Macrophages polarized towards the M2 phenotype can produce FGF2 (Jetten et al., 2014) and are a source of FGF2 in EAE (Liu et al., 1998). These data suggest FGF9 produced by macrophages in MS might be a result of anti-inflammatory M2 macrophages. Taken together, this research provides several avenues to explore in the search for the trigger of FGF9 expression in MS. The aims of experiments in this chapter were to assess the ability of a range of factors associated with MS to induce FGF9 up regulation in CNS and macrophage cultures.

4.2 Results

4.2.1 Inflammatory mediators had little effect on myelination *in vitro*

To address the possibility of cytokines inducing FGF9 expression in MS, myelinating cultures were treated with a range of inflammatory and anti-inflammatory cytokines involved in MS (Durán et al., 2001, Romme Christensen et al., 2012, Maimone et al., 1991, Tsukada et al., 1991) as described in section 2.2.6.4. PGE₂ and the AhR agonist, benzo[a]pyrene (BaP) (Machala et al., 2001) were tested in conjunction with inflammatory mediators. PGE₂ and BaP were reconstituted in DMSO (dimethyl sulfoxide) so DMSO alone was also tested as a control. The first step was to assess myelination and axon densities following treatment with each factor. Myelinating cultures were treated with 100 ng/mL of each factor from DIV 18 - 28 and stained with antibodies against MOG and neurofilament (SMI31). Cultures were imaged using immunofluorescence microscopy. Myelination and axon density were calculated in CellProfiler as described in section 2.2.8. Of all the factors tested, only IFN γ inhibited myelination (10d C = 14.9 \pm 0.2%, 10d IFN γ = 6.9 \pm 3.3%) (Figure 4.1 A). Axon densities were unaffected by any treatment at DIV 28 (Figure 4.1 B).

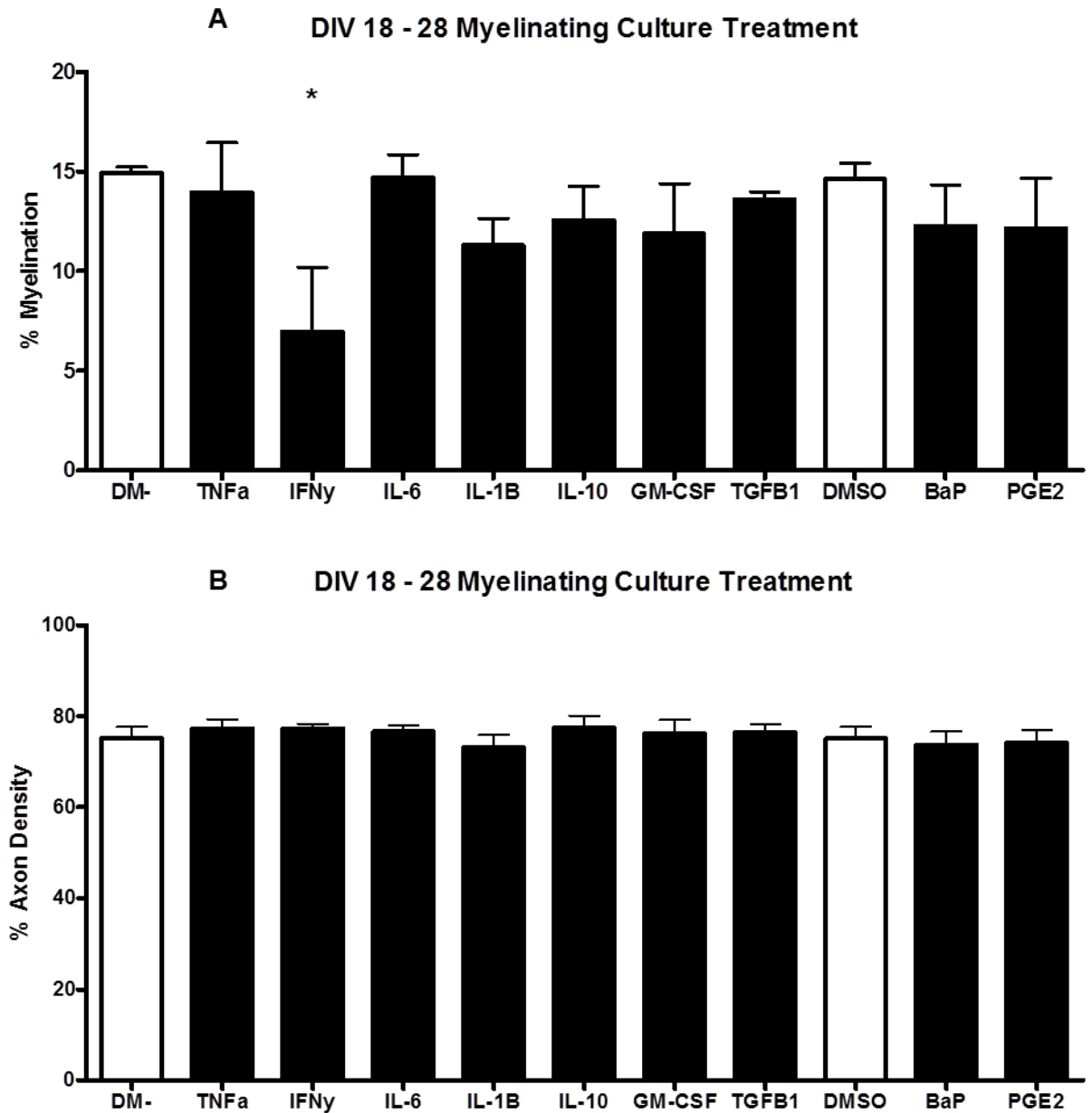


Figure 4.1. A selection of inflammatory mediators had little effect on myelination or axon density. Myelinating cultures were treated with a range of inflammatory cytokines previously shown to be expressed in MS lesions. Cultures were treated with factors at 100 ng/mL from DIV 18 – 28. Cultures were fixed and stained with antibodies against MOG (Z2) and axons (SMI31). Myelination rates and axon densities were calculated in CellProfiler. Data presented are the means \pm SD. This experiment was performed three times. *, $p < 0.05$, (one-way ANOVA with Dunnett's Multiple Comparison Test).

4.2.2 Treatment with inducers of FGF9 in cancer or inflammatory mediators did not induce expression of FGFs

DIV 18 myelinating cultures were treated with each factor for 24 hours then processed for qPCR as described in section 2.4. No significant changes in expression of *Fgf1* (Figure 4.2), *Fgf2* (Figure 4.3), or *Fgf9* (Figure 4.4) were detected following treatment with any of the factors at each of three concentrations tested.

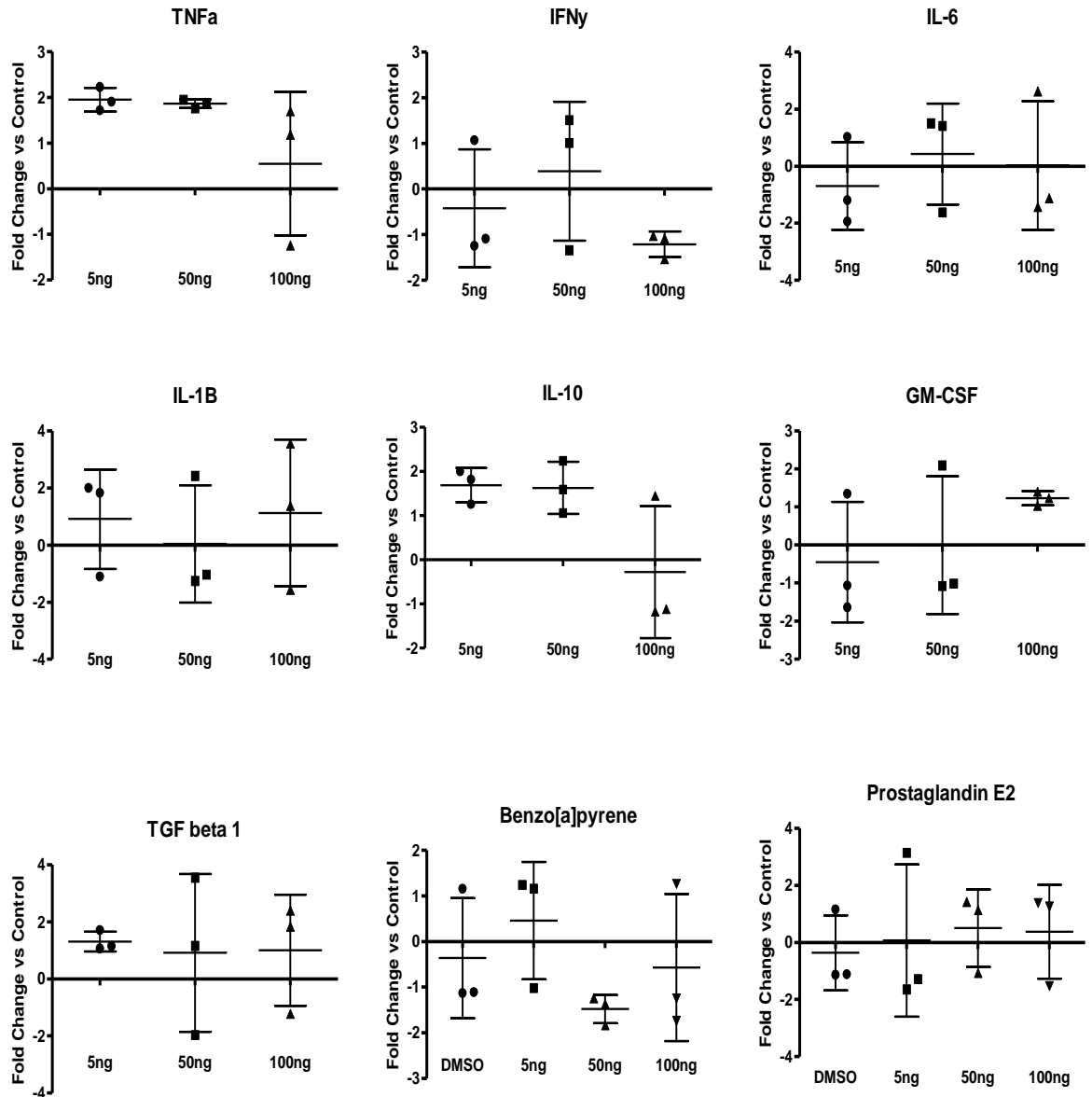


Figure 4.2. Inflammatory mediators did not upregulate *Fgf1* expression in myelinating cultures. Myelinating cultures were treated with a range of inflammatory cytokines previously shown to be expressed in MS lesions. Cultures were treated with 5, 50, or 100 ng/mL of each factor for 24 hours on DIV 18. The cells were lysed and processed for RNA extraction and cDNA synthesis. qPCR was performed using primers for *Fgf1* and *Gapdh* as the housekeeping standard. Expression of *Fgf1* was unaffected by treatment with any factor tested. Fold changes in gene expression are shown relative to untreated control values, data presented are the means \pm SD. This experiment was performed three times. (one-way ANOVA with Dunnett's Multiple Comparison Test was performed on the delta CT values).

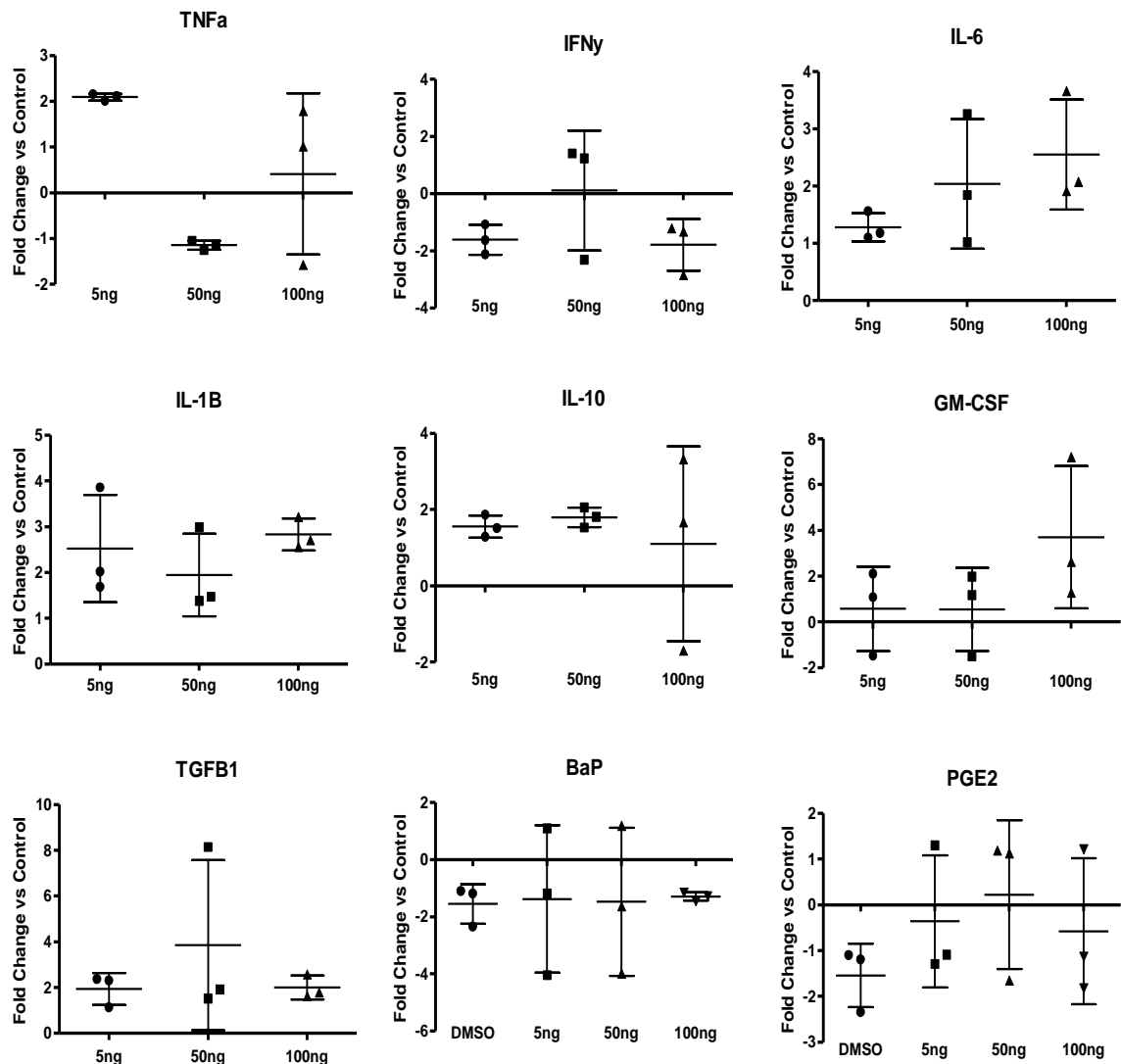


Figure 4.3. Inflammatory mediators did not upregulate *Fgf2* expression in myelinating cultures. Myelinating cultures were treated with a range of inflammatory cytokines previously shown to be expressed in MS lesions. Cultures were treated with 5, 50, or 100 ng/mL of each factor for 24 hours on DIV 18. The cells were lysed and processed for RNA extraction and cDNA synthesis. qPCR was performed using primers for *Fgf2* and *Gapdh* as the housekeeping standard. Expression of *Fgf2* was unaffected by treatment with any factor tested. Fold changes in gene expression are shown relative to untreated control values, data presented are the means \pm SD. This experiment was performed three times. (one-way ANOVA with Dunnett's Multiple Comparison Test was performed on the delta CT values).

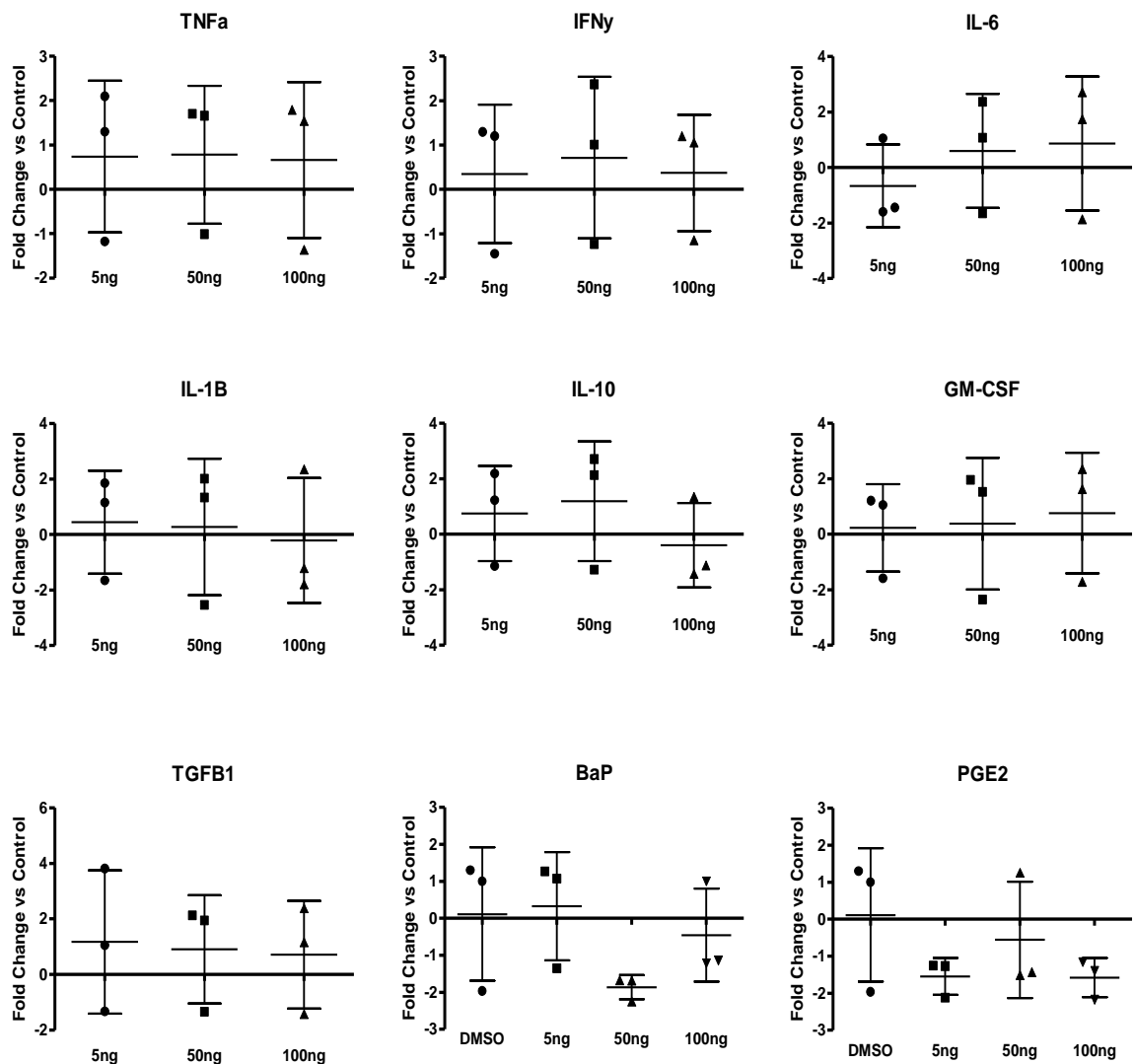


Figure 4.4. Inflammatory mediators did not upregulate *Fgf9* expression in myelinating cultures. Myelinating cultures were treated with a range of inflammatory cytokines previously shown to be expressed in MS lesions. Cultures were treated with 5, 50, or 100 ng/mL of each factor for 24 hours on DIV 18. The cells were lysed and processed for RNA extraction and cDNA synthesis. qPCR was performed using primers for *Fgf9* and *Gapdh* as the housekeeping standard. Expression of *Fgf9* was unaffected by treatment with any factor tested. Fold changes in gene expression are shown relative to untreated control values, data presented are the means \pm SD. This experiment was performed three times (one-way ANOVA with Dunnett's Multiple Comparison Test was performed on the delta CT values).

4.2.3 Inflammatory mediators did not induce FGF9 expression at the protein level

Myelinating cultures were treated as in the previous sections in this chapter from DIV 18 – 21. Cultures were stained with an anti-FGF9 antibody and imaged using fluorescence microscopy. FGF9 expression was determined by calculating the mean fluorescent intensity (MFI) of staining in each image using CellProfiler. In DIV 28 control myelinating cultures, FGF9 staining was observed mostly in astrocytes (Figure 4.5 A, B) and axons (Figure 4.5 B). In treated cultures, levels of FGF9 expression did not significantly differ from control values for any factor tested (Figure 4.6).

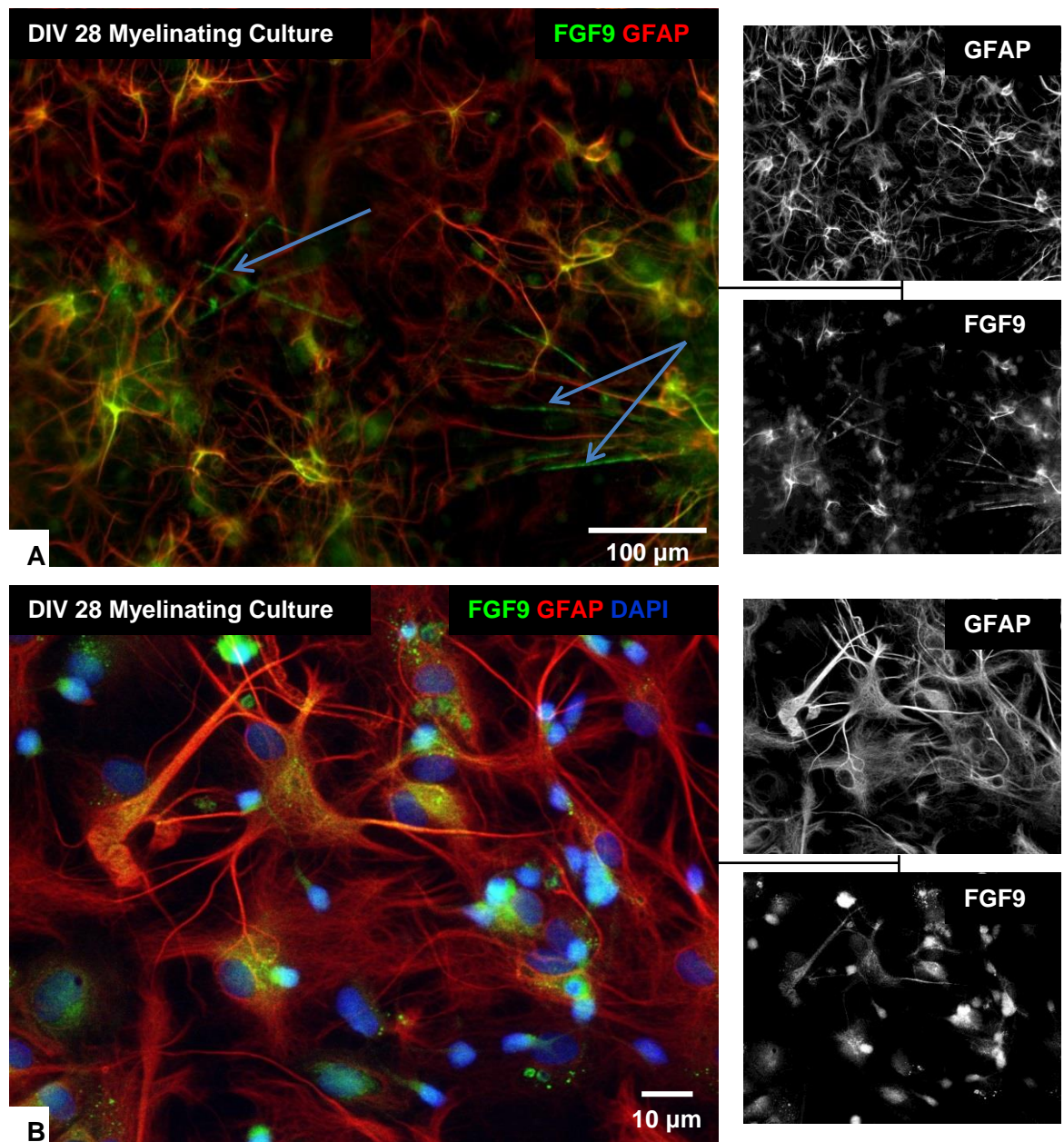


Figure 4.5. Representative images FGF9 and GFAP staining in control myelinating cultures on DIV 28. Cultures were fixed and stained with antibodies against FGF9 and GFAP. FGF9 mainly stains in astrocytes and axons, denoted with blue arrows. FGF9 staining is observed throughout some, but not all, astrocyte cell bodies at high magnification.

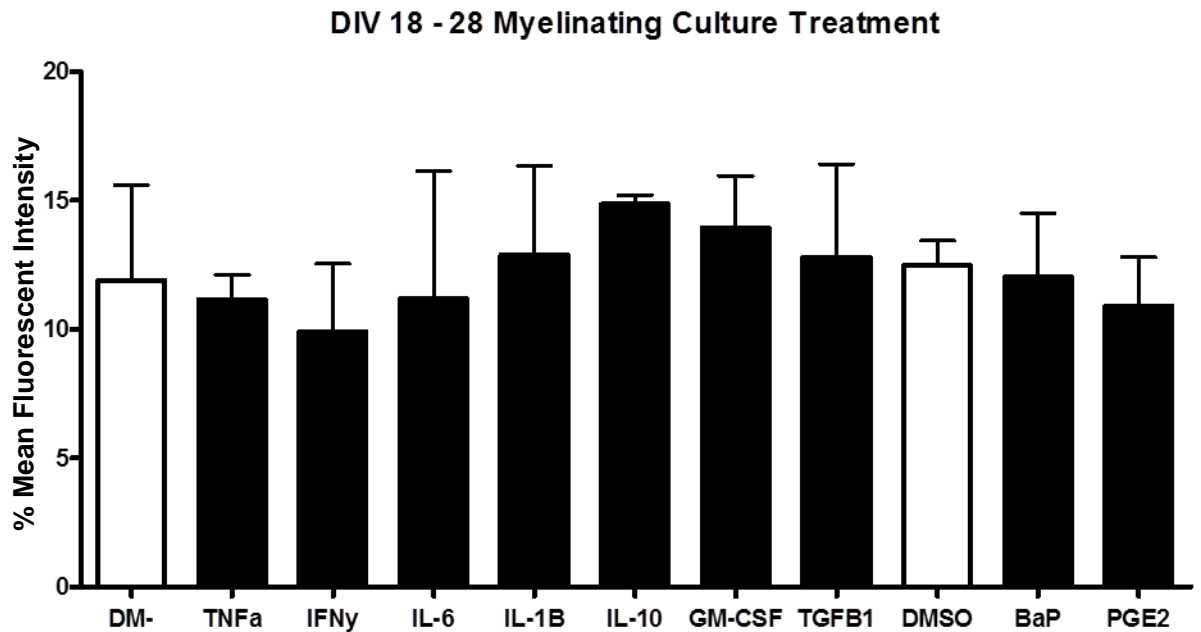


Figure 4.6. FGF9 was not induced at the protein level by inflammatory mediators. Myelinating cultures were treated with a range of inflammatory cytokines previously shown to be expressed in MS lesions. Cultures were treated with factors at 100 ng/mL from DIV 18 – 21. Cultures were fixed and stained with an anti-FGF9 antibody. FGF9 expression was quantified as the mean fluorescent intensity of FGF9 staining using CellProfiler as described in section 2.2.7. Data presented are the means \pm SD. This experiment was performed three times. *, $p < 0.05$, (one-way ANOVA with Dunnett's Multiple Comparison Test).

4.2.4 Hypoxia upregulated FGF9 in myelinating cultures

The first experiments in this set were to test the viability of myelinating cultures exposed to hypoxia. DIV 18 myelinating cultures and astrocyte monolayers were incubated in a hypoxic chamber according to the schematic on page 111. From the two biological replicates performed, after 24 hours in a hypoxic chamber with 1% O₂, cultures appeared to have less myelin than controls and there was a slight reduction in axonal density. (Figure 4.7, 4.8B). After 24 hours in hypoxia and 24 hours reperfusion, myelin and axons were completely wiped out (Figure 4.7, 4.8 D). Cultures in Figure 4.8 D displayed a random scattering of MOG and SMI31 positive cellular debris.

Cultures from these same conditions were stained with an antibody against FGF9 and the MFI of staining was measured as described previously in this chapter. Baseline FGF9 fluorescent intensity in DIV 19 and DIV 20 control cultures was around 7% (Figure 4.9.). Following 24-hour hypoxia, FGF9 levels increased slightly and after 24-hour reperfusion more than doubled (Figure 4.9) however as only two repeats of this experiment were performed, additional repeats will be necessary to confirm this finding. Despite the complete loss of axons and myelin, underlying astrocyte monolayers remained intact after hypoxia and reperfusion (Figure 4.10 B, D) and more intense FGF9 staining is visible after reperfusion.

The expression of FGF genes and a surrogate marker for hypoxia, Hexokinase 2 (HK2) (Menendez et al., 2015), were then measured in myelinating cultures. *Hk2* expression was increased around 20 fold after 24 hours in hypoxia and returned to baseline after reperfusion (Figure 4.11 A). *Fgf1* expression did not appear to be affected by hypoxia or subsequent reperfusion (Figure 4.11 B). *Fgf2* expression was upregulated around seven fold after hypoxia and equally after reperfusion (Figure 4.11 C). *Fgf9* expression was downregulated around two fold after both hypoxia and reperfusion. Additionally these experiments will require repetition before statistical analysis can be performed.

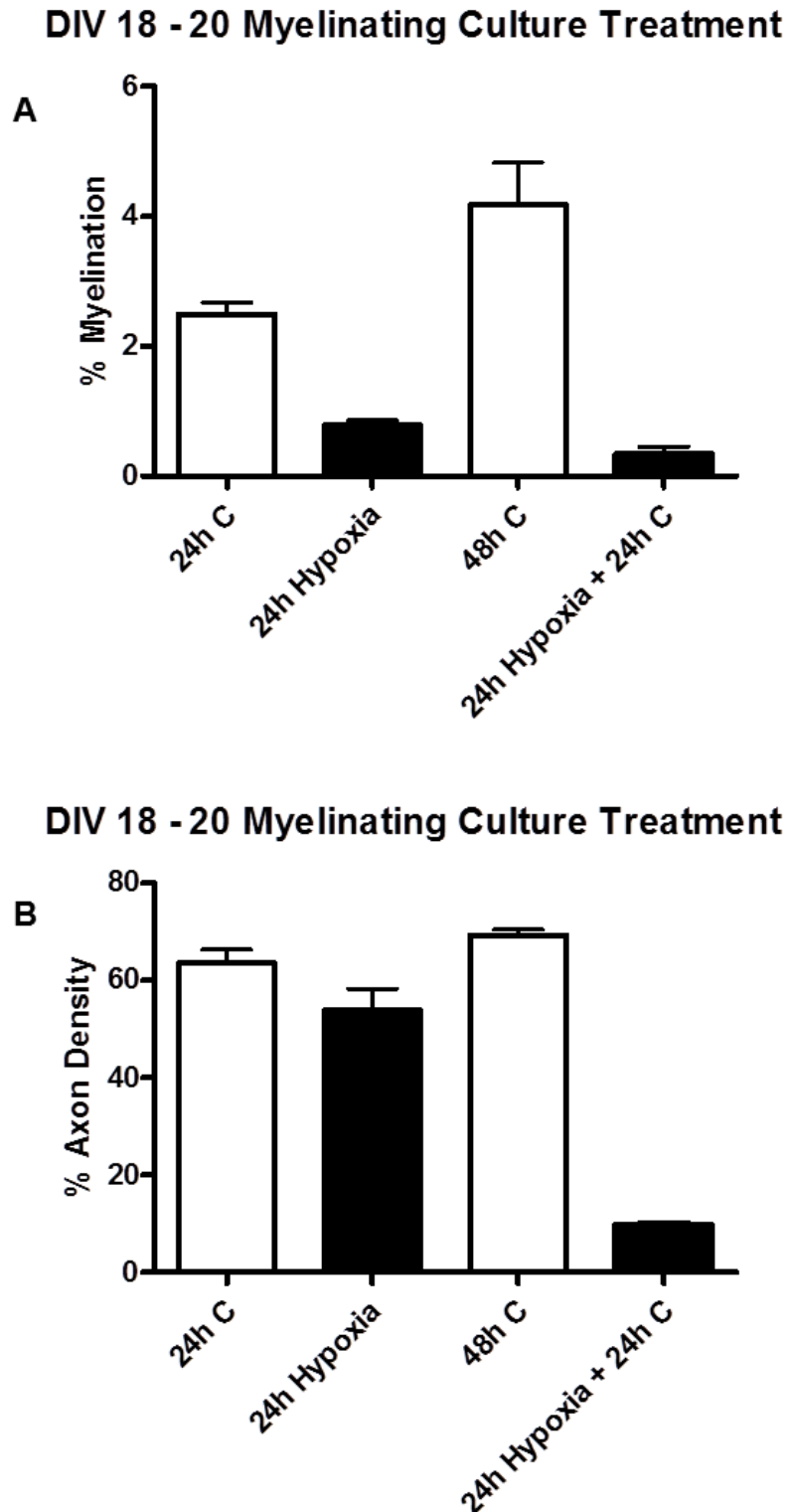


Figure 4.7. Myelinating cultures lost axons and myelin following hypoxia and reperfusion. Myelinating cultures at DIV 18 were incubated in a hypoxic chamber at 1% O_2 for 24 hours. The cultures were then fixed or transferred into a 7% CO_2 /93% air incubator for a further 24 hours to simulate reperfusion. Cultures were fixed and stained with antibodies against MOG (Z2) and axons (SMI31). Myelination percentages and axon densities were calculated in CellProfiler. Myelination was reduced in hypoxic cultures at both time points (A). Axonal density was slightly reduced after 24 hours hypoxia and severely reduced following reperfusion (B). Data presented are the means \pm SD, this experiment was performed twice.

Experimental design of hypoxia experiments.

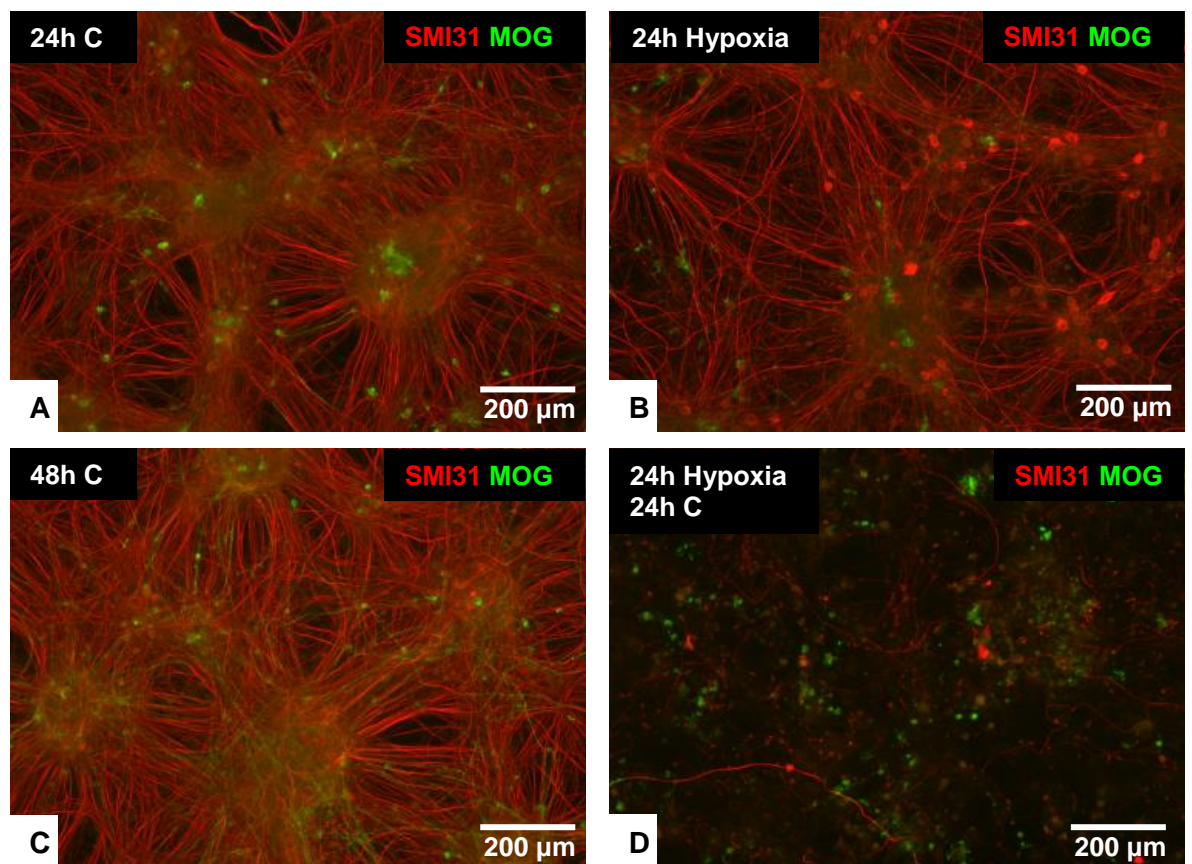
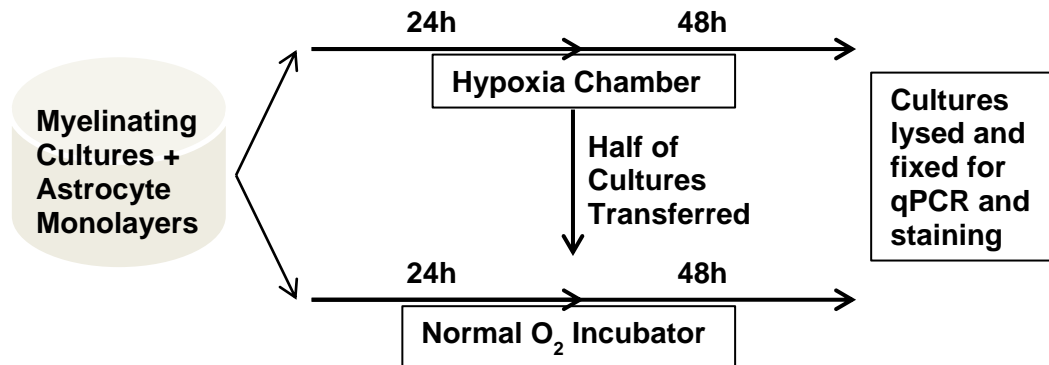


Figure 4.8. Representative images of myelin and axons in hypoxia experiment. Myelinating cultures at DIV 18 were incubated in a hypoxic chamber at 1% O_2 for 24 hours. The cultures were then fixed or transferred into a 7% CO_2 /93% air incubator for a further 24 hours to simulate reperfusion. Cultures were fixed and stained with antibodies against MOG (Z2) and axons (SMI31). Myelination is reduced after 24 hours hypoxia and SMI31 staining appears more punctate (B). Following reperfusion myelin and axons are totally eliminated from the cultures (D).

DIV 18 - 20 Myelinating Culture Treatment

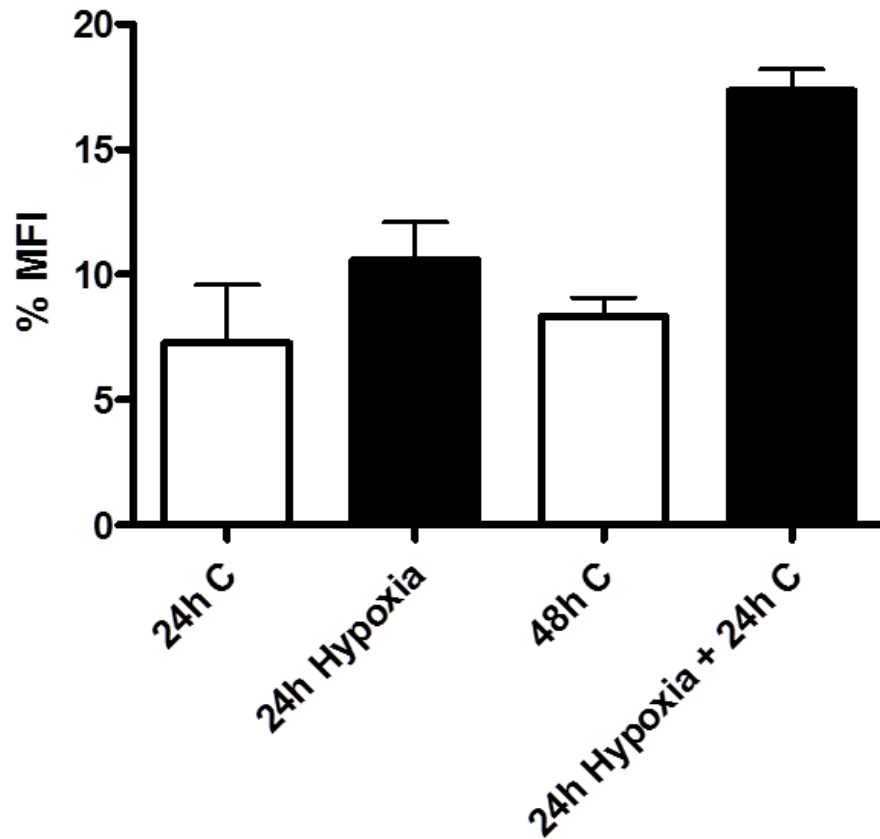


Figure 4.9. Astrocytes increased FGF9 expression in response to hypoxia. Myelinating cultures at DIV 18 were incubated in a hypoxic chamber at 1% O_2 for 24 hours. The cultures were then fixed or transferred into a 7% CO_2 /93% air incubator for a further 24 hours to simulate reperfusion. Cultures were fixed and stained with an anti-FGF9 antibody and expression was quantified as the MFI of staining using CellProfiler as described in section 2.2.7. Data presented are the means \pm SD. This experiment was performed twice.

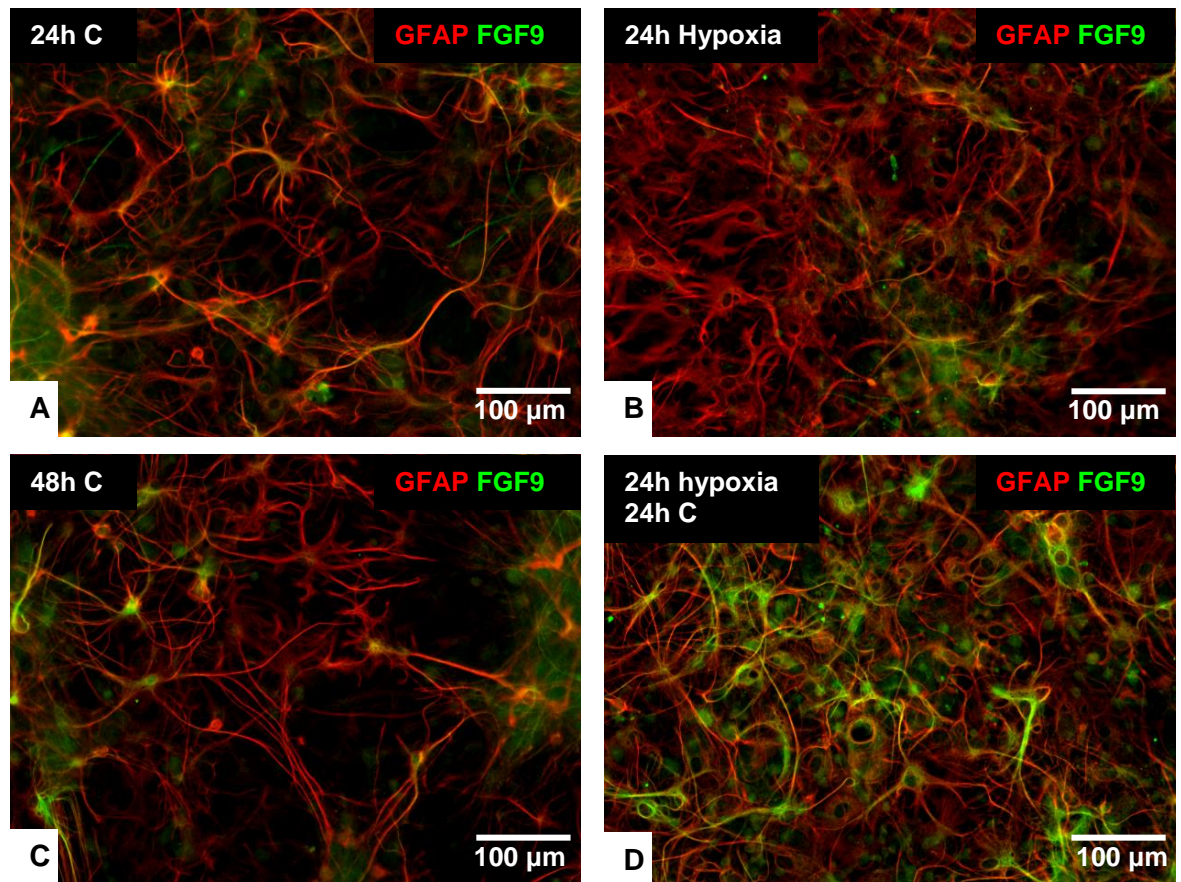


Figure 4.10. Representative images of astrocytes and FGF9 in hypoxia experiment. Myelinating cultures at DIV 18 were incubated in a hypoxic chamber at 1% O₂ for 24 hours. The cultures were then fixed or transferred into a 7% CO₂ /93% air incubator for a further 24 hours to simulate reperfusion. Cultures were fixed and stained with an anti-FGF9 antibody. FGF9 staining appears in a subset of astrocytes in controls with diffuse staining in the background (A, C). FGF9 stained much more intensely in astrocytes following hypoxia and reperfusion.

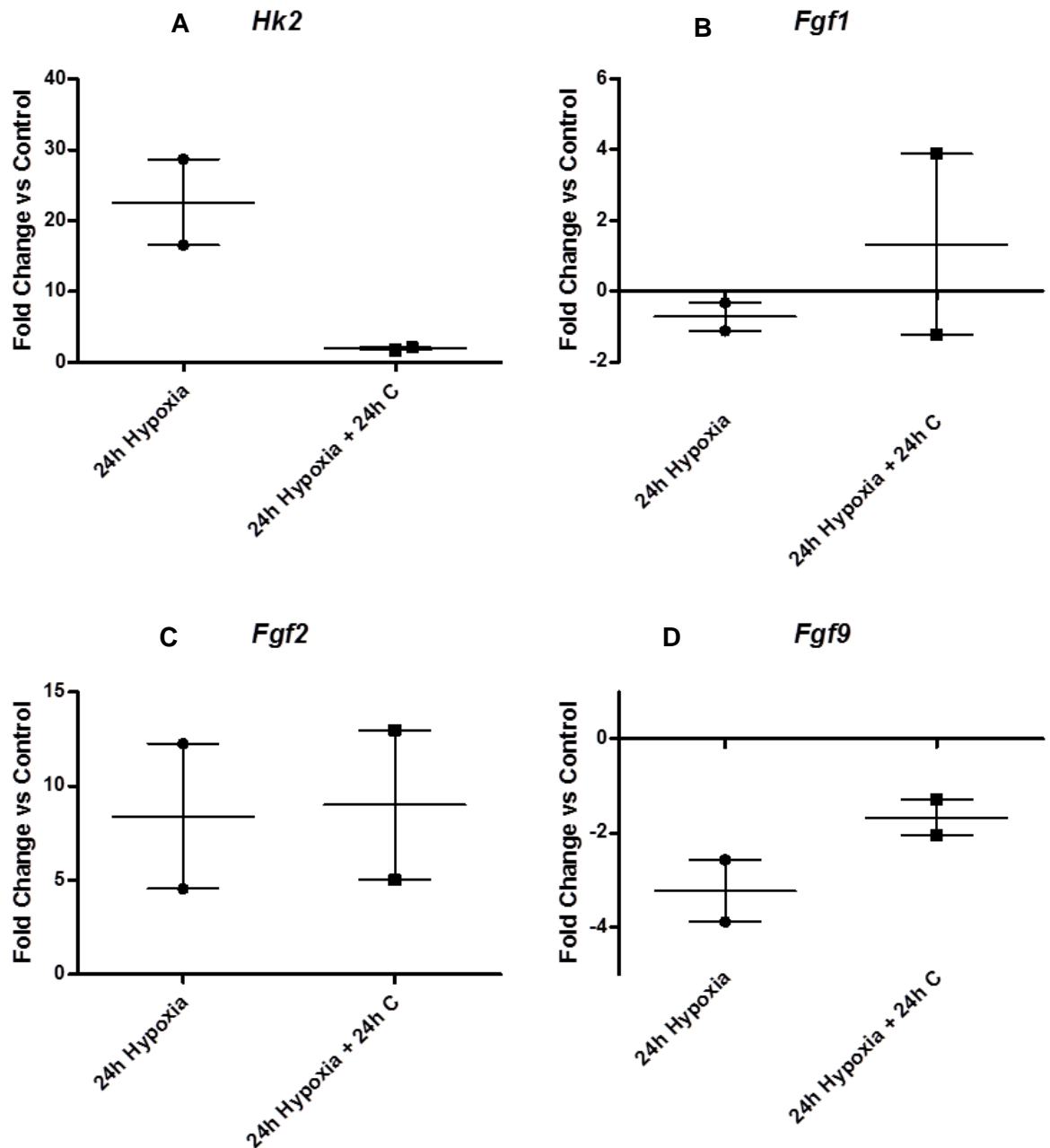


Figure 4.11. FGF9 expression was reduced at the mRNA level following hypoxia while FGF2 expression was elevated. Myelinating cultures at DIV 18 were incubated in a hypoxic chamber at 1% O_2 for 24 hours. cells were lysed and processed for RNA extraction and cDNA synthesis. qPCR was performed using primers for *Fgf1*, *Fgf2*, *Fgf9*, and *Gapdh* as the housekeeping standard. *Hk2* expression was increased after 24 hours in hypoxia and returned to baseline following reperfusion (A). *Fgf1* expression did not appear to vary far from control values in either condition (B). *FGF2* levels were similarly elevated following each treatment (C) and *Fgf9* was downregulated after hypoxia and reperfusion (D). Data presented are the means \pm SD, this experiment was performed twice.

4.2.5 Macrophages polarised towards an anti-inflammatory phenotype upregulate FGF9 gene expression

Experiments detailed in the previous chapter showed that macrophages in acute CNS lesions are immunoreactive for FGF9. Macrophages in a lesion setting display a range of phenotypes geared towards promoting or reducing inflammation, healing, and fibrosis. To study the expression of FGFs by macrophage lineage cells, BMDMs were cultured for one week then treated with the M1 and M2 polarizing cytokines, IFN γ and IL-13 as detailed in Section 2.2.6.6.

In the first experiments, cultured BMDMs were treated with polarizing cytokines for 24 hours then processed for qPCR. *Nos2* expression is robustly increased following 24 or 48-hour treatment with IFN γ (Figure 4.12 A). 24h IFN γ = 4838.2 \pm 1863.7 fold, 48h IFN γ = 6652 \pm 52.9 fold. *Arg1* expression is induced with IL-13 treatment (Figure 4.12 B) but this change only became statistically significant after 48 hours. 48h IL-13 = 79.3 \pm 66.1 fold). FGF expression in polarized BMDMs was then assessed. *Fgf1* levels fluctuated around baseline in BMDMs polarized to M1 or M2 and were never significantly elevated or decreased (Figure 4.13 A). FGF2 expression was increased 24 hours after polarization with IL-13, 15.1 \pm 5.4 fold, (Figure 4.13 B). FGF9 expression appeared slightly elevated after 24 hours of M2 polarization but was not significantly increased until 48 hours after treatment, 82.2 \pm 66.2 fold, (Figure 4.13 C).

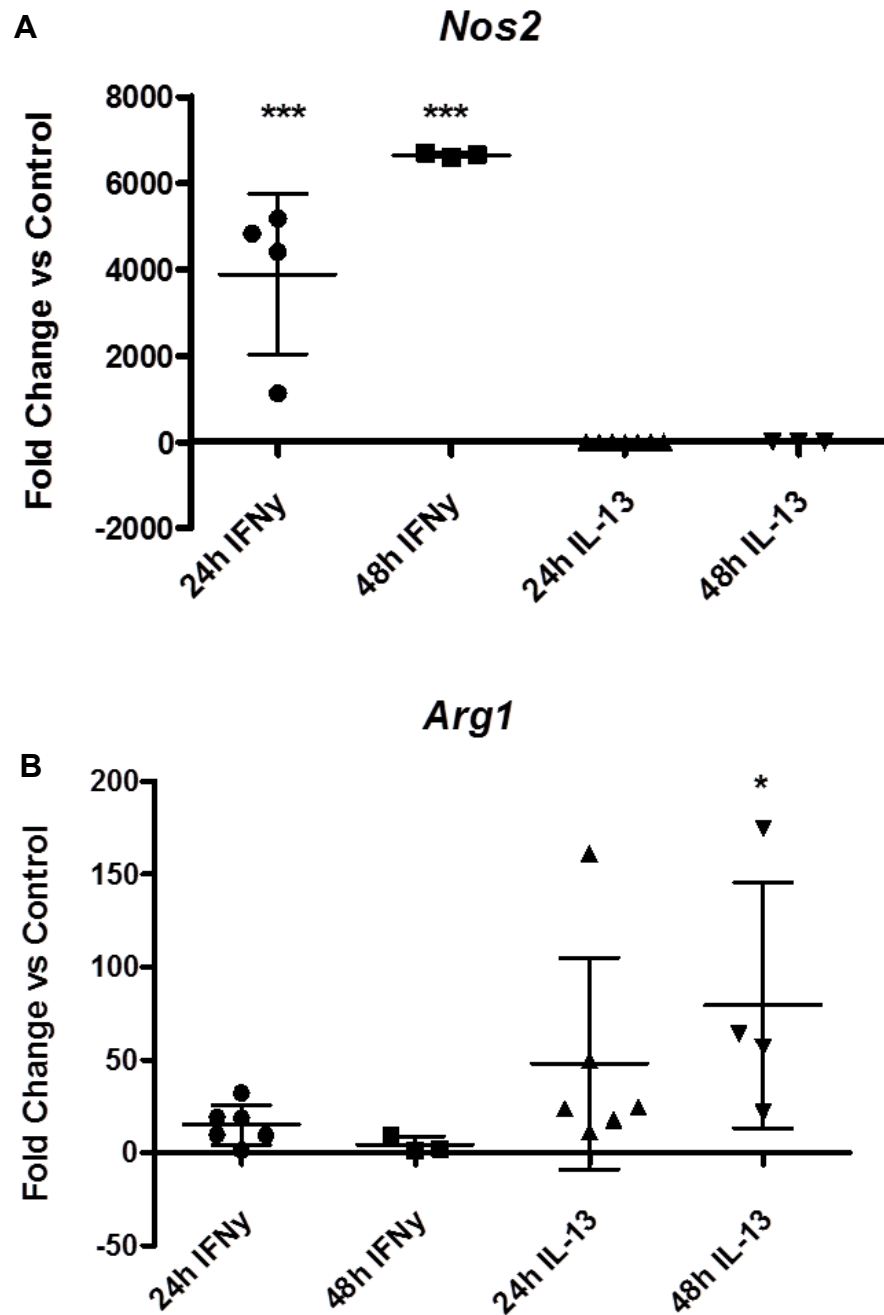


Figure 4.12. Polarization of bone marrow-derived macrophages with IFN γ and IL-13. BMDMs were cultured with M-CSF for 7 days followed by treatment with 100 ng/mL IFN γ or IL-13. Cells were lysed and processed for RNA extraction and cDNA synthesis. qPCR was performed using primers for *Nos2*, *Arg1*, and *Gapdh* as the housekeeping standard. *Nos2* expression was robustly upregulated after 24 and 48 hour treatment with IFN γ (A). *Arg1* upregulation reached significance after 48 hours of IL-13 treatment. Fold changes in gene expression are shown relative to untreated control values, data presented are the means \pm SD. This experiment was performed seven times. *, $p < 0.05$, *** $p < 0.001$ (one-way ANOVA with Bonferroni's Multiple Comparison Test).

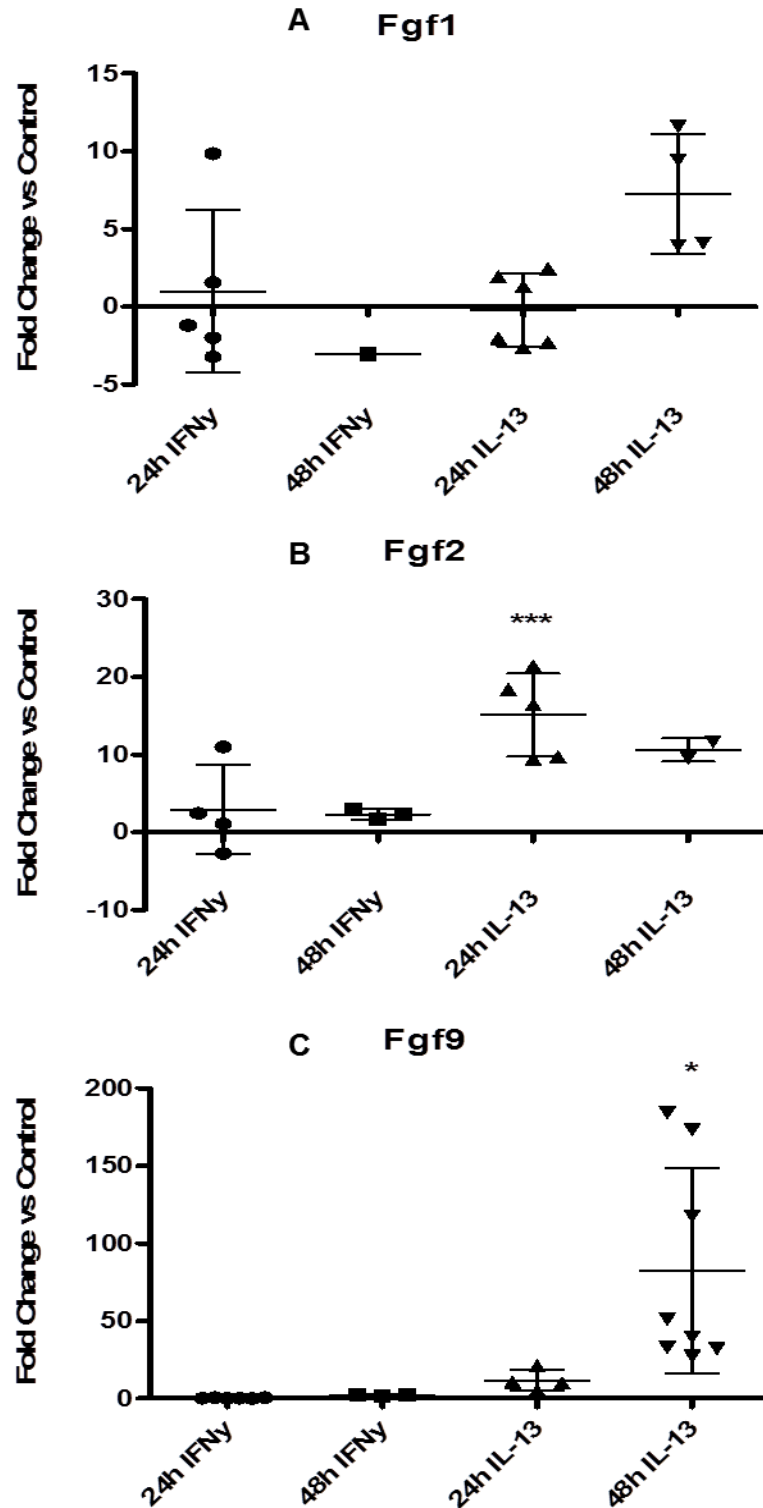


Figure 4.13. FGF 2 and FGF9 were induced by IL-13 in BMDMs. BMDMs were cultured with M-CSF for 7 days followed by treatment with 100 ng/mL IFN γ or IL-13. Cells were lysed and processed for RNA extraction and cDNA synthesis. qPCR was performed using primers for *Fgf1*, *Fgf2*, *Fgf9*, and *Gapdh* as the housekeeping standard. IL-13 had no effect on FGF1 expression (A) but significantly upregulated FGF2 (B) after 24 hours and FGF9 (C) after 48 hours. Fold changes in gene expression are shown relative to untreated control values. Data presented are the means \pm SD. This experiment was performed seven times. *, $p < 0.05$, ** $p < 0.01$ (one-way ANOVA with Bonferroni's Multiple Comparison Test).

4.2.6 FGF-treatment does not induce feedback inhibitor expression or alter cytokine production in polarised macrophages

Following the finding that macrophages polarised towards an anti-inflammatory phenotype express FGF9, the next step was to determine what effects, if any, FGFs have on macrophages. Using Sprouty and DUSP expression as readouts, macrophages were treated with polarizing cytokines in combination with FGF1, 2, or 9, for 24 hours. Macrophages were then processed for qPCR as in the previous section. IFN γ and IL-13 induced no upregulation of *Spry2*, *Spry4*, *Dusp5*, or *Dusp6* (Figure 4.14). Combination treatment with polarising cytokines and FGFs also led to no increase in feedback inhibitor expression. M1 polarization with IFN γ led to a marked but variable downregulation of each of the four feedback inhibitors which again, was not affected by the presence of FGFs. Relative expression of M1 and M2-associated genes *Nos2*, *Arg1*, *Tnf* and *il10* were also unaffected by FGFs (Figure 4.15). Results in these graphs were normalised to the effects of polarizing cytokines alone.

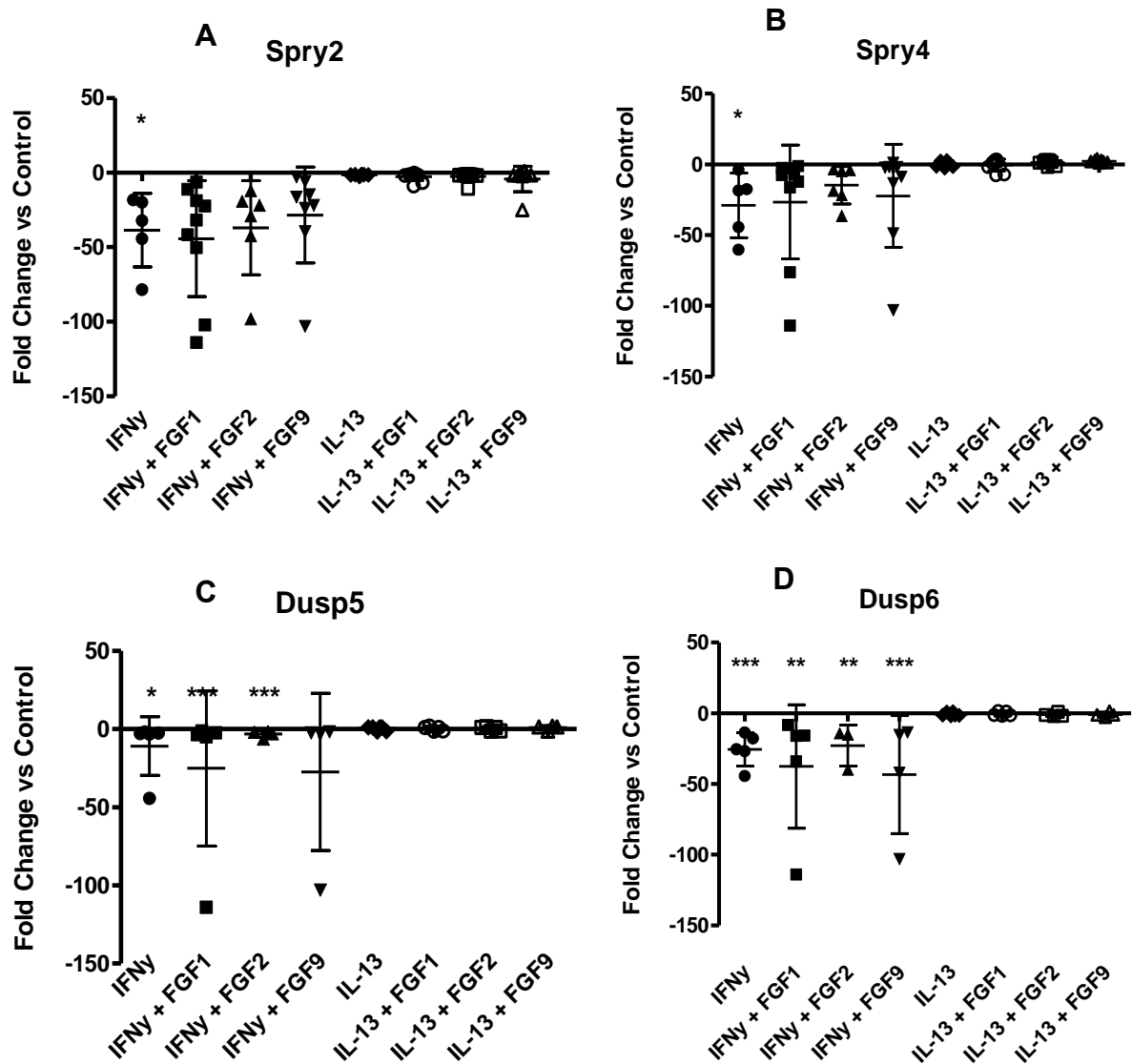


Figure 4.14. FGF treatment did not induce feedback inhibitor expression in macrophages. BMDMs were cultured with M-CSF for 7 days followed by 24-hour treatment with 100 ng/mL IFN γ or IL-13 in combination with FGF1, 2, or 9. Cells were then lysed and processed for RNA extraction and cDNA synthesis. qPCR was performed using primers for *Spry2*, *Spry4*, *Dusp5*, *Dusp6*, and *Gapdh* as the housekeeping standard. IFN γ reduced expression of all inhibitors, which was not affected by the presence of FGFs compared to unpolarised controls. IL-13 alone or in combination with FGFs did not induce upregulation of feedback inhibitors. Fold changes in gene expression are shown relative to untreated control values, data presented are the means \pm SD. This experiment was performed 7 times. *, $p < 0.05$, ** $p < 0.01$, ***, $p < 0.001$ (one-way ANOVA with Bonferroni's Multiple Comparison Test).

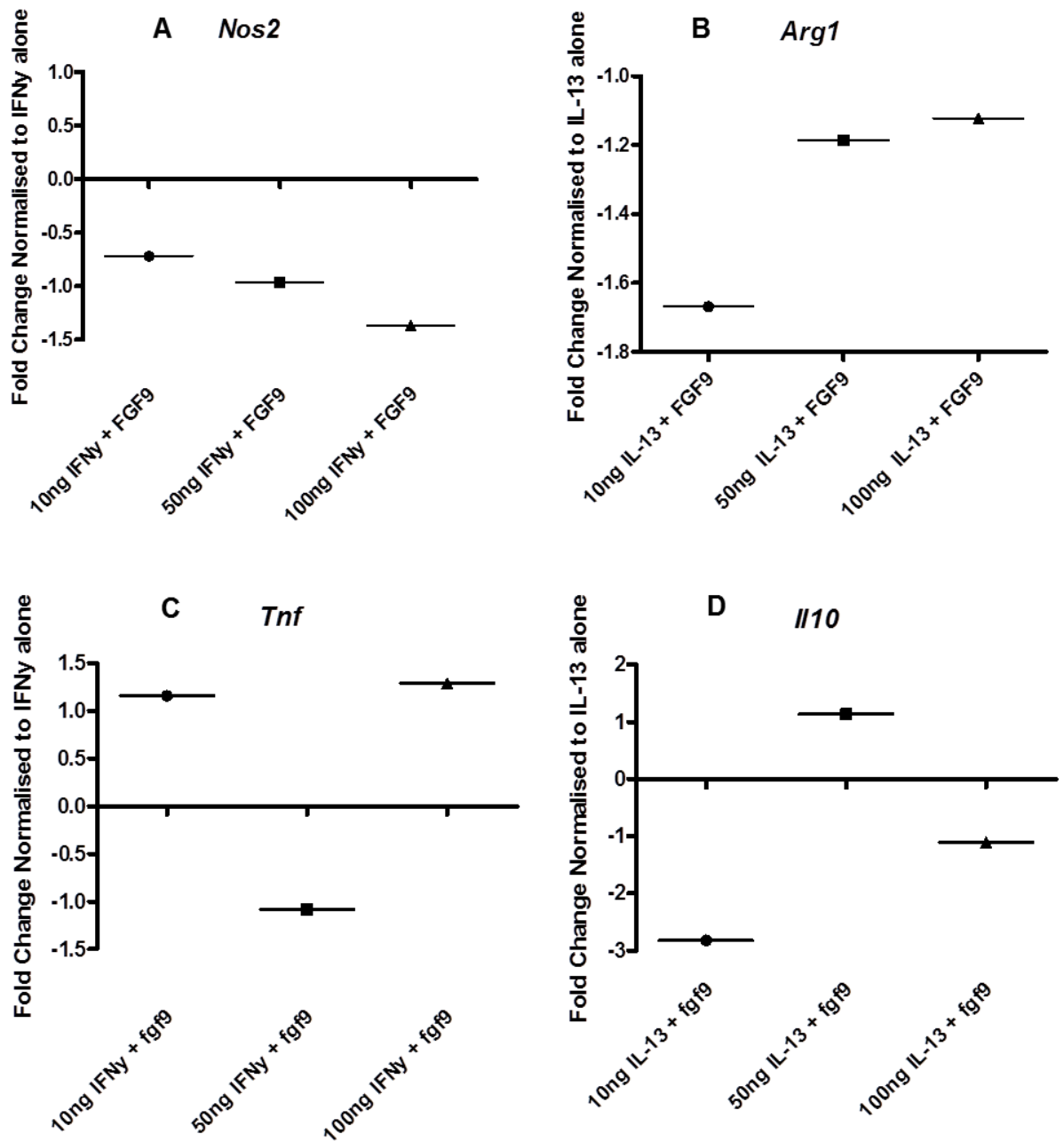


Figure 4.15. FGF9 did not influence macrophage polarization or cytokine expression. BMDMs were cultured with M-CSF for 7 days followed by 24-hour treatment with 10, 50, or 100 ng/mL IFN γ or IL-13 in combination with 100 ng/mL FGF9. *Nos2* expression increases in a dose-dependent manner with IFN γ treatment (A) and FGF treatment alone does not induce *Nos2* expression. Similarly *Arg1* is induced by treatment with IL-13, and FGF treatment alone had no effect (B). Normalising fold change between FGF9-treated and untreated macrophages revealed that FGF9 had no effect on M1 (C) or M2 (D) polarization. Inflammatory cytokine *Tnf- α* (E) and anti-inflammatory cytokine *il10* (F) expression were also unaffected by the presence of FGF9 in polarizing conditions. Fold changes in gene expression are shown relative to untreated control values, this experiment was performed once.

4.3 Discussion

Acute inflammatory exacerbations are considered to be the main driver of lesion development in RRMS and acute lesions were found to have higher levels of FGF9 compared to chronic lesions (Lindner et al., 2015). This was correlated with higher FGF9 expression and suggests aspects of the inflammatory response might drive expression of FGF9 in MS. Studies investigating cytokine profiles of MS lesions and the CSF of MS patients have found that TNF α , IFN γ , IL-6, IL-1 β , IL-10, GM-CSF, and TGF β 1 are the most prominent cytokines produced in acute MS (Romme Christensen et al., 2012, Durán et al., 2001, Tsukada et al., 1991, Maimone et al., 1991). PGE₂ has been shown to play a role in the regulation of FGF9 and might be involved in the pathogenesis of MS (Chuang et al., 2006, Mattsson et al., 2009). AhR activation has been linked to upregulation of FGF9 in adenocarcinoma and inflammation in MS (Wang et al., 2009, Quintana et al., 2008). These factors were tested for their ability to induce FGF9 expression at the mRNA and protein level in myelinating cultures as they are a good representation of the CNS, can be used for protein and RNA detection, and contain astrocyte and OLs which express FGF9 in acute MS lesions (Lindner et al., 2015).

Each factor was tested for its ability to inhibit myelination in the same manner as FGF9 treatment: 100 ng/mL from DIV 18 – 28. Most of the factors, with exception to TNF α (Cammer and Zhang, 1999) IFN γ (Agresti et al., 1996), and IL-6 (Zhang et al., 2006) have not been studied with regards to myelination *in vitro*. IFN γ was the only factor tested that had any significant effect on myelination (Figure 4.1 A). TNF α inhibited myelination in the study referenced above, however it had no effect in this myelinating culture system. IL-6 has been demonstrated to increase myelin production by cultured OLs (Zhang et al., 2006) but no effect was observed in the myelinating cultures (Figure 4.1A) The difference in effects on myelination seen in these experiments and the others mentioned may be due to the differences in the culture systems used. Treatment doses and durations also varied between studies making direct comparisons difficult. Axonal density was not reduced by treatment with any factor, which indicates that axonal integrity is not affected by long-term exposure to these inflammatory mediators alone (Figure 4.1 B).

FGF9 in myelinating cultures was measured at the messenger and protein level due to the different ways PGE₂, Ahr activation, and hypoxia have been shown to

regulate FGF9 expression (Wang et al., 2009, Chuang et al., 2006, Chen et al., 2014). qPCR for *Fgf1*, *Fgf2*, and *Fgf9* following 24-hour treatments showed no significant differences between any of the treatments and control cultures (Figure 4.2 – 4.4). These findings indicate that none of the inflammatory mediators tested are involved in FGF gene transcription in cells of the CNS in this culture system. BaP and PGE₂ have both been shown in other experimental models to up regulate FGF9 mRNA expression (Wang et al., 2009, Chuang et al., 2006) and that they did not here may be due to the different cell types that make up each model system. Myelinating cultures lack the immune cells that populate MS lesions and these may be necessary to facilitate a downstream effect on FGF9 expression. Lack of inflammation and damage in the cultures may also be inhibiting any effect of the factors as the multiple regulatory mechanisms of FGF9 expression may need to be disrupted for these factors to have an effect. BaP and PGE₂ were shown to upregulate FGF9 in cancer models. FGF signalling dysregulation is a hallmark of many cancers so these models may be associated with underlying FGF dysregulation that is not present in the myelinating cultures.

FGF9 protein expression in cells of myelinating cultures was assessed by immunofluorescence. Immunohistochemical studies of human and rat CNS tissues have shown that FGF9 is expressed by neurons, with the highest levels being in motor neurons in the spinal cord (Garcès et al., 2000, Nakamura et al., 1999, Nakamura et al., 1997). Myelinating rat cultures are composed of spinal cord-derived neurons and oligodendrocytes, and an underlying monolayer of striatum-derived astrocytes. Staining for FGF9 in the cultures shows that some axons are clearly immunoreactive for FGF9 (Figure 4.5 A). Astrocytes also stained for FGF9 against a background of diffuse FGF9 reactivity (Figure 4.5 A, B). Diffuse staining is likely due to FGF9 bound to cell surfaces and ECM components. The intermittent expression of FGF9 conserved in axons is likely due to some portions of the axons lying out of focus in another layer of the culture. These findings are similar to those observed in rat and human CNS, particularly the spinal cord. Cultures were treated from DIV 18 with each factor for three days and then stained for FGF9. Images were taken and analysed to calculate the MFI of FGF9 staining in each condition. None of the factors affected the levels of FGF9 protein expression in the cultures at 100 ng/mL. These results suggest inflammatory mediators, PGE₂, and AhR activation do not induce in FGF9 upregulation in

healthy CNS cells in myelinating and astrocyte cultures and may be relevant to elucidating the triggers for FGF9 upregulation in MS. Baseline levels of FGF9 in myelinating cultures appeared surprisingly high, which is not the case in the adult CNS. This may be due to the age of the cells being examined as myelinating cultures are derived from rat pup and embryonic cells. FGF9 is most highly expressed during development and levels in the brain are lower in adults (Nakamura et al., 1999).

Following the lack of induction observed by the panel of inflammatory mediators, other mechanisms of FGF9 upregulation in MS were investigated. Hypoxia was chosen for study due to its well documented roles in FGF regulation and evidence showing MS lesions can become hypoxic (Ganat et al., 2002, Yang et al., 2015, Aboul-Enein et al., 2003). Reduced oxygen concentration in cells activates HIF1 α , the master regulator of the cellular response to hypoxia (Pagé et al., 2002), which enters the nucleus and induces gene transcription. HIF1 α has also been detected in the nuclei of cells in MS CNS tissue.

(Chen et al., 2014) established a link between hypoxia and FGF9 expression in colon cancer and HEK293 cells. FGF9 protein expression was increased in cancerous sections compared to control colon and correlated with HIF1 α activation. HEK293 cells cultured under hypoxic conditions also upregulated FGF9 protein but had a reduced number of FGF9 mRNA transcripts. This suggested FGF9 expression was mediated by translational regulation hypoxia. These findings suggested hypoxia might be involved in FGF9 regulation in MS.

To determine whether hypoxia could induce FGF9 *in vitro*, myelinating cultures were incubated in a sealed chamber flooded with 1% O₂ for 24 hours. To test the effects of reperfusion, some cultures were transferred into a standard incubator for 24 hours following hypoxia. Myelination increased slightly between DIV 19 and 20 in control cultures (Figure 4.7 A; 4.8 A, C), whereas virtually no myelin was present in cultures exposed to hypoxia (Figure 4.7 A; 4.8 B, D). Axonal density was slightly reduced by 24 hours hypoxia but following reperfusion axons were completely absent from the cultures (Figure 4.7 B; 4.8 B, D). This would seem to suggest that the duration of treatment was too long and hypoxia lead to total cell death in myelinating cultures. However, this was not the case as astrocytes survived hypoxia and reperfusion (Figure 4.10). Staining for FGF9 in the surviving

astrocytes at 24 hours revealed a slight increase in MFI (Figure 4.9). Following reperfusion, astrocytic FGF9 expression was more than double control levels. These results are only representative of two experiments that will need to be repeated, however these findings suggest hypoxia leads to upregulation of FGF9 in astrocytes. Astrocytes have been shown to increase their use of glycolysis in hypoxia which might explain why they survived treatment (Marrif and Juurlink, 1999).

The next step in these experiments was to investigate gene expression in myelinating cultures following hypoxia. qPCR studies showed that *Hk2* expression is increased in myelinating cultures around 20 fold following 24 hours of hypoxia and returns to baseline after reperfusion (Figure 4.11A). HIF1 α expression is regulated translationally (Pagé et al., 2002), so Hif1 α mRNA levels are not a useful marker for hypoxia. *Hk2* encodes an enzyme involved in glycolysis that is upregulated by HIF1 α as part of the cellular response to hypoxia (Menendez et al., 2015). HIF1 α is constitutively expressed by all cells and is activated, but not upregulated, by hypoxia. Therefore HK2 is often used as a surrogate marker for HIF1 α activation. FGF1 mRNA levels were not affected by hypoxia or reperfusion (Figure 4.11B). *Fgf2* expression on the other hand was upregulated around seven fold following hypoxia and reperfusion (Figure 4.11C). FGF2 upregulation has been well documented in response to hypoxia, so this result was expected. It also suggests that astrocytes produce FGF2 and FGF9 in hypoxia. *Fgf9* expression was decreased two to three fold after hypoxia and reperfusion (Figure 4.11 D). This finding combined with the effects observed on FGF9 protein levels indicates that FGF9 levels in myelinating cultures exposed to hypoxia is regulated by hypoxia-induced translational activation as described by Chen et al. (Chen et al., 2014).

In the previous chapter, macrophages in acute MS were shown to be immunoreactive for FGF9. In these experiments, BMDMs were treated with polarizing cytokines and their FGF mRNA expression was analysed. IFN γ robustly induced *Nos2* expression in BMDMs after 24 and 48 hours, and this effect had mostly dissipated 24 hours after IFN γ withdrawal (Figure 4.12 A). *Arg1* expression was significantly increased only after 48 hours treatment with IL-13 (Figure 4.12 B). *FGF1* expression was unaffected in IFN γ and IL-13-polarised macrophages (Figure 4.13 A). *FGF2* levels were unchanged by IFN γ but were significantly

elevated after 24-hour treatment with IL-13 but these levels decreased slightly after a further 24 hours and the change was no longer significant (Figure 4.13 B). Macrophages polarised towards a repair phenotype have been shown to produce FGF2 in previous studies (Jetten et al., 2014) and this result is in line with those findings. *Fgf9* mRNA was increased in IL-13-polarised BMDMs to a variable extent after 24 hours but only became significantly upregulated after 48 hours (Figure 4.13 C). *Fgf9* was only increased after *Arg1* was also significantly elevated and the levels were variable but overall higher than those seen for *Fgf2* upregulation. M1 polarization of BMDMs had no effect on the expression of any FGFs tested which suggests FGF production is a feature of anti-inflammatory macrophages.

The next question to be answered concerning macrophages was whether FGFs influence macrophage phenotype and function. BMDMs were treated with polarising cytokines in the presence or absence of FGF1, 2, or 9, and screened for expression of FGF-feedback inhibitors, polarisation markers, and associated cytokines. None of the FGFs tested induced feedback inhibitor upregulation in macrophages polarized with IFN γ or IL-13, suggesting that macrophages are not a target for FGF signaling (Figure 4.15). In addition to these results, no differences in *Nos2*, *Arg1*, *Tnf*, or *Il10* expression were seen in macrophages polarised in the presence or absence of FGFs (Figure 4.16). This experiment has only been performed once and will have to be repeated but the results are in line with the results in Figure 4.14.

Interestingly, expression of all four feedback inhibitors was reduced in IFN γ treated macrophages, indicating that downregulation of MAPK signaling inhibitors is a component of M1 polarisation. Sprouty2 downregulation in IFN γ treated macrophages has been described before (Atomura et al., 2016) and in this study small-interfering RNA knockdown of Sprouty2 expression drove macrophages towards the M2 phenotype. This would suggest that reduced expression of MAPK inhibitors promotes an anti-inflammatory phenotype in macrophages and may be a component of intrinsic regulation of inflammation in macrophages. Together these data support the finding that macrophages are a source of FGF9 in MS and predict that FGF9⁺ macrophages in MS lesions will exhibit a repair phenotype and express *Arg1*. Additionally, macrophage polarisation and cytokine expression profile is not influenced by the presence of FGFs associated with MS lesions.

In this chapter, potential mechanisms involved in the induction of FGF9 in MS were investigated in *in vitro* CNS cultures. Inflammatory and anti-inflammatory mediators produced in MS lesions did not induce FGF9 mRNA or protein expression in myelinating cultures. Hypoxia was lethal for most CNS cell types but astrocytes persisted and up regulated FGF9 protein expression while mRNA levels fell. This suggests FGF9 in myelinating and astrocyte cultures is subject to the same regulatory pathways triggered by hypoxia as those described for colon cancer (Chen et al., 2014). Macrophages were also shown to up regulate FGF9 when polarized towards an anti-inflammatory phenotype. Together these findings suggest FGF9 up regulation in myelinating cultures is a consequence of normal repair mechanisms, and the failure of the lesion to resolve results in chronically increased production of FGF9. These findings suggest that hypoxia may play a role in FGF9 up regulation in MS and future studies should examine the expression of FGF9 and markers of hypoxia in MS brains to determine whether there is a correlation.

CHAPTER FIVE

**FGF9 DISRUPTED MYELINATION AND
INDUCED AXONAL PATHOLOGY**

5 FGF9 DISRUPTED MYELINATION AND INDUCED AXONAL PATHOLOGY

5.1 Introduction

The main drivers of symptoms and disability in MS are loss of myelin sheaths required for saltatory conduction, and loss of axons at which point, damage becomes irreparable. Targeting both of these pathogenic mechanisms therapeutically would restore functional nerve transmission, and preserve and protect axons (Chandran et al., 2008). This is especially true in progressive MS where inflammation is less prevalent and a range of neurodegenerative mechanisms drive disease progression.

In earlier stages of MS, OPCs efficiently repopulate demyelinated lesions and do not lose proliferative capacity after several bouts of demyelination (Penderis et al., 2003). Despite robust replacement of progenitors, complete remyelination only occurs in a small subset of MS patients and becomes less efficient with age and increasing disease duration (Patrikios et al., 2006, Sim et al., 2002). The proposed reasons for remyelination failure in MS are myriad which in itself suggests many contributing factors create a lesion environment that is impermissible to remyelination. As the problem does not appear to lie with replacement of progenitors, the point of remyelination failure likely occurs as OPCs try to differentiate and produce myelin. Complex growth factor and intracellular signaling pathways regulate the processes of OPC differentiation and myelination, which are perturbed by the complex inflammatory cytokine and growth factor signaling environment of the MS lesion (Franklin, 2002). FGF9 is one such contributing factor to remyelination failure as it promotes OPC proliferation but inhibits their differentiation via astrocyte-secreted factors (Lindner et al., 2015). A feature of FGF9-treated myelinating cultures is the appearance of round MOG⁺ cells, which may represent a failed attempt at OPC differentiation (unpublished observation).

The pathogenic mechanisms underlying axonal loss in progressive MS are discussed in section 1.1.2.2. Loss of myelin sheaths leave axons more vulnerable to damage and increases metabolic stress. Similar processes underpin neuronal damage in other neurodegenerative diseases such as Alzheimer's and Parkinson's disease. Dystrophic neurites and astrocytes are immunoreactive for

FGF9 in Alzheimer's plaques, suggesting it plays a role in disease pathology (Nakamura et al., 1998). Several studies demonstrated a neuroprotective role for FGF9 in different toxin-induced neurodegeneration models (Huang et al., 2009, Huang and Chuang, 2010, Kanda et al., 1999). In myelination experiments, FGF9 inhibited myelination without affecting the density of underlying axons (Figure 1.3). Immunohistochemical analysis of post-mortem MS brains (Lindner et al., 2015) showed FGF9 is expressed in acute lesions, and to a lesser degree, in chronic-active lesions. So far, investigation of FGF9 using the myelinating culture system has mainly focused on its effects on primary myelination. While this provides insight into the roles of FGF9 in remyelination, it does not address the impact of FGF9 expression during other stages of MS. The myelinating culture system can be used to address these questions:

1. Does longer-term treatment with FGF9 have additional pathological effects that are not apparent at DIV 28?
2. In addition to inhibition of myelination, can FGF9 cause demyelination?
3. Can myelination recover in cultures that have been treated with FGF9?

To answer these questions the following experiments were performed: 10 and 20-day FGF9 treatments were performed in myelinating cultures between DIV 18 and 38. 10-day FGF9 treatments were started on DIV 18 (onset of myelination) or DIV 28 (when the majority of myelination has occurred). FGF9 was withdrawn from DIV 18 – 28 treated cultures that were then maintained in control media until DIV 38. Control cultures were maintained in control media throughout, or treated with FGF9 from DIV 18 – 38.

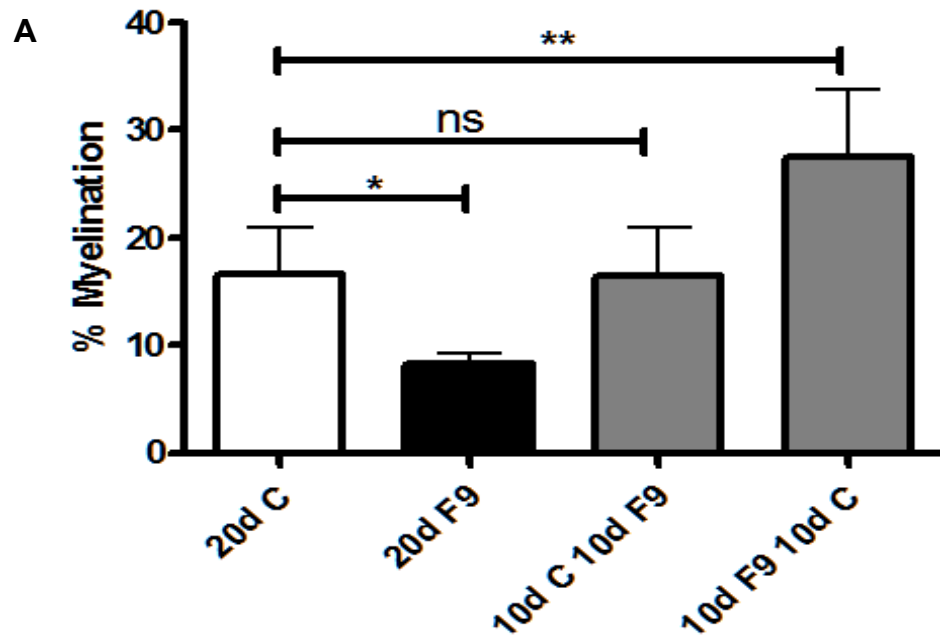
5.2 Results

5.2.1 FGF9 had different effects depending on the duration of treatment and age of cultures when treatment was initiated

5.2.1.1 FGF9 did not cause demyelination after 10-day treatment

Myelinating cultures produce the majority of their myelin sheathes between DIV 18 and 28. Treating cultures with FGF9 between these time points results in near total inhibition of myelination (Figure 1.3, 1.4). To determine if FGF9 is a demyelinating factor, as well as a myelin-inhibitory factor, myelinating cultures were treated with FGF9 from DIV 28 – 38. At DIV 38, cultures were fixed and stained as described in section 2.2.7. The percentage of myelinated axons and axon densities were calculated using CellProfiler as described in section 2.2.8. Cultures treated in this fashion had comparable levels of myelination to control cultures at DIV 38, indicating FGF9 does not directly cause demyelination (Figure 5.1 A, 5.2 C). Although FGF9 did not appear to affect mature OLs, brightly staining MOG⁺ round cells were numerous in these cultures (Figure 5.2). These cells are a common feature of myelinating cultures treated with FGF9 at any time point and suggest that FGF9 has a detrimental effect on the OPC population in myelinating cultures and leads to aberrant maturation and production of myelin proteins.

DIV 18 - 38 Myelinating Culture Treatment



DIV 18 - 38 Myelinating Culture Treatment

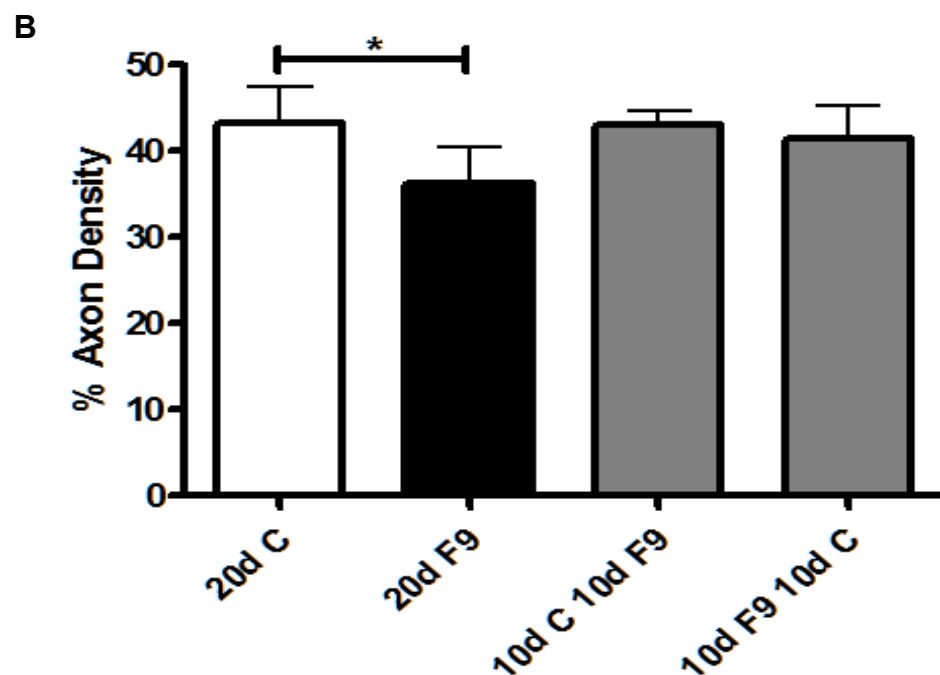


Figure 5.1. FGF9 was not a demyelinating factor and pre-treatment increased myelin production. Myelinating cultures were alternately treated with FGF9 for 10 days from DIV 18 followed by 10 days in control media or vice versa. Control cultures were treated with FGF9 or DM- for 20 days to compare the effects of alternating treatment. Cultures were fixed and stained with antibodies against MOG (Z2) and axons (SMI31). Myelination rates and axon densities were calculated in CellProfiler. Adding FGF9 at DIV 28 did not demyelinate cultures after 10-day treatment. Removing FGF9 at DIV 28 after 10-day treatment caused a significant increase in myelination by DIV 38. 20-day treatment with FGF9 led to a small but significant decrease in axon density. Data presented are the means \pm SD. This experiment was performed three times. *, $p < 0.05$, **, $p < 0.01$ (one-way ANOVA with Dunnett's Multiple Comparison Test).

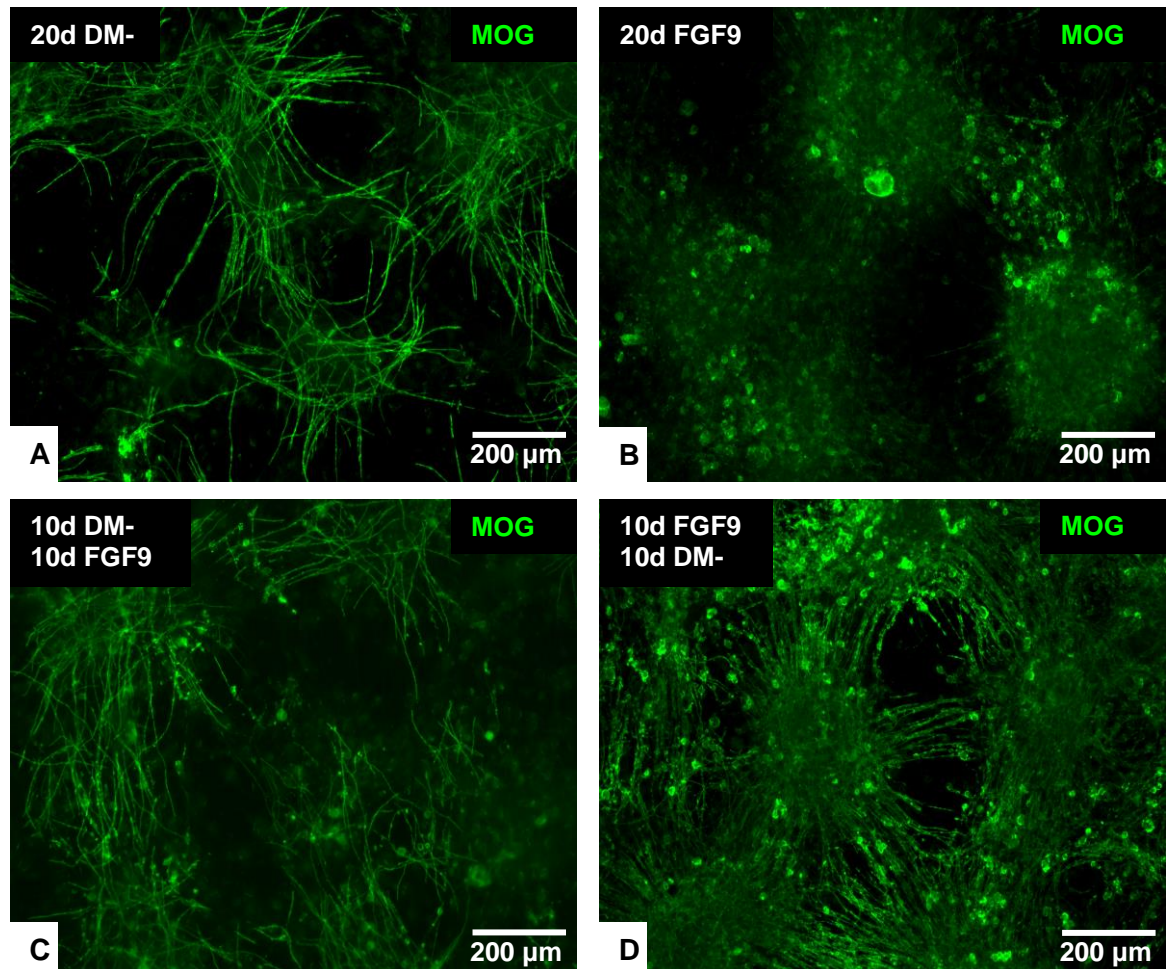


Figure 5.2. Representative images of myelinating cultures after alternating FGF9 treatment. Myelinating cultures were alternately treated with FGF9 for 10 days from DIV 18 followed by 10 days in control media or vice versa. Control cultures were treated with FGF9 or DM- for 20 days to compare the effects of alternating treatment. Cultures were fixed and stained with antibodies against MOG (Z2) and axons (SMI31). Representative images show myelination in 20 DIV (A) control cultures, and 20 DIV (B) FGF9-treated cultures, and cultures were FGF9 was added at DIV 28 (C) or removed at DIV 28 (D).

5.2.1.2 Removing FGF9 from cultures treated from DIV 18 - 28 led to increased but aberrant myelination

FGF9 treatment from DIV 18 and 28 inhibits myelination in myelinating cultures. This is associated with a massive increase in OPC numbers (Lindner et al., 2015) and the appearance of round MOG⁺ cells, thought to be the product of disrupted OPC maturation. This raised the question of whether OPCs generated from FGF9 treatment can facilitate normal myelination, or are they already on the path to defective maturation like the round MOG⁺ cells? To address this, FGF9 was withdrawn from cultures treated from DIV 18 – 28. These cultures were treated with control DM- for a further 10 days before fixation and processing for immunofluorescence.

Assessing myelination using CellProfiler revealed that levels were greater in FGF9-withdrawal cultures than DIV 38 control cultures (10d F9 10d C: 27.5% ± 6.4%; 20d C 16.6% ± 4.4%, $p < 0.01$) (Figure 5.1 A). MOG⁺ round cells were observed in these cultures 10 days after FGF9 treatment was stopped (Figure 5.2 D). Under confocal microscopy the myelin produced in 10d F9 10d C cultures appears starkly different to myelin in untreated controls (Figure 5.3). Myelin sheathes in 20d C cultures present as long, continuous strands of an even thickness that envelop long portions of axons (Figure 5.3 A). Some normal-appearing myelin sheathes are visible in 10d F9 10d C cultures (Figure 5.3 B), however, the majority of myelin sheathes appear irregular with significant membrane blebbing and separation from underlying axons (Figure 5.3 B, C).

MOG⁺PLP⁺ cells appear after FGF9 treatment (Lindner et al., 2015) and resemble pre-myelinating OLs described in chronic MS lesions (Chang et al., 2002). These same cells persisted 10 days after FGF9 treatment. Cultures were stained with antibodies against MOG and PLP, and imaged by confocal microscopy. Examples of double-labelled cells are shown in Figure 5.4. Cell bodies and processes are filled with a mixture of MOG and PLP staining. The cell shown in Figure 5.4 A has produced a network of processes filled with punctate granules of MOG and PLP. The cell in Figure 5.4 B stains strongly for each myelin protein in the cell body, surrounded by a fine web of processes, which contain little of each protein. The appearance of these cells is highly variable and irregular and does not reflect the appearance of any stage of normal OL maturation.

Membrane blebbing and the punctate appearance of myelin proteins in these cultures somewhat resembles myelin breakdown products in MS and EAE. In these conditions, degrading myelin is rapidly phagocytosed by macrophages and microglia, and myelin proteins can be detected in phagocytic vacuoles (Boven et al., 2006). To determine if the irregular myelin seen in 10d F9 10d C myelinating cultures is also undergoing phagocytosis, cultures were double-labelled with IBA1 and MOG. Searching under confocal microscopy, no colocalization of myelin in microglia membranes was detected suggesting the irregular myelin is not the result of myelin destruction and phagocytosis (Figure 5.5).

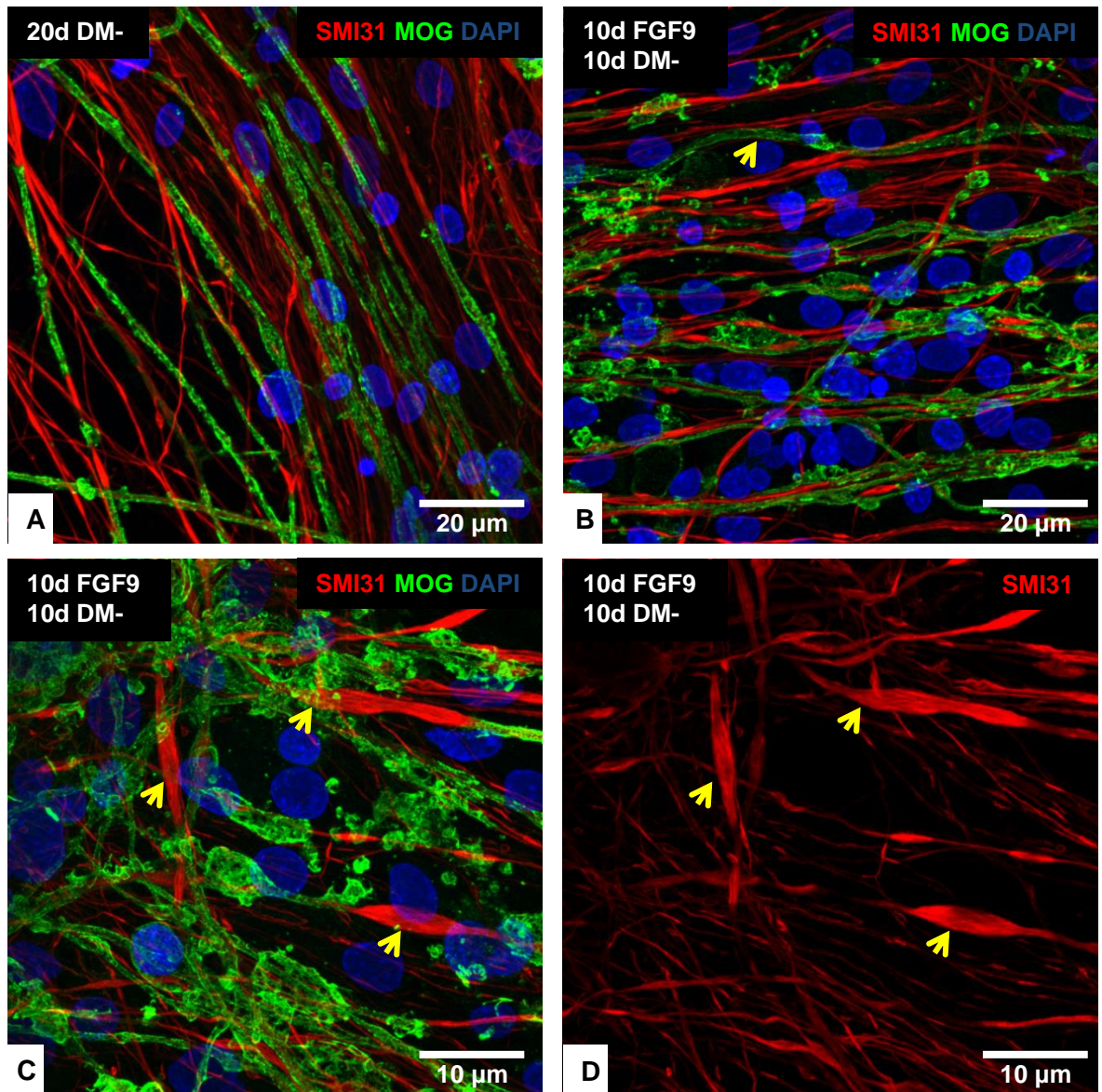


Figure 5.3 Pre-treatment with FGF9 disrupted myelination and causes an axonal pathology. Myelinating cultures were alternately treated with FGF9 for 10 days from DIV 18 followed by 10 days in control media or vice versa. Cultures were fixed and stained with antibodies against MOG (Z2) (green) and axons (SMI31) (red), which label myelin and axons respectively. Myelin sheaths in controls (A) appear uniform and continuous whereas myelin produced 10 days after FGF9 withdrawal appears highly irregular with intermittent thick and thin portions, and extensive membrane blebbing (B, C). The underlying axons in image C are shown in D and display several axonal swellings (arrows), which are shown in C to be unmyelinated.

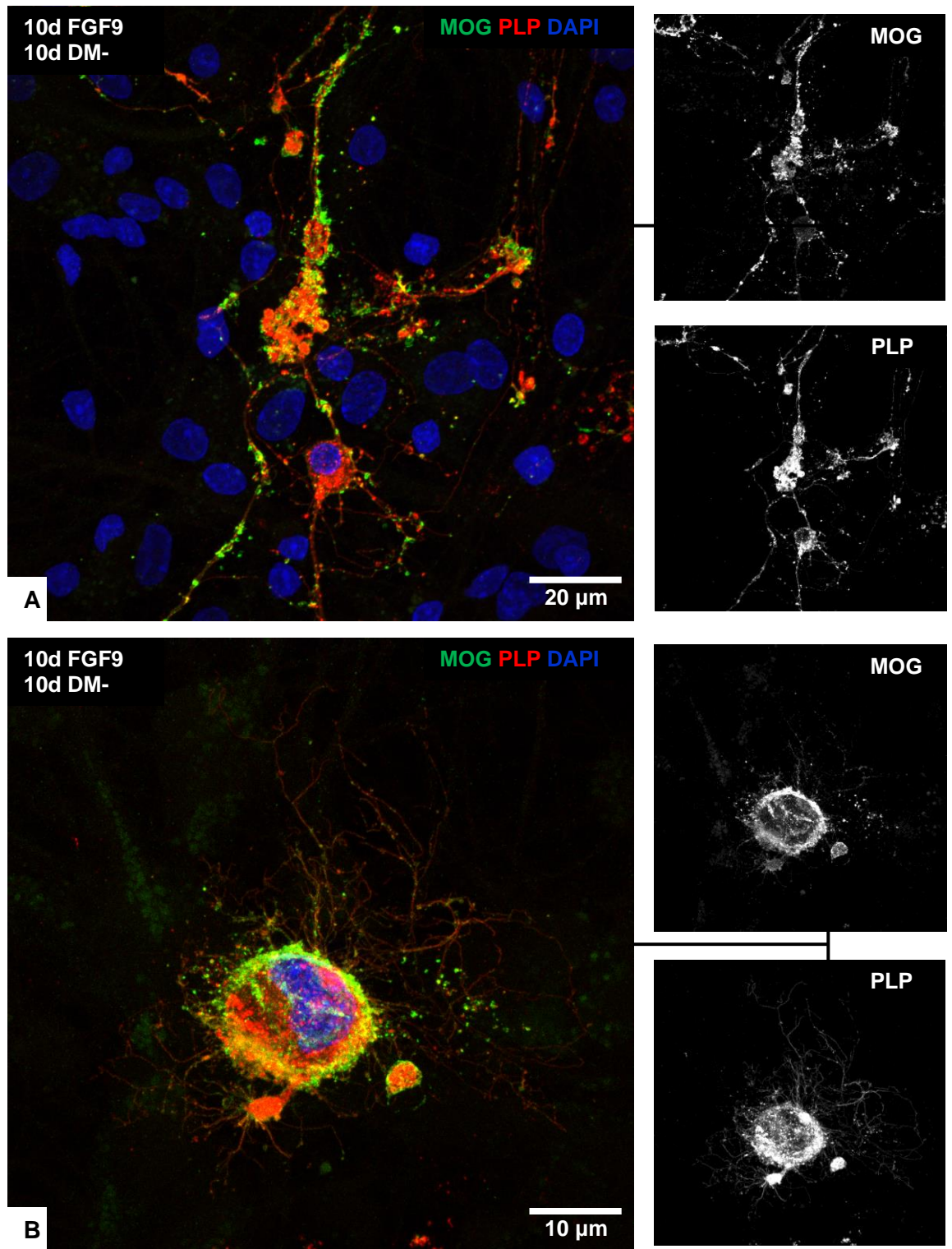


Figure 5.4 Confocal imaging of MOG⁺PLP⁺ cells reveals stark morphological differences from normal OLs. MOG positive cells observed in FGF9-treated myelinating cultures were stained together with an anti-PLP antibody, and imaged using confocal microscopy. High magnification revealed overlapping and distinct areas of PLP and MOG expression within the same cells. MOG⁺PLP⁺ cells were frequently observed to produce extensive processes which also contain myelin proteins.

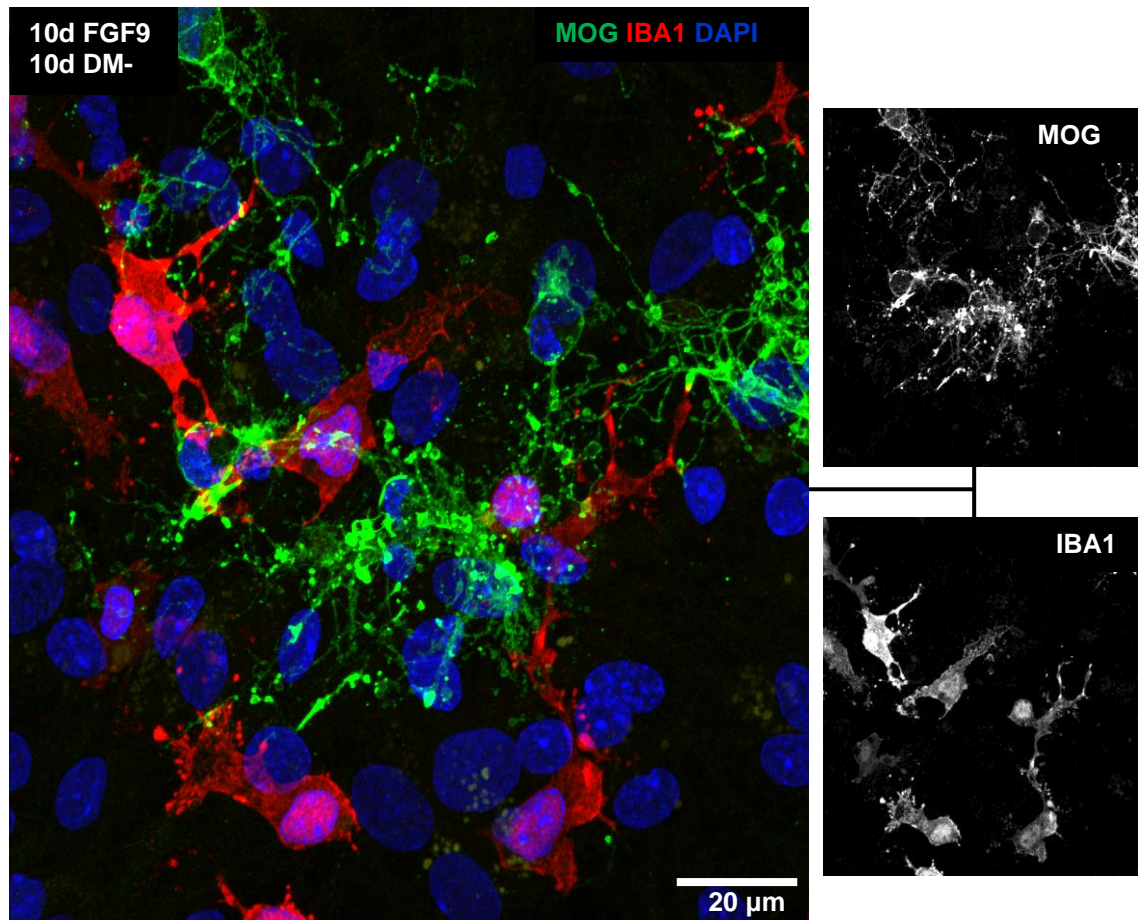


Figure 5.5 Microglia did not phagocytose irregular myelin produced as a result of FGF9-treatment. Myelinating cultures were alternately treated with FGF9 for 10 days from DIV 18 followed by 10 days in control media or vice versa. Control cultures were treated with FGF9 or DM- for 20 days to compare the effects of alternating treatment. Cultures were fixed and stained with anti-MOG (green) and anti-IBA1 (red) which label myelin and microglial respectively. Using confocal microscopy myelin was not observed within microglial membranes.

5.2.1.3 Long term treatment with FGF9 was detrimental to axons in myelinating cultures

Myelinating cultures treated with FGF9 for 10 days (DIV 18 - 28) have comparable levels of axonal density to control cultures (Figure 1.3, 1.4). Doubling the length of treatment (DIV 18 – 38) led to a small but significant reduction in axonal density compared to control cultures (20d C = 43% \pm 4%; 20 F9 = 36% \pm 4.1%, $p < 0.05$) (Figure 5.1 B). This effect was not observed in cultures treated for just 10 days from DIV 18 or DIV 28, and 10 days after FGF9 withdrawal (Figure 5.1 B). This finding suggests that axons can remain intact through a short course of FGF9 treatment but begin to suffer damage after chronic exposure.

When examining axons in 10d F9 10d C-treated myelinating cultures under high power magnification, abnormalities in neurofilament (SMI31) staining and axon structure were observed (Figure 5.3 C, D). Axons in control cultures appear continuous with an even distribution of SMI31 staining along individual axons (Figure 5.3 A). Intermittent bright and dark regions of neurofilament are apparent along the length of axons treated with FGF9, 10 days after its withdrawal. Axonal swellings are also apparent in FGF9-treated cultures, and are seen in areas of the axons that lack myelin (Figure 5.3 C, D). This suggests they have become damaged as a result of not being myelinated, or the areas of swelling are not able to undergo normal myelination. Re-examining the cultures used for Figure 5.1, under higher magnification, revealed axonal pathology is present after 10-day FGF9 treatment. Control axons at DIV 28 (Figure 5.6 A) and 38 (Figure 5.6 B) appear similarly healthy and uniform. Cultures treated with FGF9 for 10 days (Figure 5.6 C, E), 20 days (Figure 5.6 D), or 10d FGF9 10d C (Figure 5.6 F) all display a similar axonal pathology characterised by swellings and more punctate neurofilament staining. Although 10-day FGF9 treatment is not associated with a reduction in axon density, this observation shows that physical changes precede loss of axons seen after 20-day FGF9 treatment.

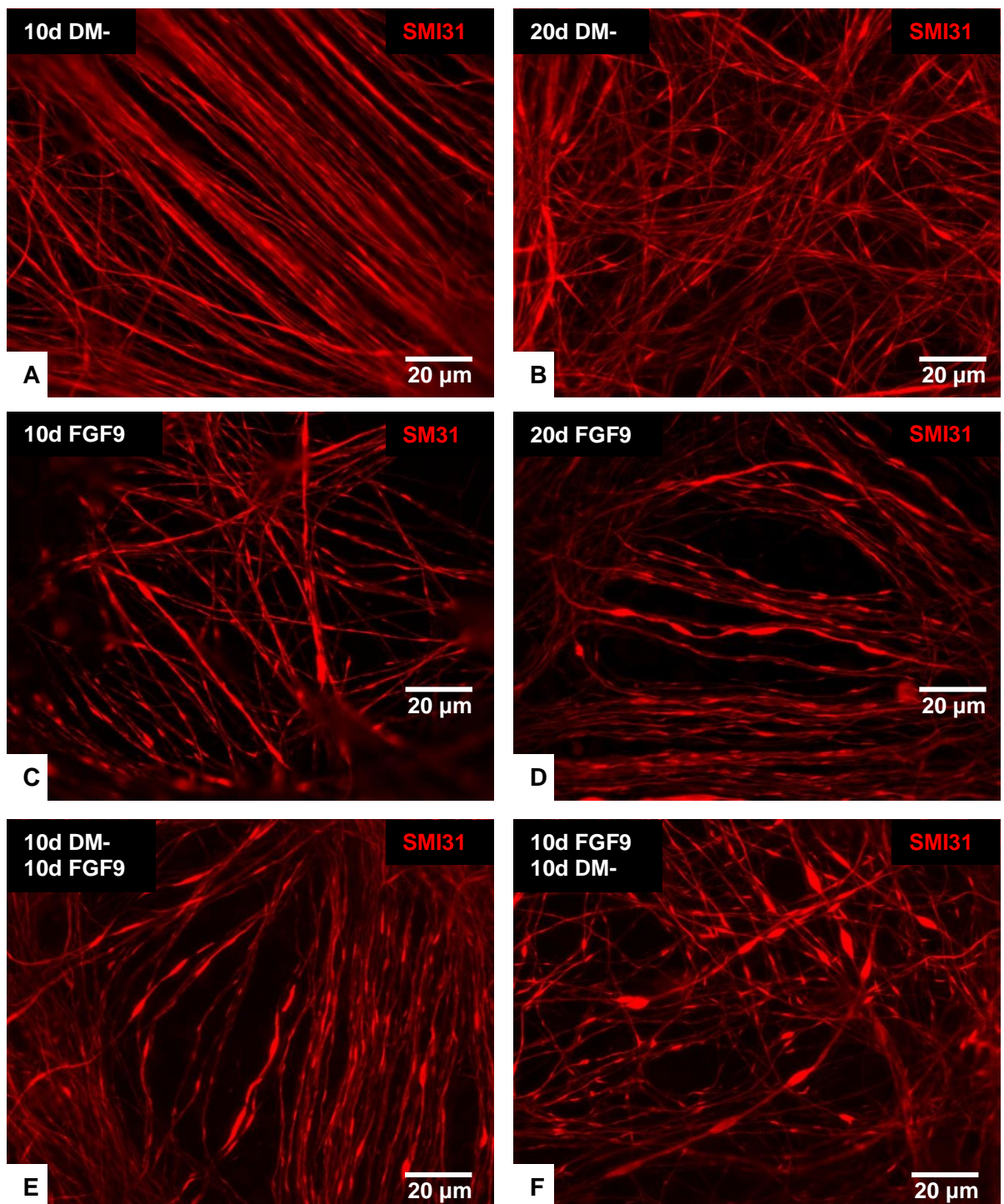


Figure 5.6. Axonal pathology preceded reduction in density in FGF9-treated myelinating cultures. Representative images show control axons at DIV 28 (A) and DIV 38 (B). Axons in FGF9-treated cultures have more punctate neurofilament staining and the presence of swellings along the length of axons after 10 (C) or 20 (D) day treatment. Axons still have an irregular appearance when treatment is started late (E) and 10 days after FGF9 withdrawal (F).

5.2.1.4 Oligodendrocyte numbers increased by FGF9 treatment return to control levels after the factor is withdrawn

OPCs proliferate rapidly in myelinating cultures in response to FGF9 and remain in a progenitor state (Lindner et al., 2015), however the fate of these cells has not been investigated. Results from the previous section suggest that many of these OPCs attempt to differentiate and produce myelin sheathes with limited success. Using the FGF9-treatment regime used in the previous sections of this chapter, myelinating cultures were fixed and stained with antibodies against NG2 (a chondroitin sulphate proteoglycan expressed on OPC cell membranes) and Olig2 (transcription factor specific to OL lineage cells). OPC numbers were counted manually in ImageJ and total OL lineage cell numbers were calculated by CellProfiler. Cells were counted from 30 fields of view per condition and results were expressed as cells/ field of view (FOV).

NG2⁺ cell numbers more than doubled in 20d F9 and 10d C 10d F9 treated cultures compared to controls (20d C = 30.2 ± 6.4 cells/FOV; 20d F9 = 81.6 ± 9.2 cells/FOV, 10d C 10d F9 = 73.3 ± 12.5 cells/FOV, $p < 0.001$) (Figure 5.7 A). NG2⁺ cell numbers reached a similar level despite one course of treatment being twice the length of the other. In 10d F9 10d C treated cultures NG2⁺ cells numbers were almost the same as in the 20d C (10d F9 10d C = 32.7 ± 4.9 cells/FOV). A similar trend was observed when total OL lineage cell numbers were quantified: 20d F9 and 10d C 10d F9 treatment increased Olig2⁺ cell numbers by 4 fold (20d C = 66.3 ± 37.1 cells/FOV; 20d F9 = 251.4 ± 60.5 cells/FOV, 10d C 10d F9 = 265.4 ± 78.8 cells/FOV, $p < 0.05$) (Figure 5.7 B). Total OL numbers remained elevated in 10d F9 10d C treated cultures, 132.9 ± 34.3 cells/FOV, however this was not significantly different from 20d C OL numbers. Representative images of NG2 and Olig2 stainings in FGF9-treated myelinating cultures are shown in Figure 5.8 and Figure 5.9 respectively.

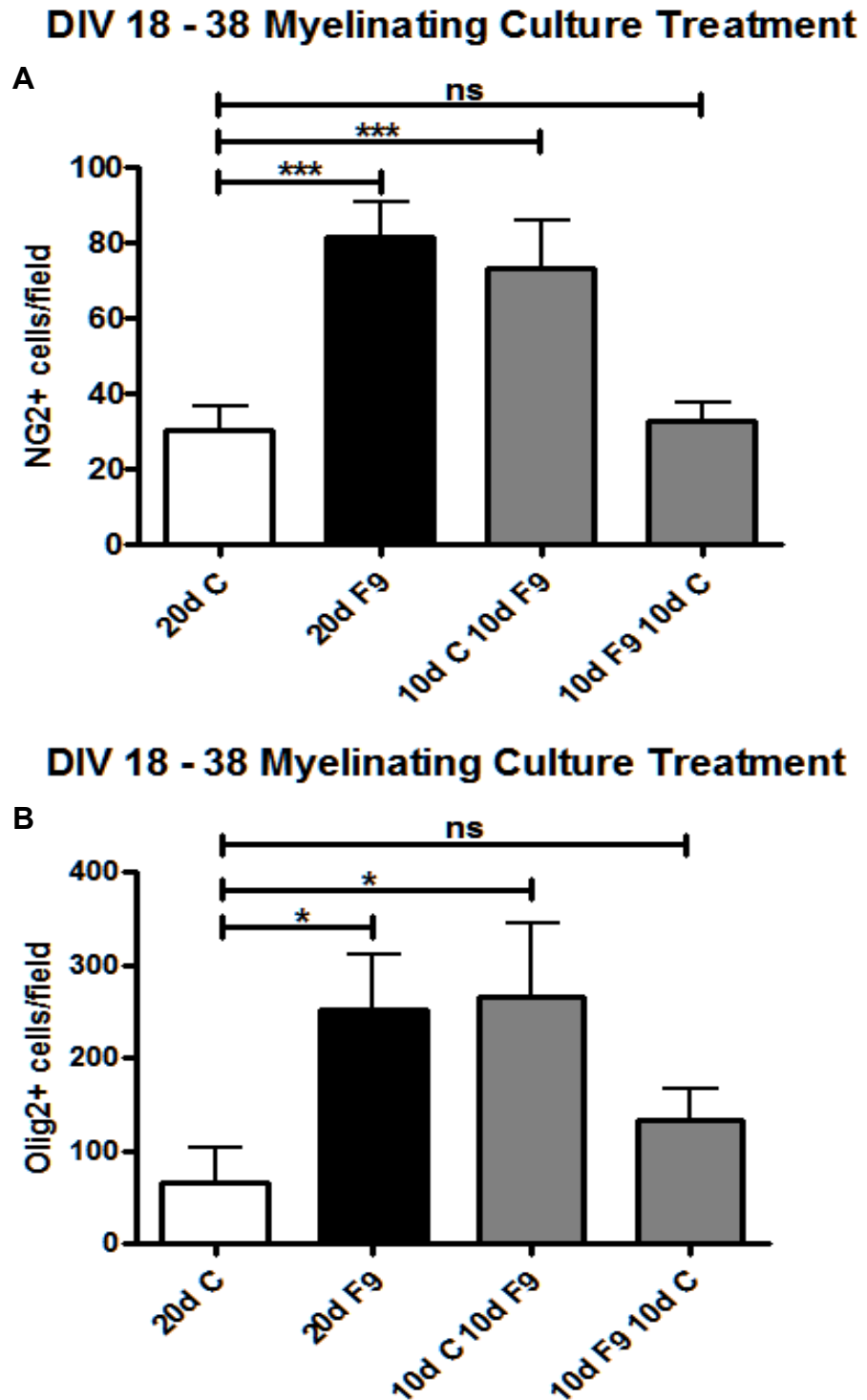


Figure 5.7. OPC and OL lineage cell numbers increased after FGF9 treatment and returned to baseline levels after it is withdrawn. Alternately treated myelinating cultures were fixed and stained with NG2 (OPCs) and Olig2 (OL lineage marker), and cell numbers were quantified. FGF9 treatment doubled NG2⁺ cell populations after 10 or 20-day treatment (A) but these numbers returned to control levels 10 days after the withdrawal of FGF9. Total OL numbers, observed as Olig2⁺ cells similarly increased and contracted following FGF9 treatment. Data presented are the means \pm SD. This experiment was performed three times. *, $p < 0.05$, ***, $p < 0.001$ (one-way ANOVA with Dunnett's Multiple Comparison Test).

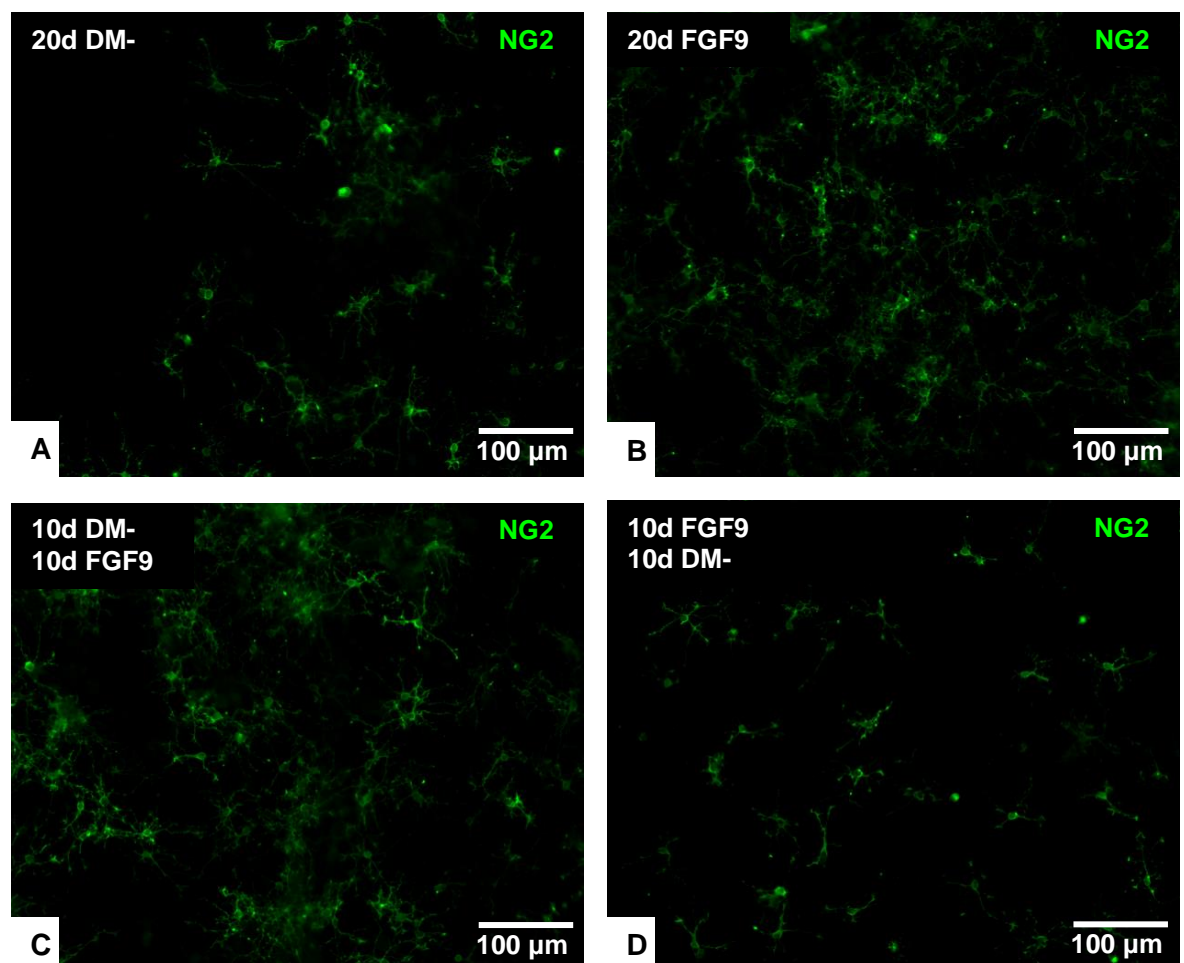


Figure 5.8. Representative images of NG2 staining after alternating FGF9 treatment. NG2+ cell numbers were similar in controls (A) and FGF9 treated cultures 10 days after it had been withdrawn (D) whereas cultures treated with FGF9 to the experiment endpoint (B, C) appeared to have much greater numbers of OPCs.

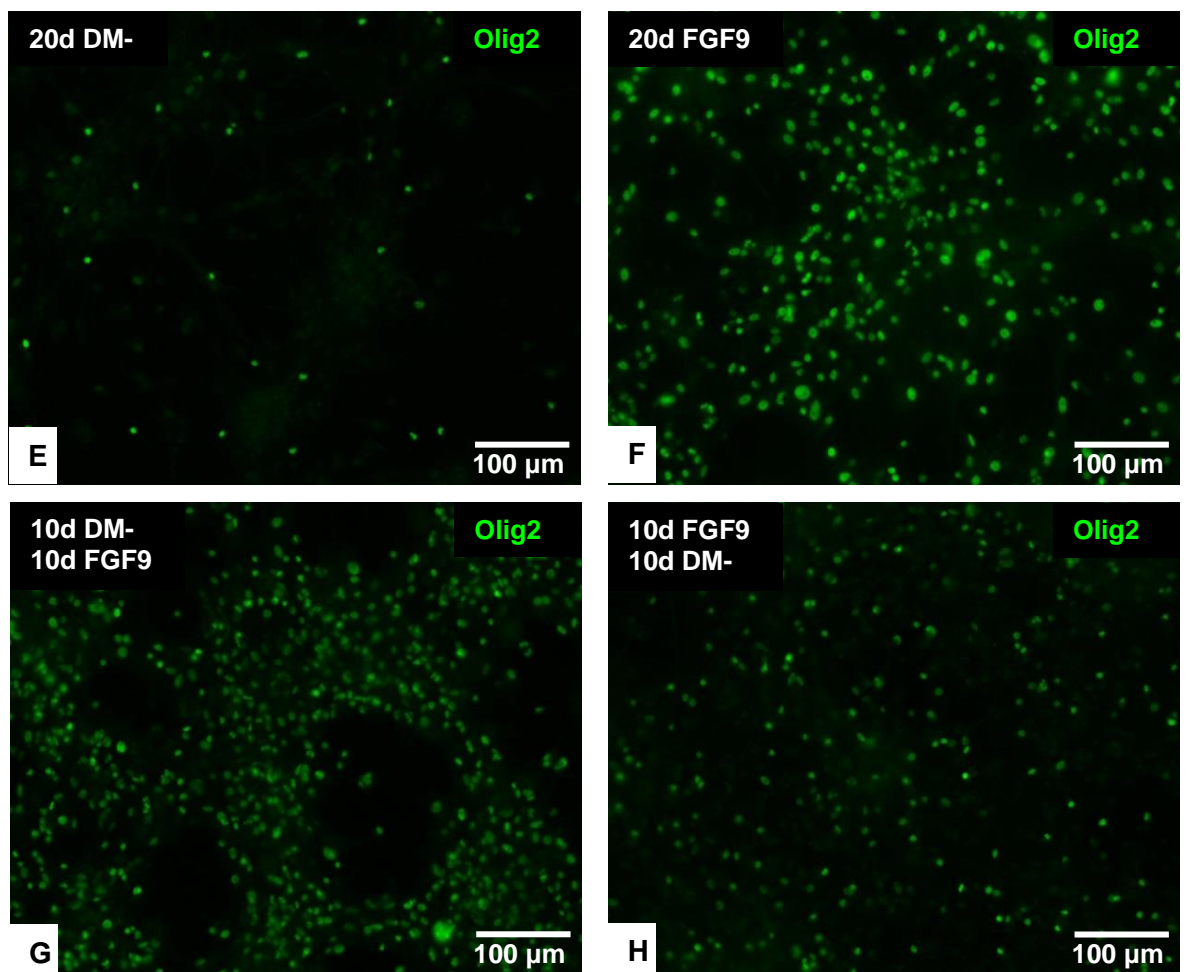


Figure 5.9. Representative images of Olig2 staining after alternating FGF9 treatment. Total OL numbers were increased following all 3 variants of FGF9 treatment compared to control cultures, but were decreased 10 days after FGF9 withdrawal.

5.2.2 FGF9 treatment reduced neuronal numbers, axonal density, and axonal transport-gene expression in enriched neuronal cultures

5.2.2.1 Expression of genes involved in axonal transport were reduced in myelinating cultures treated with FGF9

Screening of the microarray performed by Lindner et al., 2015 revealed FGF9 treatment led to a reduction in expression of genes associated with axonal transport (Table 5.1). Neurofilament light, medium, and heavy chains comprise components of the neuronal cytoskeleton (*Nefl*, *Nefm*, *NefH*). *Dnah3*, *Dnah6*, *Dnah9*, *Dync1i1*, and *Dynlrb2* encode members of the dynein motor protein family. *Kif5a* encodes a member of the kinesin motor protein family, and *SV2B* encodes Synaptic Vesicle Glycoprotein 2B, which is involved in vesicle trafficking and exocytosis. *Rbfox3* and *Tubb3* encode NeuN and β -tubulin III respectively, both of which are neuron-specific markers. After 24-hour or 10-day treatment with FGF1 or FGF2, some of these genes were variably downregulated, however after 10-day treatment with FGF9, all genes shown were downregulated more than 1.4 fold. Some of the genes were downregulated at 24 hours with FGF9, but the effect was more pronounced after 10 days suggesting this is an effect of chronic exposure to FGF9.

Validation of the microarray results by qPCR showed a similar pattern of downregulation of axonal transport genes after 10-day FGF9 treatment (Figure 5.10). *Nefh* (-2.6 ± 1.2 fold), *Dnah6* (-4.7 ± 2.9 fold), *Dnah9* (-3.3 ± 1.8 fold), *Dync1i1* (-2.9 ± 1.5 fold), *Kif5a* (-3.1 ± 2 fold), *Sv2b* (3.8 ± 1.4 fold), *Rbfox3* (-3 ± 1 fold), and *Tubb3* (-5 ± 3.1 fold) were all significantly downregulated in FGF9 treated myelinating cultures (Figure 5.10 A). *Dnah3*, *Dynlrb2*, and *Tubb3* expression trended towards downregulation but the changes were not statistically significant. *Ccl2* (11.7 ± 9.5 fold), and *Ccl7* (20.7 ± 18.4) fold changes were used as positive controls as they are upregulated by FGF9 in myelinating cultures (Figure 5.10 B) (Lindner et al., 2015).

Gene	FGF1		FGF2		FGF9	
	24 hours	10 Days	24 hours	10 Days	24 hours	10 Days
<i>Nefl</i>	-1.14265	-1.0903	-1.14096	-1.54368	-1.14265	-2.36118
<i>Nefm</i>	-1.22304	-1.31223	-1.30605	-2.25285	-1.22304	-4.331
<i>Nefh</i>	-1.2605	-1.30119	-1.43455	-2.50954	-1.2605	-6.09924
<i>Dnah3</i>	-5.52951	-1.05453	-3.20084	-2.18922	-5.52951	-8.77238
<i>Dnah6</i>	-4.25718	1.0832	-3.37902	-1.63581	-4.25718	-10.5408
<i>Dnah9</i>	-3.32719	1.19712	-2.86807	-1.49013	-3.32719	-6.99545
<i>Dync1i1</i>	-1.31006	-1.02431	-1.35517	-1.89736	-1.31006	-3.52551
<i>Dynlrb2</i>	-4.46907	-1.07507	-3.62441	-1.40705	-4.46907	-5.40226
<i>Kif5a</i>	-1.25404	-1.03218	-1.28978	-1.42876	-1.25404	-2.80844
<i>Sv2b</i>	-1.24524	-1.03132	-1.53362	-1.54508	-1.24524	-4.73995
<i>Rbfox3</i>	-1.28059	-1.08793	-1.35543	-1.59024	-1.28059	-2.78494
<i>Tubb3</i>	-1.14227	1.05834	-1.11176	-1.24627	-1.14227	-2.55708

Table 5.1 Differentially expressed neuronal genes in myelinating cultures treated with FGF1, 2, or 9, for 24 hours and 10 days. Microarray analysis of FGF-associated gene expression shows that axonal transport genes, neurofilament genes, and neuronal differentiation genes are reduced in myelinating cultures following 10-day treatment with FGF9. 24-hour treatment with FGF9 or the other FGFs had little or no effect on gene expression. Data derived from Microarray performed by Lindner et al., 2015

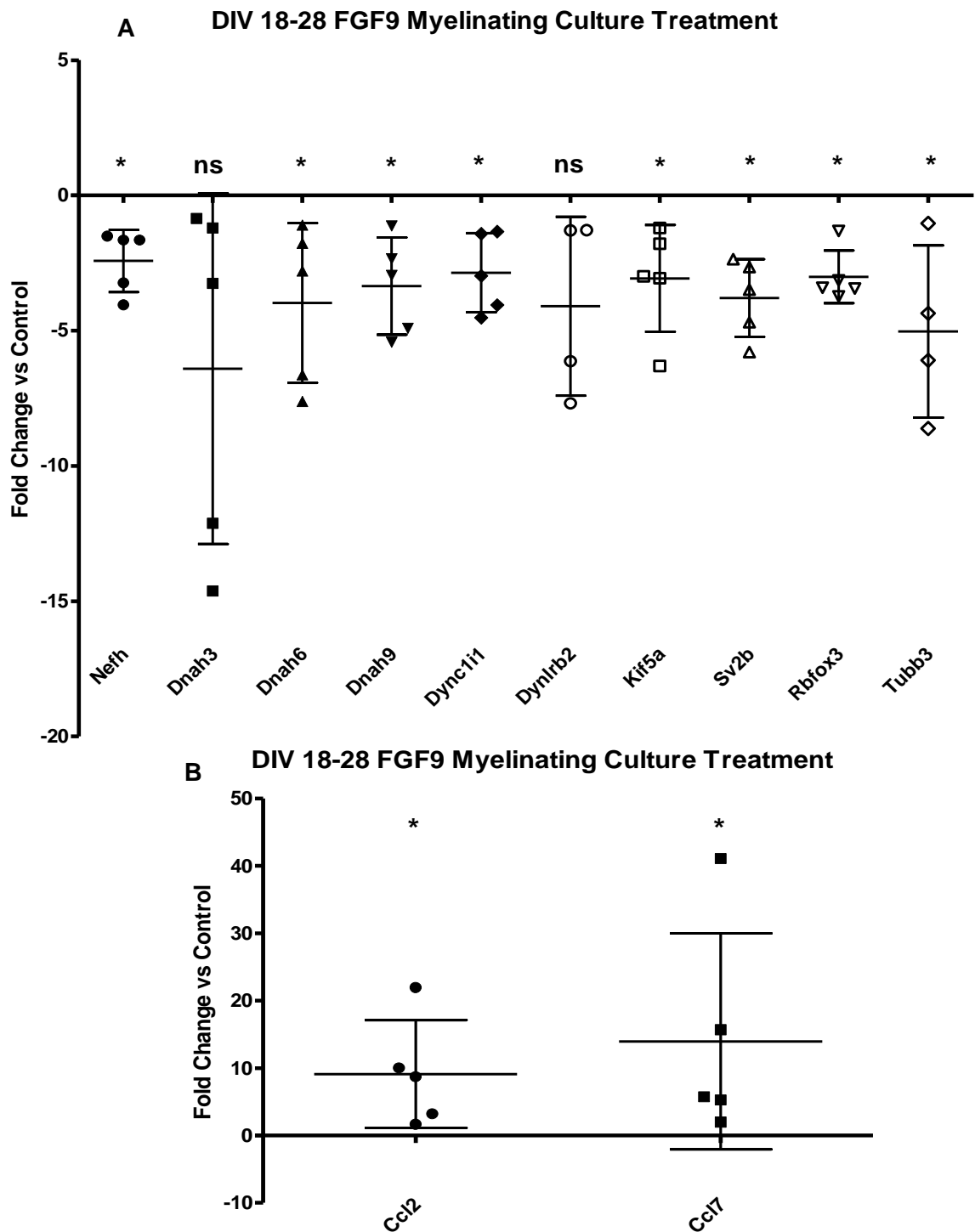


Figure 5.10 Axonal transport gene expression was reduced by FGF9 treatment. Myelinating cultures were treated with 100 ng/mL recombinant human FGF9 for 10 days from DIV 18. The cells were lysed and processed for RNA extraction and cDNA synthesis. qPCR was performed using primers for neuronal genes and *GAPDH* as the housekeeping standard. Expression of all genes analysed showed reduced expression in FGF9-treated cultures compared to controls similar to downregulation seen in the microarray (A). *Ccl2* and *Ccl7* were used as positive controls (B). Fold changes in gene expression are shown relative to untreated control values, data presented are the means \pm SD. This experiment was performed 6 times. *, $p < 0.05$, **, $p < 0.01$ (Wilcoxon matched pairs tests were performed on delta CT values).

5.2.2.2 Neuronal cell numbers and axon density were reduced by FGF9 treatment

Data from previous sections in this chapter provide evidence that FGF9, a neuroprotective survival factor, can actually damage axons and contribute to neurodegeneration. The next step in this vein of research was to determine if FGF9 mediated its effects on neurons directly or acted via other cell types as is the case with its effect on myelination. To address this question, enriched neuronal cultures were generated as described in section 2.2.5. Neurons were cultured for 6 days to allow them to fully differentiate, then treated with 100 ng/mL FGF9 for a further 10 days. At DIV 16, neurons were fixed and stained with SMI31 and MAP2 antibodies to visualise axons and neuronal cell bodies respectively. MAP2+ cells numbers were counted manually in ImageJ and axon densities were calculated using CellProfiler.

FGF9 treatment significantly reduced axonal density in neuronal cultures (10d C = $19.5 \pm 4\%$ MFI; 10d F9 = $12 \pm 0.4\%$ MFI, $p < 0.05$) (Figure 5.11 A). This was associated with a marked reduction in number of MAP2+ neurons compared to controls, however due to high variation in cell numbers between different experiments this result was not significant (10d C = 32.8 ± 12.2 cells/FOV; 10d F9 = 13.2 ± 5.8 cells/FOV, $p = 0.0546$) (Figure 5.11 B). FGF9 treatment also led to an increase in proliferation of non-neuronal cells in culture as DAPI staining shows in Figure 5.12 B. To prevent the proliferation of contaminating glial cells in neuronal cultures treated with FGF9, FdU, a potent cytotoxic agent that drives apoptosis in proliferating cells, was added from DIV 4. FdU alone decreases axon density and neuron cell numbers compared to untreated neurons (Figure 5.11 C, D). FdU also prevented the explosion in DAPI+ nuclei numbers observed after FGF9 treatment (Figure 5.11 B, D). Axonal density and neuronal cell counts were virtually the same as controls in FGF9-treated cultures that were co-treated with FdU (Figure 5.11 C, D).

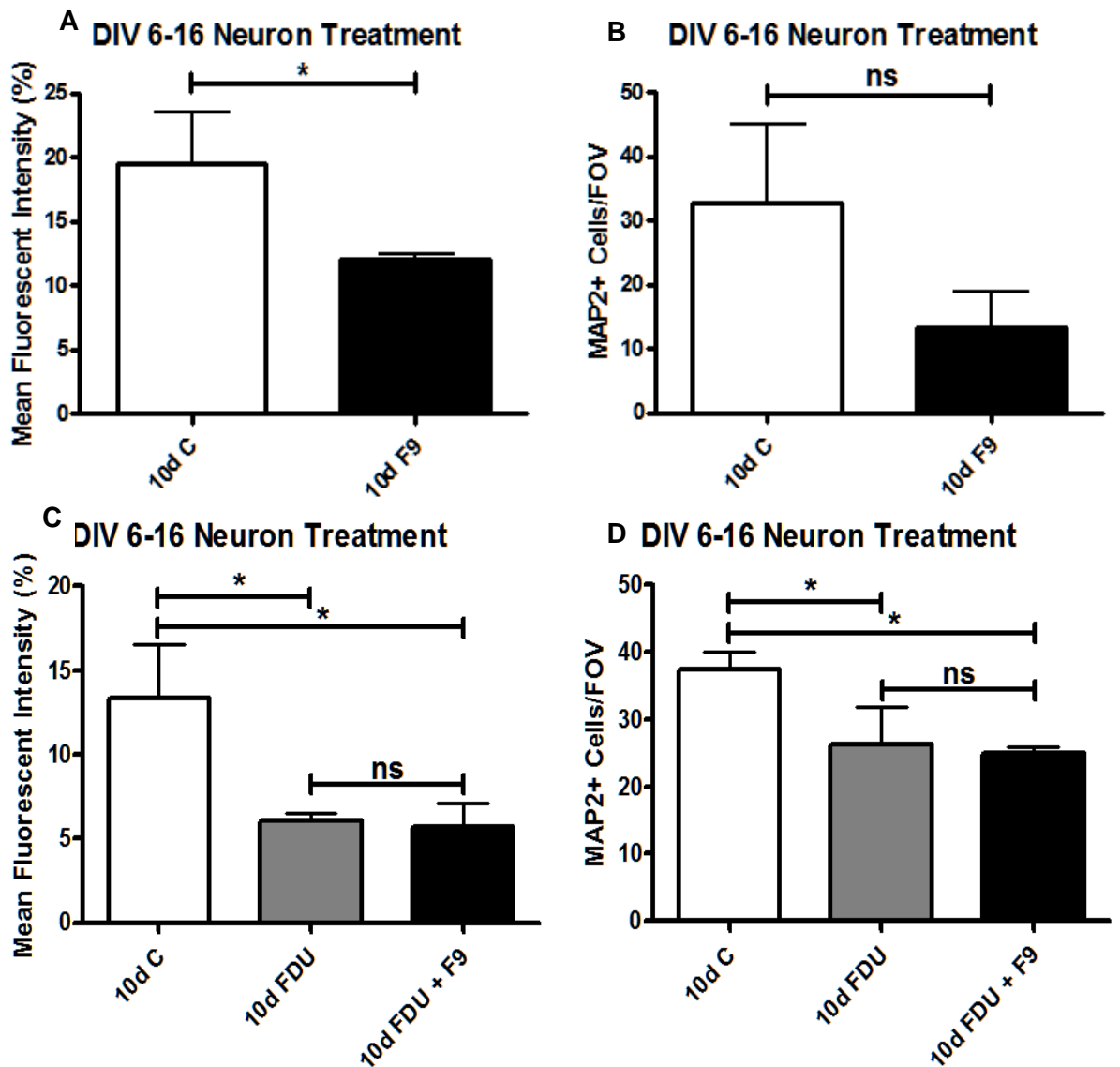


Figure 5.11. Axon density and neuronal cell counts were reduced in neuronal cultures following 10-day FGF9 treatment. Neurons were purified as described in section 2.2.5 and cultured in neuro-basal medium for 6 days. Cultures were treated with FGF9 for 10 days from DIV6 before being fixed and processed for immunofluorescence. Cells were stained with MAP2 and SMI31 to visualise neuronal cell bodies and axons respectively. MAP2+ cells were counted manually and MFI of SMI31 staining was quantified using CellProfiler. 10-day FGF9 treatment reduced MFI of SMI31 staining (A). Neuron numbers in FGF9-treated cultures were also reduced but not significantly (B). Treating neurons with FdU reduced neuron numbers and axon density but completely abrogated the effect of FGF9 (C, D). Data presented are the means \pm SD. These experiments were performed three times. *, $p < 0.05$, (Wilcoxon matched pairs test A, B) (one-way ANOVA with Tukey's Multiple Comparison Test C, D).

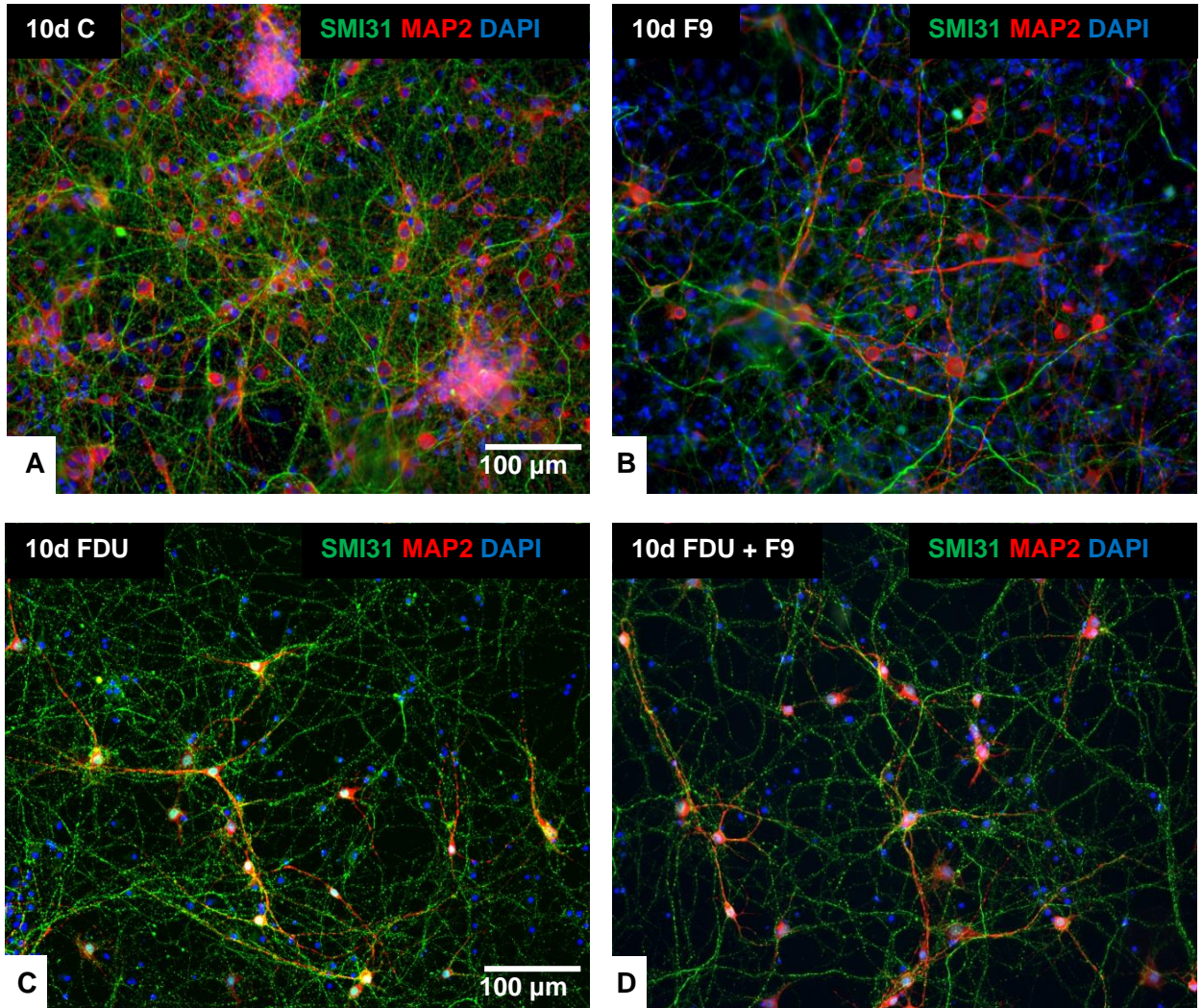


Figure 5.12. Representative images of neurons and axons in FGF9-treated neuronal cultures. Neurons were purified as described in section 2.2.5 and cultured in neuro-basal medium for 6 days. Cultures were treated with FGF9 for 10 days from DIV6 before being fixed and processed for immunofluorescence. Cells were stained with MAP2 (red) and SMI31 (green) to visualise neuronal cell bodies and axons respectively. MAP2⁺ cells were counted manually and MFI of SMI31 staining was quantified using CellProfiler. 10-day FGF9 treatment reduced SMI31 staining and neuron cell counts, and dramatically increased numbers of DAPI+ nuclei (B) versus control (A). FdU treatment alone reduced neuron number and axon density versus untreated neurons (C) but cancelled out the effects of FGF9 (D).

5.3 Discussion

MS is a complex disease with several pathogenic mechanisms contributing to demyelination and damage to axons. Inflammatory and neurodegenerative pathways drive progression at different stages of disease, however the majority of treatments currently available (Table 1.1) target the immune system in RRMS. Neurodegenerative pathways, described in section 1.1.2.2, are the primary cause of axonal pathology in PPMS. Loss of axons represents the point of no return, after which repair is no longer possible. Understanding the mechanisms responsible for remyelination failure and axonal degeneration is critically important if therapeutics targeting later stages of MS are to be developed.

FGF9 was shown previously to inhibit primary myelination *in vitro* and remyelination in cerebellar slice cultures (Lindner et al., 2015). These studies did not address whether FGF9 has any effects on established myelin and mature OLs. FGF9-treatment also greatly increases OPC numbers, but these new cells had not been tested for their capability to produce functional myelin. The primary receptor for FGF9 is FGFR3c, but like most other FGFs, FGF9 is promiscuous and can signal through FGFR2c and 1c (Zhang et al., 2006). FGFR3c expression on OL lineage cells is lost by the time they have fully matured, FGFR2c is expressed on myelin membranes, and FGFR1c is expressed on OL cell bodies (Miyake et al., 1996). In maturing OLs (A2B5⁻, O4⁺, O1⁺ cells that have extended membrane processes but have not yet produced myelin sheathes) FGF9 treatment reduces expression of FGFR2 (Figure 3.8) as well as MBP and PLP (Cohen and Chandross, 2000). This suggests FGF9 can cause de-differentiation in OL lineage cells. It was not known if the same is true for mature OLs that have produced myelin sheathes as this had not been investigated.

To answer the question of whether FGF9 is a demyelinating factor, myelinating cultures were treated for 10 days from DIV 28, when most myelination has occurred. Other cultures were treated with FGF9 from DIV 18 – 28. FGF9-media was then removed and the cultures were maintained in control media for a further 10 days. This was to show if cultures in which myelination had been inhibited could myelinate when FGF9 treatment was stopped. As these experiments were performed over 20 days, control cultures were treated with FGF9 or maintained in control media for the full 20-day duration. As expected, myelin and axons in DIV

38 control cultures were virtually identical to DIV 28 control cultures used in previous experiments (Figure 5.2 A). Cultures treated with FGF9 for 20 days mostly lacked myelin and contained numerous MOG⁺ round cells (Figure 5.2 B). Myelination rate was the same in DIV 38 control cultures as DIV 28 - 38 FGF9-treated cultures (Figure 5.1 A). This result shows FGF9 did not induce demyelination in mature myelinating cultures.

Cultures treated with FGF9 from DIV 18 - 28 produced almost double the myelin seen in control cultures at DIV 38 (Figure 5.1 A, 5.2 D). This suggested cultures treated with FGF9 for 10 days might have an increased myelination capacity due to the increase in OPC numbers associated with treatment (Lindner et al., 2015). It also suggests a subpopulation of OPCs are responsible for the appearance of MOG⁺PLP⁺ cells observed in FGF9 treated myelinating cultures, and that other OPCs can mature following FGF9 withdrawal. Examination of myelin generated after FGF9 treatment using confocal microscopy revealed this was not the case. Myelin in these cultures had a highly irregular structure compared with control myelin (Figure 5.3 C, D). Normal myelin sheathes are continuous, evenly thick, and always associated with underlying axons (Figure 5.3 A). In contrast, myelin membranes in FGF9-treated cultures are loosely associated with axons and appear to balloon at different points along their length. Some MOG staining also appears in small dense granules adjacent to these irregular myelin membranes. Overall, it appears as though OLs have attempted to myelinate axons but the process has been disrupted.

In normal OLs PLP stains in the cell body and myelin sheathes whereas MOG is localized only to the myelin sheath. The detection of MOG⁺PLP⁺ cells 10 days after FGF9 withdrawal suggests they are the product of disrupted OL maturation (Figure 5.4). Under high power magnification, these cells have a highly variable appearance. The cell shown in Figure 5.4 A has an extensive network of processes that are laden with MOG and PLP at random intervals. None of the processes appear to be forming myelin sheathes and the cell body almost exclusively contains PLP with a few surrounding specks of MOG. The cell in Figure 5.4 B contains densely packed granules of MOG and PLP in the cell body with a surrounding network of processes containing little of each protein. These are two examples of a wide array of phenotypes displayed by MOG⁺PLP⁺ cells in FGF9-treated myelinating cultures.

FGF signaling is involved in every aspect of OL development and myelination (Fortin et al., 2005). FGF2 and FGF9 induce process elongation in mature OLs and OL signaling regulates myelin sheath thickness (Fortin et al., 2005, Furusho et al., 2012). Several groups have also shown the ability of FGF2 to induce de-differentiation of mature OLs (Bansal and Pfeiffer, 1997, Fressinaud et al., 1995, Butt and Dinsdale, 2005). This is associated with downregulation of myelin genes, re-expression of OPC markers, and uncompacting of myelin membranes. It is likely that similar events in FGF9-treated myelinating cultures are causing aberrant OL maturation and producing the strange, myelin-protein filled cell bodies and membranes described here. Further characterisation of these cells is required however, and co-staining with A2B5, NG2, O4, and MBP will help to characterise this variant of OL lineage cell. It would also be interesting to find out how long MOG⁺PLP⁺ cells can persist after treatment, which could be determined by maintaining the cultures for a longer period after FGF9-withdrawal.

If the aberrant myelin produced in FGF9-treated cultures is undergoing degradation, it may undergo phagocytosis by microglia. To find out if this was the case, cultures were stained for MOG and the microglia marker, IBA1. The cultures were searched for the presence of myelin in microglial membranes using confocal microscopy. Producing 3D reconstructions showed microglia surrounding frilly myelin membranes but myelin was never detected within a microglial cell. A representative image of myelin and microglia in FGF9-treated myelinating cultures is shown in Figure 5.5.

Myelinating cultures treated with FGF9 for 20 days showed a decrease in axon density (Figure 5.1 B). This was surprising as previous experiments with FGF9 administered for 10 days found no change in the axons (Figure 1.3). In the experiments shown in this chapter, 10-day FGF9 treatments initiated at DIV 18 or 28 produced no change in axon density compared to control cultures. This suggested that FGF9 has a detrimental effect on axons, but only after chronic exposure. When examining myelin at high magnification, axonal abnormalities were observed in FGF9-treated cultures (Figure 5.2 C, D). These can be characterised as swellings or beading along axons with bright and dim regions of neurofilament staining. Interestingly, regions of axons that were swollen also lacked myelin (yellow arrows in Figure 5.3 C, D) even though the axon at either side of the swelling was myelinated. This raises two possibilities: either aberrant

myelination leaves regions of axons nude and these become swollen, or axon swelling occurs first and these portions lose their myelin sheathes. A similar axonal phenotype was observed in FGF9-treated cultures regardless of the duration or initiation point of treatment (Figure 5.6). 10 and 20-day FGF9-treated cultures display swellings and variable brightness of neurofilament staining indicating that even though axon density is not reduced by short treatments, an underlying axonal pathology is taking place. 10 days after FGF9 withdrawal this pathology is still present (Figure 5.6 F), which suggests even short exposure to high levels of FGF9 can induce a prolonged axonal pathology. To continue this research a system of quantification of axonal swellings will need to be developed in order to compare pathology following different lengths of FGF9 treatment.

The next experiments performed in this chapter looked at OL lineage cell numbers in myelinating cultures following alternating FGF9 treatment. It was hypothesised that the increase in myelination observed in 10d FGF9 10d C cultures would be associated with a decrease in OPC numbers, but an overall increase in OL cell number. To assess this, myelinating cultures were treated with FGF9 and stained with antibodies against NG2 and Olig2. NG2⁺ cell numbers were greatly elevated immediately following FGF9 treatment for 10 or 20 days (Figure 5.7 A, 5.8 B, C). NG2⁺ cell numbers were almost the same following 10 and 20-day FGF9 treatment suggesting that there is a ceiling to the number of OL progenitors that can be generated in this culture system. 10 days after FGF9 withdrawal (Figure 5.7 A, 5.8 D), NG2⁺ numbers had returned to control levels, suggesting that progenitors in these cultures had differentiated. This finding fits with the idea that OPCs in the CNS are maintained as a constant reservoir during homeostasis and that, absent any interference, this pool will be regulated at a constant level (Hughes et al., 2013). Total OL numbers closely matched OPC numbers in FGF9-treated cultures (Figure 5.7 B, 5.9). Olig2⁺ cell numbers were similarly elevated following 10 and 20-day FGF9 treatments, and were still elevated, albeit to a lesser degree 10 days after FGF9 withdrawal. Olig2⁺ numbers in these cultures were roughly twice that of the controls; however, the difference was not significant due to a large amount of variation between cultures. Lower OL numbers observed 10 days after withdrawal of FGF9 suggests a degree of OL death following withdrawal of FGF9, however further experiments would be required to confirm this.

Axonal swellings and reduced axonal density are features of progressive MS and chronic inactive lesions in particular (Fisher et al., 2007). Axonal swellings are also a hallmark of defective axonal transport (Van Den Berg et al., 2017) which is a contributing factor to neurodegeneration in progressive MS. The presence of axonal swellings and reduction in axonal density in FGF9-treated myelinating cultures suggests there may be a deficit in axonal transport. Axonal trafficking of proteins, lipids, and mitochondria is essential for neuronal and synaptic function (Millecamps and Julien, 2013). Due to the extreme length of some axons, transport deficits in any region can lead to axonal degeneration and neuronal cell death. Defects in the cytoskeleton, microtubule organisation and motor protein expression can lead to breakdown of transport between the cell body and axon tip. Axonal transport deficits have been shown to play a role in the pathology of numerous neurodegenerative diseases.

Following the finding that FGF9 is detrimental to axons in myelinating cultures, the microarray performed by Lindner et al., 2015 was screened for differences in axonal transport genes. Results from the microarray are shown in Table 5.1. Genes involved in axonal transport, structure, and neuronal differentiation and are significantly downregulated following 10-day FGF9 treatment. Some of the genes are downregulated at 24 hours however, the effect is more pronounced at 10 days. FGF2 also downregulated these genes following 10-day treatment but to a lesser degree than with FGF9. Validation of these results by qPCR found that all the genes in Table 5.1 were downregulated by FGF9 except *Dnac3*, *Tubb3*, and *Dynlrb2* (Figure 5.10). This suggests FGF9 might interfere with axonal transport by directly or indirectly downregulating gene expression which may be the reason for the axonal pathology shown in Figure 5.1, 5.3, and 5.6. As discussed in Chapter 1, FGFs are differentiation and survival factors for neurons and function mostly during embryonic development. Their potential roles in axon transport have not yet been investigated.

The next step in the investigation of the effect of FGF9 on neurons and axons was to produce enriched neuronal cultures. This was performed as described in section 2.2.6.8. Neurons in these cultures are fully differentiated by DIV 6, therefore this time point was chosen to begin treatment. Neurons were treated with FGF9 for 10 days, then fixed and stained with antibodies against neuronal cell bodies (MAP2) and axons (SMI31). The cells were imaged and neuronal cell counts and axon

densities were quantified. 10-day FGF9 treatment reduced axon density at DIV 16 by almost 50% (Figure 5.11 A). Neuron numbers were also reduced by around 50% however, due to variation in the cultures this result was not significant and will have to be repeated (Figure 5.11 B). As neuronal differentiation peaks by DIV 6, reduction in axon density and neuron number most likely represents a loss of neurons as a result of FGF9 treatment.

As this is an enriched culture system, generated from whole cortex, some contaminating CNS cells are present. These include astrocytes, microglia, OLs, and undifferentiated neuroprogenitor cells. B27 supplement in neuron differentiation media inhibits glial cell development but does not prevent 100% of glial cell generation. Contaminating OLs and astrocytes are believed to cause the massive increase in DAPI⁺ nuclei seen after FGF9 treatment (Figure 5.12 B). As inhibition of myelination by FGF9 is an indirect effect facilitated by astrocytes, it is possible that the effects of FGF9 on neurons also results from FGF9 signaling via another cell type. It is also possible that the massive proliferation induced by FGF9 indirectly damages neurons, perhaps through increased metabolic stress. To address these issues, the experiment was repeated with the addition of FdU from DIV 4. FdU kills dividing cells so will eliminate contaminating glia that proliferate in the presence of FGF9 while leaving neurons intact. This ensures any indirect effects of FGF9 via contaminating cells are prevented.

Addition of FdU alone reduced axon density and neuron numbers (Figure 5.11 C, D; 5.12 C, D). This may be due to a loss of trophic support provided by contaminating astrocytes and OLs being lost to FdU treated neurons, or a loss of neurons that were still undergoing differentiation. Ultimately, co-treatment with FdU completely abrogated the effects of FGF9 on neurons and axon density (Figure 5.11 C) and cell counts (Figure 5.11 D) were unchanged versus controls. This result does not resolve whether the effect of FGF9 on neurons is due to downstream signaling via other cell types or due to metabolic stress as a result of massive proliferation; however, it shows that FGF9 is not detrimental to neurons directly.

Further experiments will be required to resolve the precise mechanism or mechanisms responsible for FGF9's detrimental effect on axons. The findings that axonal pathology in myelinating cultures resembles axonal transport deficit, and

axonal transport genes are downregulated by FGF9 strongly suggests that this is at least a contributing factor. Axons observed in FGF9-treated cultures share characteristics with degenerating axons in progressive MS suggesting FGF9 might be contributing to disease pathogenesis. In addition to the effects on axons, pre-treatment with FGF9 also interferes with OL differentiation and myelination and therefore likely contributes to failure of remyelination even when the factor is downregulated. These findings have wider implications in the investigation of FGF signaling as a therapeutic target in MS.

CHAPTER SIX

**CHRONIC OVER-EXPRESSION OF FGF9
INDUCED DEMYELINATION AND AXONAL
PATHOLOGY**

6. CHRONIC OVER-EXPRESSION OF FGF9 INDUCED DEMYELINATION AND AXONAL PATHOLOGY

6.1 INTRODUCTION

Results from the previous chapter show pre-treatment with FGF9 can perturb myelination, and therefore, increased OPC proliferation due to FGF9 may yield no therapeutic benefit in MS. Surprisingly, prolonged FGF9 treatment also led to axonal pathology and reduced neuron numbers *in vitro*. Several studies have shown FGF9 to be a neuroprotective factor: spinal and basal forebrain neurons survive longer *in vitro* with FGF9 treatment (Kanda et al., 1999, Garcès et al., 2000, Kanda et al., 2000). FGF9 also enhanced choline acetyltransferase activity in neurons (Kanda et al., 2000, Kanda et al., 1999). FGF9 treatment protected dopaminergic neurons from 1-methyl-4-phenylpyridinium toxicity and blocking endogenous FGF9 induced neuronal apoptosis (Huang et al., 2009, Huang and Chuang, 2010). Contrary to the findings of these studies, results from the previous chapter indicate FGF9 can also be pathogenic to neurons.

Increases in FGF9 expression have been demonstrated in response to several CNS pathologies but the effects of prolonged over-expression on the CNS have not yet been investigated. The aim of this chapter was to investigate the effects of chronic over-expression of FGF9 in the CNS. Adeno Associated viral vectors (AAVs) are single stranded DNA viruses that require other viruses to replicate making them ideal transduction vectors (Naso et al., 2017). They have been used extensively in transduction studies as they do not cause disease or severe immune responses, they can infect dividing and quiescent cells, and their genes do not integrate into the host genome. This ability to infect non-dividing cells is especially useful when studying the brain as neurons do not undergo cell division (Yu et al., 2013). Adeno-associated virus serotype 6 (AAV6) is the most neuron-specific of all AAV serotypes in rat brain (Salegio et al., 2013). Gene expression resulting from AAV6 gene transfer has also been shown to persist for several months (Yu et al., 2013) allowing the effects of long-term over expression of FGF9 to be investigated.

To study the effects of chronic FGF9 treatment in isolation and delineate them from other factors at work in MS, an *in vivo* model of chronic over-expression was established. AAV6 containing FGF9 or enhanced green fluorescent protein (eGFP) sequences were injected into the cortex of Lewis rats as detailed in section 2.6.2. Gene expression was placed under control of the GFAP promoter in an attempt to target expression in astrocytes. Brains from these animals were harvested and processed for immunohistochemical/ immunofluorescence analysis ten days, thirty days, three months, and 9 months following the gene transfer procedure.

6.2 Results

6.2.1 FGF9 expression appeared in neurons following AAV6 infection

The initial step in these experiments was to determine when FGF9 expression began and how long it persisted for in the cortex following gene transfer. Spinal cord motor neurons are known to be the main source of FGF9 in the CNS, therefore spinal cord sections were used as a positive control for FGF9 expression (Nakamura et al., 1997) (Figure 6.1 A). Brains from each time point, 10 days, 30 days, 3 months, and 9 months post injection (PI) were stained for FGF9 expression and analysed by immunofluorescence microscopy. No FGF9 staining was detected at the injection site 10 days PI (Figure 6.1 B). By 30 days PI, robust FGF9 staining was observed in cells morphologically identified as neurons (Figure 6.1 C). At 3 months and 9 months PI (Figure 6.1 D, E) FGF9 was still being expressed around the injection site.

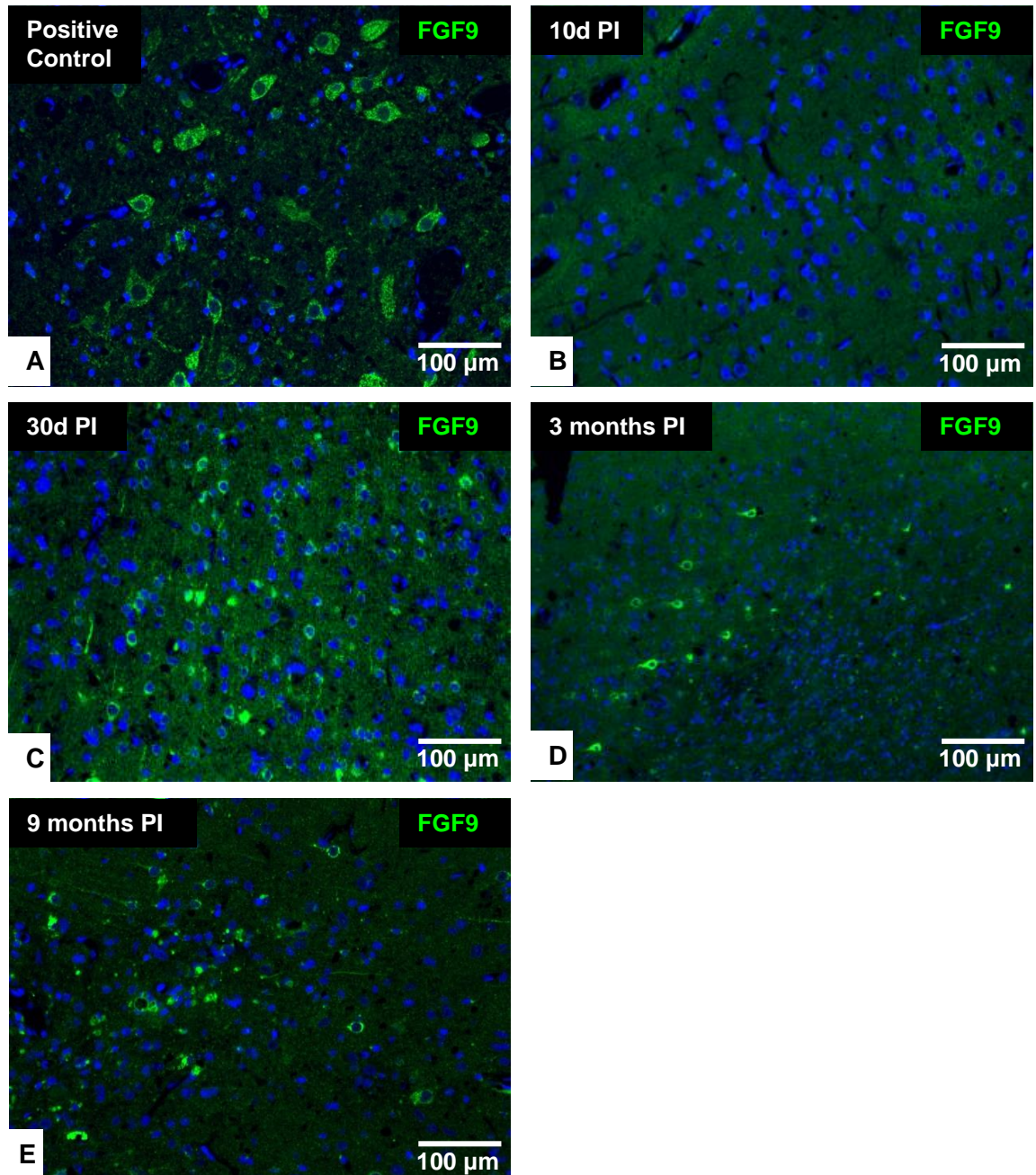


Figure 6.1. FGF9 was expressed by neurons following injection with AAV6-*Fgf9* vectors. Infections were performed using (AAV-6)-based vectors containing *Egfp* (pAAV-*egfp*) and *Fgf9* (AAV6-*Fgf9*) as described in section 2.6.2. Spinal cord motor neurons were used as a positive control for FGF9 staining (A) FGF9 was absent 10 days PI (B) but was robustly expressed by cells morphologically identified as neurons after 30 days (C), 3 months (D), and 9 months (E).

6.2.2 FGF9 overexpression caused extensive demyelination

After establishing that FGF9 expression is maintained throughout the full course of these experiments, the first question asked was what effect such chronic exposure would have on myelin in these animals. Cortical sections from each time point were stained with antibodies against five myelin proteins: CNPase, MAG, MBP, MOG, and PLP. 10 days PI, no differences between myelin adjacent to the injection site and the rest of the cortex were detected in AAV6-*Fgf9* rats (Figure 6.2 A). By 30 days PI, an area of reduced myelin density demarcated by a sharp border, shown in Figure 6.2 B, could be seen extending from the cortex into the white matter. After 3 months PI, the area surrounding the injection site was almost completely devoid of PLP staining (Figure 6.2 C). Little change was then observed at 9 months PI and the lesion remained completely demyelinated (Figure 6.2 D).

To quantify these changes in myelination, FIJI (ImageJ) software was used to calculate DAB deposition for each of the myelin proteins in lesions from their first appearance at 30 days PI to 9 months as described in section 2.6.3. This method only allowed myelination to be quantified after the onset of lesion development, as a border must be visible to select out an area of myelin for analysis. At 1 month PI, lesions in AAV6-*Fgf9* brains appear fairly normal with regards to myelination and a subtle area of myelin loss is only just identifiable compared to the surrounding grey and white matter. At this stage, the area of lesions covered by all five myelin proteins averaged around 40% (Figure 6.3). By 3 months, deposition of all myelin proteins had decreased, but to variable degrees: e.g. MBP covered 25% of the lesioned area at this stage while PLP stained in only 6%. There was little change in the area covered by each myelin protein at 9 months indicating that demyelination had reached its maximum by 3 months PI. Numbers of lesions stained at each time point varied between two and five so statistical analysis could not be performed on this data.

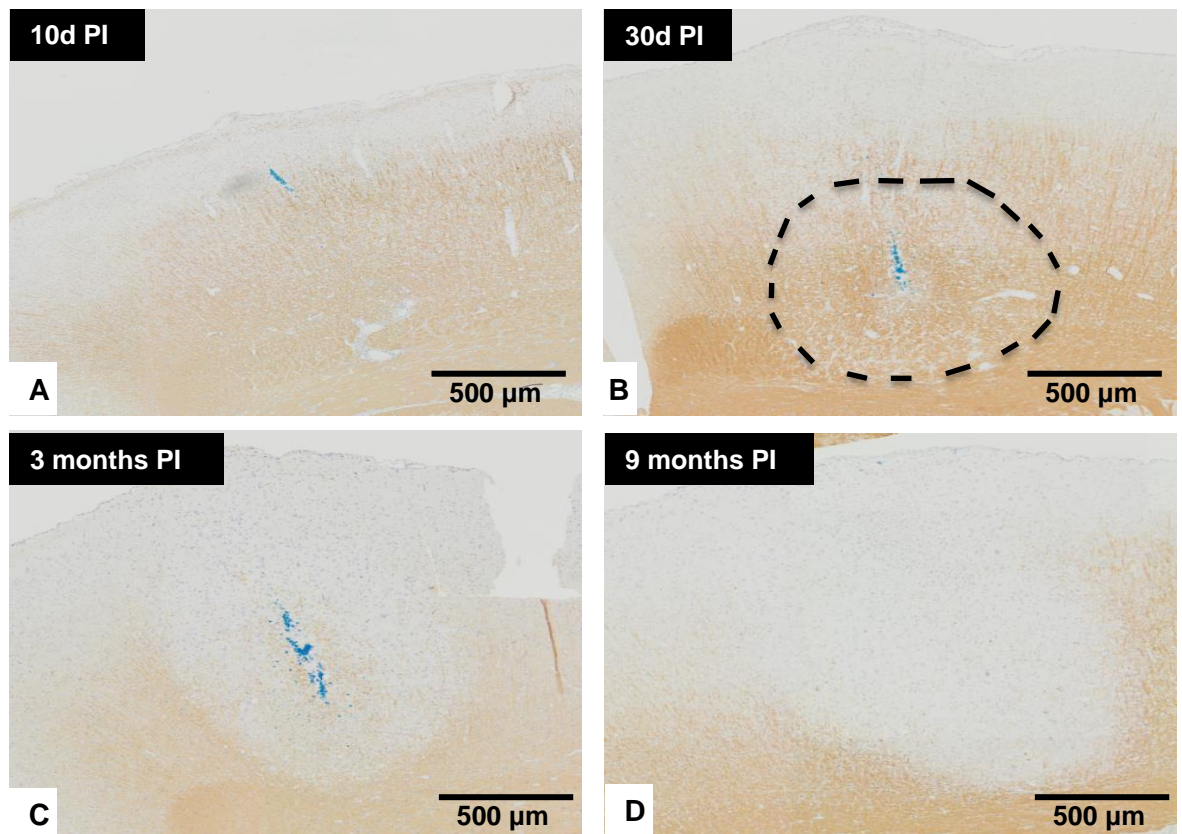


Figure 6.2. Representative images of progressive demyelination in AAV6-*Fgf9* lesions. Infections were performed using (AAV-6)-based vectors containing the *Fgf9* (pAAV-*Fgf9*) as described in section 2.6.2. Rats were euthanized at each time point and their brains were fixed and processed for immunohistochemical analysis. Sections from lesions at different time points were stained for the presence of five myelin proteins. 10 days PI (A) PLP staining is normal and no lesion can be defined at the site of injection. By 30 days, an area of disrupted PLP staining with a distinct border can be defined (B). At 3 months these lesions have lost most or all PLP staining (C), which remains unchanged 9 months PI (D).

Myelin Loss in AAV6-*Fgf9* Lesions

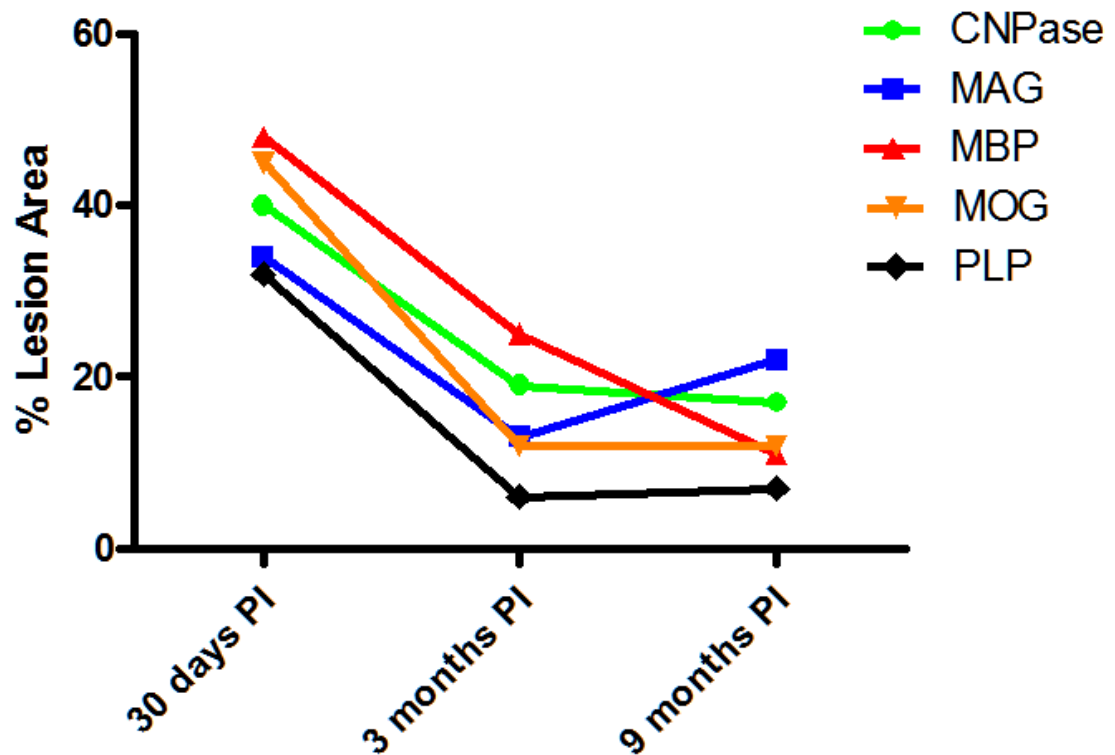


Figure 6.3. Demyelination took place between one and three months following injection with AAV6-*Fgf9*. Sections from lesions at different time points were stained for the presence of five myelin proteins. Area of myelination per lesion was calculated using particle analyser in ImageJ, described in section 2.6.3. No lesions were detected 10 days PI. The expression of each myelin protein correlates strongly at each stage of lesion development and decreases from a mean of 40% of lesion myelinated to 15% at 1 month and 3 months respectively.

6.2.3 Demyelinated lesions accumulated β -APP⁺ axonal swellings over time

To determine whether the axonal pathology observed in *in vitro* cultures treated with FGF9 also occurs *in vivo*, FGF9-overexpression lesions were stained for the presence of beta-amyloid precursor protein (β -APP⁺) axonal swellings. Sections from AAV6-*egfp* and AAV6-*Fgf9* animals from each time point were stained and β -APP⁺ swellings per mm² were quantified by light microscopy. No β -APP⁺ swellings were found at the injection site in either treatment group 10 days PI (Figure 6.4 A, E). At no time point PI were β -APP⁺ axons detected in AAV6-*egfp* animals (Figure 6.4 A – D). In one of three AAV6-*Fgf9* animals at 30 days PI, β -APP⁺ axonal swellings were detected (Figure 6.4 F), suggesting lesion formation begins at around 30 days. By 3 months PI, all three animals in the AAV6-*Fgf9* treatment group displayed β -APP⁺ axons. β -APP⁺ swellings were more numerous at 3 months (Figure 6.4 G) and 9 months PI (Figure 6.4 H) suggesting chronic exposure to FGF9 causes a progressive axonal pathology. Quantification of β -APP⁺ axonal swellings (Figure 6.5) found this to be the case: 1 month PI = 110 ± 190.5 β -APP count/mm². 3 months PI = 383.3 ± 65.1 β -APP count/mm². 9 months PI = 760 ± 72.1 β -APP count/mm².

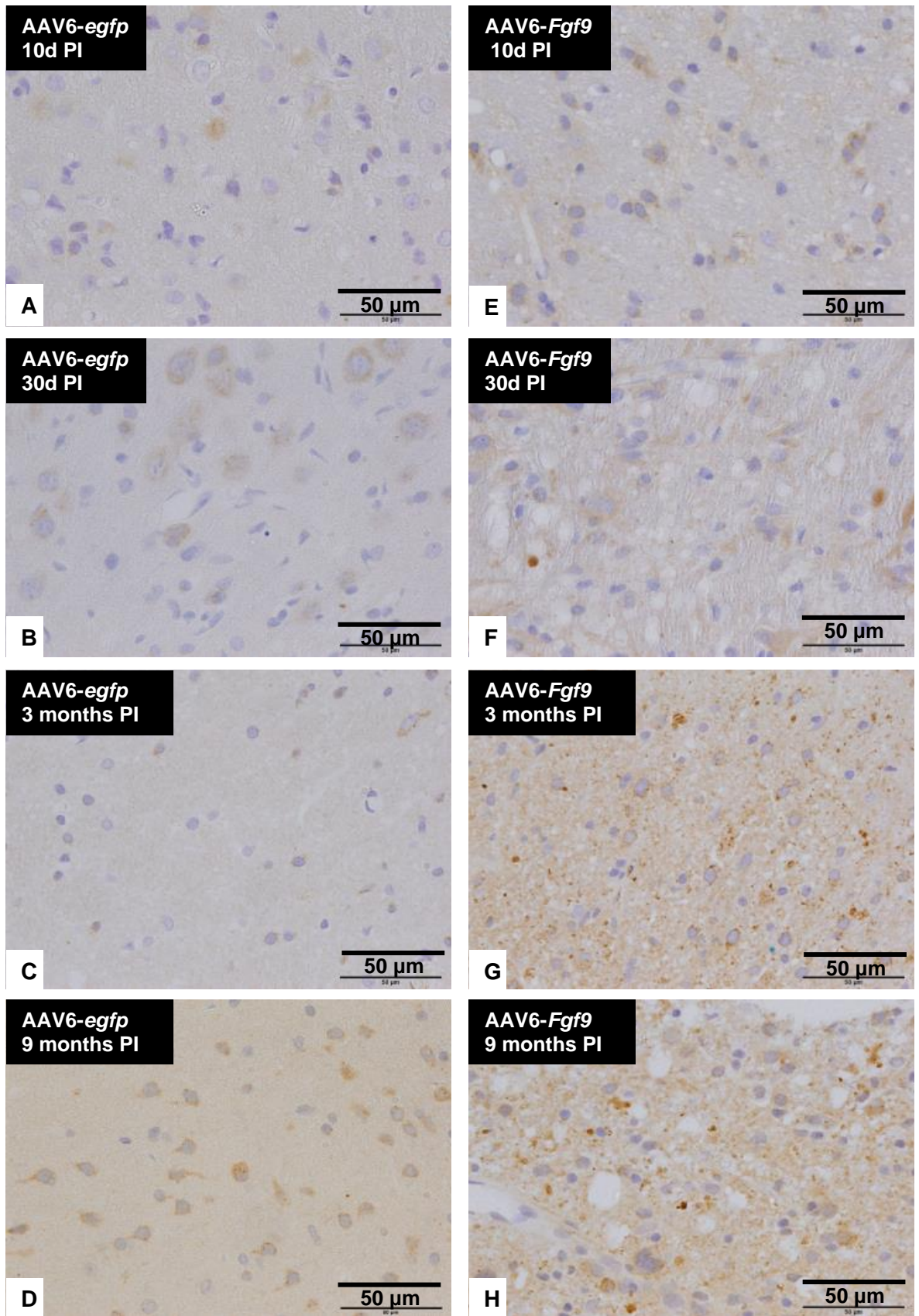


Figure 6.4. Representative images of β -APP staining in rat cortex following AAV6 infection. No β -APP⁺ axons were detected in AAV6-*egfp* animals at 10 days, 30 days, 3 months, or 9 months (A – D). AAV6-*Fgf9* animals appear normal at 10 days PI (E) but have begun to display β -APP⁺ axons at 30 days (B) β -APP⁺ axons numbers continue to increase at 3 months (G) and 9 months (H) PI.

β -APP Counts in AAV6-*Fgf9* Lesions

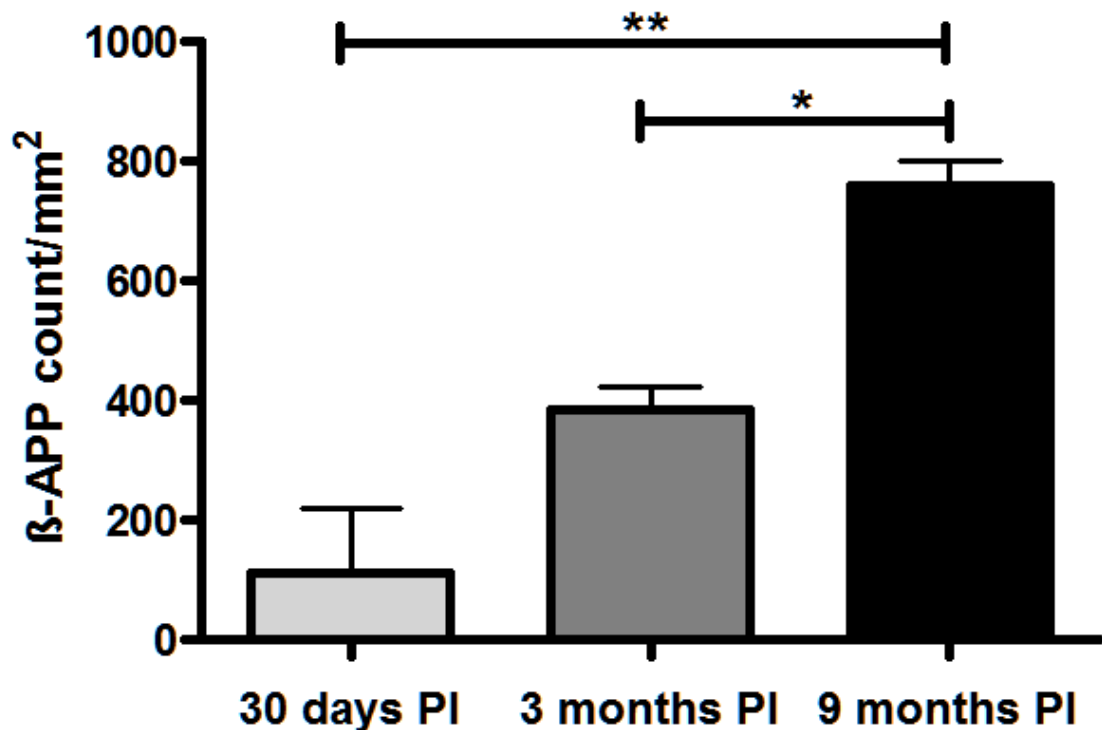


Figure 6.5. β -APP⁺ axonal swellings appeared 30 days PI in pAAV-*Fgf9* lesions and accumulated as lesions persisted. Sections from lesions at different time points were stained for the presence of β -APP. β -APP counts from three brains per time point were performed under a light microscope at 40X magnification and repeated once. Quantification of β -APP shows that axonal damage is absent before the onset of demyelination at 10 days but by 30 days 1 lesion had β -APP⁺ axonal swellings whose number increase at 3 months and 9 months PI. Data presented are the means \pm SD, *P<0.05; **P<0.01 (one way ANOVA with Bonferroni's multiple comparison test).

6.2.4 Astrocytes in FGF9-overexpressing lesions upregulated Sprouty2 but not FGF9

Lesions in *AAV6-Fgf9* rats share many characteristics with MS lesions such as demyelination and axonal pathology. To determine whether astrocytes were induced to express FGF9 in the rat model, as they have been shown to do in MS (Lindner et al., 2015), lesion sections were double-stained with FGF9 and GFAP antibodies. *In vivo*, GFAP staining is strongly associated with reactive gliosis (Pekny and Pekna, 2014). 10 days after injection with eGFP and FGF9 vectors, reactive astrocytes can be seen along the needle tract (Figure 6.6 A, B). A few reactive astrocytes persist in *AAV6-egfp* animals at 1 month and 3 months PI (Figure 6.6 C, E) but FGF9 staining is not detected at any time point in these animals. In contrast, *AAV6-Fgf9* animals display a marked increase in astrocyte reactivity associated with expression of FGF9 at 1 month and 3 months PI (Figure 6.6 D, F). No colocalization of FGF9 in GFAP⁺ astrocytes was observed, suggesting FGF9 overexpression and the resulting demyelination and axonal pathology are not drivers of astrocytic FGF9 expression.

FGF signaling feedback inhibitor expression is associated with FGF9 expression and treatment in MS lesions and myelinating cultures respectively, as demonstrated in chapter 3. In *AAV6-egfp* animals, no FGF9 or Sprouty2 was detected 10 days, 30 days, or 3 months PI (Figure 6.7 A – C). 10 days PI no FGF9 or Sprouty2 expression was detected in *AAV6-Fgf9* animals (Figure 6.7 D). By 30 days PI FGF9 expression is robust and astrocytes have become reactive. Astrocytic expression of Sprouty2 also greatly increases (Figure 6.7 E). Sprouty2 expression persisted at 3 months in FGF9 over-expressing animals (Figure 6.7 F).

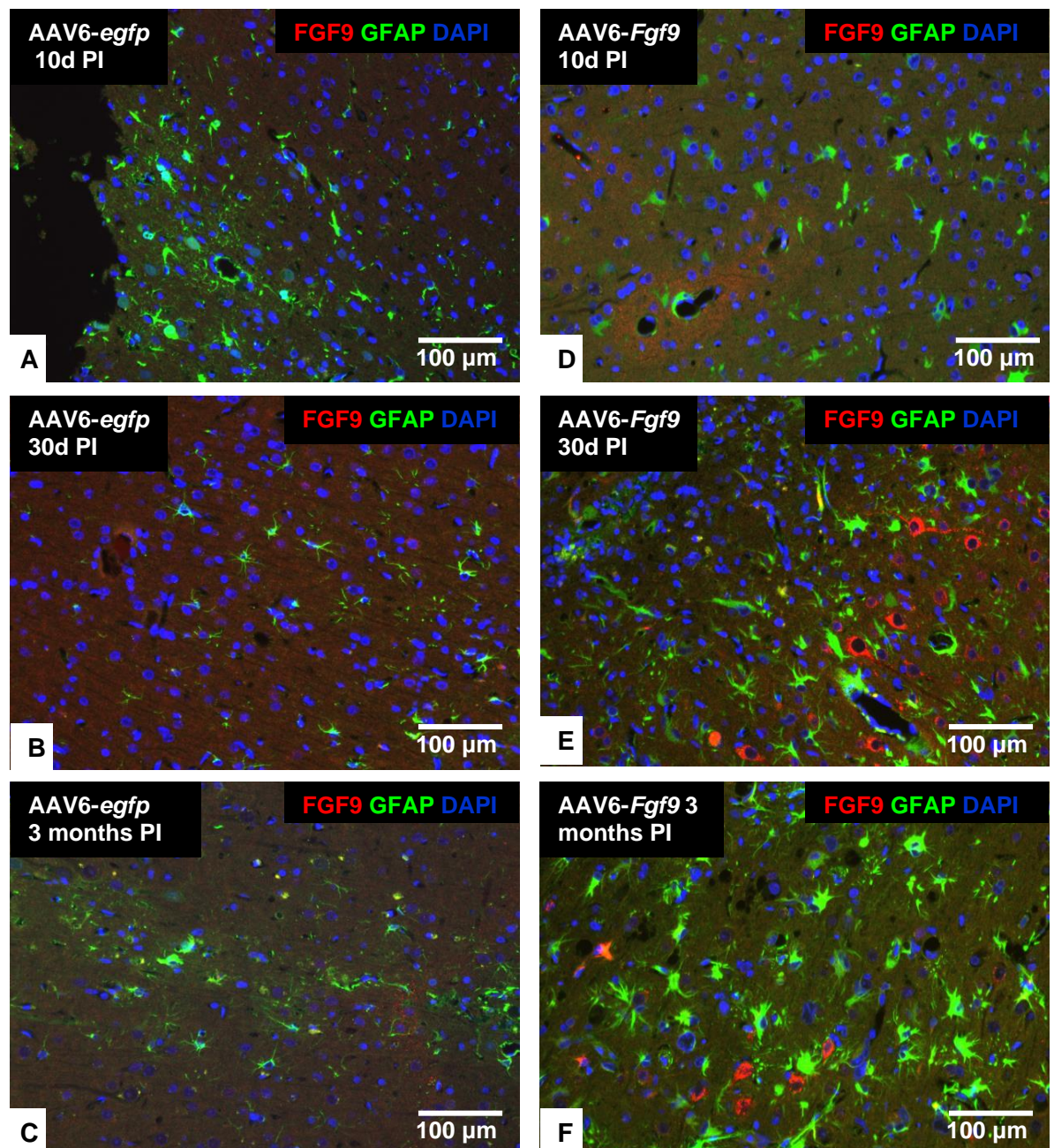


Figure 6.6. Astrocytes did not express FGF9 in AAV6-*Fgf9* lesions. Sections from AAV6-*egfp* and AAV6-*Fgf9* brains were double labelled with antibodies against FGF9 and GFAP. Some astrocytic GFAP upregulation is observed at 10 days PI along the needle tract in AAV6-*egfp* brains and this persists at 30 days and 3 months PI (A – C). No FGF9 expression was detected in these animals. AAV6-*Fgf9* brains display similar GFAP staining as AAV6-*egfp* controls, with no FGF9 expression at 10 days PI (D). 30 days (E) and 3 months (F) PI more extensive astrocyte activation is observed but this was not associated with astrocytic expression of FGF9.

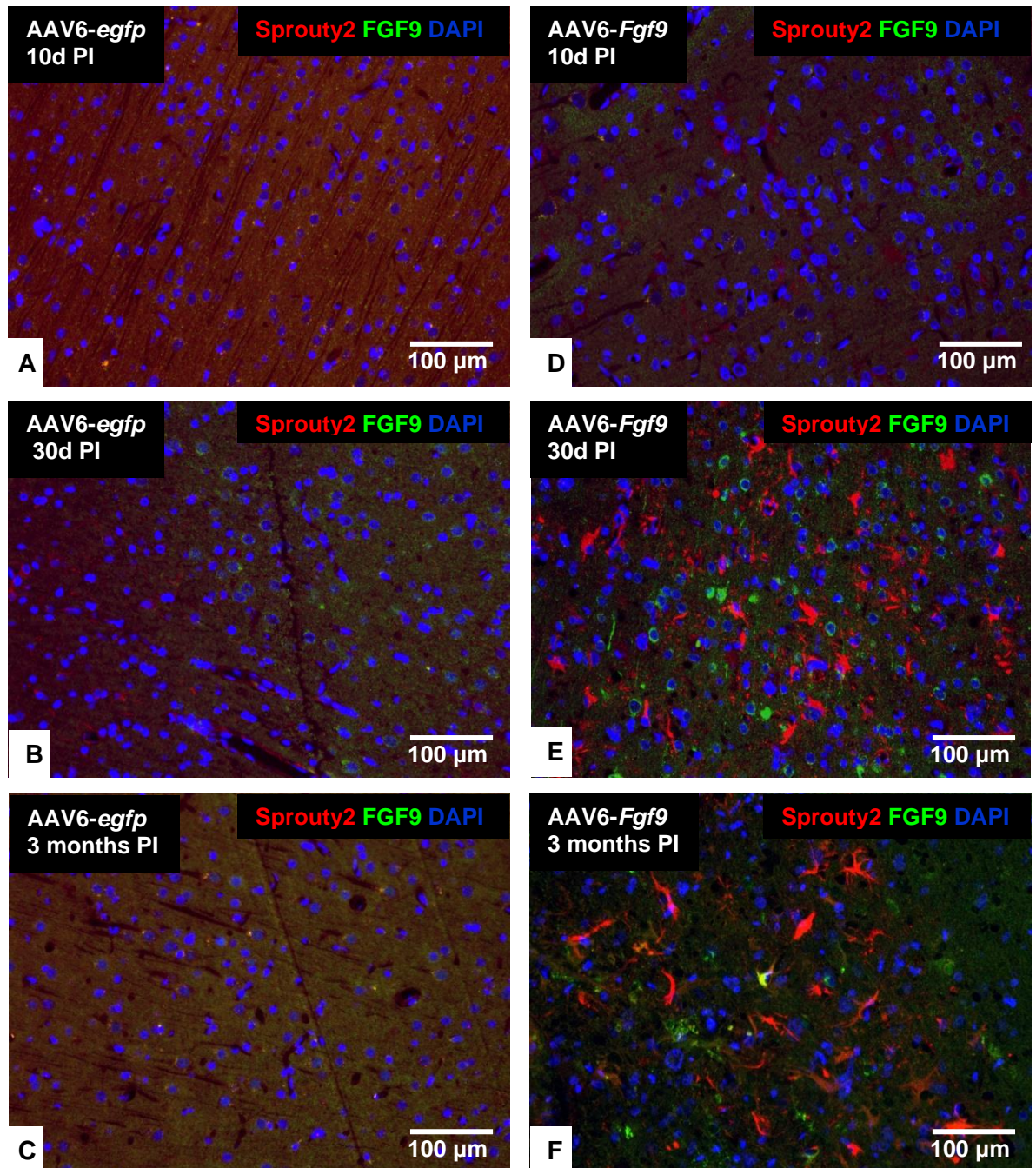


Figure 6.7. Sprouty2 staining appeared in astrocytes in AAV6-*Fgf9* lesions. Sections from AAV6-*egfp* and AAV6-*Fgf9* brains were double labelled with antibodies against FGF9 and Sprouty2. No cells stained with either antibody in the controls or AAV6-*Fgf9* animals 10 days PI (A – D). Sprouty2 staining appeared in cells morphologically identified as astrocytes 30 days (E) and 3 months (F) after AAV6-*Fgf9* injection.

6.3 Discussion

Most of the data so far generated regarding FGF9 in the CNS has focused on its roles in embryonic development and cancer. The functions of FGF9 in the healthy human CNS are still relatively unclear and as FGF signaling is so complex, are unlikely to be fully understood any time soon. FGF9 was identified as a potential therapeutic target in MS through imaging of MS lesions and by testing FGFs in myelinating cultures (Lindner et al., 2015). FGF9 signaling in the CNS is so complex because of its interactions with neurons, astrocytes, and OLs (Chapter 3). It can also induce a plethora of direct and indirect effects by utilising multiple signaling pathways. As a result, there is likely to be a lot of functional overlap with other factors that are expressed in MS, such as FGF2 for example. In order to delineate the effects of dysregulated FGF9 signaling from the complexity that is the MS lesion signaling environment, the effects of FGF9 in the CNS have to be studied in the absence of complicating factors.

Dr Claudia Wrsoz set up a model of chronic FGF9 overexpression in collaboration with Prof Christine Stadelmann's research group at the University of Göttingen. (Lindner et al., 2015) proposed that FGF9 contributes to the pathogenesis of MS by preventing remyelination and promoting the recruitment of inflammatory cells via chemokine induction. Therefore, this model was established under the hypothesis that if FGF9-overexpressing animals were given EAE, higher levels of FGF9 would enhance inflammation and limit remyelination which would hamper functional recovery. However, immunohistological characterisation of the area surrounding the injection site in these animals revealed FGF9 overexpression to have profound detrimental effects, which resembled some of the histopathological features of MS lesions.

Astrocytes were the intended target of FGF9 expression in this model as they are abundant in the CNS and were shown to express FGF9 in MS lesions (Lindner et al., 2015). FGF9 expression was placed under control of the GFAP promotor however, astrocytic expression of FGF9 was never detected at any time point following AAV6 injection, and neurons appeared to be the only cell type that expressed the growth factor (Figure 6.1). This is perhaps due to a leaky promotor and the high propensity of AAV6 vectors to preferentially infect neurons (Salegio et

al., 2013). Expression of FGF9 was still present after 9 months, as would be expected with AAV transduction (Zincarelli et al., 2008), however no expression was observed at 10 days (Figure 6.1 A). Gene expression following AAV6 transduction has been shown as early as 3 days after treatment in mouse heart (Zincarelli et al., 2010) but there is likely some variation in expression time depending on the type of cell being targeted and the gene being transduced. Robust FGF9 expression was detected at 30 days (Figure 6.1 B) so it is likely expression began soon after the 10-day time point.

Lesion formation was first detected in FGF9 overexpressing rats 30 days PI as a slight decrease in DAB deposition and irregular distribution of myelin proteins surrounding the injection site (Figure 6.2 B). Lesions remained confined to the area surrounding the injection site and were progressively demyelinated. By 3 months PI (Figure 6.2 C), virtually no myelin protein staining was detected within the lesioned area and myelin loss persisted until the end of the experiment at 9 months (Figure 6.2 D). Myelin in AAV6-*egfp* animals appeared normal throughout the experiment. The sharp border between the demyelinated lesion and surrounding NAWM is likely due to the very limited diffusion distance of paracrine/autocrine FGFs; HSPGs on the surface of cells and the ECM prevent diffusion more than a few cell-widths from the site of secretion (Storey et al., 1998). Quantification of myelin protein staining in FGF9 overexpressing lesions revealed demyelination occurred between 1 and 3 months PI and then little change occurred between 3 and 9 months PI (Figure 6.3).

These results were interesting as previous studies have shown that FGF9 reduces myelin protein expression and differentiation in developing OLs (Cohen and Chandross, 2000), however, in mature OLs FGF9 only enhanced process elongation and did not induce de-differentiation (Fortin et al., 2005). Results in the last chapter showed that 10-day FGF9 treatment from DIV 28 - 38 did not induce demyelination in myelinating cultures (Figure 5.1). The difference between *in vivo* and *in vitro* findings is perhaps due to a timing discrepancy, as disruption of myelin did not become apparent until 30 days PI in AAV6-*Fgf9* rats so perhaps longer treatment with FGF9 *in vitro* would cause demyelination. There may also be influence from the immune system *in vivo* which precipitated the observed demyelination.

These findings resemble those from (Butt and Dinsdale, 2005) who demonstrated that continuous injection of FGF2 into rat CSF disrupted mature OLs and caused demyelination. Chronic high levels of FGF9 appear to have a similar effect but demyelination occurred after just 3 days in the FGF2 experiments suggesting different mechanisms are involved.

Axonal β -APP immunoreactivity is a commonly used marker for axonal injury (Sherriff et al., 1994). No β -APP⁺ axons were detected in AAV6-*egfp* brains at any time point and AAV6-*Fgf9* brains at 10 days PI (Figure 6.4 A – E). β -APP⁺ axonal swellings appeared concurrent with the onset of demyelination in FGF9-over-expressing lesions (Figure 6.4 F). β -APP⁺ axons were not detected in any sections in which myelin disturbances were not also apparent suggesting axonal pathology follows myelin disruption in this model. While demyelination peaked at 3 months PI in FGF9 over-expressing animals, β -APP⁺ axon counts doubled between 3 and 9 months PI. This suggests high levels of FGF9 causes a slowly progressing axonal pathology. Loss of myelin and the associated trophic support and metabolic strain is a likely contributing factor to axonal pathology seen in these lesions (Nave, 2010). As discussed in the introduction to this chapter, FGF9 has neuroprotective properties, and it is unclear if FGF9 is performing any of these functions in AAV6-*Fgf9* rats. It is possible the pro-survival functions of FGF9 in neurons are simply incapable of compensating for the impact of prolonged demyelination and astrocyte activation brought on by its over-expression. There may be a dose effect in that a certain concentration of FGF9 protects neurons in the brain and above this threshold becomes damaging, or FGF9 is protective in the short term but becomes pathogenic with chronic exposure. Hopefully, future experiments will be able to answer these questions. These results also support *in vitro* findings from the previous chapter that showed FGF9 could be detrimental to neurons and axons.

Astrocyte activation, or reactive astrogliosis, is a common feature of MS lesions and is thought to exacerbate and mitigate pathogenesis in MS (Correale and Farez, 2015). (Lindner et al., 2015) demonstrated that inhibition of myelination by FGF9 is dependent on astrocytes and this effect was accompanied by a pro-inflammatory chemokine response predicted to drive inflammation. Astrocyte activation was extensive in FGF9-over-expressing lesions, in which strong GFAP

reactivity was detected from 30 days PI and persisted to at least 3 months PI (Figure 6.6, 6.7). FGF9 staining did not colocalize with GFAP in AAV6-*Fgf9* lesions suggesting FGF9 does not drive its own expression in astrocytes. These findings also indicate that myelin and axonal damage observed in AAV6-*Fgf9* lesions do not drive FGF9 expression directly. This suggests that similar destruction in MS may also not be responsible for FGF9 expression associated with MS but further studies will be required to test this hypothesis.

In Chapter 3, the FGF feedback inhibitors Sprouty2 and Sprouty4 were visualised mostly in astrocytes in MS lesions. FGF9 induced feedback inhibitor expression in myelinating cultures while FGF1 and FGF2 did not. Astrocytes upregulated feedback inhibitor expression at the mRNA and protein level only in response to FGF9. These findings suggested that feedback inhibitor expression in astrocytes is mainly a response to FGF9 signaling. Sprouty2 was visualised in astrocytes adjacent to FGF9-expressing neurons 30 days and 3 months PI in AAV6-*Fgf9* lesions (Figure 6.7). Astrocytic Sprouty2 expression corresponded with onset of demyelination and axonal pathology. As inhibition of myelination *in vitro* is astrocyte dependant and astrocytes respond to FGF9 in AAV6-*Fgf9* lesions, it is tempting to speculate that demyelination in these lesions is also astrocyte dependant but further experiments will be required to determine if this is the case. Pinpointing the exact time within the first 30 days of FGF9 expression, astrocytic Sprouty2 expression, and demyelination take place, would reveal whether astrocytes are activated before or after the onset of demyelination.

In MS, FGF9 is thought to contribute to pathogenesis by inhibiting remyelination and inducing pro-inflammatory chemokine production, both of which are dependent on astrocytes. By inducing FGF9-over-expression in rat cortex, results in this chapter have shown increased levels of FGF9 are sufficient to induce formation of demyelinated lesions with extensive axonal pathology, the two major hallmarks of MS. These lesions progressively demyelinated over months and were accompanied by a sustained astrocytic response. Data from Figure 5.12 demonstrated FGF9 does not induce axonal pathology directly. This suggests FGF9 might be causing axonal damage via astrocytes in a similar fashion to how FGF9 inhibits myelination. In summary, these results combined with findings from the previous chapter support a role for FGF9 as a neurodegenerative agent in MS.

CHAPTER SEVEN

GENERAL DISCUSSION

7 GENERAL DISCUSSION

FGF signaling represents a relatively unexplored area of research in the study of MS pathogenesis. FGF9 has long been a factor of interest in the study of several cancers as it is a potent mitogen and survival factor that promotes tumorigenesis (Todo et al., 1998). Some studies have alluded to a role for FGF9 in the CNS as a protective factor in neurodegenerative diseases like Parkinson's, ALS, and Alzheimer's disease (Nakamura et al., 1998b, Nakamura et al., 1998a, Huang et al., 2009, Huang and Chuang, 2010). In these studies, the presence of FGF9 protected neurons from death from a variety of toxic insults. FGF9 emerged as an interesting target in the study of demyelinating disease when it was found to inhibit myelination in a screen of myelinating cultures (Lindner et al., 2015). This effect was associated with the appearance of OLs displaying a premyelinating phenotype that also expressed mature myelin proteins. OLs in these experiments resembled OLs seen in chronic MS lesions (Chang et al., 2002). Further research led to the discovery that astrocyte-dependant mechanisms are responsible for inhibition of myelination seen with FGF9. Although FGF9 inhibited myelination, it promoted OPC proliferation, which is believed to be a beneficial process in trying to promote remyelination in MS. Despite these findings, relatively little is known about the functions of this pleiotropic growth factor in MS and experiments in the course of this thesis have set out to address this problem. In particular, this work has focused on elucidating which cell types respond to FGF9 signaling in the CNS. Experiments were performed to screen inflammatory factors associated with MS to determine whether any caused induction of FGF9 in CNS cells. The effects of long-term exposure to FGF9 were investigated *in vitro* and *in vivo*, and neuronal cultures were studied with regard to the effects of FGF9 on axonal integrity and transport.

The first set of experiments performed in the course of this research went back into human brain samples used by Lindner et al. to try to determine the targets of FGF9 signaling in MS. MS brains displayed higher levels of FGF-feedback inhibitors, correlating with the presence of FGF9. The same cell types associated with FGF9 expression in MS, astrocytes and OLs, were found to express FGF-feedback inhibitors. Feedback inhibitor expression was also more common in acute MS than chronic MS, as is FGF9. In acute lesions, astrocytes, OLs, and macrophages were FGF9⁺ and most often, these cells were Sprouty⁺ as well.

FGF9 was expressed at lower levels in chronic lesions and the same was true for the Sproutys. Expression of FGF9 and Sproutys was mostly limited to astrocytes in chronic lesions, likely due to the paucity of OLs and macrophages present at this stage of disease. In summary, there was strong correlation between the cells expressing FGF9 and those expressing Sproutys in MS. These studies were limited in scope due to difficulty with using human tissue. Unlike with *in vivo* tissue or *in vitro* cells, there is often a long delay between death and fixation, which allows degradation of the tissue to take place and makes staining more difficult. Of the dozen antibodies specific for members of FGF-signaling pathways, only three were efficacious enough for staining. This limited the research that could be performed using archived MS brain samples.

The expression of negative feedback inhibitors of FGF signaling, Sproutys and DUSPs, were then assessed in FGF-treated *in vitro* cultures. OLs and neurons responded similarly to FGF2 and FGF9 but astrocytes only upregulated feedback inhibitors in response to FGF9. This is despite the fact FGF1 and FGF2 are the most promiscuous FGFs and astrocytic responses to FGF1 and FGF2 have been demonstrated by other groups in the past (Cassina et al., 2005, Gómez-Pinilla et al., 1995, Eclancher et al., 1996). In myelinating cultures, FGF9 induced feedback inhibitor expression while FGF1 and FGF2 did not, suggesting this may be a feature exclusive to FGF9. Interestingly, FGF1 had almost no effect on any of the cells studied in these experiments. The reasons for discrepancies in feedback inhibitor expression are a mystery and warrant further investigation as these cell types are well documented to express FGFRs and feedback-inhibitor expression is a robust downstream signaling event following FGF-FGFR interactions, however this was not the case in these experiments. These findings were not anticipated as feedback inhibitor expression is the response most strongly associated with FGF signaling and the two are often intrinsically linked. Examining other aspects of FGF signaling in these cells, such as MAPK, AKT, and PLC γ activation should be investigated to determine if these cells were responding to FGF signaling at all. There may also be some discrepancy between previous studies that have shown FGF-feedback inhibitor expression mostly through *in vivo* staining and imaging, and these studies, which relied on *in vitro* cultures. Although myelinating cultures have all CNS cell types represented they are still very different from the *in vivo* environment, one major difference is these cultures are produced from embryos

and very young animals whereas most MS research focuses on the adult. These cultures also lack a functional immune and circulatory system which may impact reactions to different treatments.

One crucial question regarding FGF9 in MS is why is it upregulated in the first place? The trigger or triggers for FGF9 expression are unknown in most contexts in which FGF9 has been investigated, but some clues have come from cancer studies. FGF9 induction has been shown in response to PGE₂ (Wang et al., 2009), AhR activation (Chuang et al., 2006), and hypoxia (Chen et al., 2014). These factors along with a host of inflammatory and anti-inflammatory cytokines associated with MS were screened for their ability to induce FGF9 upregulation in myelinating cultures. None of the factors used in these experiments succeeded in upregulating FGF9 except hypoxia. Hypoxia was incredibly damaging to myelinating cultures as it killed neurons and OLs while sparing only astrocytes. Astrocytes survived hypoxia and reperfusion, and responded by increasing their expression of FGF9. Hypoxia is a well described component of MS pathogenesis (Lassmann, 2003) and these findings suggested it may also be involved in driving FGF9 expression by astrocytes in MS lesions. Colocalization studies of HIF1 α in nuclei and FGF9 in cytoplasm of astrocytes in MS lesions could confirm whether hypoxia is indeed a trigger for FGF9 expression in MS. Macrophages polarised towards an anti-inflammatory phenotype were also induced to upregulate FGF9, at the mRNA level. This suggested an additional mechanism whereby FGF9 expression could be induced by macrophages in a tissue repair context. This could also be investigated in MS as results from Chapter 3 showed that, where present, macrophages stained for the presence of FGF9. Future experiments should examine the phenotype of FGF9⁺ macrophages in MS lesions and determine whether there is a correlation between an anti-inflammatory phenotype and FGF9 expression. In additional experiments looking at the effects of FGFs on macrophages directly, macrophages did not respond to FGF treatment by upregulating feedback inhibitor expression, or altering their polarization state or cytokine profile suggesting they are not targets of FGF signaling.

Experiments performed in Chapter 5 attempted to address some basic questions about FGF9 and its effects on myelin using myelinating cultures. The most obvious consideration was whether FGF9 is a demyelinating factor. To test this query,

myelinating cultures were maintained until DIV 28, before treatment with FGF9 was initiated. Myelinating cultures produce the majority of their myelin between DIV 18 and DIV 28 so this approach allowed for the effects of FGF9 on mature myelin to be observed, as opposed to previous research that focused on the effect of FGF9 treatment on primary myelination (Lindner et al., 2015). Using this model it was found that FGF9 did not induce demyelination in cultures after ten days suggesting that FGF9 is not a demyelinating factor. Withdrawing FGF9 from cultures that were treated from DIV 18 – 28, and maintaining them in control media for a further ten days had surprising results. Pre-treatment with FGF9 led to greatly increased myelin production, determined through greatly increased MOG⁺ staining, compared to control cultures at DIV 38. Analysis of these cultures under high power microscopy revealed the myelin produced following withdrawal of FGF9 at DIV 28 differed greatly from myelin in control cultures. This myelin had an irregular structure with large segments that were only loosely associated with axons, and a striking variety in the thickness of the myelin sheath along the length of one internode. This suggested there was a defect in differentiation and myelin production in OLs that have been exposed to FGF9, even when the factor is removed.

Findings from the previous section raised the question: what happens to OPCs that are produced as a result of FGF9-induced proliferation? Can they go onto mature and myelinate or does FGF9 irreparably alter them in some way? In these cultures it appeared as though OLs had attempted to mature and myelinate but were unable to do so following the withdrawal of FGF9. Further staining and imaging studies revealed the presence of MOG⁺PLP⁺ OLs with the proteins randomly distributed throughout cell bodies and processes. This effect had not been described before and these cells somewhat resemble mature OLs that undergo de-differentiation when treated with FGF2 (Bansal and Pfeiffer, 1997). This suggested similar mechanisms might underlie the appearance of aberrant myelin in FGF9-treated cultures and the de-differentiation observed in FGF2-treated OLs. Future studies along this line of enquiry should focus on the effects of FGF9 pre-treatment on OL maturation and myelination, and try to determine at which point in differentiation OLs begin to exhibit these unusual characteristics. As these effects were observed ten days after treatment was ended, these findings suggest exposure to high levels of FGF9 may render OLs produced from FGF9-

induced proliferation unable to develop normally. This would have potential implications on the failure of remyelination observed in many MS cases.

Examining axons in cultures from the previous section under confocal microscopy revealed that long-term treatment with FGF9 resulted in axonal loss and the appearance of axonal swellings. These findings somewhat resembled features of axonal transport deficit so axonal transporter gene expression was assessed in FGF9-treated myelinating cultures. The outcome of this experiment was a downregulation of axonal transporter genes following FGF9 treatment suggesting FGF9 may actually be detrimental to neurons, in contradiction to the current literature. Following these results, enriched neuronal cultures were generated and treated with FGF9 and these cultures displayed a reduction in total neuronal cell counts and axonal density. This effect could be overcome by the addition of FdU, a cytotoxic agent that kills proliferating cells. This showed the effects of FGF9 on neurons was indirect, and likely a result of astrocyte-dependant signaling or metabolic stress. Additionally, neurons express FGFR1 and FGFR4 while FGF9 is specific for FGFR2 and FGFR3 further supporting the hypothesis that FGF9 does not signal in neurons directly to mediate these detrimental effects. These experiments showed for the first time that FGF9 could be harmful to neurons while most other research has focused on its neuroprotective capabilities. To continue this line of experimentation, FGF9-treated astrocyte supernatants should be administered to neuronal cultures to determine whether a soluble astrocyte-derived factor is responsible for these effects as is the case for myelination (Lindner et al., 2015). Following this the microarray from FGF9-treated myelinating cultures mentioned previously in this thesis should be screened for upregulated candidates that regulate axonal transport and neuronal survival. These factors could then be tested on neurons to see if the effects observed with FGF9 can be replicated.

Chapter 6 focused on the over-expression of FGF9 in rat cortex. Unexpectedly, chronic over-expression of FGF9 induced demyelination and axonal pathology over the course of nine months. By 30 days, the formation of demyelinated lesions and the appearance of β -APP axonal swellings were apparent in FGF9-over expressing brains while brains injected with a control vector remained healthy throughout the experiment. These lesions had completely demyelinated by three

months and axonal β -APP swellings continued to accumulate until the end of the experiment at nine months. Lesions in FGF9 over-expressing animals were associated with Sprouty2 staining in astrocytes. These lesions displayed characteristics strikingly similar to MS lesions, such as demyelination, axonal pathology, astrocyte activation and Sprouty2 expression. This suggests that FGF9 may be also be involved in MS lesion development, as well as failure of remyelination and axonal pathology and further *in vivo* research should focus on more robustly examining lesion development in FGF9-overexpressing cortex. Future *in vivo* experiments should also address the potential roles of FGF9 in EAE as one of the most widely used models of MS.

Taken together, the results shown in this thesis support the hypothesis that FGF9 can mediate a host of detrimental effects on cells of the CNS and may be a more prominent factor in MS lesion development and progression than previously thought. Before commencement of experiments in this thesis, FGF9 was believed to contribute to remyelination failure in MS and promote inflammation via inflammatory chemokine expression but this research expands on the potential detrimental mechanisms of FGF9 in the CNS. In *in vitro* and *in vivo* models, FGF9 has been shown to negatively impact OL differentiation, myelination, axonal integrity, and neuronal numbers. This work also showed astrocytes appear to be particularly receptive to FGF9 signaling compared to other cell types in the CNS. Astrocytes also produce FGF9 in response to hypoxia, a common feature of MS lesions. Infiltrating macrophages are also sources of FGF9 in MS lesions and experiments shown here suggest this is largely a feature of repair-oriented macrophages. In addition to inhibiting myelination, FGF9 was shown to perturb myelination by OPCs generated as a result of FGF9 treatment. This suggests FGF9 induces long lasting changes in cells of the OPC lineage that interfere with maturation. Chronic over-expression of FGF9 also led to the formation of demyelinating lesions. In summary, these experiments show that, in a variety of model systems, FGF9 is involved in demyelination and axonal damage as well as inhibition of myelination, the three major characteristic of MS.

CHAPTER EIGHT

APPENDICES

8 APPENDICES

8.1 Positive control stainings for Sprouty, DUSP, and FGF9 antibodies

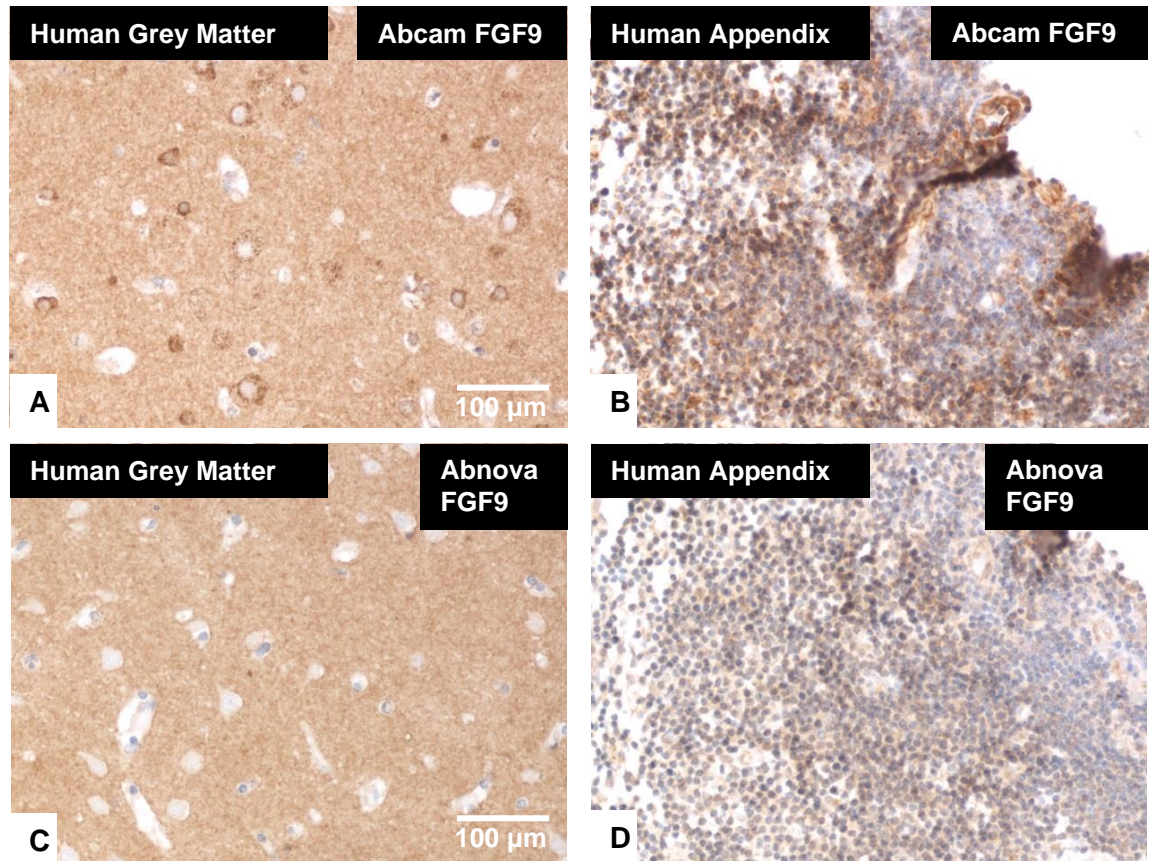


Figure 8.1. Positive control stainings for FGF9 antibodies used in immunohistochemistry and immunofluorescence. Antibodies against FGF9 were tested on tissues known to express each protein according to the Human Protein Atlas (<https://www.proteinatlas.org/>) and antibody specification sheets. Abcam FGF9 was more effective for immunohistochemistry while Abnova FGF9 was more effective for immunofluorescence.

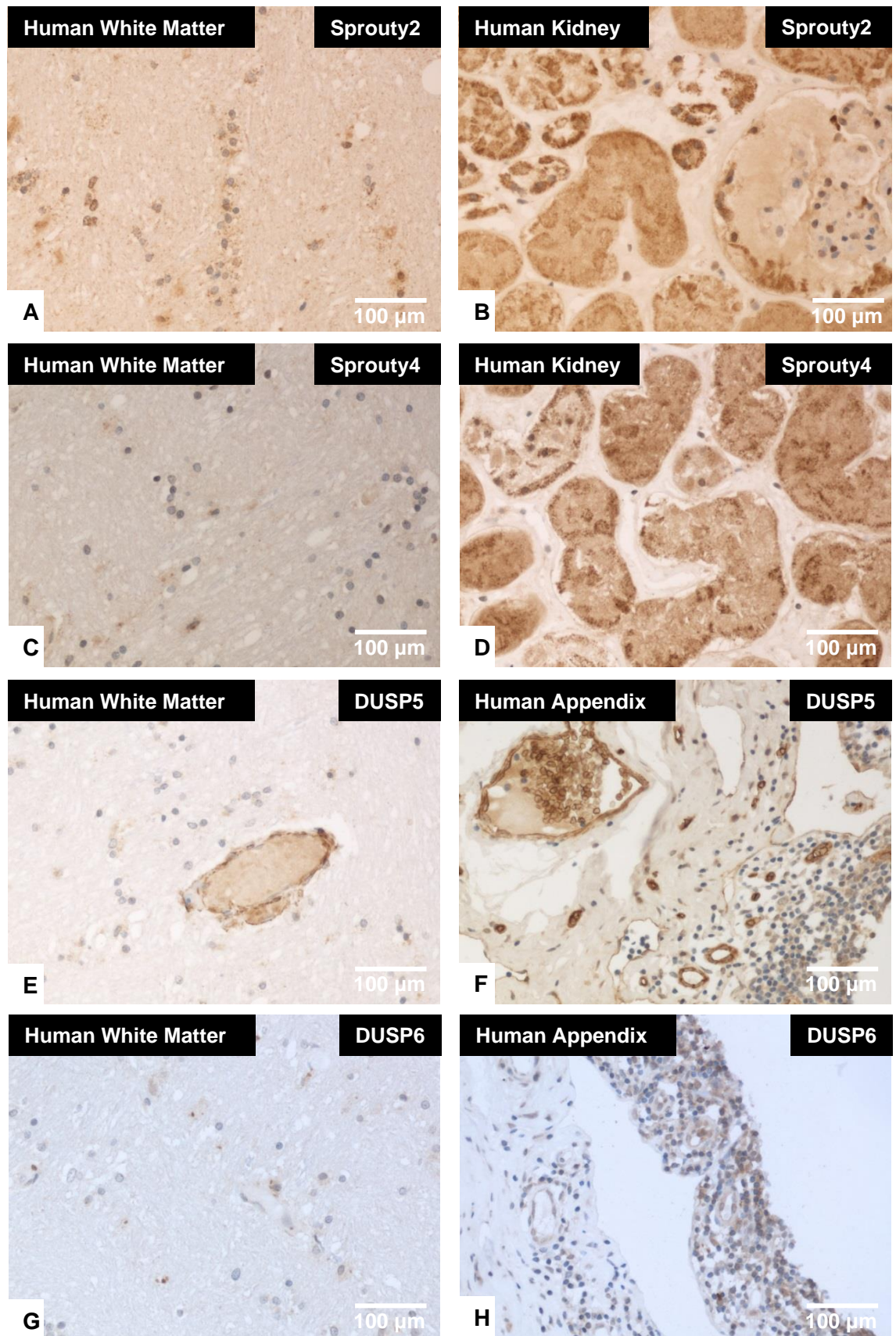


Figure 8.2. Positive control stainings for antibodies used in immunohistochemistry and immunofluorescence. Antibodies against Sprouty2 (A, B), Sprouty4 (C, D), DUSP5 (E, F), and DUSP6 were tested on tissues known to express each protein according to the Human Protein Atlas (<https://www.proteinatlas.org/>) and antibody specification sheets.

8.2 Cell culture purity analysis

To assess their purity, astrocyte monolayers were stained with antibodies against markers of CNS cells (Figure 8.3). Monolayers were fixed at DIV 7 as this is when they are used for experiments or seeded with spinal cord progenitors to generate myelinating cultures. Astrocytes were not counted directly in this experiment as their density and irregular shape made this too difficult to do accurately. The only contaminating cell type was found to be OL lineage cells due to the prevalence of Olig2 staining in astrocyte monolayers.

As enriched neuronal cultures were used in experiments involving FGF9, a potent proliferative factor, it was important to investigate purity in the cultures. NeuN⁺ cells, signifying neuronal differentiation, appeared at DIV 3 and then remained at a steady level (Figure 8.4 B). As with astrocyte monolayers, OL lineage cells were the main contaminating cell type, proliferating exponentially between DIV 3 – 10 (Figure 8.4 C). Astrocytes were rare in neuronal cultures but were detected from DIV5 and continued to proliferate to DIV 10 (Figure 8.4 D). Microglia were very rare or absent in most of the cultures examined (Figure 8.4 E).

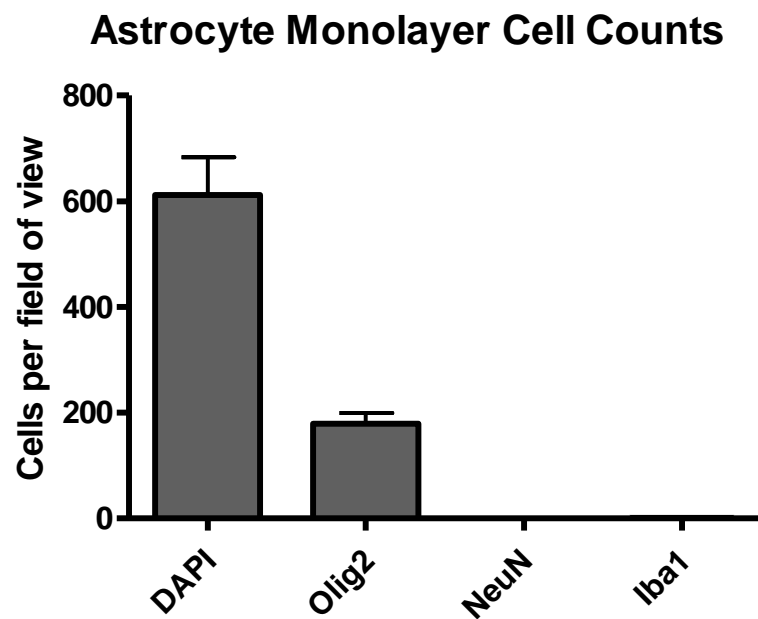


Figure 8.3. Quantification of different cell types in astrocyte monolayers. Astrocyte monolayers were generated as described in section 2.2.1.2 and fixed for staining at DIV 7. Monolayers were stained with antibodies against cell nuclei (DAPI) OL lineage cells (Olig2), neurons (NeuN), and microglia (Iba1). Olig2⁺ cells were the most abundant contaminating cell type in astrocyte monolayers while neurons and microglia were never detected. This experiment was performed three times.

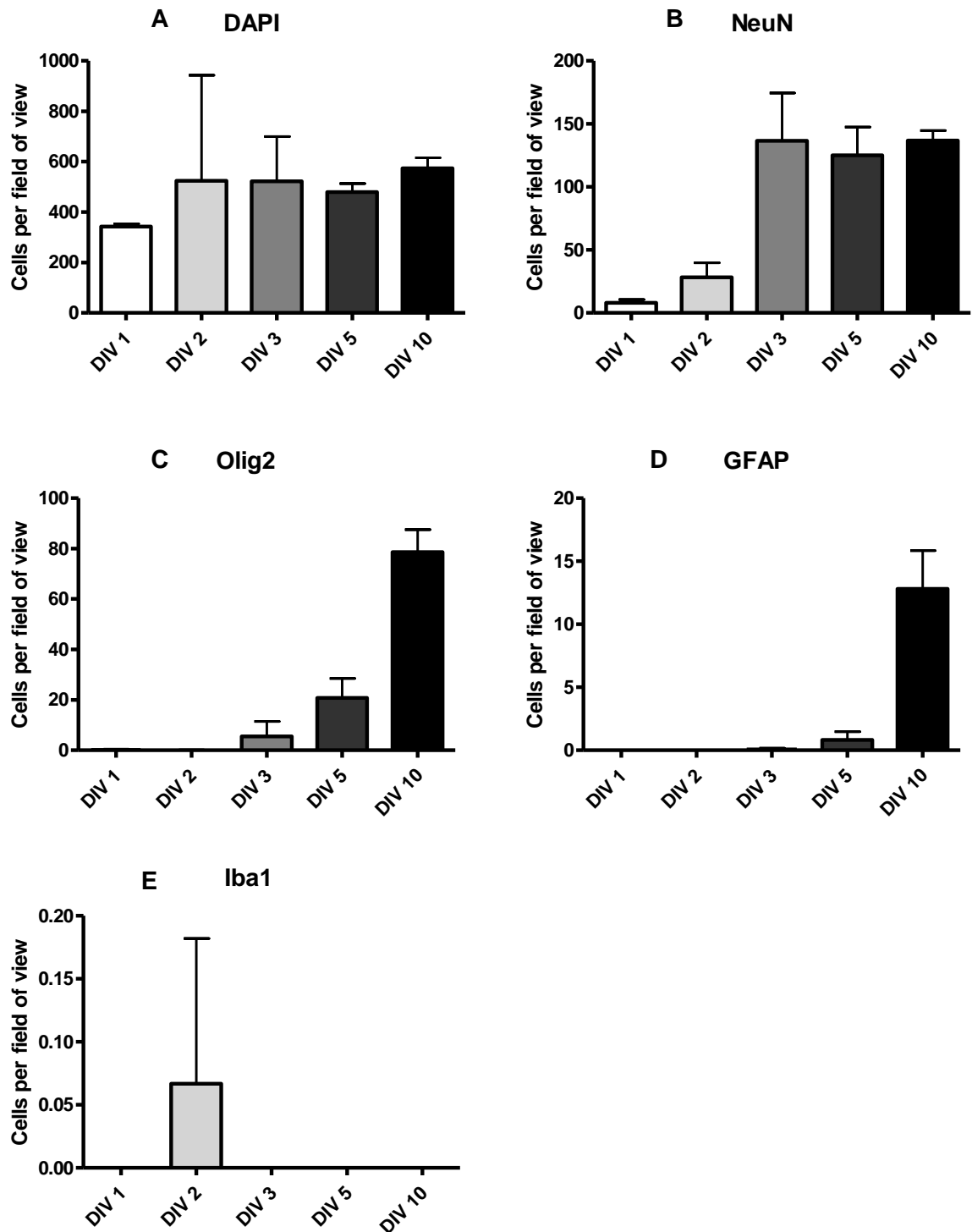


Figure 8.4. Quantification of different cell types in enriched neuronal cultures. Neurons were purified as described in section 2.2.5.8 and cultured in neuro-basal medium from 1 to 10 days before being fixed and processed for immunofluorescence. Cultures were stained for Olig2, NeuN, Iba1, and GFAP to identify oligodendrocytes, neurons, microglia, and astrocytes respectively. Cell numbers from each time point were quantified by manual counting except for Olig2 and DAPI counts which were done using CellProfiler. Overall cell numbers remained fairly constant from DIV1-10 (A). NeuN⁺ cells are present from DIV1 but reach and remain at their peak from DIV3 (B) Olig2⁺ cells begin appearing at DIV3 and these numbers increase rapidly by DIV 10 (C). Astrocytes appear around DIV5 and quickly proliferate by DIV10. Microglia were very rarely seen at any time in the cultures (E). This experiment was performed once.

8.3 FGF9 induced proliferation in astrocytes

Low-density astrocyte cultures were generated as described in section 2.2.2. After 1 week in culture, astrocytes were treated with 100 ng/mL FGF1, 2, or 9 for 3 days. Astrocyte numbers were quantified by counting DAPI nuclei per field of view using CellProfiler. FGF9 induced a significant proliferative response by 3 days while FGF1 and FGF2 had no effect on cell numbers. C = 98.4 ± 36.5 cells/FOV, FGF9 = 160.5 ± 59 cells/FOV.

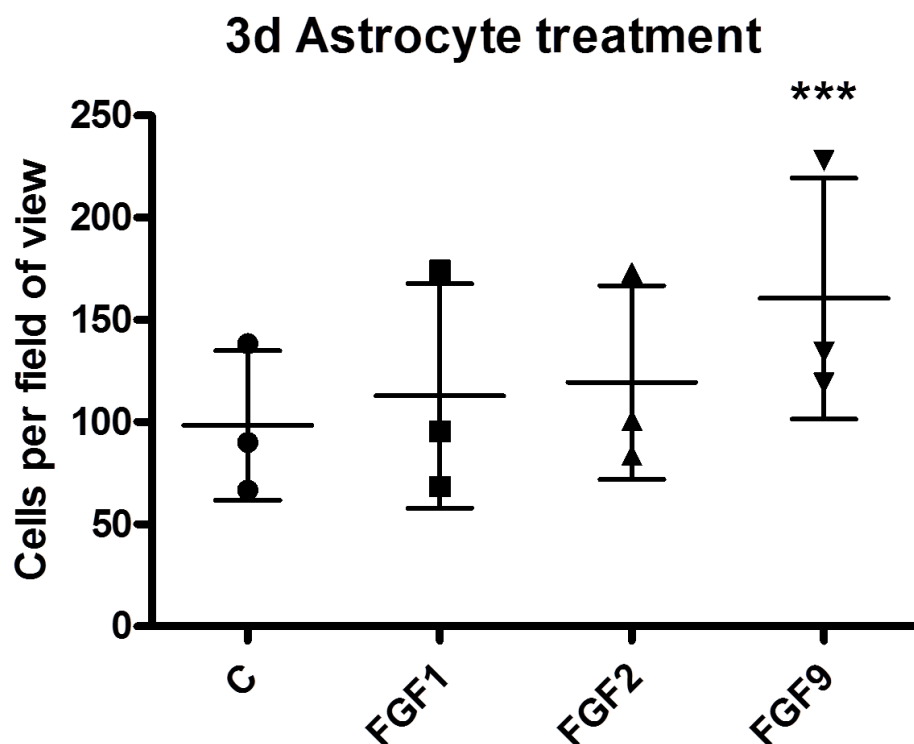


Figure 8.5 FGF9 induced proliferation in astrocytes *in vitro*. Low-density astrocyte cultures were generated as described in section 2.2.2 and treated for 72 hours with 100 ng/mL FGF1, 2, or 9. Cells were fixed and stained and DAPI-positive nuclei were quantified using CellProfiler. Following FGF9 treatment cell numbers were increased 50% where as FGF1 and FGF2 appeared to have a slight but insignificant proliferative effect. This experiment was performed three times. ***, $p < 0.001$, (one-way ANOVA with Dunnett's Multiple Comparison Test).

8.4 Expression of FGFs and feedback inhibitors in EAE

To investigate the expression and functions of FGF9 in EAE, Lewis rats were immunised against MOG. 100 μ L complete Freund's adjuvant containing 50 μ g MOG₁₋₁₂₅ was injected into rats subcutaneously at the base of the tail (n = 6). Animals were monitored for symptoms of EAE and sacrificed at the peak of the second phase of disease. Clinical scores and weights from control and EAE animals are shown in Figure 8.6. Animals were scored based on the criteria laid out in section 2.6.1.1. Symptoms first appeared at day 10 PI and peaked at a score of four on day 13. Weight decreased by an average of 35g in EAE rats by this time point. This was followed by a brief recovery period and clinical scores decreased to an average of two. By day 21, all but one animal in the EAE group developed severe disease and the experiment was stopped. Animals in both groups were sacrificed and the lumbar portions of their spinal cords were prepared for qPCR and immunohistological analysis.

The first studies looked at expression of inflammatory markers in EAE vs control spinal cords. The polarized macrophage markers *Nos2* and *Arg1* were not up or down regulated in EAE cords compared to controls (Figure 8.7 A). Expression of inflammatory cytokine genes, *Tnfa*, and *Ifny* were significantly up regulated in EAE cords (*Tnfa* = 17.7 \pm 13.4 fold, *Ifny* = 51.4 \pm 72.6 fold). Expression of *Fgf1* and *Fgf9* did not vary strongly from control levels (Figure 8.7 B). *Fgf2* expression was slightly elevated, 2.2 \pm 0.7 fold. FGF feedback inhibitor genes, *Spry2* and *Dusp5* were unchanged in EAE spinal cords (Figure 8.7 C). *Spry4* was down regulated - 2.4 \pm 1.1 fold, while *Dusp6* was up regulated 5.5 \pm 3.2 fold.

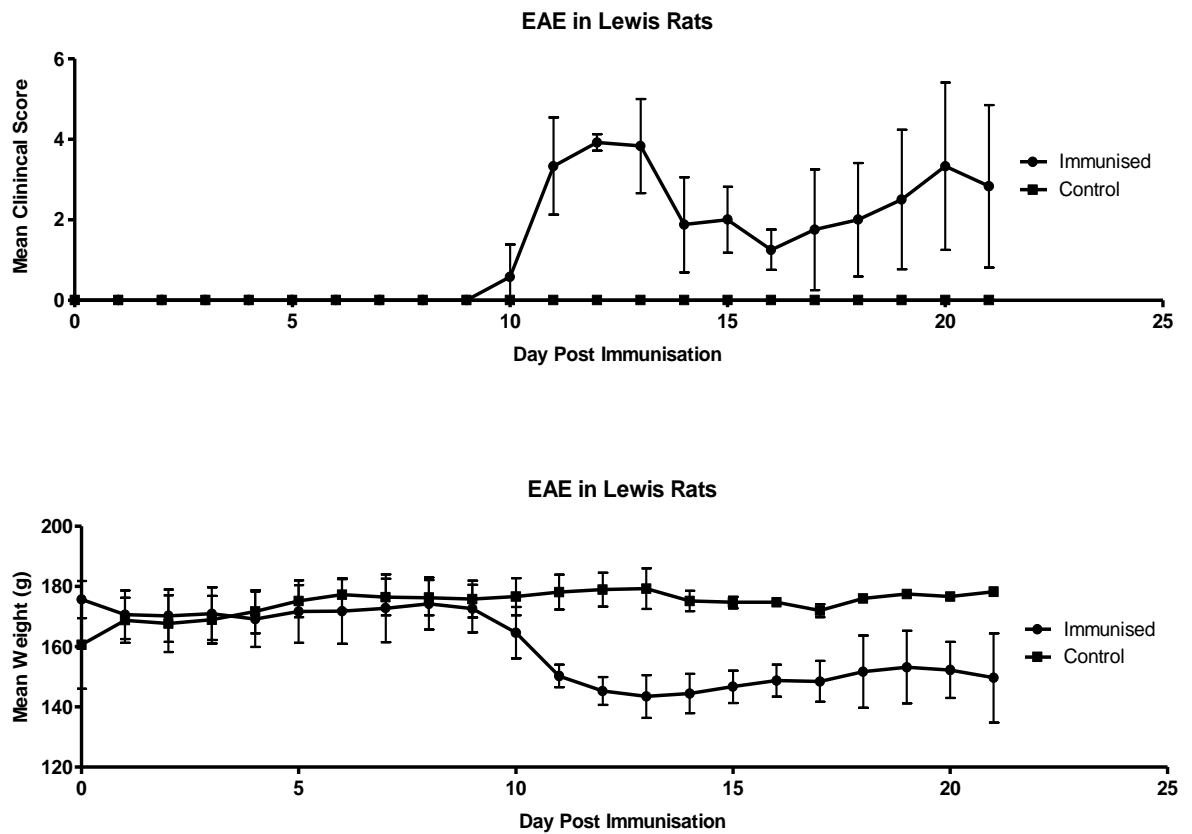


Figure 8.6. MOG₁₋₁₂₅ induced EAE caused biphasic disease in Lewis rats. 10 12-week-old female Lewis rats were immunised with 100 μ L complete Freund's adjuvant containing 50 μ g MOG₁₋₁₂₅ as described in section 2.6.1. Animals began showing symptoms and losing weight 10 days PI and the first phase of disease peaked at day 13. Animals partially recovered until day 16 when the second phase began. At day 21 some of the animals progressed to a clinical score of 6 so the experiment was stopped at this stage and the animals euthanized.

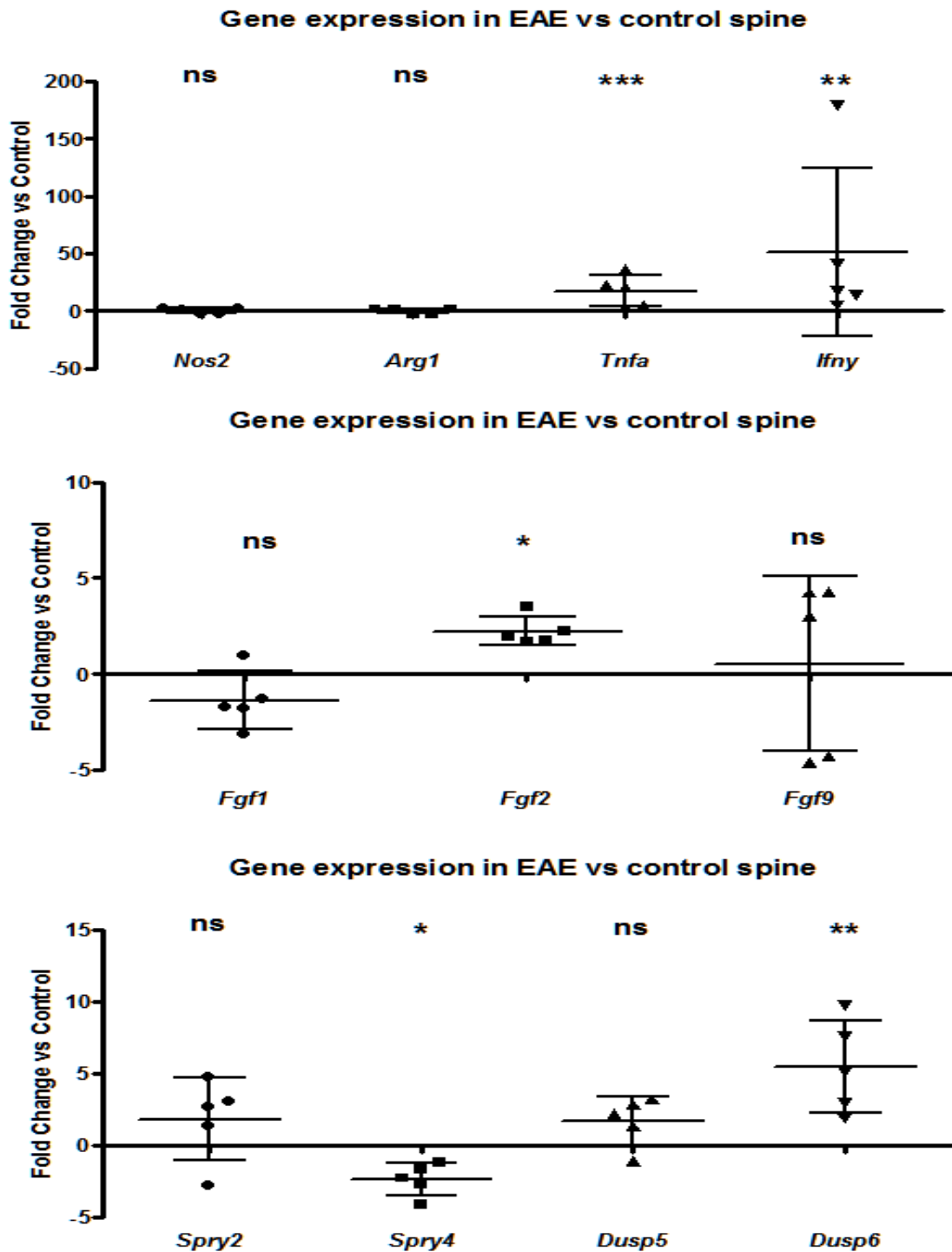


Figure 8.7. FGF and feedback inhibitor expression was variable in EAE. The lumbar regions of spinal cords from EAE and control rats were harvested and processed for qPCR as described in section 2.6.1.2. qPCRs were ran with *Gapdh* as a house keeping control. CT values from 3 controls were averaged for each gene analysed and this value was used as the control. There was no change in *Nos2* or *Arg1* expression in EAE (A) but *Tnfa* and *Ifny* were significantly up regulated. *Fgf2* expression was increased while expression of *Fgf1* and *Fgf9* were not significantly up or down regulated (B). *Spry4* expression was decreased slightly and *Dusp6* was significantly up regulated while *Spry2* and *Dusp5* expression were unaffected by EAE (C). Data presented are the means \pm SD. *, $p < 0.05$, **, $p < 0.01$ (Two-tailed T test of delta CT values).

8.5 FGF9 and Sprouty2 were associated with macrophages in EAE

Results from the previous section suggest that FGF signaling is not a major feature of MOG induced EAE. To determine whether any changes in FGF9 expression could be detected, EAE cords were fixed and prepared for immunohistochemistry. Sections were stained with antibodies against FGF9 and Sprouty2 in combination with GFAP, the OL markers P25 and Olig2, and the macrophage/microglia markers ED1 and IBA1. FGF9 staining was extensive in White matter regions and was not associated with GFAP in EAE (Figure 8.8 A) or P25 (Figure 8.8 B). There was strong colocalization of FGF9 and ED1 surrounding blood vessels indicating that infiltrating macrophages are producing FGF9 (Figure 8.8 C). Sprouty2 staining did not colocalize in astrocytes (Figure 8.8 D) stained in a few OL nuclei (Figure 8.8 E) and macrophage/microglia cell bodies (Figure 8.8 F). Due to time constraints further analysis was not performed.

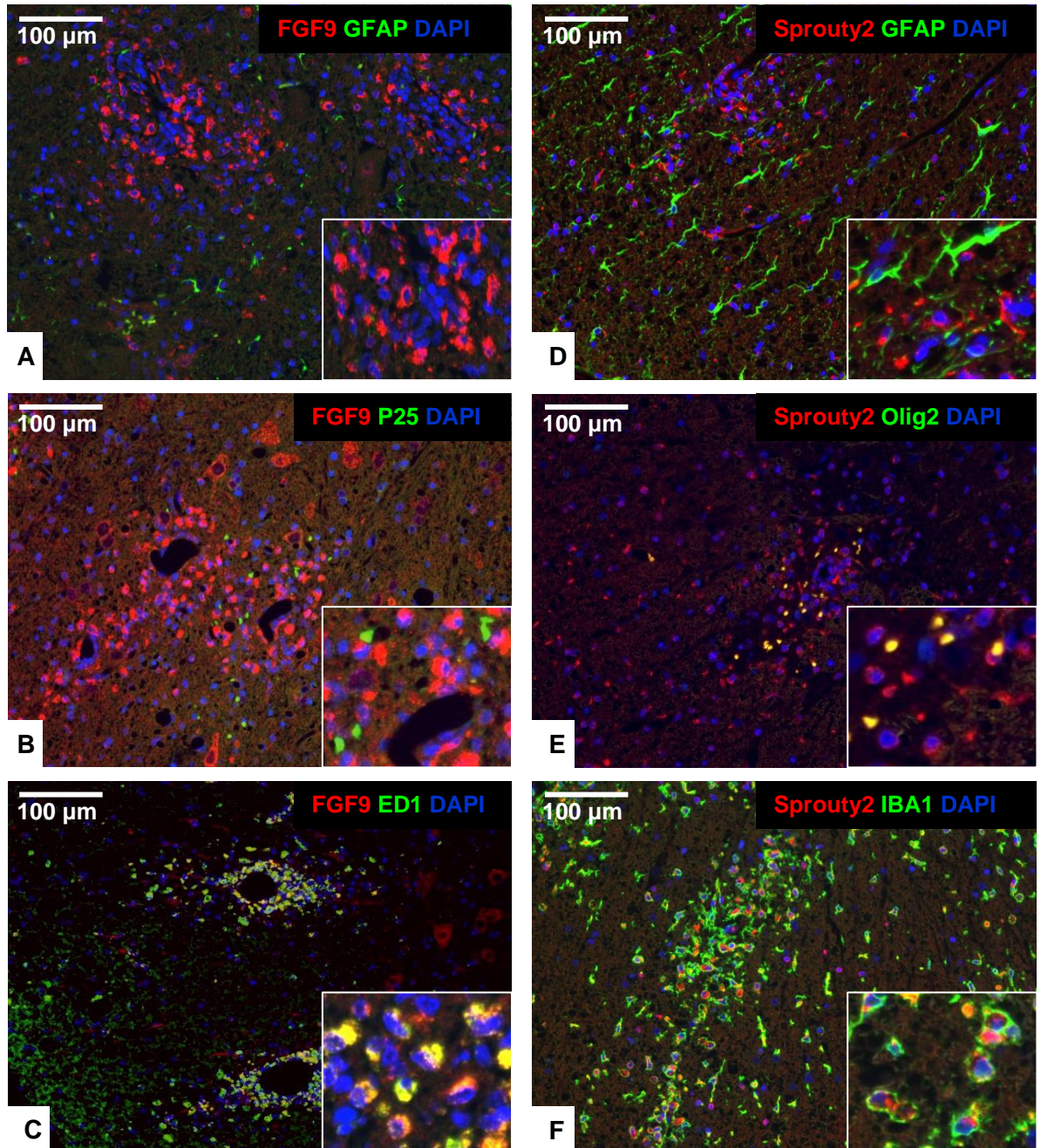


Figure 8.8. FGF9 and Sprouty2 expression was visualised in macrophages/microglia in EAE. Spinal cords from EAE rats were perfused with PFA and the lumbar portion prepared for immunohistochemistry as described in section 2.6.1.2. Sections were double labelled with antibodies against FGF9 or Sprouty2 in combination with markers for astrocytes, OLs, and macrophages. FGF9 staining did not colocalize with GFAP (A) or the OL marker P25 (B), but was seen in ED1⁺ macrophages (C). Sprouty2 was also not detected in astrocytes (D) but did stain in OLs (E) and macrophages (F).

REFERENCES

- Abe, M. & Naski, M. C. 2004. Regulation of sprouty expression by PLCgamma and calcium-dependent signals. *Biochem Biophys Res Commun*, 323, 1040-7.
- Aboul-Enein, F., Rauschka, H., Kornek, B., Stadelmann, C., Stefferl, A., Brück, W., Lucchinetti, C., Schmidbauer, M., Jellinger, K. & Lassmann, H. 2003. Preferential loss of myelin-associated glycoprotein reflects hypoxia-like white matter damage in stroke and inflammatory brain diseases. *J Neuropathol Exp Neurol*, 62, 25-33.
- Agresti, C., D'urso, D. & Levi, G. 1996. Reversible inhibitory effects of interferon-gamma and tumour necrosis factor-alpha on oligodendroglial lineage cell proliferation and differentiation in vitro. *Eur J Neurosci*, 8, 1106-16.
- Akbulut, S., Reddi, A. L., Aggarwal, P., Ambardekar, C., Canciani, B., Kim, M. K., Hix, L., Vilimas, T., Mason, J., Basson, M. A., Lovatt, M., Powell, J., Collins, S., Quatela, S., Phillips, M. & Licht, J. D. 2010. Sprouty proteins inhibit receptor-mediated activation of phosphatidylinositol-specific phospholipase C. *Mol Biol Cell*, 21, 3487-96.
- Alam, K. Y., Frosthalm, A., Hackshaw, K. V., Evans, J. E., Rotter, A. & Chiu, I. M. 1996. Characterization of the 1B promoter of fibroblast growth factor 1 and its expression in the adult and developing mouse brain. *J Biol Chem*, 271, 30263-71.
- Albrecht, P. J., Dahl, J. P., Stoltzfus, O. K., Levenson, R. & Levison, S. W. 2002. Ciliary neurotrophic factor activates spinal cord astrocytes, stimulating their production and release of fibroblast growth factor-2, to increase motor neuron survival. *Exp Neurol*, 173, 46-62.
- Albrecht, P. J., Murtie, J. C., Ness, J. K., Redwine, J. M., Enterline, J. R., Armstrong, R. C. & Levison, S. W. 2003. Astrocytes produce CNTF during the remyelination phase of viral-induced spinal cord demyelination to stimulate FGF-2 production. *Neurobiol Dis*, 13, 89-101.
- Alharbi, F. M. 2015. Update in vitamin D and multiple sclerosis. *Neurosciences (Riyadh)*, 20, 329-35.
- Allen, B. L. & Rapraeger, A. C. 2003. Spatial and temporal expression of heparan sulfate in mouse development regulates FGF and FGF receptor assembly. *Journal of Cell Biology*, 163, 637-648.
- Allen, I. V., Mcquaid, S., Mirakhur, M. & Nevin, G. 2001. Pathological abnormalities in the normal-appearing white matter in multiple sclerosis. *Neurol Sci*, 22, 141-4.
- Alonso, A., Sasin, J., Bottini, N., Friedberg, I., Osterman, A., Godzik, A., Hunter, T., Dixon, J. & Mustelin, T. 2004. Protein tyrosine phosphatases in the human genome. *Cell*, 117, 699-711.
- Antoine, M., Reimers, K., Dickson, C. & Kiefer, P. 1997. Fibroblast growth factor 3, a protein with dual subcellular localization, is targeted to the nucleus and nucleolus by the concerted action of two nuclear localization signals and a nucleolar retention signal. *J Biol Chem*, 272, 29475-81.

- Arakawa, Y., Sendtner, M. & Thoenen, H. 1990. Survival effect of ciliary neurotrophic factor (CNTF) on chick embryonic motoneurons in culture: comparison with other neurotrophic factors and cytokines. *J Neurosci*, 10, 3507-15.
- Armelin, H. A. 1973. PITUITARY EXTRACTS AND STEROID-HORMONES IN CONTROL 3T3-CELL GROWTH. *Proceedings of the National Academy of Sciences of the United States of America*, 70, 2702-2706.
- Armstrong, R. C., Le, T. Q., Flint, N. C., Vana, A. C. & Zhou, Y. X. 2006. Endogenous cell repair of chronic demyelination. *J Neuropathol Exp Neurol*, 65, 245-56.
- Armstrong, R. C., Le, T. Q., Frost, E. E., Borke, R. C. & Vana, A. C. 2002. Absence of fibroblast growth factor 2 promotes oligodendroglial repopulation of demyelinated white matter. *Journal of Neuroscience*, 22, 8574-8585.
- Atomura, R., Sanui, T., Fukuda, T., Tanaka, U., Toyoda, K., Taketomi, T., Yamamichi, K., Akiyama, H. & Nishimura, F. 2016. Inhibition of Sprouty2 polarizes macrophages toward an M2 phenotype by stimulation with interferon γ and *Porphyromonas gingivalis* lipopolysaccharide. *Immun Inflamm Dis*, 4, 98-110.
- Au-Yeung, N., Mandhana, R. & Horvath, C. M. 2013. Transcriptional regulation by STAT1 and STAT2 in the interferon JAK-STAT pathway. *JAKSTAT*, 2, e23931.
- Aurbach, E. L., Inui, E. G., Turner, C. A., Hagenauer, M. H., Prater, K. E., Li, J. Z., Absher, D., Shah, N., Blandino, P., Bunney, W. E., Myers, R. M., Barchas, J. D., Schatzberg, A. F., Watson, S. J. & Akil, H. 2015. Fibroblast growth factor 9 is a novel modulator of negative affect. *Proc Natl Acad Sci U S A*, 112, 11953-8.
- Azin, M., Mirnajafi-Zadeh, J. & Javan, M. 2015. Fibroblast Growth Factor-2 Enhanced The Recruitment of Progenitor Cells and Myelin Repair in Experimental Demyelination of Rat Hippocampal Formations. *Cell J*, 17, 540-456.
- Ballabriga, J., Pozas, E., Planas, A. M. & Ferrer, I. 1997. bFGF and FGFR-3 immunoreactivity in the rat brain following systemic kainic acid administration at convulsant doses: localization of bFGF and FGFR-3 in reactive astrocytes, and FGFR-3 in reactive microglia. *Brain Res*, 752, 315-8.
- Bansal, R. & Pfeiffer, S. E. 1997. FGF-2 converts mature oligodendrocytes to a novel phenotype. *Journal of Neuroscience Research*, 50, 215-228.
- Barnett, S. C. L., Christopher 2012. Myelination: Do Astrocytes Play a Role? *The Neuroscientist*.
- Baron, O., Ratzka, A. & Grothe, C. 2012. Fibroblast growth factor 2 regulates adequate nigrostriatal pathway formation in mice. *J Comp Neurol*, 520, 3949-61.
- Beenken, A. & Mohammadi, M. 2009. The FGF family: biology, pathophysiology and therapy. *Nat Rev Drug Discov*, 8, 235-53.
- Berghoff, S. A., Gerndt, N., Winchenbach, J., Stumpf, S. K., Hosang, L., Odoardi, F., Ruhwedel, T., Böhler, C., Barrette, B., Stassart, R., Liebetanz, D., Dibaj, P.,

Möbius, W., Edgar, J. M. & Saher, G. 2017. Dietary cholesterol promotes repair of demyelinated lesions in the adult brain. *Nat Commun*, 8, 14241.

Bernfield, M., Gotte, M., Park, P. W., Reizes, O., Fitzgerald, M. L., Lincecum, J. & Zako, M. 1999. Functions of cell surface heparan sulfate proteoglycans. *Annual Review of Biochemistry*, 68, 729-777.

Bethel, A., Kirsch, J. R., Koehler, R. C., Finklestein, S. P. & Traystman, R. J. 1997. Intravenous basic fibroblast growth factor decreases brain injury resulting from focal ischemia in cats. *Stroke*, 28, 609-15; discussion 615-6.

Bharti, A. R., Woods, S. P., Ellis, R. J., Cherner, M., Rosario, D., Potter, M., Heaton, R. K., Everall, I. P., Masliah, E., Grant, I. & Letendre, S. L. 2016. Fibroblast growth factors 1 and 2 in cerebrospinal fluid are associated with HIV disease, methamphetamine use, and neurocognitive functioning. *HIV AIDS (Auckl)*, 8, 93-9.

Bitsch, A., Schuchardt, J., Bunkowski, S., Kuhlmann, T. & Brück, W. 2000. Acute axonal injury in multiple sclerosis. Correlation with demyelination and inflammation. *Brain*, 123 (Pt 6), 1174-83.

Bogie, J. F., Stinissen, P. & Hendriks, J. J. 2014. Macrophage subsets and microglia in multiple sclerosis. *Acta Neuropathol*, 128, 191-213.

Bouvier, M. M. & Mytilineou, C. 1995. Basic fibroblast growth factor increases division and delays differentiation of dopamine precursors in vitro. *J Neurosci*, 15, 7141-9.

Boven, L. A., Van Meurs, M., Van Zwam, M., Wierenga-Wolf, A., Hintzen, R. Q., Boot, R. G., Aerts, J. M., Amor, S., Nieuwenhuis, E. E. & Laman, J. D. 2006. Myelin-laden macrophages are anti-inflammatory, consistent with foam cells in multiple sclerosis. *Brain*, 129, 517-26.

Branney, P. A., Faas, L., Steane, S. E., Pownall, M. E. & Isaacs, H. V. 2009. Characterisation of the Fibroblast Growth Factor Dependent Transcriptome in Early Development. *Plos One*, 4.

Brondello, J. M., Pouyssegur, J. & McKenzie, F. R. 1999. Reduced MAP kinase phosphatase-1 degradation after p42/p44(MAPK)-dependent phosphorylation. *Science*, 286, 2514-2517.

Brück, W., Porada, P., Poser, S., Rieckmann, P., Hanefeld, F., Kretschmar, H. A. & Lassmann, H. 1995. Monocyte/macrophage differentiation in early multiple sclerosis lesions. *Ann Neurol*, 38, 788-96.

Bsibsi, M., Peferoen, L. A., Holtman, I. R., Nacken, P. J., Gerritsen, W. H., Witte, M. E., Van Horssen, J., Eggen, B. J., Van Der Valk, P., Amor, S. & Van Noort, J. M. 2014. Demyelination during multiple sclerosis is associated with combined activation of microglia/macrophages by IFN- γ and alpha B-crystallin. *Acta Neuropathol*, 128, 215-29.

Butt, A. M. & Dinsdale, J. 2005. Fibroblast growth factor 2 induces loss of adult oligodendrocytes and myelin in vivo. *Exp Neurol*, 192, 125-33.

- Böttcher, R. T., Pollet, N., Delius, H. & Niehrs, C. 2004. The transmembrane protein XFLRT3 forms a complex with FGF receptors and promotes FGF signalling. *Nat Cell Biol*, 6, 38-44.
- Calabrese, M., Poretto, V., Favaretto, A., Alessio, S., Bernardi, V., Romualdi, C., Rinaldi, F., Perini, P. & Gallo, P. 2012. Cortical lesion load associates with progression of disability in multiple sclerosis. *Brain*, 135, 2952-61.
- Cammer, W. & Zhang, H. 1999. Maturation of oligodendrocytes is more sensitive to TNF alpha than is survival of precursors and immature oligodendrocytes. *J Neuroimmunol*, 97, 37-42.
- Carballada, R., Yasuo, H. & Lemaire, P. 2001. Phosphatidylinositol-3 kinase acts in parallel to the ERK MAP kinase in the FGF pathway during *Xenopus* mesoderm induction. *Development*, 128, 35-44.
- Casci, T., Vinos, J. & Freeman, M. 1999. Sprouty, an intracellular inhibitor of Ras signaling. *Cell*, 96, 655-665.
- Casper, D. & Blum, M. 1995. Epidermal growth factor and basic fibroblast growth factor protect dopaminergic neurons from glutamate toxicity in culture. *J Neurochem*, 65, 1016-26.
- Cassina, P., Pehar, M., Vargas, M. R., Castellanos, R., Barbeito, A. G., Estévez, A. G., Thompson, J. A., Beckman, J. S. & Barbeito, L. 2005. Astrocyte activation by fibroblast growth factor-1 and motor neuron apoptosis: implications for amyotrophic lateral sclerosis. *J Neurochem*, 93, 38-46.
- Caster, O. & Edwards, I. R. 2015. Quantitative benefit-risk assessment of methylprednisolone in multiple sclerosis relapses. *BMC Neurol*, 15, 206.
- Ceccarelli, A., Rocca, M. A., Falini, A., Tortorella, P., Pagani, E., Rodegher, M., Comi, G., Scotti, G. & Filippi, M. 2007. Normal-appearing white and grey matter damage in MS. A volumetric and diffusion tensor MRI study at 3.0 Tesla. *J Neurol*, 254, 513-8.
- Chambers, D. & Mason, I. 2000. Expression of sprouty2 during early development of the chick embryo is coincident with known sites of FGF signalling. *Mechanisms of Development*, 91, 361-364.
- Chandran, S., Hunt, D., Joannides, A., Zhao, C., Compston, A. & Franklin, R. J. 2008. Myelin repair: the role of stem and precursor cells in multiple sclerosis. *Philos Trans R Soc Lond B Biol Sci*, 363, 171-83.
- Chang, A., Tourtellotte, W. W., Rudick, R. & Trapp, B. D. 2002. Premyelinating oligodendrocytes in chronic lesions of multiple sclerosis. *N Engl J Med*, 346, 165-73.
- Chang, Z., Meyer, K., Rapraeger, A. C. & Friedl, A. 2000. Differential ability of heparan sulfate proteoglycans to assemble the fibroblast growth factor receptor complex in situ. *FASEB J*, 14, 137-44.
- Chaudhuri, A. & Behan, P. O. 2005. Multiple sclerosis: looking beyond autoimmunity. *J R Soc Med*, 98, 303-6.

Chen, P.-Y., Qin, L., Zhuang, Z. W., Tellides, G., Lax, I., Schlessinger, J. & Simons, M. 2014a. The docking protein FRS2 α is a critical regulator of VEGF receptors signaling. *Proceedings of the National Academy of Sciences*, 111, 5514-5519.

Chen, T.-M., Shih, Y.-H., Tseng, J. T., Lai, M.-C., Wu, C.-H., Li, Y.-H., Tsai, S.-J. & Sun, H. S. 2014b. Overexpression of FGF9 in colon cancer cells is mediated by hypoxia-induced translational activation. *Nucleic Acids Research*, 42, 2932-2944.

Choi, S. R., Howell, O. W., Carassiti, D., Magliozzi, R., Gveric, D., Muraro, P. A., Nicholas, R., Roncaroli, F. & Reynolds, R. 2012. Meningeal inflammation plays a role in the pathology of primary progressive multiple sclerosis. *Brain*, 135, 2925-37.

Choubey, L., Collette, J. C. & Smith, K. M. 2017. Quantitative assessment of fibroblast growth factor receptor 1 expression in neurons and glia. *PeerJ*, 5, e3173.

Chuang, P. C., Sun, H. S., Chen, T. M. & Tsai, S. J. 2006. Prostaglandin E2 induces fibroblast growth factor 9 via EP3-dependent protein kinase Cdelta and Elk-1 signaling. *Mol Cell Biol*, 26, 8281-92.

Clemente, D., Ortega, M. C., Arenzana, F. J. & De Castro, F. 2011. FGF-2 and Anosmin-1 are selectively expressed in different types of multiple sclerosis lesions. *J Neurosci*, 31, 14899-909.

Cohen, R. I. & Chandross, K. J. 2000. Fibroblast growth factor-9 modulates the expression of myelin related proteins and multiple fibroblast growth factor receptors in developing oligodendrocytes. *Journal of Neuroscience Research*, 61, 273-287.

Colvin, J. S., White, A. C., Pratt, S. J. & Ornitz, D. M. 2001. Lung hypoplasia and neonatal death in Fgf9-null mice identify this gene as an essential regulator of lung mesenchyme. *Development*, 128, 2095-2106.

Compston, A. 1988. The 150th anniversary of the first depiction of the lesions of multiple sclerosis. *J Neurol Neurosurg Psychiatry*, 51, 1249-52.

Correale, J. & Farez, M. F. 2015. The Role of Astrocytes in Multiple Sclerosis Progression. *Front Neurol*, 6, 180.

Couderc, B., Prats, H., Bayard, F. & Amalric, F. 1991. Potential oncogenic effects of basic fibroblast growth factor requires cooperation between CUG and AUG-initiated forms. *Cell Regul*, 2, 709-18.

Coughlin, S. R., Barr, P. J., Cousens, L. S., Fretto, L. J. & Williams, L. T. 1988. Acidic and basic fibroblast growth factors stimulate tyrosine kinase activity in vivo. *J Biol Chem*, 263, 988-93.

Cox, F. F., Berezin, V., Bock, E. & Lynch, M. A. 2013. The neural cell adhesion molecule-derived peptide, FGL, attenuates lipopolysaccharide-induced changes in glia in a CD200-dependent manner. *Neuroscience*, 235, 141-8.

- Cummings, B. J., Yee, G. J. & Cotman, C. W. 1992. bFGF promotes the survival of entorhinal layer II neurons after perforant path axotomy. *Brain Res*, 591, 271-6.
- Dehghan, S., Javan, M., Pourabdolhossein, F., Mirnajafi-Zadeh, J. & Baharvand, H. 2012. Basic fibroblast growth factor potentiates myelin repair following induction of experimental demyelination in adult mouse optic chiasm and nerves. *J Mol Neurosci*, 48, 77-85.
- Deloulme, J. C., Gensburger, C., Sarhan, S., Seiler, N. & Sensenbrenner, M. 1991. Effects of basic fibroblast growth factor on the development of GABAergic neurons in culture. *Neuroscience*, 42, 561-8.
- Deng, Y. Y., Lu, J., Ling, E. A. & Kaur, C. 2010. Microglia-derived macrophage colony stimulating factor promotes generation of proinflammatory cytokines by astrocytes in the periventricular white matter in the hypoxic neonatal brain. *Brain Pathol*, 20, 909-25.
- Donnelly, D. J. & Popovich, P. G. 2008. Inflammation and its role in neuroprotection, axonal regeneration and functional recovery after spinal cord injury. *Exp Neurol*, 209, 378-88.
- Dono, R., Texido, G., Dussel, R., Ehmke, H. & Zeller, R. 1998. Impaired cerebral cortex development and blood pressure regulation in FGF-2-deficient mice. *EMBO J*, 17, 4213-25.
- Dudka, A. A., Sweet, S. M. & Heath, J. K. 2010. Signal transducers and activators of transcription-3 binding to the fibroblast growth factor receptor is activated by receptor amplification. *Cancer Res*, 70, 3391-401.
- Durán, I., Martínez-Cáceres, E. M., Brieva, L., Tintoré, M. & Montalban, X. 2001. Similar pro- and anti-inflammatory cytokine production in the different clinical forms of multiple sclerosis. *Mult Scler*, 7, 151-6.
- Durán, R. V. & Hall, M. N. 2012. Regulation of TOR by small GTPases. *EMBO Rep*, 13, 121-8.
- Dutta, R., McDonough, J., Yin, X., Peterson, J., Chang, A., Torres, T., Gudz, T., Macklin, W. B., Lewis, D. A., Fox, R. J., Rudick, R., Mirnics, K. & Trapp, B. D. 2006. Mitochondrial dysfunction as a cause of axonal degeneration in multiple sclerosis patients. *Ann Neurol*, 59, 478-89.
- Désiré, L., Courtois, Y. & Jeanny, J. C. 1998. Suppression of fibroblast growth factors 1 and 2 by antisense oligonucleotides in embryonic chick retinal cells in vitro inhibits neuronal differentiation and survival. *Exp Cell Res*, 241, 210-21.
- Ebers, D. G. C. 1998. Randomised double-blind placebo-controlled study of interferon beta-1a in relapsing/remitting multiple sclerosis. PRISMS (Prevention of Relapses and Disability by Interferon beta-1a Subcutaneously in Multiple Sclerosis) Study Group. *Lancet*, 352, 1498-504.
- Eckenstein, F. P. 1994. FIBROBLAST GROWTH-FACTORS IN THE NERVOUS-SYSTEM. *Journal of Neurobiology*, 25, 1467-1480.

- Eclancher, F., Kehrl, P., Labourdette, G. & Sensenbrenner, M. 1996. Basic fibroblast growth factor (bFGF) injection activates the glial reaction in the injured adult rat brain. *Brain Res*, 737, 201-14.
- Eisen, A. A. & Norris, J. W. 1969. Adrenal steroid therapy in neurological disease. Part I. *Can Med Assoc J*, 100, 27-30.
- Elde, R., Cao, Y. H., Cintra, A., Brelje, T. C., Pelto-Huikko, M., Junntila, T., Fuxe, K., Pettersson, R. F. & Hökfelt, T. 1991. Prominent expression of acidic fibroblast growth factor in motor and sensory neurons. *Neuron*, 7, 349-64.
- Elian, M., Nightingale, S. & Dean, G. 1990. Multiple sclerosis among United Kingdom-born children of immigrants from the Indian subcontinent, Africa and the West Indies. *J Neurol Neurosurg Psychiatry*, 53, 906-11.
- Eming, S. A., Krieg, T. & Davidson, J. M. 2007. Inflammation in wound repair: molecular and cellular mechanisms. *J Invest Dermatol*, 127, 514-25.
- Fang, X., Stachowiak, E. K., Dunham-Ems, S. M., Klejbor, I. & Stachowiak, M. K. 2005. Control of CREB-binding protein signaling by nuclear fibroblast growth factor receptor-1: a novel mechanism of gene regulation. *J Biol Chem*, 280, 28451-62.
- Fisher, E., Chang, A., Fox, R. J., Tkach, J. A., Svarovsky, T., Nakamura, K., Rudick, R. A. & Trapp, B. D. 2007. Imaging correlates of axonal swelling in chronic multiple sclerosis brains. *Ann Neurol*, 62, 219-28.
- Fisniku, L. K., Brex, P. A., Altmann, D. R., Miszkiel, K. A., Benton, C. E., Lanyon, R., Thompson, A. J. & Miller, D. H. 2008. Disability and T2 MRI lesions: a 20-year follow-up of patients with relapse onset of multiple sclerosis. *Brain*, 131, 808-17.
- Fon Tacer, K., Bookout, A. L., Ding, X., Kurosu, H., John, G. B., Wang, L., Goetz, R., Mohammadi, M., Kuro-O, M., Mangelsdorf, D. J. & Kliewer, S. A. 2010. Research resource: Comprehensive expression atlas of the fibroblast growth factor system in adult mouse. *Mol Endocrinol*, 24, 2050-64.
- Ford-Perriss, M., Abud, H. & Murphy, M. 2001. Fibroblast growth factors in the developing central nervous system. *Clin Exp Pharmacol Physiol*, 28, 493-503.
- Fortin, D., Rom, E., Sun, H., Yayon, A. & Bansal, R. 2005. Distinct fibroblast growth factor (FGF)/FGF receptor signaling pairs initiate diverse cellular responses in the oligodendrocyte lineage. *J Neurosci*, 25, 7470-9.
- Fox, E. J. 2006. Management of worsening multiple sclerosis with mitoxantrone: a review. *Clin Ther*, 28, 461-74.
- Frank, M. J., Dawson, D. W., Bensinger, S. J., Hong, J. S., Knosp, W. M., Xu, L., Balatoni, C. E., Allen, E. L., Shen, R. R., Bar-Sagi, D., Martin, G. R. & Teitell, M. A. 2009. Expression of sprouty2 inhibits B-cell proliferation and is epigenetically silenced in mouse and human B-cell lymphomas. *Blood*, 113, 2478-2487.
- Franklin, R. J. 2002. Why does remyelination fail in multiple sclerosis? *Nat Rev Neurosci*, 3, 705-14.

- Fransson, L. A., Belting, M., Cheng, F., Jonsson, M., Mani, K. & Sandgren, S. 2004. Novel aspects of glypican glycobiochemistry. *Cellular and Molecular Life Sciences*, 61, 1016-1024.
- Frautschy, S. A., Walicke, P. A. & Baird, A. 1991. Localization of basic fibroblast growth factor and its mRNA after CNS injury. *Brain Res*, 553, 291-9.
- Fressinaud, C., Vallat, J. M. & Labourdette, G. 1995. Basic fibroblast growth factor down-regulates myelin basic protein gene expression and alters myelin compaction of mature oligodendrocytes in vitro. *J Neurosci Res*, 40, 285-93.
- Frischer, J. M., Bramow, S., Dal-Bianco, A., Lucchinetti, C. F., Rauschka, H., Schmidbauer, M., Laursen, H., Sorensen, P. S. & Lassmann, H. 2009. The relation between inflammation and neurodegeneration in multiple sclerosis brains. *Brain*, 132, 1175-89.
- Fu, Z. & Tindall, D. J. 2008. FOXOs, cancer and regulation of apoptosis. *Oncogene*, 27, 2312-2319.
- Fuhrmann, V., Kinkl, N., Leveillard, T., Sahel, J. & Hicks, D. 1999. Fibroblast growth factor receptor 4 (FGFR4) is expressed in adult rat and human retinal photoreceptors and neurons. *J Mol Neurosci*, 13, 187-97.
- Fujita, E., Jinbo, A., Matuzaki, H., Konishi, H., Kikkawa, U. & Momoi, T. 1999. Akt phosphorylation site found in human caspase-9 is absent in mouse caspase-9. *Biochemical and Biophysical Research Communications*, 264, 550-555.
- Fukui, S., Nawashiro, H., Otani, N., Ooigawa, H., Nomura, N., Yano, A., Miyazawa, T., Ohnuki, A., Tsuzuki, N., Katoh, H., Ishihara, S. & Shima, K. 2003. Nuclear accumulation of basic fibroblast growth factor in human astrocytic tumors. *Cancer*, 97, 3061-7.
- Furusho, M., Dupree, J. L., Nave, K. A. & Bansal, R. 2012. Fibroblast growth factor receptor signaling in oligodendrocytes regulates myelin sheath thickness. *J Neurosci*, 32, 6631-41.
- Furusho, M., Roulois, A. J., Franklin, R. J. & Bansal, R. 2015. Fibroblast growth factor signaling in oligodendrocyte-lineage cells facilitates recovery of chronically demyelinated lesions but is redundant in acute lesions. *Glia*, 63, 1714-28.
- Gage, F. H., Coates, P. W., Palmer, T. D., Kuhn, H. G., Fisher, L. J., Suhonen, J. O., Peterson, D. A., Suhr, S. T. & Ray, J. 1995. Survival and differentiation of adult neuronal progenitor cells transplanted to the adult brain. *Proc Natl Acad Sci U S A*, 92, 11879-83.
- Gallagher, J. T. 2001. Heparan sulfate: growth control with a restricted sequence menu. *Journal of Clinical Investigation*, 108, 357-361.
- Ganat, Y., Soni, S., Chacon, M., Schwartz, M. L. & Vaccarino, F. M. 2002. Chronic hypoxia up-regulates fibroblast growth factor ligands in the perinatal brain and induces fibroblast growth factor-responsive radial glial cells in the sub-ependymal zone. *Neuroscience*, 112, 977-91.

- Gandoglia, I., Ivaldi, F., Laroni, A., Benvenuto, F., Solaro, C., Mancardi, G., Kerlero De Rosbo, N. & Uccelli, A. 2017. Teriflunomide treatment reduces B cells in patients with MS. *Neurol Neuroimmunol Neuroinflamm*, 4, e403.
- Garcès, A., Nishimune, H., Philippe, J. M., Pettmann, B. & Delapeyrière, O. 2000. FGF9: a motoneuron survival factor expressed by medial thoracic and sacral motoneurons. *J Neurosci Res*, 60, 1-9.
- Ghazavi, H., Hoseini, S. J., Ebrahimzadeh-Bideskan, A., Mashkani, B., Mehri, S., Ghorbani, A., Sadri, K., Mahdipour, E., Ghasemi, F., Forouzanfar, F., Hoseini, A., Pasdar, A. R., Sadeghnia, H. R. & Ghayour-Mobarhan, M. 2017. Fibroblast Growth Factor Type 1 (FGF1)-Overexpressed Adipose-Derived Mesenchymal Stem Cells (AD-MSC(FGF1)) Induce Neuroprotection and Functional Recovery in a Rat Stroke Model. *Stem Cell Rev*.
- Goddard, D. R., Berry, M., Kirvell, S. L. & Butt, A. M. 2002. Fibroblast growth factor-2 induces astroglial and microglial reactivity in vivo. *J Anat*, 200, 57-67.
- Goetz, R. & Mohammadi, M. 2013. Exploring mechanisms of FGF signalling through the lens of structural biology. *Nat Rev Mol Cell Biol*, 14, 166-80.
- Goldshmit, Y., Frisca, F., Pinto, A. R., Pébay, A., Tang, J. K., Siegel, A. L., Kaslin, J. & Currie, P. D. 2014. Fgf2 improves functional recovery-decreasing gliosis and increasing radial glia and neural progenitor cells after spinal cord injury. *Brain Behav*, 4, 187-200.
- Gritti, A., Parati, E. A., Cova, L., Frolichsthal, P., Galli, R., Wanke, E., Faravelli, L., Morassutti, D. J., Roisen, F., Nickel, D. D. & Vescovi, A. L. 1996. Multipotential stem cells from the adult mouse brain proliferate and self-renew in response to basic fibroblast growth factor. *J Neurosci*, 16, 1091-100.
- Gross, I., Bassit, B., Benezra, M. & Licht, J. D. 2001. Mammalian sprouty proteins inhibit cell growth and differentiation by preventing ras activation. *J Biol Chem*, 276, 46460-8.
- Groth, C. & Lardelli, M. 2002. The structure and function of vertebrate Fibroblast Growth Factor Receptor 1. *International Journal of Developmental Biology*, 46, 393-400.
- Gómez-Pinilla, F., Miller, S., Choi, J. & Cotman, C. W. 1997. Heparan sulfate potentiates the autocrine action of basic fibroblast growth factor in astrocytes: an in vivo and in vitro study. *Neuroscience*, 76, 137-45.
- Gómez-Pinilla, F., Vu, L. & Cotman, C. W. 1995. Regulation of astrocyte proliferation by FGF-2 and heparan sulfate in vivo. *J Neurosci*, 15, 2021-9.
- Habuchi, H., Habuchi, O. & Kimata, K. 1998. Biosynthesis of heparan sulfate and heparin how are the multifunctional glycosaminoglycans built up? *Trends in Glycoscience and Glycotechnology*, 10, 65-80.
- Hacohen, N., Kramer, S., Sutherland, D., Hiromi, Y. & Krasnow, M. A. 1998. sprouty encodes a novel antagonist of FGF signaling that patterns apical branching of the Drosophila airways. *Cell*, 92, 253-263.

Hafler, D. A., Compston, A., Sawcer, S., Lander, E. S., Daly, M. J., De Jager, P. L., De Bakker, P. I., Gabriel, S. B., Mirel, D. B., Ivinson, A. J., Pericak-Vance, M. A., Gregory, S. G., Rioux, J. D., Mccauley, J. L., Haines, J. L., Barcellos, L. F., Cree, B., Oksenberg, J. R., Hauser, S. L. & Consortium, I. M. S. G. 2007. Risk alleles for multiple sclerosis identified by a genomewide study. *N Engl J Med*, 357, 851-62.

Hall, H., Williams, E. J., Moore, S. E., Walsh, F. S., Prochiantz, A. & Doherty, P. 1996. Inhibition of FGF-stimulated phosphatidylinositol hydrolysis and neurite outgrowth by a cell-membrane permeable phosphopeptide. *Current Biology*, 6, 580-587.

Hammond, S. R., English, D. R. & Mcleod, J. G. 2000. The age-range of risk of developing multiple sclerosis: evidence from a migrant population in Australia. *Brain*, 123 (Pt 5), 968-74.

Han, M. H., Hwang, S. I., Roy, D. B., Lundgren, D. H., Price, J. V., Ousman, S. S., Fernald, G. H., Gerlitz, B., Robinson, W. H., Baranzini, S. E., Grinnell, B. W., Raine, C. S., Sobel, R. A., Han, D. K. & Steinman, L. 2008. Proteomic analysis of active multiple sclerosis lesions reveals therapeutic targets. *Nature*, 451, 1076-81.

Hanafusa, H., Torii, S., Yasunaga, T. & Nishida, E. 2002. Sprouty1 and Sprouty2 provide a control mechanism for the Ras/MAPK signalling pathway. *Nature Cell Biology*, 4, 850-858.

Harirchian, M. H., Tekieh, A. H., Modabbernia, A., Aghamollaii, V., Tafakhori, A., Ghaffarpour, M., Sahraian, M. A., Naji, M., Yazdankhah, M. & Yazdanbakhsh, M. 2012. Serum and CSF PDGF-AA and FGF-2 in relapsing-remitting multiple sclerosis: a case-control study. *Eur J Neurol*, 19, 241-7.

Hart, K. C., Robertson, S. C., Kanemitsu, M. Y., Meyer, A. N., Tynan, J. A. & Donoghue, D. J. 2000. Transformation and Stat activation by derivatives of FGFR1, FGFR3, and FGFR4. *Oncogene*, 19, 3309-20.

Hartwig, J. H., Thelen, M., Rosen, A., Janmey, P. A., Nairn, A. C. & Aderem, A. 1992. MARCKS IS AN ACTIN FILAMENT CROSS-LINKING PROTEIN REGULATED BY PROTEIN-KINASE-C AND CALCIUM CALMODULIN. *Nature*, 356, 618-622.

Hauser, S. L., Bar-or, A., Comi, G., Giovannoni, G., Hartung, H. P., Hemmer, B., Lublin, F., Montalban, X., Rammohan, K. W., Selmaj, K., Traboulsee, A., Wolinsky, J. S., Arnold, D. L., Klingelschmitt, G., Masterman, D., Fontoura, P., Belachew, S., Chin, P., Mairon, N., Garren, H., Kappos, L. & Investigators, O. I. A. O. I. C. 2017. Ocrelizumab versus Interferon Beta-1a in Relapsing Multiple Sclerosis. *N Engl J Med*, 376, 221-234.

Havrdova, E., Horakova, D. & Kovarova, I. 2015. Alemtuzumab in the treatment of multiple sclerosis: key clinical trial results and considerations for use. *Ther Adv Neurol Disord*, 8, 31-45.

Hebenstreit, D., Horejs-Hoeck, J. & Duschl, A. 2005. JAK/STAT-dependent gene regulation by cytokines. *Drug News Perspect*, 18, 243-9.

Higginson, J. R., Thompson, S. M., Santos-Silva, A., Guimond, S. E., Turnbull, J. E. & Barnett, S. C. 2012. Differential Sulfation Remodelling of Heparan Sulfate by Extracellular 6-O-Sulfatases Regulates Fibroblast Growth Factor-Induced Boundary Formation by Glial Cells: Implications for Glial Cell Transplantation. *Journal of Neuroscience*, 32, 15902-15912.

Hogan, P. G., Chen, L., Nardone, J. & Rao, A. 2003. Transcriptional regulation by calcium, calcineurin, and NFAT. *Genes Dev*, 17, 2205-32.

Holmøy, T. 2006. A Norse contribution to the history of neurological diseases. *Eur Neurol*, 55, 57-8.

House, S. L., Branch, K., Newman, G., Doetschman, T. & Schultz, J. L. J. 2005. Cardioprotection induced by cardiac-specific overexpression of fibroblast growth factor-2 is mediated by the MAPK cascade. *Am J Physiol Heart Circ Physiol*, 289, H2167-75.

Hu, Y., Fang, X., Dunham, S. M., Prada, C., Stachowiak, E. K. & Stachowiak, M. K. 2004. 90-kDa ribosomal S6 kinase is a direct target for the nuclear fibroblast growth factor receptor 1 (FGFR1): role in FGFR1 signaling. *J Biol Chem*, 279, 29325-35.

Huang, J. Y. & Chuang, J. I. 2010. Fibroblast growth factor 9 upregulates heme oxygenase-1 and gamma-glutamylcysteine synthetase expression to protect neurons from 1-methyl-4-phenylpyridinium toxicity. *Free Radic Biol Med*, 49, 1099-108.

Huang, J. Y., Hong, Y. T. & Chuang, J. I. 2009. Fibroblast growth factor 9 prevents MPP⁺-induced death of dopaminergic neurons and is involved in melatonin neuroprotection in vivo and in vitro. *J Neurochem*, 109, 1400-12.

Huang, S. S. & Huang, J. S. 1986. Association of bovine brain-derived growth factor receptor with protein tyrosine kinase activity. *J Biol Chem*, 261, 9568-71.

Hughes, E. G., Kang, S. H., Fukaya, M. & Bergles, D. E. 2013. Oligodendrocyte progenitors balance growth with self-repulsion to achieve homeostasis in the adult brain. *Nat Neurosci*, 16, 668-76.

Hutchinson, M. 2007. Natalizumab: A new treatment for relapsing remitting multiple sclerosis. *Ther Clin Risk Manag*, 3, 259-68.

Iberg, N., Rogelj, S., Fanning, P. & Klagsbrun, M. 1989. Purification of 18- and 22-kDa forms of basic fibroblast growth factor from rat cells transformed by the ras oncogene. *J Biol Chem*, 264, 19951-5.

Ishiyama, J., Saito, H. & Abe, K. 1991. Epidermal growth factor and basic fibroblast growth factor promote the generation of long-term potentiation in the dentate gyrus of anaesthetized rats. *Neurosci Res*, 12, 403-11.

Issa, R., Alqteishat, A., Mitsios, N., Saka, M., Krupinski, J., Tarkowski, E., Gaffney, J., Slevin, M., Kumar, S. & Kumar, P. 2005. Expression of basic fibroblast growth factor mRNA and protein in the human brain following ischaemic stroke. *Angiogenesis*, 8, 53-62.

- Itoh, N. 2007. The Fgf families in humans, mice, and zebrafish: their evolutionary processes and roles in development, metabolism, and disease. *Biol Pharm Bull*, 30, 1819-25.
- Itoh, N., Ohta, H. & Konishi, M. 2015. Endocrine FGFs: Evolution, Physiology, Pathophysiology, and Pharmacotherapy. *Front Endocrinol (Lausanne)*, 6, 154.
- Itoh, N. & Ornitz, D. M. 2011. Fibroblast growth factors: from molecular evolution to roles in development, metabolism and disease. *Journal of Biochemistry*, 149, 121-130.
- Jetten, N., Verbruggen, S., Gijbels, M. J., Post, M. J., De Winther, M. P. & Donners, M. M. 2014. Anti-inflammatory M2, but not pro-inflammatory M1 macrophages promote angiogenesis in vivo. *Angiogenesis*, 17, 109-18.
- Jimenez Hamann, M. C., Tator, C. H. & Shoichet, M. S. 2005. Injectable intrathecal delivery system for localized administration of EGF and FGF-2 to the injured rat spinal cord. *Exp Neurol*, 194, 106-19.
- Jin, K., Lafevre-Bernt, M., Sun, Y., Chen, S., Gafni, J., Crippen, D., Logvinova, A., Ross, C. A., Greenberg, D. A. & Ellerby, L. M. 2005. FGF-2 promotes neurogenesis and neuroprotection and prolongs survival in a transgenic mouse model of Huntington's disease. *Proc Natl Acad Sci U S A*, 102, 18189-94.
- Johnson, D. E. & Williams, L. T. 1993. STRUCTURAL AND FUNCTIONAL DIVERSITY IN THE FGF RECEPTOR MULTIGENE FAMILY. *Advances in Cancer Research*, 60, 1-41.
- Joy, A., Moffett, J., Neary, K., Mordechai, E., Stachowiak, E. K., Coons, S., Rankin-Shapiro, J., Florkiewicz, R. Z. & Stachowiak, M. K. 1997. Nuclear accumulation of FGF-2 is associated with proliferation of human astrocytes and glioma cells. *Oncogene*, 14, 171-83.
- Kalil, K., Szebenyi, G. & Dent, E. W. 2000. Common mechanisms underlying growth cone guidance and axon branching. *J Neurobiol*, 44, 145-58.
- Kanda, T., Iwasaki, T., Nakamura, S., Kurokawa, T., Ikeda, K. & Mizusawa, H. 2000. Self-secretion of fibroblast growth factor-9 supports basal forebrain cholinergic neurons in an autocrine/paracrine manner. *Brain Res*, 876, 22-30.
- Kanda, T., Iwasaki, T., Nakamura, S., Ueki, A., Kurokawa, T., Ikeda, K. & Mizusawa, H. 1999. FGF-9 is an autocrine/paracrine neurotrophic substance for spinal motoneurons. *International Journal of Developmental Neuroscience*, 17, 191-200.
- Kang, W., Balordi, F., Su, N., Chen, L., Fishell, G. & Hébert, J. M. 2014. Astrocyte activation is suppressed in both normal and injured brain by FGF signaling. *Proc Natl Acad Sci U S A*, 111, E2987-95.
- Katoh, M. & Katoh, M. 2006. FGF signaling network in the gastrointestinal tract (Review). *International Journal of Oncology*, 29, 163-168.
- Kebir, H., Kreymborg, K., Ifergan, I., Dodelet-Devillers, A., Cayrol, R., Bernard, M., Giuliani, F., Arbour, N., Becher, B. & Prat, A. 2007. Human TH17 lymphocytes

- promote blood-brain barrier disruption and central nervous system inflammation. *Nat Med*, 13, 1173-5.
- Keegan, K., Johnson, D. E., Williams, L. T. & Hayman, M. J. 1991. Isolation of an additional member of the fibroblast growth factor receptor family, FGFR-3. *Proc Natl Acad Sci U S A*, 88, 1095-9.
- Khatri, B. O. 2016. Fingolimod in the treatment of relapsing-remitting multiple sclerosis: long-term experience and an update on the clinical evidence. *Ther Adv Neurol Disord*, 9, 130-47.
- Kieseier, B. C. 2011. The mechanism of action of interferon- β in relapsing multiple sclerosis. *CNS Drugs*, 25, 491-502.
- Kimura, H., Tooyama, I. & Mcgeer, P. L. 1994. Acidic FGF expression in the surroundings of senile plaques. *Tohoku J Exp Med*, 174, 279-93.
- Kiyota, T., Ingraham, K. L., Jacobsen, M. T., Xiong, H. & Ikezu, T. 2011. FGF2 gene transfer restores hippocampal functions in mouse models of Alzheimer's disease and has therapeutic implications for neurocognitive disorders. *Proc Natl Acad Sci U S A*, 108, E1339-48.
- Kouhara, H., Hadari, Y. R., Spivakkroizman, T., Schilling, J., Barsagi, D., Lax, I. & Schlessinger, J. 1997. A lipid-anchored Grb2-binding protein that links FGF-receptor activation to the Ras/MAPK signaling pathway. *Cell*, 89, 693-702.
- Kramer, S., Okabe, M., Hacohen, N., Krasnow, M. A. & Hiromi, Y. 1999. Sprouty: a common antagonist of FGF and EGF signaling pathways in Drosophila. *Development*, 126, 2515-25.
- Kucharska, A., Rushworth, L. K., Staples, C., Morrice, N. A. & Keyse, S. M. 2009. Regulation of the inducible nuclear dual-specificity phosphatase DUSP5 by ERK MAPK. *Cell Signal*, 21, 1794-805.
- Kutzelnigg, A., Lucchinetti, C. F., Stadelmann, C., Bruck, W., Rauschka, H., Bergmann, M., Schmidbauer, M., Parisi, J. E. & Lassmann, H. 2005. Cortical demyelination and diffuse white matter injury in multiple sclerosis. *Brain*, 128, 2705-2712.
- Kuzet, S. E. & Gaggioli, C. 2016. Fibroblast activation in cancer: when seed fertilizes soil. *Cell Tissue Res*, 365, 607-19.
- La Spada, A. R. 2005. Huntington's disease and neurogenesis: FGF-2 to the rescue? *Proc Natl Acad Sci U S A*, 102, 17889-90.
- Lamothe, B., Yamada, M., Schaeper, U., Birchmeier, W., Lax, I. & Schlessinger, J. 2004. The docking protein Gab1 is an essential component of an indirect mechanism for fibroblast growth factor stimulation of the phosphatidylinositol 3-kinase/Akt antiapoptotic pathway. *Molecular and Cellular Biology*, 24, 5657-5666.
- Lan, M., Tang, X., Zhang, J. & Yao, Z. 2017. Insights in pathogenesis of multiple sclerosis: nitric oxide may induce mitochondrial dysfunction of oligodendrocytes. *Rev Neurosci*.

Lang, H. L., Jacobsen, H., Ikemizu, S., Andersson, C., Harlos, K., Madsen, L., Hjorth, P., Sondergaard, L., Svejgaard, A., Wucherpfennig, K., Stuart, D. I., Bell, J. I., Jones, E. Y. & Fugger, L. 2002a. A functional and structural basis for TCR cross-reactivity in multiple sclerosis. *Nat Immunol*, 3, 940-3.

Lang, K. J., Kappel, A. & Goodall, G. J. 2002b. Hypoxia-inducible factor-1alpha mRNA contains an internal ribosome entry site that allows efficient translation during normoxia and hypoxia. *Mol Biol Cell*, 13, 1792-801.

Lassmann, H. 2003. Hypoxia-like tissue injury as a component of multiple sclerosis lesions. *J Neurol Sci*, 206, 187-91.

Lassmann, H., Brück, W., Lucchinetti, C. & Rodriguez, M. 1997. Remyelination in multiple sclerosis. *Mult Scler*, 3, 133-6.

Lassmann, H., Van Horssen, J. & Mahad, D. 2012. Progressive multiple sclerosis: pathology and pathogenesis. *Nat Rev Neurol*, 8, 647-56.

Lax, I., Wong, A., Lamothe, B., Lee, A., Frost, A., Hawes, J. & Schlessinger, J. 2002. The docking protein FRS2 alpha controls a MAP kinase-mediated negative feedback mechanism for signaling by FGF receptors. *Molecular Cell*, 10, 709-719.

Lee, P. L., Johnson, D. E., Cousens, L. S., Fried, V. A. & Williams, L. T. 1989. Purification and complementary DNA cloning of a receptor for basic fibroblast growth factor. *Science*, 245, 57-60.

Lee, S. H., Schloss, D. J., Jarvis, L., Krasnow, M. A. & Swain, J. L. 2001. Inhibition of angiogenesis by a mouse sprouty protein. *J Biol Chem*, 276, 4128-33.

Lemmon, S. K. & Bradshaw, R. A. 1983. Purification and partial characterization of bovine pituitary fibroblast growth factor. *J Cell Biochem*, 21, 195-208.

Levin, L. I., Munger, K. L., Rubertone, M. V., Peck, C. A., Lennette, E. T., Spiegelman, D. & Ascherio, A. 2003. Multiple sclerosis and Epstein-Barr virus. *JAMA*, 289, 1533-6.

Levy, Y. A., Fainberg, K. M., Amidror, T., Regev, K., Auriel, E. & Karni, A. 2013. High and dysregulated secretion of epidermal growth factor from immune cells of patients with relapsing-remitting multiple sclerosis. *J Neuroimmunol*, 257, 82-9.

Li, C., Scott, D. A., Hatch, E., Tian, X. & Mansour, S. L. 2007. Dusp6 (Mkp3) is a negative feedback regulator of FGF-stimulated ERK signaling during mouse development. *Development*, 134, 167-76.

Li, H., Rao, A. & Hogan, P. G. 2011. Interaction of calcineurin with substrates and targeting proteins. *Trends in Cell Biology*, 21, 91-103.

Li, Y., Xie, P., Fan, X. & Tang, H. 2009. Balò's concentric sclerosis presenting with benign clinical course and multiple sclerosis-like lesions on magnetic resonance images. *Neurol India*, 57, 66-8.

Liberto, C. M., Albrecht, P. J., Herx, L. M., Yong, V. W. & Levison, S. W. 2004. Pro-regenerative properties of cytokine-activated astrocytes. *J Neurochem*, 89, 1092-100.

- Lim, J., Yusoff, P., Wong, E. S. M., Chandramouli, S., Lao, D. H., Fong, C. W. & Guy, G. R. 2002. The cysteine-rich sprouty translocation domain targets mitogen-activated protein kinase inhibitory proteins to phosphatidylinositol 4,5-bisphosphate in plasma membranes. *Molecular and Cellular Biology*, 22, 7953-7966.
- Lin, W. F., Chen, C. J., Chang, Y. J., Chen, S. L., Chiu, I. M. & Chen, L. 2009. SH2B1beta enhances fibroblast growth factor 1 (FGF1)-induced neurite outgrowth through MEK-ERK1/2-STAT3-Egr1 pathway. *Cell Signal*, 21, 1060-72.
- Lin, X., Deng, F. Y., Lu, X. & Lei, S. F. 2015. Susceptibility Genes for Multiple Sclerosis Identified in a Gene-Based Genome-Wide Association Study. *J Clin Neurol*, 11, 311-8.
- Lindner, M., Thümmler, K., Arthur, A., Brunner, S., Elliott, C., Mcelroy, D., Mohan, H., Williams, A., Edgar, J. M., Schuh, C., Stadelmann, C., Barnett, S. C., Lassmann, H., Mücklich, S., Mudaliar, M., Schaeren-Wiemers, N., Meinl, E. & Lington, C. 2015. Fibroblast growth factor signalling in multiple sclerosis: inhibition of myelination and induction of pro-inflammatory environment by FGF9. *Brain*.
- Linker, R. A. & Haghikia, A. 2016. Dimethyl fumarate in multiple sclerosis: latest developments, evidence and place in therapy. *Ther Adv Chronic Dis*, 7, 198-207.
- Liu, X., Mashour, G. A., Webster, H. F. & Kurtz, A. 1998. Basic FGF and FGF receptor 1 are expressed in microglia during experimental autoimmune encephalomyelitis: temporally distinct expression of midkine and pleiotrophin. *Glia*, 24, 390-7.
- Livak, K. J. & Schmittgen, T. D. 2001. Analysis of relative gene expression data using real-time quantitative PCR and the 2(T)(-Delta Delta C) method. *Methods*, 25, 402-408.
- Lloyd, A. F. & Miron, V. E. 2016. Cellular and Molecular Mechanisms Underpinning Macrophage Activation during Remyelination. *Front Cell Dev Biol*, 4, 60.
- Logan, A., Frautschy, S. A., Gonzalez, A. M. & Baird, A. 1992. A time course for the focal elevation of synthesis of basic fibroblast growth factor and one of its high-affinity receptors (flg) following a localized cortical brain injury. *J Neurosci*, 12, 3828-37.
- Lucchinetti, C., Brück, W., Parisi, J., Scheithauer, B., Rodriguez, M. & Lassmann, H. 2000. Heterogeneity of multiple sclerosis lesions: implications for the pathogenesis of demyelination. *Ann Neurol*, 47, 707-17.
- Lum, M., Turbic, A., Mitrovic, B. & Turnley, A. M. 2009. Fibroblast Growth Factor-9 Inhibits Astrocyte Differentiation of Adult Mouse Neural Progenitor Cells. *Journal of Neuroscience Research*, 87, 2201-2210.
- Lycke, J. 2015. Monoclonal antibody therapies for the treatment of relapsing-remitting multiple sclerosis: differentiating mechanisms and clinical outcomes. *Ther Adv Neurol Disord*, 8, 274-93.

Lyons, A., Downer, E. J., Crotty, S., Nolan, Y. M., Mills, K. H. & Lynch, M. A. 2007. CD200 ligand receptor interaction modulates microglial activation in vivo and in vitro: a role for IL-4. *J Neurosci*, 27, 8309-13.

Lysaght, A. C., Yuan, Q., Fan, Y., Kalwani, N., Caruso, P., Cunnane, M., Lanske, B. & Stanković, K. M. 2014. FGF23 deficiency leads to mixed hearing loss and middle ear malformation in mice. *PLoS One*, 9, e107681.

Machala, M., Vondráček, J., Bláha, L., Ciganek, M. & Neca, J. V. 2001. Aryl hydrocarbon receptor-mediated activity of mutagenic polycyclic aromatic hydrocarbons determined using in vitro reporter gene assay. *Mutat Res*, 497, 49-62.

Madiai, F., Hussain, S. R., Goettl, V. M., Burry, R. W., Stephens, R. L. & Hackshaw, K. V. 2003. Upregulation of FGF-2 in reactive spinal cord astrocytes following unilateral lumbar spinal nerve ligation. *Exp Brain Res*, 148, 366-76.

Magliozzi, R., Howell, O., Vora, A., Serafini, B., Nicholas, R., Puopolo, M., Reynolds, R. & Aloisi, F. 2007. Meningeal B-cell follicles in secondary progressive multiple sclerosis associate with early onset of disease and severe cortical pathology. *Brain*, 130, 1089-104.

Maimone, D., Gregory, S., Arnason, B. G. & Reder, A. T. 1991. Cytokine levels in the cerebrospinal fluid and serum of patients with multiple sclerosis. *J Neuroimmunol*, 32, 67-74.

Manning, B. D. & Cantley, L. C. 2007. AKT/PKB signaling: navigating downstream. *Cell*, 129, 1261-74.

Marrif, H. & Juurlink, B. H. 1999. Astrocytes respond to hypoxia by increasing glycolytic capacity. *J Neurosci Res*, 57, 255-60.

Martinez, F. O. & Gordon, S. 2014. The M1 and M2 paradigm of macrophage activation: time for reassessment. *F1000Prime Rep*, 6, 13.

Martone, M. E., Hu, B. R. & Ellisman, M. H. 2000. Alterations of hippocampal postsynaptic densities following transient ischemia. *Hippocampus*, 10, 610-6.

Mashayekhi, F., Hadavi, M., Vaziri, H. R. & Najji, M. 2010. Increased acidic fibroblast growth factor concentrations in the serum and cerebrospinal fluid of patients with Alzheimer's disease. *J Clin Neurosci*, 17, 357-9.

Mattson, M. P., Kumar, K. N., Wang, H., Cheng, B. & Michaelis, E. K. 1993. Basic FGF regulates the expression of a functional 71 kDa NMDA receptor protein that mediates calcium influx and neurotoxicity in hippocampal neurons. *J Neurosci*, 13, 4575-88.

Mattsson, N., Yaong, M., Rosengren, L., Blennow, K., Månsson, J. E., Andersen, O., Zetterberg, H., Haghighi, S., Zho, I. & Pratico, D. 2009. Elevated cerebrospinal fluid levels of prostaglandin E2 and 15-(S)-hydroxyeicosatetraenoic acid in multiple sclerosis. *J Intern Med*, 265, 459-64.

Mayer, M., Bogler, O. & Noble, M. 1993. THE INHIBITION OF OLIGODENDROCYTIC DIFFERENTIATION OF O-2A PROGENITORS CAUSED

BY BASIC FIBROBLAST GROWTH-FACTOR IS OVERRIDDEN BY ASTROCYTES. *Glia*, 8, 12-19.

Małeckı, J., Wesche, J., Skjerpen, C. S., Wiedłocha, A. & Olsnes, S. 2004. Translocation of FGF-1 and FGF-2 across vesicular membranes occurs during G1-phase by a common mechanism. *Mol Biol Cell*, 15, 801-14.

Mccubrey, J. A., May, W. S., Duronio, V. & Mufson, A. 2000. Serine/threonine phosphorylation in cytokine signal transduction. *Leukemia*, 14, 9-21.

Mckinnon, R. D., Matsui, T., Dubois-dalcq, M. & Aaronson, S. A. 1990. FGF MODULATES THE PDGF-DRIVEN PATHWAY OF OLIGODENDROCYTE DEVELOPMENT. *Neuron*, 5, 603-614.

Mckinnon, R. D., Smith, C., Behar, T., Smith, T. & Dubois-Dalcq, M. 1993. Distinct effects of bFGF and PDGF on oligodendrocyte progenitor cells. *Glia*, 7, 245-54.

Menendez, M. T., Teygong, C., Wade, K., Florimond, C. & Blader, I. J. 2015. siRNA Screening Identifies the Host Hexokinase 2 (HK2) Gene as an Important Hypoxia-Inducible Transcription Factor 1 (HIF-1) Target Gene in *Toxoplasma gondii*-Infected Cells. *MBio*, 6, e00462.

Messersmith, D. J., Murtie, J. C., Le, T. Q., Frost, E. E. & Armstrong, R. C. 2000. Fibroblast growth factor 2 (FGF2) and FGF receptor expression in an experimental demyelinating disease with extensive remyelination. *Journal of Neuroscience Research*, 62, 241-256.

Mierzwa, A. J., Zhou, Y.-X., Hibbits, N., Vana, A. C. & Armstrong, R. C. 2013. FGF2 and FGFR1 signaling regulate functional recovery following cuprizone demyelination. *Neuroscience Letters*, 548, 280-285.

Miki, T., Fleming, T. P., Bottaro, D. P., Rubin, J. S., Ron, D. & Aaronson, S. A. 1991. EXPRESSION CDNA CLONING OF THE KGF RECEPTOR BY CREATION OF A TRANSFORMING AUTOCRINE LOOP. *Science*, 251, 72-75.

Millecamps, S. & Julien, J. P. 2013. Axonal transport deficits and neurodegenerative diseases. *Nat Rev Neurosci*, 14, 161-76.

Miller, D. L., Ortega, S., Bashayan, O., Basch, R. & Basilico, C. 2000. Compensation by fibroblast growth factor 1 (FGF1) does not account for the mild phenotypic defects observed in FGF2 null mice. *Mol Cell Biol*, 20, 2260-8.

Milligan, N. M., Newcombe, R. & Compston, D. A. 1987. A double-blind controlled trial of high dose methylprednisolone in patients with multiple sclerosis: 1. Clinical effects. *J Neurol Neurosurg Psychiatry*, 50, 511-6.

Minowada, G., Jarvis, L. A., Chi, C. L., Neubuser, A., Sun, X., Hacohen, N., Krasnow, M. A. & Martin, G. R. 1999. Vertebrate Sprouty genes are induced by FGF signaling and can cause chondrodysplasia when overexpressed. *Development*, 126, 4465-4475.

Miyake, A., Hattori, Y., Ohta, M. & Itoh, N. 1996. Rat oligodendrocytes and astrocytes preferentially express fibroblast growth factor receptor-2 and -3 mRNAs. *J Neurosci Res*, 45, 534-41.

Mizuno, T. 2014. [Neuronal dysfunction in multiple sclerosis]. *Rinsho Shinkeigaku*, 54, 1066-8.

Mohammadi, M., Dionne, C. A., Li, W., Li, N., Spivak, T., Honegger, A. M., Jaye, M. & Schlessinger, J. 1992. POINT MUTATION IN FGF RECEPTOR ELIMINATES PHOSPHATIDYLINOSITOL HYDROLYSIS WITHOUT AFFECTING MITOGENESIS. *Nature*, 358, 681-684.

Mohammadi, M., Olsen, S. K. & Ibrahimi, O. A. 2005. Structural basis for fibroblast growth factor receptor activation. *Cytokine & Growth Factor Reviews*, 16, 107-137.

Mohan, H., Friese, A., Albrecht, S., Krumbholz, M., Elliott, C. L., Arthur, A., Menon, R., Farina, C., Junker, A., Stadelmann, C., Barnett, S. C., Huitinga, I., Wekerle, H., Hohlfeld, R., Lassmann, H., Kuhlmann, T., Linington, C. & Meinl, E. 2014. Transcript profiling of different types of multiple sclerosis lesions yields FGF1 as a promoter of remyelination. *Acta Neuropathol Commun*, 2, 168.

Mori, F., Rossi, S., Piccinin, S., Motta, C., Mango, D., Kusayanagi, H., Bergami, A., Studer, V., Nicoletti, C. G., Buttari, F., Barbieri, F., Mercuri, N. B., Martino, G., Furlan, R., Nisticò, R. & Centonze, D. 2013. Synaptic plasticity and PDGF signaling defects underlie clinical progression in multiple sclerosis. *J Neurosci*, 33, 19112-9.

Morrison, R. S., Sharma, A., De Vellis, J. & Bradshaw, R. A. 1986. Basic fibroblast growth factor supports the survival of cerebral cortical neurons in primary culture. *Proc Natl Acad Sci U S A*, 83, 7537-41.

Moscatelli, D. 1987. HIGH AND LOW AFFINITY BINDING-SITES FOR BASIC FIBROBLAST GROWTH-FACTOR ON CULTURED-CELLS - ABSENCE OF A ROLE FOR LOW AFFINITY BINDING IN THE STIMULATION OF PLASMINOGEN-ACTIVATOR PRODUCTION BY BOVINE CAPILLARY ENDOTHELIAL-CELLS. *Journal of Cellular Physiology*, 131, 123-130.

Mosser, D. M. & Edwards, J. P. 2008. Exploring the full spectrum of macrophage activation. *Nat Rev Immunol*, 8, 958-69.

Munger, K. L., Levin, L. I., Hollis, B. W., Howard, N. S. & Ascherio, A. 2006. Serum 25-hydroxyvitamin D levels and risk of multiple sclerosis. *JAMA*, 296, 2832-8.

Murphy, M., Drago, J. & Bartlett, P. F. 1990. Fibroblast growth factor stimulates the proliferation and differentiation of neural precursor cells in vitro. *J Neurosci Res*, 25, 463-75.

Murphy, M., Reid, K., Ford, M., Furness, J. B. & Bartlett, P. F. 1994. FGF2 REGULATES PROLIFERATION OF NEURAL CREST CELLS, WITH SUBSEQUENT NEURONAL DIFFERENTIATION REGULATED BY LIF OR RELATED FACTORS. *Development*, 120, 3519-3528.

Murray, T. J. 2009. Robert Carswell: the first illustrator of MS. *Int MS J*, 16, 98-101.

Myhr, K. M. & Mellgren, S. I. 2009. Corticosteroids in the treatment of multiple sclerosis. *Acta Neurol Scand Suppl*, 73-80.

- Nakamura, S., Arima, K., Haga, S., Aizawa, T., Motoi, Y., Otsuka, M., Ueki, A. & Ikeda, K. 1998a. Fibroblast growth factor (FGF)-9 immunoreactivity in senile plaques. *Brain Research*, 814, 222-225.
- Nakamura, S., Arima, K., Kanda, T., Motoi, Y., Ikeda, K. & Ueki, A. 1998b. Fibroblast growth factor-9 immunoreactivity in spinal cord of patients with amyotrophic lateral sclerosis. *Society for Neuroscience Abstracts*, 24, 487-487.
- Nakamura, S., Todo, T., Haga, S., Aizawa, T., Motoi, Y., Ueki, A., Kurokawa, T. & Ikeda, K. 1997a. Motor neurons in human and rat spinal cord synthesize fibroblast growth factor-9. *Neurosci Lett*, 221, 181-4.
- Nakamura, S., Todo, T., Haga, S., Aizawa, T., Motoi, Y., Ueki, A., Kurokawa, T. & Ikeda, K. 1997b. Motor neurons in human and rat spinal cord synthesize fibroblast growth factor-9. *Neuroscience Letters*, 221, 181-184.
- Nakamura, S., Todo, T., Motoi, Y., Haga, S., Aizawa, T., Ueki, A. & Ikeda, K. 1999. Glial expression of fibroblast growth factor-9 in rat central nervous system. *Glia*, 28, 53-65.
- Nakata, N., Kato, H. & Kogure, K. 1993. Protective effects of basic fibroblast growth factor against hippocampal neuronal damage following cerebral ischemia in the gerbil. *Brain Res*, 605, 354-6.
- Nakazawa, T., Nakazawa, C., Matsubara, A., Noda, K., Hisatomi, T., She, H., Michaud, N., Hafezi-Moghadam, A., Miller, J. W. & Benowitz, L. I. 2006. Tumor necrosis factor-alpha mediates oligodendrocyte death and delayed retinal ganglion cell loss in a mouse model of glaucoma. *J Neurosci*, 26, 12633-41.
- Nandoskar, A., Raffel, J., Scalfari, A. S., Friede, T. & Nicholas, R. S. 2017. Pharmacological Approaches to the Management of Secondary Progressive Multiple Sclerosis. *Drugs*, 77, 885-910.
- Naruo, K., Seko, C., Kuroshima, K., Matsutani, E., Sasada, R., Kondo, T. & Kurokawa, T. 1993. NOVEL SECRETORY HEPARIN-BINDING FACTORS FROM HUMAN GLIOMA-CELLS (GLIA-ACTIVATING FACTORS) INVOLVED IN GLIAL-CELL GROWTH - PURIFICATION AND BIOLOGICAL PROPERTIES. *Journal of Biological Chemistry*, 268, 2857-2864.
- Naso, M. F., Tomkowicz, B., Perry, W. L. & Strohl, W. R. 2017. Adeno-Associated Virus (AAV) as a Vector for Gene Therapy. *BioDrugs*, 31, 317-334.
- Nave, K. A. 2010. Myelination and the trophic support of long axons. *Nat Rev Neurosci*, 11, 275-83.
- Nave, K. A. & Trapp, B. D. 2008. Axon-glial signaling and the glial support of axon function. *Annu Rev Neurosci*, 31, 535-61.
- Neuhaus, O., Farina, C., Wekerle, H. & Hohlfeld, R. 2001. Mechanisms of action of glatiramer acetate in multiple sclerosis. *Neurology*, 56, 702-8.
- Noda, M., Takii, K., Parajuli, B., Kawanokuchi, J., Sonobe, Y., Takeuchi, H., Mizuno, T. & Suzumura, A. 2014. FGF-2 released from degenerating neurons

- exerts microglial-induced neuroprotection via FGFR3-ERK signaling pathway. *J Neuroinflammation*, 11, 76.
- Ohkubo, Y., Uchida, A. O., Shin, D., Partanen, J. & Vaccarino, F. M. 2004. Fibroblast growth factor receptor 1 is required for the proliferation of hippocampal progenitor cells and for hippocampal growth in mouse. *J Neurosci*, 24, 6057-69.
- Olerup, O. & Hillert, J. 1991. HLA class II-associated genetic susceptibility in multiple sclerosis: a critical evaluation. *Tissue Antigens*, 38, 1-15.
- Olsen, S. K., Ibrahim, O. A., Raucchi, A., Zhang, F., Eliseenkova, A. V., Yayon, A., Basilico, C., Linhardt, R. J., Schlessinger, J. & Mohammadi, M. 2004. Insights into the molecular basis for fibroblast growth factor receptor autoinhibition and ligand-binding promiscuity. *Proc Natl Acad Sci U S A*, 101, 935-40.
- Ong, S. H., Guy, G. R., Hadari, Y. R., Laks, S., Gotoh, N., Schlessinger, J. & Lax, I. 2000. FRS2 proteins recruit intracellular signaling pathways by binding to diverse targets on fibroblast growth factor and nerve growth factor receptors. *Molecular and Cellular Biology*, 20, 979-989.
- Ornitz, D. M. & Itoh, N. 2015. The Fibroblast Growth Factor signaling pathway. *Wiley Interdiscip Rev Dev Biol*, 4, 215-66.
- Orrurtreger, A., Bedford, M. T., Burakova, T., Arman, E., Zimmer, Y., Yayon, A., Givol, D. & Lonai, P. 1993. DEVELOPMENTAL LOCALIZATION OF THE SPLICING ALTERNATIVES OF FIBROBLAST GROWTH-FACTOR RECEPTOR-2 (FGFR2). *Developmental Biology*, 158, 475-486.
- Orton, S. M., Herrera, B. M., Yee, I. M., Valdar, W., Ramagopalan, S. V., Sadovnick, A. D., Ebers, G. C. & Group, C. C. S. 2006. Sex ratio of multiple sclerosis in Canada: a longitudinal study. *Lancet Neurol*, 5, 932-6.
- Osterhout, D. J., Ebner, S., Xu, J. S., Ornitz, D. M., Zazanis, G. A. & Mckinnon, R. D. 1997. Transplanted oligodendrocyte progenitor cells expressing a dominant-negative FGF receptor transgene fail to migrate in vivo. *Journal of Neuroscience*, 17, 9122-9132.
- Otto, D., Frotscher, M. & Unsicker, K. 1989. Basic fibroblast growth factor and nerve growth factor administered in gel foam rescue medial septal neurons after fimbria fornix transection. *J Neurosci Res*, 22, 83-91.
- Owens, D. M. & Keyse, S. M. 2007. Differential regulation of MAP kinase signalling by dual-specificity protein phosphatases. *Oncogene*, 26, 3203-3213.
- Pagé, E. L., Robitaille, G. A., Pouysségur, J. & Richard, D. E. 2002. Induction of hypoxia-inducible factor-1alpha by transcriptional and translational mechanisms. *J Biol Chem*, 277, 48403-9.
- Partanen, J., Mäkelä, T. P., Eerola, E., Korhonen, J., Hirvonen, H., Claesson-Welsh, L. & Alitalo, K. 1991. FGFR-4, a novel acidic fibroblast growth factor receptor with a distinct expression pattern. *EMBO J*, 10, 1347-54.

- Pasquale, E. B. 1990a. A DISTINCTIVE FAMILY OF EMBRYONIC PROTEIN-TYROSINE KINASE RECEPTORS. *Proceedings of the National Academy of Sciences of the United States of America*, 87, 5812-5816.
- Pasquale, E. B. 1990b. A distinctive family of embryonic protein-tyrosine kinase receptors. *Proc Natl Acad Sci U S A*, 87, 5812-6.
- Patel, M. N. & Mcnamara, J. O. 1995. Selective enhancement of axonal branching of cultured dentate gyrus neurons by neurotrophic factors. *Neuroscience*, 69, 763-70.
- Patrikios, P., Stadelmann, C., Kutzelnigg, A., Rauschka, H., Schmidbauer, M., Laursen, H., Sorensen, P. S., Brueck, W., Lucchinetti, C. & Lassmann, H. 2006. Remyelination is extensive in a subset of multiple sclerosis patients. *Brain*, 129.
- Patterson, K. I., Brummer, T., O'brien, P. M. & Daly, R. J. 2009. Dual-specificity phosphatases: critical regulators with diverse cellular targets. *Biochemical Journal*, 418, 475-489.
- Pawson, T., Olivier, P., Rozakisadcock, M., Mcglade, J. & Henkemeyer, M. 1993. PROTEINS WITH SH2 AND SH3 DOMAINS COUPLE RECEPTOR TYROSINE KINASES TO INTRACELLULAR SIGNALING PATHWAYS. *Philosophical Transactions of the Royal Society of London Series B-Biological Sciences*, 340, 279-285.
- Pekny, M. & Pekna, M. 2014. Astrocyte reactivity and reactive astrogliosis: costs and benefits. *Physiol Rev*, 94, 1077-98.
- Penderis, J., Shields, S. A. & Franklin, R. J. 2003. Impaired remyelination and depletion of oligodendrocyte progenitors does not occur following repeated episodes of focal demyelination in the rat central nervous system. *Brain*, 126, 1382-91.
- Pera, E. M., Acosta, H., Gouignard, N., Climent, M. & Arregi, I. 2014. Active signals, gradient formation and regional specificity in neural induction. *Exp Cell Res*, 321, 25-31.
- Perkins, L. A. & Cain, L. D. 1995. Basic fibroblast growth factor (bFGF) increases the survival of embryonic and postnatal basal forebrain cholinergic neurons in primary culture. *Int J Dev Neurosci*, 13, 51-61.
- Perrimon, N. & Bernfield, M. 2000. Specificities of heparan sulphate proteoglycans in developmental processes. *Nature*, 404, 725-728.
- Planque, N. 2006. Nuclear trafficking of secreted factors and cell-surface receptors: new pathways to regulate cell proliferation and differentiation, and involvement in cancers. *Cell Commun Signal*, 4, 7.
- Plotnikov, A. N., Hubbard, S. R., Schlessinger, J. & Mohammadi, M. 2000. Crystal structures of two FGF-FGFR complexes reveal the determinants of ligand-receptor specificity. *Cell*, 101, 413-24.
- Polman, C. H., Reingold, S. C., Banwell, B., Clanet, M., Cohen, J. A., Filippi, M., Fujihara, K., Havrdova, E., Hutchinson, M., Kappos, L., Lublin, F. D., Montalban,

- X., O'Connor, P., Sandberg-Wollheim, M., Thompson, A. J., Waubant, E., Weinshenker, B. & Wolinsky, J. S. 2011. Diagnostic criteria for multiple sclerosis: 2010 revisions to the McDonald criteria. *Ann Neurol*, 69, 292-302.
- Preger, E., Ziv, I., Shabtay, A., Sher, I., Tsang, M., Dawid, I. B., Altuvia, Y. & Ron, D. 2004. Alternative splicing generates an isoform of the human Sef gene with altered subcellular localization and specificity. *Proc Natl Acad Sci U S A*, 101, 1229-34.
- Presta, M., Andres, G., Leali, D., Dell'era, P. & Ronca, R. 2009. Inflammatory cells and chemokines sustain FGF2-induced angiogenesis. *European Cytokine Network*, 20, 39-50.
- Prineas, J. W., Kwon, E. E., Cho, E. S., Sharer, L. R., Barnett, M. H., Oleszak, E. L., Hoffman, B. & Morgan, B. P. 2001. Immunopathology of secondary-progressive multiple sclerosis. *Ann Neurol*, 50, 646-57.
- Proescholdt, M. A., Jacobson, S., Tresser, N., Oldfield, E. H. & Merrill, M. J. 2002. Vascular endothelial growth factor is expressed in multiple sclerosis plaques and can induce inflammatory lesions in experimental allergic encephalomyelitis rats. *J Neuropathol Exp Neurol*, 61, 914-25.
- Proia, P., Schiera, G., Mineo, M., Ingrassia, A. M., Santoro, G., Savettieri, G. & Di Liegro, I. 2008. Astrocytes shed extracellular vesicles that contain fibroblast growth factor-2 and vascular endothelial growth factor. *Int J Mol Med*, 21, 63-7.
- Qian, X. M., Davis, A. A., Goderie, S. K. & Temple, S. 1997. FGF2 concentration regulates the generation of neurons and glia from multipotent cortical stem cells. *Neuron*, 18, 81-93.
- Quintana, F. J., Basso, A. S., Iglesias, A. H., Korn, T., Farez, M. F., Bettelli, E., Caccamo, M., Oukka, M. & Weiner, H. L. 2008. Control of T(reg) and T(H)17 cell differentiation by the aryl hydrocarbon receptor. *Nature*, 453, 65-71.
- Rafalski, V. A. & Brunet, A. 2011. Energy metabolism in adult neural stem cell fate. *Prog Neurobiol*, 93, 182-203.
- Ramirez, J. J., Finklestein, S. P., Keller, J., Abrams, W., George, M. N. & Parakh, T. 1999. Basic fibroblast growth factor enhances axonal sprouting after cortical injury in rats. *Neuroreport*, 10, 1201-4.
- Reilly, J. F. & Maher, P. A. 2001. Importin beta-mediated nuclear import of fibroblast growth factor receptor: role in cell proliferation. *J Cell Biol*, 152, 1307-12.
- Reilly, J. F., Maher, P. A. & Kumari, V. G. 1998. Regulation of astrocyte GFAP expression by TGF-beta1 and FGF-2. *Glia*, 22, 202-10.
- Reuss, B., Hertel, M., Werner, S. & Unsicker, K. 2000. Fibroblast growth factors-5 and -9 distinctly regulate expression and function of the gap junction protein connexin43 in cultured astroglial cells from different brain regions. *Glia*, 30, 231-41.

Reynolds, B. A. & Weiss, S. 1996. Clonal and population analyses demonstrate that an EGF-responsive mammalian embryonic CNS precursor is a stem cell. *Dev Biol*, 175, 1-13.

Ribatti, D., Nico, B. & Vacca, A. 2006. Importance of the bone marrow microenvironment in inducing the angiogenic response in multiple myeloma. *Oncogene*, 25, 4257-4266.

Riccio, P. & Rossano, R. 2017. Diet, Gut Microbiota, and Vitamins D + A in Multiple Sclerosis. *Neurotherapeutics*.

Robertson, N. P., O'riordan, J. I., Chataway, J., Kingsley, D. P., Miller, D. H., Clayton, D. & Compston, D. A. 1997. Offspring recurrence rates and clinical characteristics of conjugal multiple sclerosis. *Lancet*, 349, 1587-90.

Romme Christensen, J., Börnsen, L., Hesse, D., Krakauer, M., Sørensen, P. S., Søndergaard, H. B. & Sellebjerg, F. 2012. Cellular sources of dysregulated cytokines in relapsing-remitting multiple sclerosis. *J Neuroinflammation*, 9, 215.

Rosenberg, R. D., Shworak, N. W., Liu, J., Schwartz, J. J. & Zhang, L. J. 1997. Heparan sulfate proteoglycans of the cardiovascular system. Specific structures emerge but how is synthesis regulated? *Journal of Clinical Investigation*, 99, 2062-2070.

Rottlaender, A., Villwock, H., Addicks, K. & Kuerten, S. 2011. Neuroprotective role of fibroblast growth factor-2 in experimental autoimmune encephalomyelitis. *Immunology*, 133, 370-8.

Rowntree, S. & Kolb, B. 1997. Blockade of basic fibroblast growth factor retards recovery from motor cortex injury in rats. *Eur J Neurosci*, 9, 2432-41.

Rungta, R. L., Choi, H. B., Tyson, J. R., Malik, A., Dissing-Olesen, L., Lin, P. J. C., Cain, S. M., Cullis, P. R., Snutch, T. P. & Macvicar, B. A. 2015. The cellular mechanisms of neuronal swelling underlying cytotoxic edema. *Cell*, 161, 610-621.

Russell, J. C., Szufflita, N., Khatri, R., Lattera, J. & Hossain, M. A. 2006. Transgenic expression of human FGF-1 protects against hypoxic-ischemic injury in perinatal brain by intervening at caspase-XIAP signaling cascades. *Neurobiol Dis*, 22, 677-90.

Salegio, E. A., Samaranch, L., Kells, A. P., Mittermeyer, G., San Sebastian, W., Zhou, S., Beyer, J., Forsayeth, J. & Bankiewicz, K. S. 2013. Axonal transport of adeno-associated viral vectors is serotype-dependent. *Gene Ther*, 20, 348-52.

Sanderson, N. S., Zimmermann, M., Eilinger, L., Gubser, C., Schaeren-Wiemers, N., Lindberg, R. L., Dougan, S. K., Ploegh, H. L., Kappos, L. & Derfuss, T. 2017. Cocapture of cognate and bystander antigens can activate autoreactive B cells. *Proc Natl Acad Sci U S A*, 114, 734-739.

Sapieha, P. S., Peltier, M., Rendahl, K. G., Manning, W. C. & Di Polo, A. 2003. Fibroblast growth factor-2 gene delivery stimulates axon growth by adult retinal ganglion cells after acute optic nerve injury. *Mol Cell Neurosci*, 24, 656-72.

Sarchielli, P., Di Filippo, M., Ercolani, M. V., Chiasserini, D., Mattioni, A., Bonucci, M., Tenaglia, S., Eusebi, P. & Calabresi, P. 2008. Fibroblast growth factor-2 levels are elevated in the cerebrospinal fluid of multiple sclerosis patients. *Neurosci Lett*, 435, 223-8.

Sasaki, A., Taketomi, T., Kato, R., Saeki, K., Nonami, A., Sasaki, M., Kuriyama, M., Saito, N., Shibuya, M. & Yoshimura, A. 2003. Mammalian Sprouty4 suppresses Ras-independent ERK activation by binding to Raf1. *Nature Cell Biology*, 5, 427-432.

Sasaki, K., Oomura, Y., Figurov, A. & Yagi, H. 1994. Acidic fibroblast growth factor facilitates generation of long-term potentiation in rat hippocampal slices. *Brain Res Bull*, 33, 505-11.

Sasaki, K., Tooyama, I., Li, A. J., Oomura, Y. & Kimura, H. 1999. Effects of an acidic fibroblast growth factor fragment analog on learning and memory and on medial septum cholinergic neurons in senescence-accelerated mice. *Neuroscience*, 92, 1287-94.

Sasisekharan, R. & Venkataraman, G. 2000. Heparin and heparan sulfate: biosynthesis, structure and function. *Current Opinion in Chemical Biology*, 4, 626-631.

Schlessinger, J. 1991. CLONING AND EXPRESSION OF TWO DISTINCT HIGH-AFFINITY RECEPTORS CROSS-REACTING WITH ACIDIC AND BASIC FIBROBLAST GROWTH FACTORS. *Journal of Cellular Biochemistry Supplement*, 209-209.

Schlessinger, J., Plotnikov, A. N., Ibrahimi, O. A., Eliseenkova, A. V., Yeh, B. K., Yayon, A., Linhardt, R. J. & Mohammadi, M. 2000. Crystal structure of a ternary FGF-FGFR-heparin complex reveals a dual role for heparin in FGFR binding and dimerization. *Molecular Cell*, 6, 743-750.

Schmittgen, T. D. & Livak, K. J. 2008. Analyzing real-time PCR data by the comparative C-T method. *Nature Protocols*, 3, 1101-1108.

Seghezzi, G., Patel, S., Ren, C. J., Gualandris, A., Pintucci, G., Robbins, E. S., Shapiro, R. L., Galloway, A. C., Rifkin, D. B. & Mignatti, P. 1998. Fibroblast growth factor-2 (FGF-2) induces vascular endothelial growth factor (VEGF) expression in the endothelial cells of forming capillaries: an autocrine mechanism contributing to angiogenesis. *J Cell Biol*, 141, 1659-73.

Sekine, K., Ohuchi, H., Fujiwara, M., Yamasaki, M., Yoshizawa, T., Sato, T., Yagishita, N., Matsui, D., Koga, Y., Itoh, N. & Kato, S. 1999. Fgf10 is essential for limb and lung formation. *Nature Genetics*, 21, 138-141.

Seo, J. H., Suenaga, A., Hatakeyama, M., Taiji, M. & Imamoto, A. 2009. Structural and functional basis of a role for CRKL in a fibroblast growth factor 8-induced feed-forward loop. *Mol Cell Biol*, 29, 3076-87.

Serafini, B., Rosicarelli, B., Franciotta, D., Magliozzi, R., Reynolds, R., Cinque, P., Andreoni, L., Trivedi, P., Salvetti, M., Faggioni, A. & Aloisi, F. 2007. Dysregulated Epstein-Barr virus infection in the multiple sclerosis brain. *J Exp Med*, 204, 2899-912.

- Sheng, Z., Liang, Y., Lin, C. Y., Comai, L. & Chirico, W. J. 2005. Direct regulation of rRNA transcription by fibroblast growth factor 2. *Mol Cell Biol*, 25, 9419-26.
- Sherriff, F. E., Bridges, L. R. & Sivaloganathan, S. 1994. Early detection of axonal injury after human head trauma using immunocytochemistry for beta-amyloid precursor protein. *Acta Neuropathol*, 87, 55-62.
- Silva, P. N., Altamentova, S. M., Kilkenny, D. M. & Rocheleau, J. V. 2013. Fibroblast growth factor receptor like-1 (FGFRL1) interacts with SHP-1 phosphatase at insulin secretory granules and induces beta-cell ERK1/2 protein activation. *J Biol Chem*, 288, 17859-70.
- Sim, F. J., Zhao, C., Penderis, J. & Franklin, R. J. 2002. The age-related decrease in CNS remyelination efficiency is attributable to an impairment of both oligodendrocyte progenitor recruitment and differentiation. *J Neurosci*, 22, 2451-9.
- Sinha, S., Boyden, A. W., Itani, F. R., Crawford, M. P. & Karandikar, N. J. 2015. CD8(+) T-Cells as Immune Regulators of Multiple Sclerosis. *Front Immunol*, 6, 619.
- Smith, K. J., Kapoor, R., Hall, S. M. & Davies, M. 2001. Electrically active axons degenerate when exposed to nitric oxide. *Ann Neurol*, 49, 470-6.
- Sorensen, A., Moffat, K., Thomson, C. & Barnett, S. C. 2008. Astrocytes, but not olfactory ensheathing cells or Schwann cells, promote myelination of CNS axons in vitro. *Glia*, 56, 750-763.
- Soulet, F., Bailly, K., Roga, S., Lavigne, A. C., Amalric, F. & Bouche, G. 2005. Exogenously added fibroblast growth factor 2 (FGF-2) to NIH3T3 cells interacts with nuclear ribosomal S6 kinase 2 (RSK2) in a cell cycle-dependent manner. *J Biol Chem*, 280, 25604-10.
- Stachowiak, M. K., Fang, X., Myers, J. M., Dunham, S. M., Berezney, R., Maher, P. A. & Stachowiak, E. K. 2003. Integrative nuclear FGFR1 signaling (INFS) as a part of a universal "feed-forward-and-gate" signaling module that controls cell growth and differentiation. *J Cell Biochem*, 90, 662-91.
- Staub, F., Mackert, B., Kempfski, O., Peters, J. & Baethmann, A. 1993. Swelling and death of neuronal cells by lactic acid. *J Neurol Sci*, 119, 79-84.
- Steinberg, F., Zhuang, L., Beyeler, M., Kälin, R. E., Mullis, P. E., Brändli, A. W. & Trueb, B. 2010. The FGFRL1 receptor is shed from cell membranes, binds fibroblast growth factors (FGFs), and antagonizes FGF signaling in *Xenopus* embryos. *J Biol Chem*, 285, 2193-202.
- Storey, K. G., Goriely, A., Sargent, C. M., Brown, J. M., Burns, H. D., Abud, H. M. & Heath, J. K. 1998. Early posterior neural tissue is induced by FGF in the chick embryo. *Development*, 125, 473-84.
- Sylvestersen, K. B., Herrera, P. L., Serup, P. & Rescan, C. 2011. Fgf9 signalling stimulates *Spred* and *Sprouty* expression in embryonic mouse pancreas mesenchyme. *Gene Expr Patterns*, 11, 105-11.

- Takami, K., Matsuo, A., Terai, K., Walker, D. G., Mcgeer, E. G. & Mcgeer, P. L. 1998. Fibroblast growth factor receptor-1 expression in the cortex and hippocampus in Alzheimer's disease. *Brain Res*, 802, 89-97.
- Takayama, H., Ray, J., Raymon, H. K., Baird, A., Hogg, J., Fisher, L. J. & Gage, F. H. 1995. Basic fibroblast growth factor increases dopaminergic graft survival and function in a rat model of Parkinson's disease. *Nat Med*, 1, 53-8.
- Tao, Y., Black, I. B. & Dicicco-Bloom, E. 1996. Neurogenesis in neonatal rat brain is regulated by peripheral injection of basic fibroblast growth factor (bFGF). *J Comp Neurol*, 376, 653-63.
- Tassi, E., McDonnell, K., Gibby, K. A., Tilan, J. U., Kim, S. E., Kodack, D. P., Schmidt, M. O., Sharif, G. M., Wilcox, C. S., Welch, W. J., Gallicano, G. I., Johnson, M. D., Riegel, A. T. & Wellstein, A. 2011. Impact of fibroblast growth factor-binding protein-1 expression on angiogenesis and wound healing. *Am J Pathol*, 179, 2220-32.
- Tejera-Alhambra, M., Casrouge, A., De Andrés, C., Seyfferth, A., Ramos-Medina, R., Alonso, B., Vega, J., Fernández-Paredes, L., Albert, M. L. & Sánchez-Ramón, S. 2015. Plasma biomarkers discriminate clinical forms of multiple sclerosis. *PLoS One*, 10, e0128952.
- Thau-Zuchman, O., Shohami, E., Alexandrovich, A. G. & Leker, R. R. 2012. Combination of vascular endothelial and fibroblast growth factor 2 for induction of neurogenesis and angiogenesis after traumatic brain injury. *J Mol Neurosci*, 47, 166-72.
- Thomson, C. E., Hunter, A. M., Griffiths, I. R., Edgar, J. M. & McCulloch, M. C. 2006. Murine spinal cord explants: A model for evaluating axonal growth and myelination in vitro. *Journal of Neuroscience Research*, 84, 1703-1715.
- Thomson, C. E., McCulloch, M., Sorenson, A., Barnett, S. C., Seed, B. V., Griffiths, I. R. & Mclaughlin, M. 2008. Myelinated, synapsing cultures of murine spinal cord - validation as an in vitro model of the central nervous system. *European Journal of Neuroscience*, 28, 1518-1535.
- Thornton, S. C., Mueller, S. N. & Levine, E. M. 1983. HUMAN-ENDOTHELIAL CELLS - USE OF HEPARIN IN CLONING AND LONG-TERM SERIAL CULTIVATION. *Science*, 222, 623-625.
- Timmer, M., Cesnulevicius, K., Winkler, C., Kolb, J., Lipokatic-Takacs, E., Jungnickel, J. & Grothe, C. 2007. Fibroblast growth factor (FGF)-2 and FGF receptor 3 are required for the development of the substantia nigra, and FGF-2 plays a crucial role for the rescue of dopaminergic neurons after 6-hydroxydopamine lesion. *J Neurosci*, 27, 459-71.
- Tkachenko, E., Rhodes, J. M. & Simons, M. 2005. Syndecans - New kids on the signaling block. *Circulation Research*, 96, 488-500.
- Todo, T., Kondo, T., Kirino, T., Asai, A., Adams, E. F., Nakamura, S., Ikeda, K. & Kurokawa, T. 1998. Expression and growth stimulatory effect of fibroblast growth factor 9 in human brain tumors. *Neurosurgery*, 43, 337-46.

- Trapp, B. D. & Nave, K. A. 2008. Multiple sclerosis: an immune or neurodegenerative disorder? *Annu Rev Neurosci*, 31, 247-69.
- Trapp, B. D. & Stys, P. K. 2009. Virtual hypoxia and chronic necrosis of demyelinated axons in multiple sclerosis. *Lancet Neurol*, 8, 280-91.
- Trowell, O. A. & Willmer, E. N. 1939. Studies on the growth of tissues in vitro VI. The effects of some tissue extracts on the growth of periosteal fibroblasts. *Journal of Experimental Biology*, 16, 60-70.
- Trueb, B., Zhuang, L., Taeschler, S. & Wiedemann, M. 2003. Characterization of FGFR1, a novel fibroblast growth factor (FGF) receptor preferentially expressed in skeletal tissues. *J Biol Chem*, 278, 33857-65.
- Tsai, M. C., Shen, L. F., Kuo, H. S., Cheng, H. & Chak, K. F. 2008. Involvement of acidic fibroblast growth factor in spinal cord injury repair processes revealed by a proteomics approach. *Mol Cell Proteomics*, 7, 1668-87.
- Tsang, M. & Dawid, I. B. 2004. Promotion and attenuation of FGF signaling through the Ras-MAPK pathway. *Science's STKE : signal transduction knowledge environment*, 2004, pe17-pe17.
- Tsang, M., Friesel, R., Kudoh, T. & Dawid, I. B. 2002. Identification of Sef, a novel modulator of FGF signalling. *Nat Cell Biol*, 4, 165-9.
- Tsukada, N., Miyagi, K., Matsuda, M., Yanagisawa, N. & Yone, K. 1991. Tumor necrosis factor and interleukin-1 in the CSF and sera of patients with multiple sclerosis. *J Neurol Sci*, 104, 230-4.
- Tumani, H. 2008. Corticosteroids and plasma exchange in multiple sclerosis. *J Neurol*, 255 Suppl 6, 36-42.
- Turner, N. & Grose, R. 2010. Fibroblast growth factor signalling: from development to cancer. *Nature Reviews Cancer*, 10, 116-129.
- Tutuncu, M., Tang, J., Zeid, N. A., Kale, N., Crusan, D. J., Atkinson, E. J., Siva, A., Pittock, S. J., Pirko, I., Keegan, B. M., Lucchinetti, C. F., Noseworthy, J. H., Rodriguez, M., Weinshenker, B. G. & Kantarci, O. H. 2013. Onset of progressive phase is an age-dependent clinical milestone in multiple sclerosis. *Mult Scler*, 19, 188-98.
- Tzartos, J. S., Friese, M. A., Craner, M. J., Palace, J., Newcombe, J., Esiri, M. M. & Fugger, L. 2008. Interleukin-17 production in central nervous system-infiltrating T cells and glial cells is associated with active disease in multiple sclerosis. *Am J Pathol*, 172, 146-55.
- Ueno, H., Gunn, M., Dell, K., Tseng, A. & Williams, L. 1992. A TRUNCATED FORM OF FIBROBLAST GROWTH-FACTOR RECEPTOR-1 INHIBITS SIGNAL TRANSDUCTION BY MULTIPLE TYPES OF FIBROBLAST GROWTH-FACTOR RECEPTOR. *Journal of Biological Chemistry*, 267, 1470-1476.
- Urness, L. D., Li, C., Wang, X. & Mansour, S. L. 2008. Expression of ERK signaling inhibitors Dusp6, Dusp7, and Dusp9 during mouse ear development. *Developmental Dynamics*, 237, 163-169.

- Vacca, A., Ribatti, D., Presta, M., Minischetti, M., Iurlaro, M., Ria, R., Albin, A., Bussolino, F. & Dammacco, F. 1999. Bone marrow neovascularization, plasma cell angiogenic potential, and matrix metalloproteinase-2 secretion parallel progression of human multiple myeloma. *Blood*, 93, 3064-3073.
- Van Den Berg, R., Hoogenraad, C. C. & Hintzen, R. Q. 2017. Axonal transport deficits in multiple sclerosis: spiraling into the abyss. *Acta Neuropathol*, 134, 1-14.
- Veldhoen, M., Hirota, K., Westendorf, A. M., Buer, J., Dumoutier, L., Renauld, J. C. & Stockinger, B. 2008. The aryl hydrocarbon receptor links TH17-cell-mediated autoimmunity to environmental toxins. *Nature*, 453, 106-9.
- Vincentz, J. W., Mcwhirter, J. R., Murre, C., Baldini, A. & Furuta, Y. 2005. Fgf15 is required for proper morphogenesis of the mouse cardiac outflow tract. *Genesis*, 41, 192-201.
- Vogel, D. Y., Vereyken, E. J., Glim, J. E., Heijnen, P. D., Moeton, M., Van Der Valk, P., Amor, S., Teunissen, C. E., Van Horssen, J. & Dijkstra, C. D. 2013. Macrophages in inflammatory multiple sclerosis lesions have an intermediate activation status. *J Neuroinflammation*, 10, 35.
- Wagner, J. P., Black, I. B. & Diccico-Bloom, E. 1999. Stimulation of neonatal and adult brain neurogenesis by subcutaneous injection of basic fibroblast growth factor. *J Neurosci*, 19, 6006-16.
- Wang, C. K., Chang, H., Chen, P. H., Chang, J. T., Kuo, Y. C., Ko, J. L. & Lin, P. 2009. Aryl hydrocarbon receptor activation and overexpression upregulated fibroblast growth factor-9 in human lung adenocarcinomas. *Int J Cancer*, 125, 807-15.
- Wang, J. K., Xu, H., Li, H. C. & Goldfarb, M. 1996. Broadly expressed SNT-like proteins link FGF receptor stimulation to activators of Ras. *Oncogene*, 13, 721-729.
- Wei, O. Y., Huang, Y. L., Da, C. D. & Cheng, J. S. 2000. Alteration of basic fibroblast growth factor expression in rat during cerebral ischemia. *Acta Pharmacol Sin*, 21, 296-300.
- Werner, S., Unsicker, K. & Von Bohlen Und Halbach, O. 2011. Fibroblast growth factor-2 deficiency causes defects in adult hippocampal neurogenesis, which are not rescued by exogenous fibroblast growth factor-2. *J Neurosci Res*, 89, 1605-17.
- Wesche, J., Małecki, J., Wiedłocha, A., Skjerpen, C. S., Claus, P. & Olsnes, S. 2006. FGF-1 and FGF-2 require the cytosolic chaperone Hsp90 for translocation into the cytosol and the cell nucleus. *J Biol Chem*, 281, 11405-12.
- Wiedłocha, A. & Sørensen, V. 2004. Signaling, internalization, and intracellular activity of fibroblast growth factor. *Curr Top Microbiol Immunol*, 286, 45-79.
- Willer, C. J., Dymont, D. A., Risch, N. J., Sadovnick, A. D., Ebers, G. C. & Group, C. C. S. 2003. Twin concordance and sibling recurrence rates in multiple sclerosis. *Proc Natl Acad Sci U S A*, 100, 12877-82.

- Wilson, H. C., Scolding, N. J. & Raine, C. S. 2006. Co-expression of PDGF alpha receptor and NG2 by oligodendrocyte precursors in human CNS and multiple sclerosis lesions. *J Neuroimmunol*, 176, 162-73.
- Wingerchuk, D. M., Hogancamp, W. F., O'brien, P. C. & Weinshenker, B. G. 1999. The clinical course of neuromyelitis optica (Devic's syndrome). *Neurology*, 53, 1107-14.
- Woodbury, M. E. & Ikezu, T. 2014. Fibroblast growth factor-2 signaling in neurogenesis and neurodegeneration. *J Neuroimmune Pharmacol*, 9, 92-101.
- Woodward, W. R., Nishi, R., Meshul, C. K., Williams, T. E., Coulombe, M. & Eckenstein, F. P. 1992. NUCLEAR AND CYTOPLASMIC LOCALIZATION OF BASIC FIBROBLAST GROWTH-FACTOR IN ASTROCYTES AND CA2 HIPPOCAMPAL-NEURONS. *Journal of Neuroscience*, 12, 142-152.
- Wu, D. Q., Kan, M. K., Sato, G. H., Okamoto, T. & Sato, J. D. 1991. Characterization and molecular cloning of a putative binding protein for heparin-binding growth factors. *J Biol Chem*, 266, 16778-85.
- Xu, H. & Goldfarb, M. 2001. Multiple effector domains within SNT1 coordinate ERK activation and neuronal differentiation of PC12 cells. *Journal of Biological Chemistry*, 276, 13049-13056.
- Xu, J. S., Liu, Z. H. & Ornitz, D. M. 2000. Temporal and spatial gradients of Fgf8 and Fgf17 regulate proliferation and differentiation of midline cerebellar structures. *Development*, 127, 1833-1843.
- Xu, X., Weinstein, M., Li, C., Naski, M., Cohen, R. I., Ornitz, D. M., Leder, P. & Deng, C. 1998. Fibroblast growth factor receptor 2 (FGFR2)-mediated reciprocal regulation loop between FGF8 and FGF10 is essential for limb induction. *Development*, 125, 753-65.
- Yamanaka, Y., Lanner, F. & Rossant, J. 2010. FGF signal-dependent segregation of primitive endoderm and epiblast in the mouse blastocyst. *Development*, 137, 715-24.
- Yang, J., Kim, W. J., Jun, H. O., Lee, E. J., Lee, K. W., Jeong, J. Y. & Lee, S. W. 2015. Hypoxia-induced fibroblast growth factor 11 stimulates capillary-like endothelial tube formation. *Oncol Rep*, 34, 2745-51.
- Yayon, A., Klagsbrun, M., Esko, J. D., Leder, P. & Ornitz, D. M. 1991. CELL-SURFACE, HEPARIN-LIKE MOLECULES ARE REQUIRED FOR BINDING OF BASIC FIBROBLAST GROWTH-FACTOR TO ITS HIGH-AFFINITY RECEPTOR. *Cell*, 64, 841-848.
- Yeh, B. K., Igarashi, M., Eliseenkova, A. V., Plotnikov, A. N., Sher, I., Ron, D., Aaronson, S. A. & Mohammadi, M. 2003. Structural basis by which alternative splicing confers specificity in fibroblast growth factor receptors. *Proceedings of the National Academy of Sciences of the United States of America*, 100, 2266-2271.
- Zajicek, J. P., Wing, M., Scolding, N. J. & Compston, D. A. 1992. Interactions between oligodendrocytes and microglia. A major role for complement and tumour

necrosis factor in oligodendrocyte adherence and killing. *Brain*, 115 (Pt 6), 1611-31.

Zeis, T., Graumann, U., Reynolds, R. & Schaeren-Wiemers, N. 2008. Normal-appearing white matter in multiple sclerosis is in a subtle balance between inflammation and neuroprotection. *Brain*, 131, 288-303.

Zhang, P. L., Izrael, M., Ainbinder, E., Ben-Simchon, L., Chebath, J. & Revel, M. 2006a. Increased myelinating capacity of embryonic stem cell derived oligodendrocyte precursors after treatment by interleukin-6/soluble interleukin-6 receptor fusion protein. *Mol Cell Neurosci*, 31, 387-98.

Zhang, X., Bao, L., Yang, L., Wu, Q. & Li, S. 2012. Roles of intracellular fibroblast growth factors in neural development and functions. *Sci China Life Sci*, 55, 1038-44.

Zhang, X., Ibrahimi, O. A., Olsen, S. K., Umemori, H., Mohammadi, M. & Ornitz, D. M. 2006b. Receptor specificity of the fibroblast growth factor family. The complete mammalian FGF family. *J Biol Chem*, 281, 15694-700.

Zhang, X., Tang, N., Hadden, T. J. & Rishi, A. K. 2011. Akt, FoxO and regulation of apoptosis. *Biochimica Et Biophysica Acta-Molecular Cell Research*, 1813, 1978-1986.

Zhang, Y., Chen, K., Sloan, S. A., Bennett, M. L., Scholze, A. R., O'keeffe, S., Phatnani, H. P., Guarnieri, P., Caneda, C., Ruderisch, N., Deng, S., Liddelov, S. A., Zhang, C., Daneman, R., Maniatis, T., Barres, B. A. & Wu, J. Q. 2014. An RNA-sequencing transcriptome and splicing database of glia, neurons, and vascular cells of the cerebral cortex. *J Neurosci*, 34, 11929-47.

Zhou, Y. X., Flint, N. C., Murtie, J. C., Le, T. Q. & Armstrong, R. C. 2006. Retroviral lineage analysis of fibroblast growth factor receptor signaling in FGF2 inhibition of oligodendrocyte progenitor differentiation. *Glia*, 54, 578-90.

Zhou, Y. X., Pannu, R., Le, T. Q. & Armstrong, R. C. 2012. Fibroblast growth factor 1 (FGFR1) modulation regulates repair capacity of oligodendrocyte progenitor cells following chronic demyelination. *Neurobiol Dis*, 45, 196-205.

Zincarelli, C., Soltys, S., Rengo, G., Koch, W. J. & Rabinowitz, J. E. 2010. Comparative cardiac gene delivery of adeno-associated virus serotypes 1-9 reveals that AAV6 mediates the most efficient transduction in mouse heart. *Clin Transl Sci*, 3, 81-9.

Zincarelli, C., Soltys, S., Rengo, G. & Rabinowitz, J. E. 2008. Analysis of AAV serotypes 1-9 mediated gene expression and tropism in mice after systemic injection. *Mol Ther*, 16, 1073-80.

Özakbaş, S. 2015. Cognitive Impairment in Multiple Sclerosis: Historical Aspects, Current Status, and Beyond. *Noro Psikiyatı Ars*, 52, S12-S15.